Study of the PPARγ Cofactor Receptor Interacting Protein 140 in Alzheimer's Disease

Katrin Gisela
Blondrath

Centre for

Neuroscience

Division of Brain

Science Department

of Medicine Faculty

of Medicine Imperial

College London

Submitted for the Diploma of Imperial College (DIC), PhD degree of Imperial College London// Clinical Medicine Research (A3Z1DM)

Copyright declaration

The copyright of this thesis rests with the author and is made available under a Creative Commons Attribution Non-Commercial No Derivatives licence. Researchers are free to copy, distribute or transmit the thesis on the condition that they attribute it, that they do not use it for commercial purposes and that they do not alter, transform or build upon it. For any reuse or redistribution, researchers must make clear to others the licence terms of this work

DECLARATION

In submitting this thesis I declare that the work presented henceforth is purely that of my own unless disclosed otherwise, in which case it is fully referenced or acknowledged.

ACKNOLWEDEMENTS

A three-year PhD studentship was awarded from Alzheimer's Research UK (ARUK) and allowed me to conduct full-time research that has led to the submission of the generated data. Special thanks go to Jamie Graham and his wife Vicki, who raised the money to fund this project. Jamie was diagnosed with early-onset Alzheimer's at just 59 years of age and he raised money by rowing 22 miles from Henley to Eton, together with former Olympic rowers Col Alexander Lindsay and Hugh Matheson amongst other crewmembers. Unfortunately Jamie died in January of this year and my thoughts and condolences go out to his family. I would also like to thank the London Neurodegenerative Diseases Brain Bank for the donation of the human brains used in the present study. My gratitude goes to my first supervisor Dr Magdalena Sastre as during my time at Imperial College, she has always been readily available for guidance, critical appraisal of my work and technical assistance. She was particularly helpful with revision, assessment and correction of the present manuscript. Secondly I would like to thank my second supervisor, Dr Mark Christian for his periodical assessment of my project and practical advise during the experimental work. I would like to thank Professor Malcolm Parker for critical discussion about the project and suggestions of new ideas as well as providing the RIP140 transgenic and knock out mouse lines. Dr. Jenny Steel helped with breeding and harvesting of the RIP140 mouse line and provided the in situ hybridization and LacZ stain images of the RIP140 knock out brains, and constantly helped with providing background knowledge about these animals, for which I am all very grateful. David Morrow helped with the part of the IBA1 and GFAP staining as well as the analyses of the NeuN staining images and I would like to thank him for his contributions to this thesis. Special thanks go out to Dr Loukia Katsouri who did most of the animal breeding, tissue harvesting and provided great expertise with the NeuN staining procedure. In addition, Loukia was always helpful with any questions exceeding the techniques above and has been a good colleague and friend during the time in and outside of the lab.

Big thanks go out to the whole group who worked under Magdalena Sastre, for providing a friendly environment. I would like to thank them for their emotional support and friendship and the fun times we had during bench time

and after that. A particular group member I would like to thank is Dr. Callum Parr. Although he left the group early his help, emotional support and technical advise regarding any method or content of the project continued over the distance of 5,886 miles and I am glad to have found a bright scientist like him who I can call a good friend whose friendship will hopefully exceed this PhD time. I would like to thank my family for their support throughout this PhD time and in particular my Mother who would jump on a plane at any minute to fly to London just to comfort me. Danke liebe Mama. I saved my last thanks to a very special person I have met in the Division of Neuroscience for whom I am eternally grateful that he has found the way into my life and let me be part of his. Thank you for your friendship, patience, scientific advice and critical assessment of my work, the way to deal with my craziness but most importantly thanks you for your love. During these four years I am so very lucky to have found more than just a PhD project and some days I think without you, I would have just left it and London behind me. You were the anchor to it when I was storming through the sea of frustration, failure and misunderstandings. Thank you for everything Dr. D. Gonzalez-Carter, te amo.

ABSTRACT

Activation of nuclear receptor Peroxisome Proliferator Activated Receptor gamma (PPARγ) has been reported to be protective in Alzheimer's disease (AD) mouse models, by decreasing inflammation and toxic Aβ levels, one of the key features hallmarking the disease. Therefore, the role of PPARγ cofactors will be critical in order to regulate the activity of PPARγ. Our aim was to study the potential role of the PPARγ cofactor Receptor Interacting Protein 140 (RIP140) in AD. Results from our lab showed that RIP140 is reduced in the brain of AD patients. Therefore, we investigated the role of RIP140 on the processing of APP initially in vitro, using a neuroblastoma cell line. Our results suggest that RIP140 over expression reduced Aβ generation and BACE1 protein expression and mRNA levels in a PPARγ activated dependent manner. Conversely, knockdown of RIP140 increased the level of BACE1 protein mRNA and promoter activity. Therefore, RIP140 seems to act as a transcriptional co-activator for PPARγ leading to reductions in BACE1 transcription. Studies performed in animal models, lacking or over expressing RIP140 indicated that many genes involved in the insulin pathway appeared to be modulated by RIP140. In the hippocampus area of mice overexpressing RIP140there was a transcriptional induction of growth factors involved in synaptic plasticity, including growth associated protein 43 (GAP43) and Insulin growth factor2 (IgF2), both being linked to the development of AD but also memory and cognition. In agreement with the in vitro results, the levels of BACE1 were found reduced in the

brain of RIP140 transgenic mice, although no alterations on endogenous mouse Aβ levels were detected. Further more, the expression of proteins being involved in the clearance of Aβ plaques, such as ApoE were found increased. RIP140 over expressing mice showed also alteration in genes associated with Tau pathology, such as a reduction of microtubule-associated proteins 1 and 2 and the Tau kinases CDK5 and GSK3. Studies in animals lacking RIP140 showed the opposite effect in most of the above genes and mRNA analysis revealed that BACE1 expression levels were increased in the frontal cortex area, which is in line with our previous results. RIP140 knockout mice showed also increases in the levels of genes involved in Tau pathology, such as GSK3, cdK5 and Mtap2. Interestingly, RIP140 appeared to be involved in the regulation of inflammatory processes in the mouse brain, showing an increase in GFAP staining for astrocytes in RIP140 knockout mice and reductions in the levels of inflammatory cytokines in RIP40 transgenic animals. The results indicate that RIP140 has neuro-protective effects and could serve as therapeutic target for AD, by reducing the levels of BACE1 (the main enzyme involved in Aβ generation), proteins involved in Tau pathology and leading to a decrease of inflammatory processes in the brain.

Contents

1 Summary **34**

1.1 Background 34

2 General Introduction **36**

2.1 Losing yourself 36

2.2 Alois Alzheimer 37

2.3 The global challenge 38

2.4 A closer look at Alzheimer's Disease: from symptoms and diagnosis to the molecular basics 39

2.4.1 Symptoms and Diagnosis 39

2.4.2 Neuropatholgy 41

2.4.2.1 Senile amyloid β plaques 43

2.4.2.2 Neurofibrillary tau tangles 45

2.4.2.3 GSK3 and Tau 47

2.4.2.4 Regulation of GSK3 47

2.4.3 CDK5 and Tau 49

2.4.3.1 Neuroinflammation 50

2.4.3.2 Risk factors for AD 50

2.4.4 The link between Alzheimer's disease and type 2 Diabetes 50

2.4.5 Amyloid precursor protein (APP) processing 51

2.4.5.1 Biological functions of APP 54

2.4.5.2 α-secretase processing . . . 56
2.4.5.3 β-secretase processing . . . 57
2.4.5.4 γ-secretase processing . . . 59
2.4.6 Mechanisms of Aβ degradation . . . 63
2.5 Peroxisome proliferation activating receptors . . . 63
2.5.1 Discovery of PPARs . . . 64
2.5.2 Isoforms . . . 65
2.5.2.1 PPARα . . . 65
2.5.2.2 PPARβ/δ . . . 65
2.5.2.3 PPARγ . . . 66
2.5.2.4 Neuroprotective functions of PPARγ . . . 67
2.5.2.5 PPARγ in AD . . . 68
2.5.2.6 Stiumlation of PPARγ: agonism vs antagonism . . . 70
2.6 PPARγ Cofactors . . . 72
2.6.1 Receptor interacting Protein 140 (RIP140) . . . 73
2.6.2 Regulation of RIP140 Activity . . . 75
2.6.3 Corepressor vs. Coactivator . . . 77
2.6.4 Effects of RIP140 on the transcription of Inflammatory genes . . . 79
2.7 Aims of the thesis . . . 79

3 Materials and Methods **81**

3.1 Cell culture . . . 83
3.1.1 Neuronal cellline N2a (N2a sw) . . . 83
3.1.2 Transfections and treatments . . . 84
3.1.2.1 Transfections . . . 84
3.1.2.2 Transfection and cell lysis for Western blot analysis . . . 84
3.1.2.3 Transfections and treatments for qPCR analyses . . . 86
3.1.2.4 Confirmation of the efficiency of Transfections by qPCR analyses . . . 87
3.1.2.5 Transfections and treatments for Luciferase assays . . . 88

3.2 SDS page and Western Blot analyses . . . 89
3.2.1 Harvesting methods . . . 89
3.2.1.1 Harvesting of cells for total protein expression assay . . . 89
3.2.1.2 Subcellular fractionation for C- terminal fragment expression assay . . . 90
3.2.2 SDS page and Western Blot immunoblotting . . . 90
3.3 Analyses of Ribonucleic Acids (RNA) . . . 92
3.3.1 RNA Isolation . . . 92
3.3.2 Digestion of genomic DNA with DNAse . . . 93
3.3.3 Reverse Transcription Polymerase Chain Reaction (RT PCR) . . . 93
3.3.4 Quantitive Real time Polymerase Chain Reaction (qPCR) . . . 94
3.4 Luciferase Promoter Activity Assay . . . 96
3.5 Immunocytochemistry . . . 97
3.6 ELISA . . . 98
3.7 Animal work . . . 98
3.7.1 RIP140 Mouse lines . . . 98
3.7.2 DNA extraction from mice ear snips . . . 100
3.7.3 Genotype Polymerase chain reaction for RIP140 knock down animals (genotype PCR) . . . 101
3.7.4 Harvesting, dissectioning and storage of brain tissue . . . 101
3.7.5 ELISA assays . . . 102
3.7.6 Immunohistochemistry (IHC) . . . 102
3.7.7 Quantification of NeuN, GFAP, and IBA1 staining . . . 103
3.7.8 Human post mortem samples . . . 103
3.8 Statistical analyses . . . 103

4 Results I: Effects of RIP140 expression on APP processing in vitro 104

4.1 Introduction . . . 104
4.1.1 Determination of RIP140 levels in the post-mortem brain from AD patients . . . 105
4.2 Results: RIP140 affects APP processing *in vitro* . . . 106
4.2.1 Human RIP140 localizes to the nucleus and can efficiently be transfected into N2a cells . . . 106

4.2.2 RIP140 overexpression decreases extracellular Aβ42 peptides and AICD levels in a ligand dependent manner . . . 110
4.2.3 BACE1 protein and mRNA levels are affected by the expression status of RIP140 . . . 117
4.2.4 Alterations of BACE1 promoter activity are induced by PPARγ agonism and linked to RIP140 expression changes . . . 122
4.3 Discussion . . . 123
4.3.1 RIP140 acts possibly as a co-activator for PPARγ in the transcriptional regula- tion of BACE1 in vitro . . . 124
4.3.2 Silencing RIP140 in vitro reverses the effects on BACE1 transcription and may contribute towards amyloid pathology . . . 125

5 Results II: Study of the brain of RIP140 knock out mice 127
5.1 Introduction . . . 127
5.1.1 RIP140 in the brain . . . 127
5.2 Results . . . 128
5.2.1 RIP140 is located mainly in the hippocampus of mouse brain . . . 128
5.2.2 Effects of RIP140 depletion on expression level of various genes implicated in AD . . . 130
5.2.3 Mice lacking RIP140 show higher BACE1 mRNA expression in the Hippocampus . . . 136
5.2.4 Endogenous Aβ40 and 42 are not significantly altered by absence of RIP140 expression . . . 140
5.2.5 Genes involved in Aβ degradation . . . 142
5.2.6 Genes involved in memory and cognition . . . 148
5.2.7 Genes involved in the tau pathology . . . 151
5.2.8 5.2.8 Effect of RIP140 knock out on the levels of inflammatory mediators in the brain . . . 155
5.3 Neuronal density in RIP140 knock out mice . . . 162
5.4 Discussion . . . 166
5.4.1 Implications on APP processing . . . 166
5.4.2 RIP140 affects the levels of the Aβ clearing enzyme ApoE but not IDE or Neprilysin . . . 167
5.4.3 RIP140 alters the expression of GAP43 . . . 168
5.4.4 RIP140 affects the expression of genes involved in the Tau pathology . . . 169

5.4.5 Inflammation in the RIP140 ko brain . . . 170

6 Study of the brain of RIP140 transgenic mice 172

6.1 Introduction . . . 172

6.2 Results . . . 173

6.2.1 Genes involved in APP processing . . . 175

6.2.2 Endogenous expression of Aβ42 and Aβ40 are not affected by RIP140 overex- pression in vivo . . . 178

6.2.2.1 Effect of RIP140 overexpression on genes involved in Aβ degradation . . . 180

6.2.3 Effect of RIP140 overexpression on genes involved in memory and cognition . . . 184

6.2.4 Effect of RIP140 overexpression on genes involved in Tau pathology . . . 187

6.2.5 Effect of RIP140 overexpression on inflammatory mediators . . . 191

6.3 Neuronal density in RIP140 trangenic mice . . . 194

6.4 Discussion of the effect of RIP140 overexpression in vivo in the ex- pression of genes involved in AD . . . 197

6.4.1 Effect of RIP140 on APP processing . . . 197

6.4.2 RIP140 overexpression results in elevation of the expression of Aβ degrading enzymes . . . 198

6.4.3 RIP140 overexpression leads to an increase in neurotrophic growth factors and neuronal density . 199

6.4.4 Effect of RIP140 overexpression in the regulation of genes involved in Tau pathology . . . 200

6.4.5 RIP140 has anti-inflammatory function . . . 201

7 General Discussion 204

7.1 Findings of the study of RIP140 . . . 204

7.1.1 Effect of RIP140 on Aβ generation . . . 206

7.1.2 Effects of RIP140 on Aβ clearance . . . 208

7.1.3 Effects on Tau pathology . . . 209

7.1.4 Effects of RIP140 on inflammation . . . 211

7.1.5 Effects of RIP140 on neuronal density, neuronal growths factors and neuroprotection . . . 211

7.2 Limitations of the study and future work . . . 212

7.3 Final Conclusion . . . 214

7.4 Literature . . . 215

List of Figures

2.1 Alois Alzheimer (A) and his first, most famous patient Auguste Deter (B). The study and post mortem examanitation of the brain of Auguste Deter, who developed at the age of 51 years unusual symptoms of dementia, made Alois Alzheimer famous for the first description of the disease which is till today named Alzheimer's Disease after him. 38

2.2 Coronal brain scan, comparing a healthy (right, blue) and atrophic (left, red) brain. In cases of Alzheimer's disease, there is an associated loss of brain tissue. Examination of brains of presenile onset reveal obvious differences of the weight of the brain in comparisons with age matched, healthy control people (taken from BBC website, article about AD (http://www.bbc.com/news/health-33617141)) 41

2.3 Silver impregnation of the two main pathological hallmarks of Alzheimer's Disease. A is showing Amyloid ß deposition in the form of radial structured plaques that accumulate extracellular. B: Formation of intracellular neurofibrillary Tau tangles with their typical pyramidal shape (taken from Wikipedia.co.uk). 42

2.4 Progression and stages of Alzheimer's Disease with correlating pathological hallmarks. As the disease prgogresses to more severe stages, Amyloid β plaques as well as neurofibrillary tangles will accumulate causing a decline in neuronal integrity leading to cell death followed by neuronal and synaptic loss (Modified from Holztmann et al., 2011). 43

2.5 Amyloid plaque deposition and their impact on a cellular level. Aβ42 generated inside the neurons gets transported to the extracellular space where it eventually oligomerises with further peptides of its kind. These cores of Aβ are surrounded by dystrophic dendrites of the neuron and microglia and reactive astrocytes in the periphery. Activated Microglia trying to clear the peptides will surround the accumulation in a radial fashion and secrete pro-inflammatory factors during the the process. The composition of this entire structure is cummulative called amyloid plaque. 45

2.6 Canonical Wnt signaling leads to the stabilization of β -catenin and translocation to the nucleus, upon which it interacts with various LEF/TCF activators and the regulation of target genes. 49

2.7 Amyloidogenic APP processing: After β-cleavage a soluble fragment (sAPPβ) is liberated and released into the extracellular space. A remaining membrane integrated 99 amino acid long fragment (C99) will be the second product of this cleavage. A further cleavage by γ-secretase of the C99 at γ- and ε-cleaving sites will finally release Aβ and second, c-terminal, trans membrane product called AICD (APP intracellular signaling domain), which can be either 49 or 50 amino acids long. The mass spectrometry above shows that these two AICDs are produce in a nearly equimolar ratio. The N-terminal fragment of this γ-cleavage will release the Aβ species of all different length to the extracellular space. Mass spectrometry of Aβ species showed that Aβ40 isoform is present in much higher levels than the more toxic Aβ42. (Taken from Dimitrov et al., 2013) 53

2.8 Influence of neurogenesis by sAPPα and AICD. sAPPα possibly functions on cells via binding with its specific receptors and positively stimulate neurogenesis by promoting neuro progenitor cell proliferation. Contrary, the release of AICD, which eventually forms a complex with Fe65, might act as a inhibitory regulator on neuronal differentiation by yet unknown mechanisms. 56

2.9 Non-amyloidogenic cleavage of APP by α.-secretases. The alpha secretase ADAM17/ TACE cleaves the APP protein within the Aβ region, preventing the generation of toxic amyloid-β species. 57

2.10 BACE1 gene expression profile in human tissues. The expression profile of BACE1 indicates that its expression is not exclusive to the brain but almost all other tissues where it appears with higher expression in the pancreas (Source: www. biogps.org). 60

2.11 Schematic view of the γ-secretase complex. γ-secretase is a multi-subunit, intra membrane protease complex. It cleaves single-pass trans membrane proteins at residues within the trans membrane domain. It consists four individual proteins: presenilin, nicastrin, APH-1 (anterior pharynx-defective 1), and PEN-2 (presenilin enhancer 2). There are two known presinilin forms, 1 and two which expression is tissue specific and they are never expressed at the same time in the same complex. APH1 consits two isoforms, APH-1a and APH-1b (taken from Tomoko Wakabayashi, Bart De Strooper, 2008). 61

2.12 General mechanism of PPARs. PPAR's belong to the nuclear receptors, hence their localization within the nucleus. Specific PPAR ligands of extracellular and intracellular origin will bind to the PPAR ligand binding domain and allow dimerization with the RXR. RXR is also abundant in the nucleus and activated by its own specific ligands form within the nucleus. The activated heterodimer complex will then bind to the PPRE. The active complex is further regulated by recruitment and de-recruitment of co-activators and co-repressors of PPAR. 64

2.13 Chemical structure of (S)- (left) and (R)- (right) Pioglitazone. The pioglitazone molecule exhibits chirality with one stereo centre leading to the two enantiomer forms of (S)- and (R)- pioglitazone. The available pharmalogical drug contains a racemic mixture of both forms as a hydochloride (taken from wikipedia.org). 71

2.14 Chemical structure of T0070907 (A) and analysis of its binding to different PPAR subtypes (B). The affinities of T0070907 for the various PPAR subtypes were determined using an SPA assay. [3H]GW2433 (5 nM) was used as a ligand for PPARα and PPARδ, and [3H]rosiglitazone (5 nM) was used for PPARγ. T0070907 Is a non-TZD ligand for PPARγ, binding PPARγ with high affinity and being capable of displacing [3H]rosiglitazone with an apparent Ki of 1 nM. (Gary Lee et al., 2002). 72

2.15 Expression of RIP140 in human tissue. RIP140 expression was detected in all tissues tested. Expression levels were particularly high in the uterus, certain areas of the brain and in CD positive immune cells. . 74

2.16 In situ hybridization for RIP140 in the mouse brain. ISH of RIP140 indicates further that RIP140 seems specifically expressed in the brains of mice. Interestingly, within the brain expression seems highest in the Hippocampus an area that has been strongly linked to AD (taken from brain explorer; Allen brain atlas; ISH data for RIP140 (http://mouse.brain-map.org/experiment/show?id=740)). 75

2.17 Cytoplasmic functions and effects on glucose metabolism by RIP140. A high fat diet will eventually lead to phosphorylation by PKCε or methylation by PRMT1 and subsequent re-localization of RIP140 from the nucleus to the cytoplasm. A Rab GTPase-activating protein, AS160 can interact in the cytoplasm with RIP140 causing inhibition of GLUT4 translocation. Further on The RIP140 AS160 complex can inhibit the Akt inactivation, normally mediated by insulin, which is up taken by the cell. 77

2.18 Processes and gene targets regulated by RIP140. RIP140 acts both as a co-activator and co-repressor in conjunction with several NRs and other transcription factors; indicated by upwards and downwards arrows, respectively. The inner periphery of the ellipse shows gene targets which are repressed by RIP140 (in red) and those that are activated (in green) against which are mentioned the processes which are affected by these gene targets. Abbreviations: Areg, amphiregulin; Bmal1, brain and muscle aryl hydrocarbon receptor nuclear trans locator (ARNT)-like; CCND1, cyclin D1; CIDEA, cell death activator; Cpt1b, carnitine palmitoyltransferase Ib; CRABP1, cellular retinoic acid binding protein; FABP3, fatty acid binding protein 3; FAS, fatty acid synthase; IL1β interleukin-1β; IL6, interleukin 6; MCAD, medium-chain acyl coenzyme A dehydrogenase; PEPCK, phosphoenolpyruvate carboxykinase; PGR, progesterone receptor; SREBP, sterol regulatory element-binding transcription factor; Stat5a, signal transducer and activator of transcription 5A; TNFα, tumor necrosis factor-alpha; UCP1, uncoupling protein 1 (taken from Nautiyal et. al, 2010). 78

3.1 Validation of RIP140 overexpression or silencing via qPCR. The cDNA construct used for RIP140 transfection encoded for the human RIP140 gene and primers were designed to pick up overexpressed RIP140 only and no endogenous mRNA. The expression of human RIP140 was around a 1700 fold higher than in cells transfected with control pcDNA3 (A). Transfection with a siRNA targeting RIP140, mRNA expression was lowered for around 50% (B). 87

3.2 Validation of RIP140 overexpression or silencing via qPCR. The cDNA construct used for RIP140 transfection encoded for the human RIP140 gene and primers were designed to pick up overexpressed RIP140 only and no endogenous mRNA. The expression of human RIP140 was around a 1700 fold higher than in cells transfected with control pcDNA3 (A). Transfection with a siRNA targeting RIP140, mRNA expression was lowered for around 50% (B). 88

3.3 The luciferase reporter gene has been put under the control of a specific BACE1 promoter so that expression of the Luciferase protein represents how often the BACE1 promoter was read. After protein translation a biochemical reaction of lucefrin, which is part of the luciferase protein will induce a light signal, which can be measured. A higher light signal indicates a higher promoter activity. 97

3.4 Genomic organization of mouse Nrip1. A 3.6-kilobase fragment containing the complete open reading frame of Nrip1, with the exception of the first 27 amino acids, was removed using NsiI and was replaced with an IRES NEO cassette to generate the targeting vector. Short thick black horizontal lines, positions of the 3' probe outside the targeted region and the RIP140 probe. B, BamHI; N, NsiI; X, XbaI; Kb, kilobase; Wt, wild-type. b, Southern blot analysis of DNA samples from wild-type (+/+), heterozygous (+/-) and RIPKO (-/-) mice, digested with BamHI. Wt, wild type; Mut, mutant. Right margin, molecular sizes (taken from White et al., 2000) 99

4.1 RIP140 is decreased in AD post-mortem brains. Representative Western blot and quantification of RIP140 levels. As control for protein loading we used β-actin. Values are expressed as mean±SEM; *P<0.05, Student's t test. (This experiment was performed preliminary to the PhD project and the figure is the courtesy of Dr. Magdalene Sastre). 107

4.2 Localization of RIP140 in vitro. Immunofluorescence labeling with the 6D7 antibody against RIP140 protein (green) shows its localization, strictly restricted to the cell nucleus. The 6E10 antibody was used to detect full length APP (red). Cells were prior stably transfected with APP cDNA construct carrying the Swedish mutation. APP expression was detected in the cytoplasm and plasmatic membrane. Nuclear staining with DAPI (blue) was used a s a control and detected all cells. 108

4.3 Evaluation of transfection efficiency and subsequent effects on BACE1 expression. A+B: Controls of GFP transfected cells showing a high transfection rate ($>$ 60%) of N2aSw cells. The expression of RIP140 was not affected by during the duration of the treatment time from 17h to 40 hours or the treatment with the PPARγ ligand Pioglitazone in comparison to vehicle DMSO alone. C: knock down of BACE1 protein by using a siRNA revealed the specificity of the antibody. Treatment with 20 μM pioglitazone alone or in cells transfected with RIP140 resulted in a decrease in BACE1 protein level with strongest effects at the long treatment (40h). The V5 antibody was used to detect the transfected RIP140, which was tagged with the V5 peptide. RIP140 level seemed to be lower after 40 hour post transfection in comparison to 17 hours but remained stable when compared to cells with the same time treatment (D). Previous experiments revealed that no changes in BACE1 protein expression were accomplished within the 17-hour treatment time span (data not shown). 110

4.4 The EC50 values were derived from dose–response curves using the Cheng–Prusoff equation, with values representing the means and standard deviations calculated from three dose–response curves. The IC50 values were derived from inhibition curves at constant GW7647 (30 nM), L-165041 (200 nM), and BRL49653 (20 nM) concentrations for PPARα, PPARδ, and PPARγ, respectively, using the Cheng–Prusoff equation, with values representing the means and standard deviations calculated from three inhibition curves (taken from Seimandi et al., 2005). 111

4.5 Legend of treatments. N2aSw cells were transfected with RIP140 cDNA to induce overexpression or siRNA to silence RIP140. Additionally, cells overexpressing RIP140 received treatment with the synthetic PPARγ agonist Pioglitazone (Pio) which was dissolved in Dimethylsulfideoxide (DMSO) hence 3 different controls had to be per- formed: cells transfected with pcDNA3 (scrambled control DNA) + DMSO and pcDNA3 + Pio alone for the RIP140 overexpression experiments and cells receiving non coding siRNA as a control for siRNA experiments. 112

4.6 Effect of RIP140 overexpression on Aβ4 levels in vitro. Conditioned medium of N2aSw cells transfected with RIP140 cDNA showed significantly lower levels of Aβ peptides in a PPARγ activated dependent manner (A,B). In same samples, level of soluble APPα remained unchanged and was used to normalize the levels of Aβ in the conditioned medium samples (B). Full-length APP from whole cell lysates showed also no differences with the different treatments (E). Cells receiving only RIP140 cDNA but no PPARγ stimulation showed a slight but non-significant decrease in Aβ levels. (n=3 with 2-3 biological samples per group. Values shown in graphs represent the mean value ±SEM and are expressed as a percentage of control. Statistical analysis included one-way ANOVA with a post Tukey test, *P<0.05). 113

4.7 ELISA for Aβ40 and Aβ42 secreted in conditioned medium from N2aSw cells. Cells overexpressing RIP140 alone do not show any difference in amounts of Aβ42 (A) or Aβ40 (B) but if stimulated with pioglitazone, Aβ42 species were significantly lower in comparison to the control group. The ratio taken of Aβ40 to Aβ42 does not show any differences (C).Knock down of RIP140 did had no effect on Aβ42 level in vitro. (n=2 with 3 biological samples per group. Values shown in graphs represent the mean value ±SEM and are expressed as a percentage of control. Statistical analysis included one-way ANOVA with a post Tukey test, *P<0.05 for A, B and C and students t-test for D). 115

4.8 Effects of RIP140 overexpression on AICD level in membrane preparations of N2aSw cells overexpressing RIP140. Pioglitazone alone and combination of overexpression of RIP140 and pioglitazone treatment decreased amounts of AICD significantly (A, with representative western blot) while full length APP remained unchanged. (n=3 with 3 biological samples per group. Values shown in graphs represent the mean value ±SEM and are expressed as a percentage of control. Statistical analysis included one-way ANOVA with a post Tukey test, **P<0.01). 117

4.9 Effects of RIP140 on BACE1 protein expression in vitro. Pioglitazone treatment and RIP140 overexpression can independently lower BACE1 protein level significantly and have a cumulative effect when combined together (A). Silencing of RIP140 increases BACE1 protein expression (B) . Differences in endogenous RIP140 expression using the 6D7 antibody were not detected for cells treated with RIP140 siRNA in comparison to control, but showed an increase using cells overexpressing exogenous RIP140 as a control. (n=3 with 2-3 biological samples per group for RIP140 overexpression and n=1 with 3 biological samples per group for RIP140 silencing. Values shown in graphs represent the mean value ±SEM and are expressed as a percentage of control. Statistical analysis included one-way ANOVA with a post Tukey test, **P<0.01 ***P<0.001 for A and students t-test for C *P<0.05). 119

4.10 Effects of RIP140 on BACE1 mRNA expression in vitro. Pioglitazone treatment and RIP140 overexpression can both lower BACE1 mRNA level but only pioglitazone alone and combined treatment (RIP140 overexpression + pioglitazone) in a significant manner (A). Expression level of exogenous human RIP140 were around a 4000 fold higher than RIP140 untransfected cells in which no RIP140 expression was detected (B). Silencing of RIP140 increases BACE1 mRNA expression significantly (C). A 50% silencing rate of endogenous RIP140 was reached using RIP140 siRNA (D). (n=3 with 3 biological samples per group for RIP140 overexpression (A and B) and RIP140 silencing (C and D). Values shown in graphs represent the mean value ±SEM and are expressed as a fold change in comparison to the normalized control. Statistical analysis included one-way ANOVA with a post Tukey test, *P<0.05 for A and students t-test for C and D *P<0.05, ***P<0.001). 121

4.11 BACE1 promoter activity. BACE1 Promoter activity was decreased when RIP140 was overexpressed alone or combined with pioglitazone treatment (white colums). Silencing of RIP140 strongly increased BACE1 promoter activity (blue colum). (n=3 with 3 biological samples per group for RIP140 overexpression and RIP140 silencing. Values shown in graphs represent the mean value ±SEM and are expressed as a fold change in comparison to the normalized control. Statistical analysis included one-way ANOVA with a post Tukey test, *P<0.05, **P<0.01,***P<0.001). 123

5.1 Localization of RIP140 in the mouse brain. In situ hybridization, using specific primer designed to detect the RIP140 transcript exhibited specific RIP140 labeling within the hippocampus area (C) on sagittal (A and C) and coronal (B) brain sections of wild-type mice. The cerebellum and olfactory bulb also showed enhanced RIP140 labeling throughout the sections for cerebellum and more inside the brain for the olfactory bulb and frontal cortex area. (Images A and C taken from: http://mouse.brain-map.org, Image B: courtesy of Dr. Jenny Steel, Imperial College London) 129

5.2 LacZ staining of RIP140 deficient mice. Mice lacking RIP140 had the gene replaced by a LacZ gene. β-Galactosidase staining shows where LacZ is expressed in the RIP140 ko brain serving as an indirect marker with expression in the dentate gyrus and cerebral cortex and highest in the hippocampus. Image is the courtesy of Dr. Jenny Steel. 130

5.3 RT2 Profiler qPCR array. A Qiagen Alzheimer's Disease qPCR profiler array specific for mouse was used to screen a wide range of genes, implicated in AD in RIP140 knockout mice. Hippocampus mRNA samples of 2 young (2 months) knock out and wild-type mice were analysed and expression differences are expressed in fold change to the baseline 1. Green arrows highlight genes exhibiting overexpression and have been selected for further analyses. Red arrows show genes down-regulated and have been selected for further analyses. (n=2, no statistical analyses on n of 2) 132

5.4 Validation of the qPCR values of the array with new primers. The same samples used in the array (Fig. 5.3) were used for further confirmation by qPCR using self-designed primer of the selected genes. Additionally, genes known to be direct targets of RIP140 were examined as well, including CIDEA, ESRR-γ, PDK4, PGC-1alpha and PPAR-α. Wild-types (white bars) have been plotted next to ko samples (black bars) for each gene. Effects observed on some genes remained the same as in the array, such as strong up-regulations in IgF2 and Mtap1, slight up-regulation of cdk5 and down-regulation of IDE. Contrary to the array data, BACE1 and GsK3 appeared down-regulated. None of the target genes of RIP140 showed any strong response to the knockout of it. The n= number remains the same as in the array above (2) and therefor no statistical analyses could have been performed 134

5.5 Protein homogenates and mRNA extracts of two brain areas and mouse lines were studied. A mouse line lacking (knockout) RIP140 and its corresponding wild-type strain (black) were studied using hippocampus (blue) and frontal cortex (green) areas of each animal. Dissections of hippocampus and frontal cortex areas of the right hemisphere were used to extract RNA for subsequent mRNA analyses via qPCR and left hemisphere dissections were lysed to produce protein homogenates for subsequent analyses of protein expression level via Western blot. 136

5.6 BACE1 and BACE2 mRNA expression. RNA preparations of 9 months old RIP140 null mice hippocampus and frontal cortex were analysed for changes in BACE1 and BACE2 mRNA expression. Mice lacking RIP140 in the Hippocampus showed a significant increase in BACE1 mRNA level in comparison to wild-type animals (A) and a mild but non-significant increase in BACE2 mRNA expression in the same area (B). Expression level of BACE1 and 2 mRNA in the frontal cortex region appeared to be unchanged (C+D).). (n=4 for RIP140 null mice and n=4 of corresponding wild-type. Values shown in graphs represent the mean value ±SEM and are expressed as a fold change in comparison to the normalized wild-type control. Statistical analysis included students t-test *P<0.05). 138

5.7 Western Blot analyses for BACE1 protein level. Protein expression of BACE1 in RIP140 null mice in Hippocampus and frontal cortex area showed no changes in comparison to matching wild-type expression (A+B). BACE1 expression was normalized to β-actin level. (n=4, RIP140 mice and n=5 matching wild-type animals for hippocampus, n=4 RIP140 null mice and matching wild-type for frontal cortex. Values shown in graphs represent the mean value ±SEM and are expressed as a fold change in comparison to the normalized wild-type control. Statistical analysis included student's t-test) 139

5.8 Endogenous level of the two Aβ species of 40 and 42 amino acids in RIP140 mice. ELISA assays with antibodies against either Aβ42 (A+C) or Aβ40 (B+D) were used to evaluate these species in brain lysates from hippocampus (A+B) and frontal cortex (C+D) of RIP140 knockout and wild-type mice. Comparison of RIP140 ko mice revealed no significant differences in either Aβ40 or 42 level and no changes in the ratio of Aβ42 to Aβ40 (D+E). (n= 3 for both wild-type and RIP140 ko. Values shown in graphs represent the mean value ±SEM and are expressed as a picogram per μL. Statistical analysis included student's t-test). 142

5.9 Neprilysin and IDE expression in RIP140 knockout mice. mRNA samples from hippocampus and frontal cortex obtained from 9 months old RIP140 null mice were analysed for changes in Neprilysin and IDE mRNA ex- pression. Mice lacking RIP140 in the Hippocampus showed a decrease in Neprilysin mRNA level in comparison to wild-type animals (A). IDE hippocampal mRNA expression remained unchanged (B).Expression level of Neprilysin and IDE mRNA in the frontal cortex region appeared to be unchanged (C+E). (n=4 for RIP140 null mice and n=4 of corresponding wild-type). Values shown in graphs represent the mean value ±SEM and are expressed as a fold change in comparison to the normalized wild-type control. Statistical analysis included student's t-test). 144

5.10 Western Blot analyses for Neprilysin and IDE protein level. Protein expression of Neprilysin in RIP140 null mice showed a roughly 20% decrease in comparison to matching wiltype expression in the frontal cortex area (B) but not in the hippocampus (A). IDE protein expression was unchanged in the hippocampus (A).Neprilysin and IDE expression were normalized to Actin level. (n=5, RIP140 mice and matching wiltype animals for both, hippocampus and frontal cortex. Values shown in graphs represent the mean value ±SEM and are expressed as a fold change in comparison to the normalized wiltype control. Statistical analysis included students t-test) 146

5.11 ApoE mRNA and protein expression in RIP140 ko mice. ApoE mRNA levels are significantly decreased in the Hippocampus of RIP140 ko mice (A). Protein levels are unaltered in both Hippocampus (B) and frontal cortex(C). (n=4, RIP140ko mice and n=5 for matching wild-type animals for both, hippocampus and frontal cortex. Values shown in graphs represent the mean value ±SEM and are expressed as % of wild-type control. Statistical analysis included students t-test, *$p<0.05$) 148

5.12 IgF2 and GAP43 mRNA expression in RIP140 ko mice. RNA extractions in hippocampus and frontal cortex of 9 months old RIP140 null mice brain were analysed for changes in IgF2 and GAP43 mRNA expression. Mice lacking RIP140 in the Hippocampus showed a non-significant decrease in IgF2 mRNA level in comparison to wild-type animals(A) and a strong, significant increase of GAP43 mRNA expression in the same area (B). Expression level of IgF2 and GAP43 mRNA in the frontal cortex region appeared to be unchanged (n=4, RIP140 mice and n=5 matching wild-type animals for hippocampus, n=4 RIP140 null mice and matching wild-type for frontal cortex). Values shown in graphs represent the mean value ±SEM and are expressed as a fold change in comparison to the normalized wild-type control. Statistical analysis included student's t-test **p<0.01). 150

5.13 MAP2 and CDK5 mRNA expression. RNA preparations of hippocampus and frontal cortex from 9 months old RIP140 null mice were checked for changes in MAP2 and CDK5 mRNA expression. Mice lacking RIP140 in the hippocampus showed a significant increase in MAP2 (A) and cdK5 (B) mRNA level in comparison to wild-type animals but no differences for these genes were observed in the frontal cortex (C,D). (MAP2: n=4 for ko animals and n=2 for matching wt. cdK5: n=4 for ko animals and n=3 for matching wt. Values shown in graphs represent the mean value ±SEM and are expressed as a fold change in comparison to the normalized wild-type control. Statistical analysis included students t-test **p=0.01, ***p=0.001) 152

5.14 GSK3β mRNA expression. GSK3β mRNA seemed increased in the hippocampus and frontal cortex, however not significant in either case (A+B). GSK3β: n=4 for ko and wt animals. Values shown in graphs represent the mean value ±SEM and are expressed as a fold change in comparison to the normalized wild-type control. Statistical analysis included student's t-test. 154

5.15 GSK3 protein expression in RIP140 knockout mice. Representative Western blot and quantification of different GSK3 subtypes (α and β) and phosphorylated GSK. No significant changes were observed for pGSK3 in cortex and hippocampus of RIP140 knockout mice(A, B). GSK3α was higher in the frontal cortex of RIP140 ko mice (E) but not the Hippocampus (C). GSK3β was up regulated in the Hippocampus (D) and frontal cortex (F) of RIP140 ko mice. (n=5, RIP140 mice and matching wild-type animals for both, hippocampus and frontal cortex). Values shown in graphs represent the mean value ±SEM and are expressed as % of wild-type control. Statistical analysis included student's t-test. *p<0.05, **p<0.01). 156

5.16 Comparison between the distribution of all plaques and IL-6 positive plaques. Plaques were measured according to the morphology in the brains of AD patients. More than 50% of plaques have characteristic neurotic signs (left). More than 70% of all plaques are diffuse plaques (right). Taken and modified from Hul et al, 1996. 158

5.17 ELISA assays for interleukin expression. Homogenates of hippocampus and frontal cortex were tested with an ELISA IL-1β or IL-6 immuno kit and level of IL-1β or IL-6 were compared between RIP140 ko and wiltype animals. There was no difference in the hippocaompus for either IL-1β or IL-6 (A+B). IL-1β showed a increase in the frontal cortex of RIP140 ko animals in comparison to wild-type animals, just below significance (C). IL-6 level also appeared to be increased in frontal cortex of RIP140 ko animals however there was a low n number and high variabilty and the changes were not significant (D). (IL-1β Hippocampus: n=4 for wt and ko animals, frontal cortex:n=3 for wt and ko animals. IL-6 Hippocampus:n=3 tg animals and n=4 for matching wt, frontal cortex: n= 2 tg animals and n=4 for matching wt. Statistical analyses included studnets t-test). 158

5.18 Microglial activation in RIP140 ko brain sections. Sections of 40μMwere prepared and immunohistochemistry using a stain against IBA1 was performed to detect activated microglia cells. Areas of Hippocampus (A, C) and Cortex (B, D) were quantified, but none of them revealed a significant difference. Values shown in graphs represent the mean value ±SEM and are expressed as % area of wild-type control. Statistical analysis included student's t-test. Staining, quantification and analyses were performed by Mr. David Morrow). 160

5.19 Astrocyte activation in RIP140 knockout brain sections. Immunohistochemistry was performed on fixed 40μMbrain sections using an anti GFAP antibody. Hippocampi of RIP140 KO mice exhibit higher level of reactive astrocytes (A). No changes were seen in the cortex (B). Values shown in graphs represent the mean value ±SEM and are expressed as % area of wild-type control. Statistical analysis included student's t-test. *p<0.05. Staining, quantification and analyses were performed by Mr. David Morrow). 162

5.20 Brain dissections stained with NeuN antibody. Fixed sections were stained with a NeuN antibody to determine neuronal density. Each hemisphere was cut into 40μMsections and layers that started to show the Hippocampus (A,1) were used. We quantified the density of neurons in Subiculum, CA1, CA3 and dentate Gyrus (B), quantification of neuronal density was done either using a cell count tool (CA3 region) or the intensity per μM square meter area was measured. The sub sectioning was performed according to the description of the Hippocampus by Ramon and Cajal (C). 164

5.21 Neuronal density in the brains of RIP140 ko mice. The hippocampal sub regions CA1 (A), Dentate Gyrus (B), CA3 (C) and Subiculum (D) did not show any changes in neuronal density or cell number in RIP140 mice in comparison to wild-types. No differences were observed in the Cortex region (E). Values shown in graphs represent the mean value ±SEM and are expressed as % Area of wild-type control. Statistical analysis included student's t-test. Quantification and analyses were performed by Mr. David Morrow). 165

6.1 Legend for brain areas and mouse lines studied in the follwoing chapter. A mouse line overexpressing (transgenic (tg)) and its corresponding wiltype strain (white) were studied using hippocampus (orange) and frontal cortex (red) areas. 174

6.2 BACE1 and BACE2 mRNA expression levels in RIP140 Tg mice. Evaluation of expression level of, BACE1 and BACE12 in hippocampus (A-B) and frontal cortex areas of RIP140 Tg mice (C-D). RIP140 transgenic mice showed mild but not statistical significant reductions of BACE 1 and BACE2 in cortex but no changes in the hippocampus (A, B).(BACE1: n=5 for tg animals and n=3 for matching wt. BACE2: n=5 for tg animals and n=3 for matching wt.). Values shown in graphs represent the mean value ±SEM and are expressed as in fold change of control. Statistical analysis included student's t-test, * p<0.05). 176

6.3 BACE1 Protein expression in RIP140 transgenic mice. BACE1 protein levels were found significantly reduced in RIP140 transgenic mice in the frontal cortex area (B), but no effect was observed in the hippocampus of the same animals (A). (Hippocampus: n=4 for Tg animals and corresponding n=5 wt, n=3 for tg animal and corresponding wt n=4; frontal cortex: n=4 for Tg animal and corresponding wt, n=3 for tg animals and corresponding wt). Values shown in graphs represent the mean value ±SEM and are expressed as in fold change of control. Statistical analysis included students t-test, **p< 0.001). 177

6.4 ELISA of endogenous Aβ40 and Aβ42 in RIP140 transgenic mice. Whole brain lysates were loaded on an ELISA plate to detect Aβ40 and Aβ42 in hippocampus and frontal cortex of a RIP140 transgenic mouse line. The reduction in Aβ42 level observed in cells overexpressing RIP140 could not be validated in the hippocampus (A) and frontal cortex (C) of RIP140 transgenic mice. No changes were also observed for Aβ40 in both brain regions(B, D) and subsequently, no differences in the Aβ40/Aβ42 ratio were detected (E,F). (n=3 for tg animal and corresponding wt). Values shown in graphs represent the mean value ±SEM and are expressed as in pico gram per milliliter of control. Statistical analysis included student's t-test. 179

6.5 Neprilysin and IDE mRNA expression level in RIP140 tg mice. Evaluation of expression level of Neprilysin and IDE in Hippocampus (A,B) and frontal cortex areas (C,D) of RIP140 tg. Neprilysin expression appeared slightly higher in the hippocampus of mice overexpressing RIP140 (A) as well as IDE expression (B). Neprilysin seemed higher in the frontal cortex but not statistically significant due to high variability in the wt group (C). No changes were observed for IDE in the frontal cortex area (D).(NEP: n=5 for tg animal and n=3 corresponding wt, IDE: n=5 tg and n=3 wt animals). Values shown in graphs represent the mean value ±SEM and are expressed as in fold change of control. Statistical analysis included student's t-test). 181

6.6 Neprylisin and IDE protein expression in RIP140 transgenic mice. Neprilysin protein levels were unchanged in the hippocampus (A) and frontal cortex (B) of RIP140 Tg mice compared to WTs. IDE protein level of RIP140 tg animals were also unchanged in comparison to wt animals in the hippocampus (A) and frontal cortex (B). (Hippocam- pus: n=5; frontal cortex: n=5.) Values shown in graphs represent the mean value ±SEM and are expressed as in % change of control. Statistical analysis included student's t-test). 183

6.8 IgF2 and GAP43 mRNA expression level in RIP140 transgenic mice. Evaluation of expression level of IgF2 and GAP43 in hippocampus (A,B) and frontal cortex areas (C,D) of RIP140 tg. IgF2 expression appeared higher in the hippocampus of mice overexpressing RIP140 reaching a p value of 0.08, there for remaining insignificant (A). GAP43 expression appeared higher but not statistically increased than wt expression level (B). IgF2 seemed higher in the frontal cortex but not statistically significant due to high variability (C) GAP43 expression is increased in the frontal cortex area, although did not reach significance (D) .(IgF2: n=4 for tg animals and n=3 corresponding wt, GAP43: n=3 tg and wt animals). Values shown in graphs represent the mean value ±SEM and are expressed as in fold change of control. Statistical analysis included student's t-test *p<0.05). 186

6.9 MAP2 and CDK5 expression level. MAP2 was up regulated in the Hippocampus (A) but decreased in the frontal cortex (C). CDK5 level were higher in the Hippocampus but unchanged in the frontal cortex (B,D).(CDK5 : n=5 for tg animal and n=3 corresponding wt, MAP2: n=3 tg animals and matching wt). Values shown in graphs represent the mean value ±SEM and are expressed as in fold change of control. Statistical analysis included students t-test, *p<0.05, **p<0.01). 188

6.10 GSK3β mRNA expression level. GSK3β expression level were unaltered in both Hippocampus (E) and frontal cortex (G), (n=5 for tg animal and n=3 corresponding wt, Mtap2: n=3 tg animals and matching wt). Values shown in graphs represent the mean value ±SEM and are expressed as in fold change of control. Statistical analysis included student's t-test. 189

6.11 GSK3 protein expression in RIP140 transgenic mice. Representative western blot and quantification of different GSK3 subtypes (α and β) and phosphorylated GSK3 protein levels in Rip140 transgenic. a 50% decrease was observed for pGSK3 in the Hippocampus (A) but no changes of pGSK3 in the frontal cortex (B) of RIP140 tg mice. GSK3α was reduced but not significantly in the frontal cortex of RIP140 ko mice (E) and the Hippocampus (C). GSK3β was unchanged in the Hippocampus (D) and frontal cortex (F) of RIP140 ko mice. (n=5, RIP140 mice and matching wild-type animals for both, hippocampus and frontal cortex). Values shown in graphs represent the mean value ±SEM and are expressed as % of wild-type control. Statistical analysis included student's t-test. *p<0.05). 191

6.12 ELISA assays for cytokine expression in RIP140 transgenic. Homogenates of hippocampus and frontal cortex were by ELISA for IL-1β or IL-6 and levels of IL-1β or IL-6 were compared between RIP140 transgenic and wild-type animals. c IL-1β levels were reduced in the hippocampus of RIP140 Tg mice (A) but not in cortex (C). However, IL-6 were found unchanged between the different strains (B) (IL-1β and IL-6: n=4 for tg animals and =3 for matching wt. Statistical analyses included student's t-test *p<0.05). 192

6.13 Microglial activation in RIP140 tg brain sections. Sections of 40μMwere stained using an antibody against IBA1 to detect activated microglia cells. Areas of Hippocampus (C) and Cortex (D) were quantified, but none of them revealed a significant difference. Values shown in graphs represent the mean value ±SEM and are expressed as % area of wild-type control. Statistical analysis included student's t-test. Staining, quantification and analyses were performed by Mr. David Morrow). 193

6.14 Astrocyte activation in RIP140 transgenic brain sections. Immunohistochemistry was performed on fixed 40μMbrain section using an anti GFAP antibody. No changes were seen in the Hippocampus (A) or Cortex (B). Values shown in graphs represent the mean value ±SEM and are expressed as % area of wild-type control. Statistical analysis included student's t-test. Staining, quantification and analyses were performed by Mr. David Morrow). 194

6.15 Neuronal density in RIP140 tg mice by NeuN staining. The hippocampal sub regions CA1 (A), CA3 (C) and Subiculum (D) did not show any changes in neuronal density or cell number in RIP140 mice in comparison to wild-types. An increase of neuronal cell density was observed in the dentate gyrus of RIP140 transgenic mice (B). No differences were observed in the Cortex region (E). Values shown in graphs represent the mean value ±SEM and are expressed as % area of wild-type control. Statistical analysis included student's t-test. *p<0.05. Quantification and analyses were performed by Mr. David Morrow). 196

6.7 ApoE mRNA and protein expression in RIP140 tg mice. ApoE mRNA levels are significantly increased in the Hippocampus of RIP140 tg mice (A) and unchanged in the frontal cortex (B). ApoE protein levels are unaltered in both Hippocampus (C) and frontal cortex (D) of RIP140 tg. (n=5, RIP140 tg mice and n=5 for matching wild-type animals for both, hippocampus and frontal cortex. Values shown in graphs represent the mean value ±SEM and are expressed as % of wild-type control. Statistical analysis included student's t-test, *p<0.05). 203

7.1 Proposed mechanism of RIP140 on APP processing. When activated by ligands, PPARγ will bind to a PPRE element in the BACE1 promoter and form a heterodimer complex with LXR (not shown) and repress BACE1 promoter activity. RIP140 co-activates by binding to PPARγ in a ligand dependent manner, repressing BACE1 promoter further and possibly increasing the stability of the complex. Consequently, less BACE1 mRNA will be transcribed leading to decreased expression of BACE1 protein. This results in a reduction of beta cleavage of APP, producing lower amounts of the toxic Aβ. 208

List of Tables

3.1 List of cDNA, shRNA and siRNA constructs used for transfections in various assays. 85

3.2 Compounds and Volumes to cast one 10%SDS Mini gel (Biorad), 1.5mm spacer and volumes for relating stacking gel. 90

3.3 Master mixes used for reverse transcription PCR. After the genomic DNA digestion, 4.5µL of the first Master mix, containing dNTPs and random Hexamers, were added to the DNAse treated RNA sample. After pre-annealing of the first master mix for 10 min at 70ºC in a thermocycler, 10µL of the second master mix containing the reverse transcriptase enzyme were added to each tube and reverse transcription was performed. 94

3.4 Master mix mixture for quantitive real time PCR. All volumes are shown for one reaction (1x) and the number was multiplied by the number of samples plus one for the negative control. 94

3.5 Cycling conditions for quantitive real time PCR 95

3.6 List of qPCR primer. The following primer was used to evaluate gene ex- pression of the indicated genes. Forward and reverse primer was designed with the NCBI primer design tool in 5'–> 3' direction. (http://www.ncbi.nlm.nih.gov/tools/primer- blast/index.cgi?ORGANISM=10090&INPUT_SEQUENCE=NM_173440

3.7 Master mix for genotyping PCR 101

3.8 Cycling conditions for genotying PCR. Master mix mixture for quantitive real time PCR. All volumes are shown for one reaction (1x) and the number was multiplied by the number of samples 102

5.1 List of selected genes potentially affected by RIP140. Initial analyses of the qPCR array revealed changes in some genes that could be potentially regulated by RIP140 and they have a link to AD. Selected genes have been subdived into groups with similar context such as: APP processing, Aβ clearance, memory and cognition and Tau pathology. 9 genes have been selected form the initial array data and 2 more have been added that weren't present on the array, including: Mtap1 and Neprilysin. 135

LIST OF ABBREVIATIONS

Aβ- Amyloid-β

AD- Alzheimer's disease

ADAM-10- α-Secretase activity of the disintegrin metalloprotease-10

ADAM-17 -α-Secretase activity of the disintegrin metalloprotease-17

ADP- Adenosine diphosphate

AICD- APP intracellular domain

AMPK- Adenosine monophosphate activated kinase

ANOVA- Analysis of variance

APLP- APP like protein

Apoε- Apolipoprotein ε

APP- Amyloid precursor protein

ATP- Adenosine triphosphate

BACE1- β-site APP cleaving enzyme-1

BACE2- β-site APP cleaving enzyme-

BSA- Bovine seurm albumin

CDK5- Cycline-dependent kinase 5

cDNA- Copy DNA

ChIP- Chromatin immunoprecipitation

CNS- Central nervous system Cntrl- Control

Ct- Cycle threshold

CTD- C-terminal domain

CTFα/β/γ-C- terminal fragment α/β/γ

CSF- Cerebrospinal fluid

DAPT- N- [N-(3,5-difluorophenacetyl)-L-alanyl]-S-phenylglycine t-butyl ester

DAPI- 4',6-diamidino-2-phenylindole DISC1- Disrupted In schizophrenia-1

DMEM- Dulbecco's modified Eagle's medium

DMSO- Dimethyl sulfoxide DNA- Deoxynucleic acid

dNTP- Deoxyribonucleic triphosphate

D-PBS- Dulbecco's PBS

DS- Down's syndrome

ECL- Enhanced chemiluminescence

EOAD- Early-onset AD

ER- Endoplasmic reticulum

FAD- Familial AD

FBS-Foetal bovine serum

FCS- Foetal calf serum

FL-APP- Full length APP

G-418- Geneticin

GAPDH- Glyceraldehyde 3-phosphate dehydrogenase

GFP- Green fluorescent protein

GSK3- Glycogen synthase kinase-3

GWAS- Genome-wide associated study

HCl- Hydrochloric

HEK- Human embryonic kidney hiN- Human induced neurons

HRP- Horseradish peroxidase protein

ICC- Immunocytochemistry

IDE- Insulin degrading enzyme

IgF- Insulin like growth factor

IL- Interleukin

IHC- Immunohistochemistry

IP- Immunoprecipitation

kDa- kilodalton

LB- Luria Bertani

LOAD- Late-onset AD

LTD- Long-term depression

LTP- Long-term potentiation

MAPK- Mitogen-activated protein kinase

Mtap- Microtubule associated protein

MCI- Mild cognitive impairment

miRNA- micro RNA

MMSE- Mini-mental state-examination

MRI- Magnetic resonance imaging

mRNA- messenger RNA

MTA- Medial temporal atrophy

N2a- Neuroblastoma 2a 1

N2aSw- N2a-Swedish

NAD- Nicotinamide adenine dinucleotide

NeuN- Neuronal Nuclei marker

NFκB- Nulear factor κB

NFT- Neurofibrillary tangles

PBS- Phosphate-buffered saline

PCC- Pearson's correlation coefficient

PCR- Polymerase chain reaction

PDB- Phosphotyrosine-binding domain

PDZ- Postsynaptic density-95, Discs large, Zona occludens

PE- Phosphatidylethanolamine

PEN2- Presenilin enhancer-2

PFA- Paraformaldehyde PH- Pleckstrin homology

PGC-1α- Peroxisome proliferator-activated receptor gamma cofactor 1α

PPAR- Peroxisome proliferator-activated receptor

PPRE- PPAR resonse element

PSEN1- Presenilin-1

PVDF- Polyvinylidene fluoride

Opti-MEM- Optimum modified Eagle's medium

PCR- Polymerase chain reaction

qPCR- RT quantitative PCR

RIP140- Receptor interacting protein 140

RIPA- Radioimmunoprecipitation

ROI- Region of interest

RPM- Revolutions per minute

RNA- Ribonucleic acid

RNAi- RNA interference

RT- Reverse transcription

SAD- Sporadic AD

sAPPα/β- Soluble APPα/β

SDS- Sodium dodecyl sulfate

SDS-PAGE- SDS polyacrylamide gel electrophoresis

SEM- Standard error of mean

shRNA- small-hairpin RNA

siRNA- small-interfering RNA

TBST-Tris-buffered saline tween

TE- Tris-EDTA

Tm- Melting temperature

UTR- Untranslated region

WB- Western blotting

Chapter 1

Summary

1.1 Background

Alzheimer's Disease is currently affecting 750,000 people in the UK and predictions say that this number will quadruple by the year 2050 costing the health systems billions of pounds each year. The progression of the disease can be devastating for family, friends and caregivers and to date, there is no efficient cure and current treatments only help managing the symptoms. This is partially due to the lack of understanding of the ultimately causes of the disease and the mechanisms involved at the cellular level. Over the past decades, better understanding on the cellular and molecular pathways involved in the progression of the disease has emerged thanks to research, however many aspects of the disease still remain in the dark. One of the molecular pathways that has been recently involved in AD is the signaling cascade of the Nuclear factor PPARγ . PPARγ activation has been described to have beneficial effects on Aß pathology and neuro-inflammation, but little is known how PPARγ can be regulated. In this study we have investigated for the first time the role of the PPARγ co-factor RIP140in the brain, using in vitro approaches as well as genetically modified mice. The co-factor RIP140 has been shown to have co-activating or co-repressing functions for PPARγ.

Here we demonstrate that RIP140 overexpression leads to a reduction of BACE1 transcription, one of the main enzymes involved in Aß generation in AD, resulting in decreased Aß secretion. Additionally, we found that enzymes responsible for clearing up Aß are up regulated by RIP140 overexpression, further contributing to regulate Aß mediated neurotoxicity in AD. Apart of regulating the levels of Aß RIP140 also seems to affect key players involved in the

formation of neurofibrillary tangles, such as certain kinases.

This study also demonstrates the anti-inflammatory role of RIP140, thereby providing further support for RIP140 as potential target for AD.

Chapter 2

General Introduction

2.1 Losing yourself

[She sits on the bed with a helpless expression.]

"What is your name?"

"Auguste" "Surname?"

"Auguste."

"What is your husband's name?"

"I believe Auguste."

"Your husband?"

"I see, my husband. . . " [She looks as if not having understood the question.] she adds later: "I have lost myself, so to speak..." This interview marks the beginning of scientific investigation into what has become known as Alzheimer's disease. It was the examination of the case of Auguste D. during her suffering and after her death conducted by Alzheimer that would let him become eponymous for the disease. Alois Alzheimer recorded many conversations with Auguste Deter and the lines above are from the day of her admission into the psychiatric institution in Frankfurt, Germany. It is November the 26th 1901 when Alzheimer met his most famous patient for the very first time and whose case continuously fascinated him as he had never encountered someone with such symptoms before. The only 51 year old aaged woman's memory increasingly failed her; she seemed confused and anxious and although she spoke clearly and well articulated, she stopped in the middle of sentences as if she were lost or indecisive. She pronounced words in

a meaningless fashion or spelled them out letter by letter. She began having difficulties organizing the household and preparing food and started to get lost in familiar situations. Later on her behavior exhibited some unusual changes such as the fear of people she knew well and she became unusually jealous against her husband. At times she believed that someone wanted to kill her and she began to shout wildly (from the journals of Alois Alzheimer in which he describes the case of Auguste Deter. Parts published in: Current Biology "Alzheimer's discovery by Ralf Dahm, 2006).

Today we know that Alzheimer's disease (AD) is a type of dementia which symptoms varies in severity and onset. AD cause problems with thinking, remembering and behavior and it becomes worse over time. In its early stages the memory loss is mild and it's hard to give a clear diagnosis for AD. Currently AD is been subdivided into different stages ranging from 1 -7 (according to Alzheimer Association, www.alz.org), exhibiting symptoms of stronger severity within the higher stages.

2.2 Alois Alzheimer

A talk given on November the 3rd in 1906 on a patient who showed symptoms of reduced comprehension and memory, disorientation, unpredictable behavior, paranoia, hallucinations and psychological impairment marked the very first description of a form of dementia. It was a young Doctor lecturing in Tübingen, Germany who presented that day his findings on studying his late patient Auguste Deter and giving the disease the name which is carried on into present days: Alois Alzheimer ((Fig. 2.1 taken from Ralf Dahm, 2006).

Alois Alzheimer was born on June 14th 1864 in Markbreit near Würzburg, Germany. He studied medicine in Berlin, Tübingen and Würzberg where worked on his doctoral thesis in 1877. In 1888 he moved to Frankfurt to work as assistant physician in the psychiatric institution at the hospital for mentally ill and epileptics and was soon promoted to the position of senior physician. It is the same place where he had his first encounters with Auguste D. and interviewed her systemically over the following years. A year later, he met Frank Nissl, now famous for his neuronal staining method and who taught Alzheimer his histo pathological techniques to study neurodegenerative disorders in which Alzheimer has previously gained increased interest in. After 14 years, Alzheimer moved to Munich to join Emil Kraeplin at the Royal Psychatric Clinic, who was one of the leading psychiatrist that time and Alzheimer himself was joined in his work by now famous scientist such as Friedrich H. Lewy, who discovered the his name bearing Lewy bodies, and Hans-Gerhard Creutzfeld and Alfons Maria Jakob, both discoverer of the Creutzfeld-Jakop disease. When Auguste Deter died on April 8th in 1906 at the age of only 56, Alzheimer examined the pathology onside her brain

and described for the first time the most famous pathological hallmarks of the Disease, which are till today subject of study in many Alzheimer's Disease research laboratories. Not only was Auguste Deter's brain highly atrophic, it also showed fibril like structures, remaining inside the neuronal cells and further unidentified plaques throughout the cerebral cortex. The description of these structures by Alzheimer's lead to ongoing years of research and the formation hypothesis of the neurofibrillary Tau tangles and the amyloid beta plaques two of the main characteristic of Alzheimer's Disease.

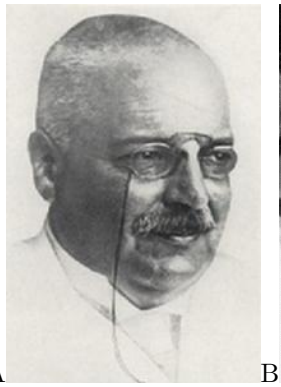
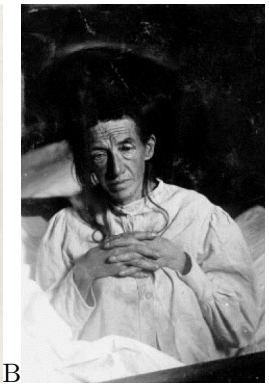
A  B 

Figure 2.1: Alois Alzheimer (A) and his first, most famous patient Auguste Deter (B). The study and post mortem examanitation of the brain of Auguste Deter, who developed at the age of 51 years unusual symptoms of dementia, made Alois Alzheimer famous for the first description of the disease which is till today named Alzheimer's Disease after him.

2.3 The global challenge

Dementia is one of the greatest challenges of our time, with 44 million cases worldwide, a number expected to triple by 2050 as a result of rapid population aging. Dementia affects approximately 820,000 cases in the UK and half of them are diagnosed with Alzheimer's disease (AD), which forms globally the most prevalent neurodegenerative disease (Alzheimer's Society and Alzheimer's Research Trust website). The number of affected people cost national health services already £24 billion per year (Lewis et al., 2014; The Trajectory of Dementia in the UK – Making a Difference, report produced by OHE for Alzheimer's Research UK). Globally it is estimated that dementia costs the economy over £360 billion each year (Wimo A, Prince M. World Alzheimer Report 2010: the global economic impact of dementia. London: Alzheimer's Disease International (ADI), September 2010).

Even though AD develops different in every individual case, there are common symptoms such as impairments

in memory and cognitive functions resulting from the neuronal loss in cortical and hippocampal areas in the brain (Frolich, 2002). AD is categorized as a neurodegenerative disorder which progresses as a dementia. There is an ongoing debate on the relative contributions of Aβ and Tau to neurodegeneration associated with AD, the lesions that Alois Alzheimer described when he examined the brain of his first patient Auguste D. Aβ are small peptides which are forming extracellular neuritic plaques and they are produced by the proteolytic cleavage of the larger amyloid precursor protein (APP) (Selkoe et al., 2003). AD brains also display intracellular neurofibrillary tangles (NFT) produced by hyper phosphorylation of the microtubule-associated protein Tau. To date, there is no known cure for AD and global studies have been conducted to investigate prevention or delay of the disease. Life style factors, such as exercise, diet and nutrition, cardiovascular risk and intellectual activities have been proposed to increase the risk for a population to develop AD, but further clinical trials will have to provide more evidence in order to make a more accurate statement if these factors can actually help to prevent or delay the onset of AD (Flicker et al., 2010).

2.4 A closer look at Alzheimer's Disease: from symptoms and diagnosis to the molecular basics

2.4.1 Symptoms and Diagnosis

The first symptoms of AD start with slow progression of memory, orientation and attention impairments. Through the progression of the disease patients will loose more and more of their independence and will eventually require 24 hours care (NHS websites). At the very early stages, the person may already feel as if he or she is having memory lapses, such as forgetting familiar words or the location of everyday objects. During the progression of mild cognitive decline problems like coming up with the right word or names of familiar objects or people will occur as well the capability to remember new names of recently introduced persons. This is accompanied by increasing difficulties to perform tasks in social or work settings and troubles with planning complex events such a dinner. Very often at this stage, people loose or misplace valuable objects. As the disease progresses towards a more severe cognitive decline, people get unable of recalling their own address or telephone number, or the high school or college they have graduated from. They can also be confused about where they are and what day it is. Finally when the disease has progressed to its latest stages, people will have lost awareness of recent experiences as well as of their surroundings. Help for dressing properly will be required as they make mistakes as putting on pyjamas during daytime or putting the left shoe on the right foot. They

experience changes in their sleep patterns and will have problems in controlling their bladder or bowels. Behavioral changes such as delusions and suspiciousness will occur. In the end people will need help with much of their daily life including eating or using the toilet as the muscles will have grown rigid and their swallowing will be impaired. All of their reflexes will act abnormal and eventually the disease is leading to the patients' death (Alzheimer's Society and NHS websites).Symptoms of AD vary with the stage and progression of the disease and may not always be easy to identify if the disease is only at early stages. Especially in the early stages of AD it is hard to distinguish between the disease and the normal, age related cognitive decline. The occurrence of different types of dementias has also to be considered before making determined conclusions about a diagnosis and possible related treatment as not all dementias progress on a molecular basis in the same way but can exhibit similar symptoms. Around 60-80% of dementia patients will actually have AD, 10-20% will be caused by front temporal dementia (FTD), vascular dementia and dementia with Lewy bodies (Holtzman et al., 2011; Barker et al., 2002). Current diagnosis mainly starts with the analysis of the patient's history and personality changes with help from caregivers as the affected person is often unaware of his or her condition and family and friends can provide important information about the daily living abilities and the decrease over time of the patient's mental function. To evaluate cognitive impairments, neuropsychological test such as the mini-mental state examination (MMSE) can be performed but more comprehensive tests are necessary for a higher reliability, especially in the early stages of disease. At advanced stages, atrophies, hypo metabolism and lower blood flow in certain brain regions can be detected using computational tomography (CT) or magnet resonance tomography (MRT) (Jack et al., 1998, Scheltens et al., 2002, Wahlund et al., 2000, Patwardhan et al., 2004). Figure 2.2 shows an atrophic brain (left) in comparison to a normal, healthy brain (right).

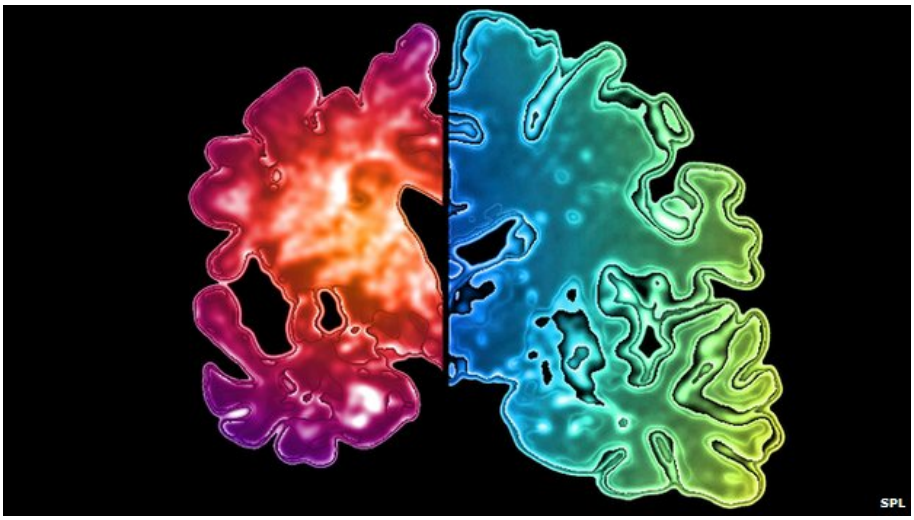


Figure 2.2: Coronal brain scan, comparing a healthy (right, blue) and atrophic (left, red) brain. In cases of Alzheimer's disease, there is an associated loss of brain tissue. Examination of brains of presenile onset reveal obvious differences of the weight of the brain in comparisons with age matched, healthy control people (taken from BBC website, article about AD (http://www.bbc.com/news/health-33617141))

The loss of brain function appears gradually and the first section of the brain starting deteriorating is often the part that controls the memory and speech functions. However, one of the main priorities of dementia research is identifying patients much earlier as currently possible. Within a decade of research, 99.6% of the trials trying to prevent or reversing the symptoms have failed and this failure is thought to be down to treating patients when it is already too late as the symptoms appear as late 10 years after the onset of the disease. Some of the most current research with the aim to identify an early blood marker may have detected such early signs for Alzheimer's disease. With an 87% accuracy they were able to predict if a patient with a mild cognitive impairment would develop AD within the next 12 months (Hye et al. 2014). In total the group has identified 10 different proteins that can predict the conversion into AD.

2.4.2 Neuropatholgy

Since Alois Alzheimer first pointed out the two primary structures, neurofibrillary tangles and amyloid β (Aβ) plaques, a lot has been added to the understanding of the pathology of the disease. Aβ are small peptides, which are forming extracellular neuritic plaques, and they are produced by the proteolytic cleavage of the larger amyloid precursor protein APP . Neurofibrillary tangles are produced by hyper phosphorylation of the microtubule-associated protein Tau (Fig.2.3

). The occurrence of pathological hallmarks during the disease progression is shown in figure 2.4

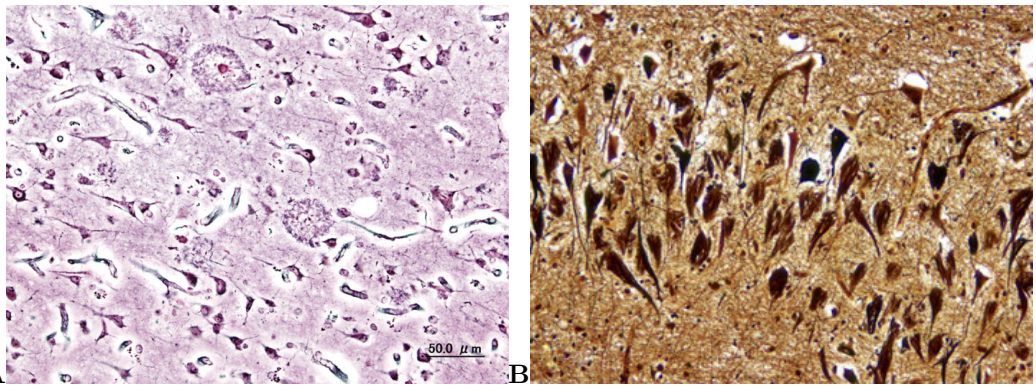


Figure 2.3: Silver impregnation of the two main pathological hallmarks of Alzheimer's Disease. A is showing Amyloid ß deposition in the form of radial structured plaques that accumulate extracellular. B: Formation of intracellular neurofibrillary Tau tangles with their typical pyramidal shape (taken from Wikipedia.co.uk).

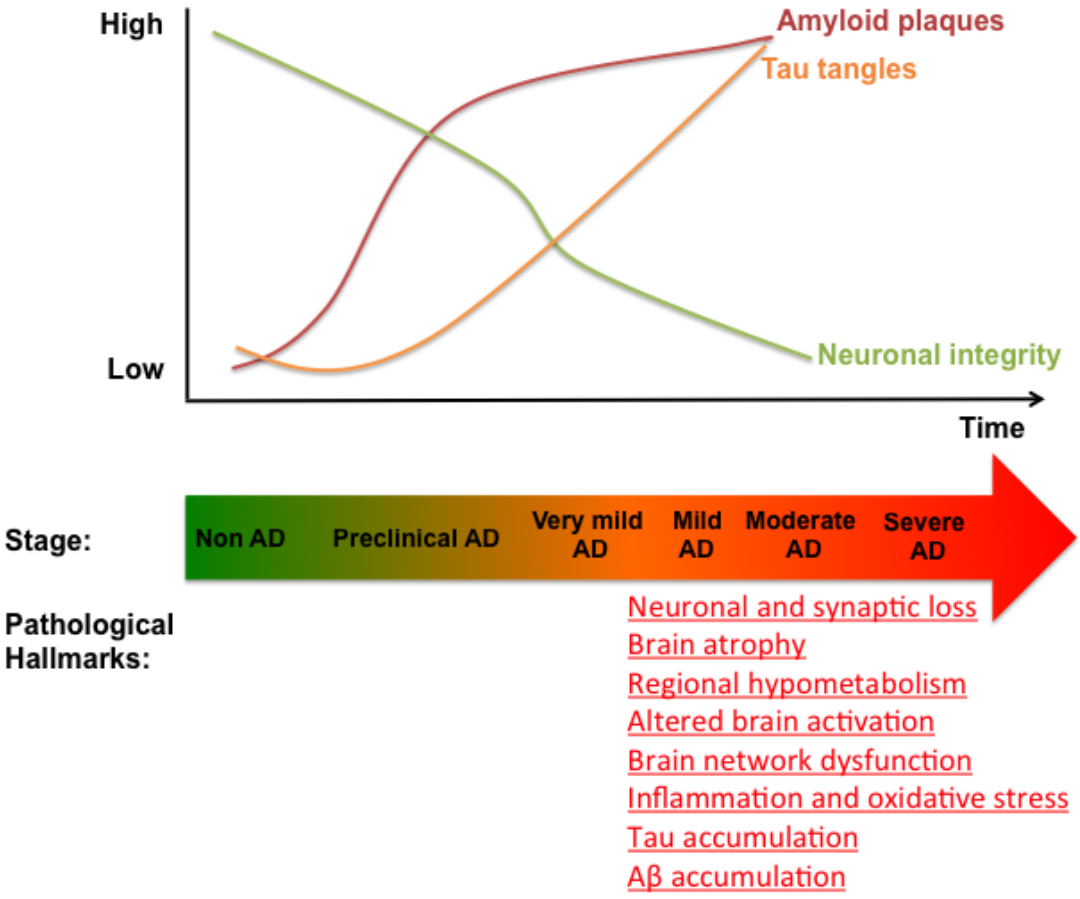


Figure 2.4: Progression and stages of Alzheimer's Disease with correlating pathological hallmarks. As the disease prgogresses to more severe stages, Amyloid β plaques as well as neurofibrillary tangles will accumulate causing a decline in neuronal integrity leading to cell death followed by neuronal and synaptic loss (Modified from Holztmann et al., 2011).

2.4.2.1 Senile amyloid β plaques

The composition of Aβ plaques mainly contains extracellular aggregates of 39-43 amino acids long Aβ, forming peptides with a total size total size of 4kD (Masters et al., 1985). Although five different forms can be generated from the cleavage of APP, Aβ plaques have been shown to be predominantly composed of Aβ42 (Wolfe et al., 2007).

The native 4kD monomers are due to their high content in α-helix secondary structure soluble cellular proteins but can convert into the pathogenic β-sheet rich isoform which is able to self-assemble to oligomers and eventually leading

to the formation of protofibrils, followed by aggregation to amyloid fibrils (Sunde et al.,1997). In the healthy brain, some unidentified chaperone proteins may prevent the aggregation of Aβ monomers.

The discoveries of the secondary structure as a β-pleated sheet conformation lead to the name Aβ (Masters et al., 1985; Beyrether et al., 1990). The beta sheet conformation allows binding to the Congo red dye causing birefringence when illuminated by polarized light, which confirms the classical, histopathological definition of an amyloid. There are truncated forms of Aβ that are more toxic than the Aβ42. These forms were described recently as pyro glutamate-modified amyloid-β (Aβ(pE3)) peptides (Jawhar et al., 2011). The structure of the senile, neuritic Aβ plaques is arranged into a core of the 4kD peptides, in a radial pattern. These round Aβ 4kD cores are surrounded by abnormally shaped or dystrophic neurons or their processes such as dendrites or axons, which can be stained with the same silver impregnation like the one to identify Tau tangles. At the periphery, reactive astrocytes and immune cells of the central nervous system (CNS), the microglia, will surround the plaque, possibly leading to an inflammatory reaction or the release of inflammatory mediators. The microglia cells also have the ability to phagocytize Aβ fibrils but not oligomers (Xiao-dong et al., 2010) which could mean that Aβ oligomers induce a potent inflammatory response, disturbing phagocytosis and clearance of Aβ fibrils by the microglia and thereby contributing to an initial neurodegenerative characteristic of AD (Xiao-dong et al., 2010). The following toxicity causes disintegration of dendrites and axons as well synaptic dysfunction leading to cell death and neuronal loss.

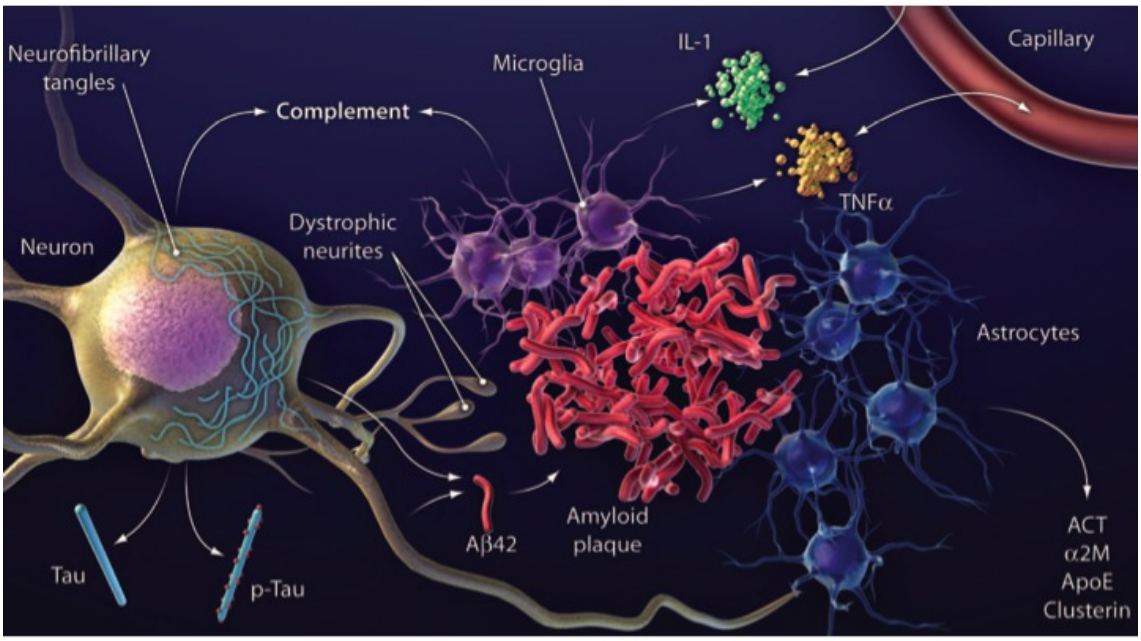


Figure 2.5: Amyloid plaque deposition and their impact on a cellular level. Aβ42 generated inside the neurons gets transported to the extracellular space where it eventually oligomerises with further peptides of its kind. These cores of Aβ are surrounded by dystrophic dendrites of the neuron and microglia and reactive astrocytes in the periphery. Activated Microglia trying to clear the peptides will surround the accumulation in a radial fashion and secrete pro-inflammatory factors during the the process. The composition of this entire structure is cummulative called amyloid plaque.

2.4.2.2 Neurofibrillary tau tangles

The other structure observed by Alzheimer was abnormal fibrous inclusion in the cytoplasm of neuronal cells, which will eventually form neurofibrillary tangles. The nature of these tangles has been extensively studied since their discovery in 1906 and a lot of knowledge about their structure has been gained. The tangles ultrastructure is build up by paired fibrils with a 10nm diameter wound in a helical shape with regular repeats of 80nm (Kidd, 1963; Wisniewski et al., 1976), this is why they also can be called paired helical filaments (PHF). PHFs main component is the hyper phosphorylated form of Tau proteins. The occurrence of these tangles appears when the phosphorylation status of the

Tau protein changes and is much higher than normally. The hyper phosphorylated Tau will start to pair with other Tau proteins, leading to fibrous structures (Goedert et al., 1991). The fibrous structures accumulate into tangles, which then leads to microtubule disintegration and collapse of the entire neuronal microtubule associated transport system (Iqbal, 2005). To this day, the presence of neurofibrillary tangles is required to make a pathological diagnosis for AD. The cellular scaffold or cytoskeleton is made up by microtubule structures and is important for the transport of other proteins and mRNA molecules within the cell, especially along the axon. Because of their function to associate with microtubule, Tau is also often called microtubule-associated protein (MAP or Mtap) and MAPs are mainly found in neurons but no other cell types, presumably due to the extensive axonal cell morphology that is required for synaptic transmission over vast distances. The stabilization of the cytoskeleton of these cell types is essential for their vitality and intracellular trafficking (Billingsley et al., 1997). However, Tau is not present in dendrites and mainly active within the axonal compartments. The stabilization of the microtubule system by Tau can be controlled in two ways, first by its phosphorylation status and secondly by different Tau isoforms. Alternative splicing of the microtubule associated Tau gene leads to six different isoforms (Goedert et al., 1988), which are different in their number of binding domains. Three isoforms have three binding domains and the remaining contain four. They are C-terminal located and exhibit a positive charge, which allows binding to the negatively charged microtubule. A knockout mouse model for Tau did not show any impact on the brain development possibly because the other Tau isoforms were able to compensate for the loss of one isoform as they may perform very similar functions (Harada et al., 1994). The longest Tau isoform contains 79 phosphorylation sites and normal Tau protein was reported to have phosphorylation's on 30 of these sites (Billingsley et al., 1997). Several kinases phosphorylate Tau, including cyclin dependent Kinase 5 (cDK5) and Glycogen synthase kinase 3 (GsK3). Both kinases may phosphorylate Tau in a either physiological or pathological manner. A study on cdK5 and GsK3 inhibition demonstrated that inhibition of these kinases leads to an increase on Aβ production (Ryder et al., 2003).

The distribution pattern of neurofibrillary tangles is AD appears to be stereotypical. Areas with high Tau tangle abundance are the CA1 and subicular regions of the hippocampus, layer II neurons of the entorhinal cortex, layers III, V and VI of the neocortex and the amygdala (Morrison et al., 1997). A correlation for strength and distribution of neurofibrillary tangles with the degree of AD dementia and duration of illness has been postulated (Hof et al., 1995; Arriagada et al., 1992). It should be kept in mind that also many other factors contribute to the pathology

2.4.2.3 GSK3 and Tau

GSK3 is a kinase that is important for the phosphorylation of Tau (Ishiguro et al,. 1988; Ishiguro et al., 1993), which has been confirmed through in vivo action of GSK3 on Tau (Hanger et al., 1992). It was further shown that there is a correlation between specific kinase sites of GSK3 within Tau and those found in pathological NFT in AD patients (Lovetsone et al., 1994). GSK3 knock in models revealed that they are able to generate Tau hyper phosphorylation, but sometimes not occurring until a relatively old age (Spittaels et al., 2000; Brownlees et al., 1997; Lucas et al., 2001). Interestingly this hyper phosphorylation was reversible through administration of a GSK3 inhibitor in double transgenic Tau knock-in mouse model (Engel et al., 2006).

GsK3 is a proline-directed serine/ threonine kinase with permanent activity. It is involved in various physiological processes including glycogen metabolism and gene transcription. Additionally, GsK3 has been linked to the pathology of AD in both familial and sporadic forms of the disease. This lead to the 'GsK3 hypothesis of AD,' which implies that GsK3 over activity is responsible for memory impairment, increased β-amyloid level, microglial inflammatory responses but also Tau hyper phosphorylation. Two genes of GsK3 exist, producing GsK3β and GSK3α and both versions are ubiquitously expressed but partially involved in different processes (Mukai et al.,2002; Schaffer et al.,2003). Both versions, GsK3β and GSK3α can lead to hyper phosphorylation of Tau. Only GSK3α knockout mice have been shown to be viable whereas GSK3β knockout mice die in utero (MacAulay et al. 2007; Hoeflich et al. 2000). GSK3 is negatively regulated by kinases that directly inhibit GSK3 by phosphorylating a regulatory N-terminal serine of GSK3 known as Ser9 (S9) of GSK3β (Jope and Johnson, 2004).

2.4.2.4 Regulation of GSK3

GSK3 is negatively regulated by kinases that directly inhibit GSK3 by phosphorylating a regulatory N-terminal serine of GSK3 known as Ser9 (S9) of GSK3β (Jope and Johnson, 2004). This regulation involves a number of pathways including insulin signaling through the PI3K/ Akt pathway (Sutherland et al., 1993). Other mechanisms include a tyrosine auto phosphorylation at the amino acid position Y216 (Lochhead et al., 2006) and a GSK3β specific serine-phosphorylation within the C-terminus (Thornton et al., 2008). This GSK3β specific regulation is mediated through the p38 MAPK axis.

One of GSK3s of its crucial regulatory role lies within the canonical Wnt cascade and serves as a perfect example for the various regulation mechanisms mentioned previously. The canonical Wnt cascade is vital for axis formation during

development and cell-fate determination In the resting state, a destruction complex made up of GSK3, casein kinase 1α (CK1α) (Liu et al., 2002), and the structural proteins, adenomatous polyposis coli (APC) and axin (Kishida et al., 1998), enable the sequestration of β-catenin leading to its phosphorylation. CK1 provides the primed phosphorylation on serine 45 (Amit et al., 2002) for the subsequent GSK3 phosphorylation on serine 33, 37 and 42 of β-catenin. These phospho-sites provide molecular cues for recognition from the ubiquitination mediator, β TrCP (Liu et al., 1999, Aberle et al., 1997) and its subsequent degradation through the 26S proteasome. Stimulation of the canonical Wnt cascade ultimately leads to the break up of this destruction complex and inactivation of GSK3. The stabilization of β-catenin leads to its translocation to the nucleus (Miller and Moon, 1997). Within this compartment, it partners with LEF/TCF transcription factors, which are usually repressed by Groucho (transcriptional repressor) and therefore up regulates the Wnt target genes (Behrens et al., 1996, van de Wetering et al., 1997). How this stabilization event occurs by stimulation of the Frizzled/LRP5/6 co-receptor complex is unknown but several mechanisms prevail. Despite this ambiguity, two key attributes provide clues.

As pharmacological inhibition of GSK3 perfectly mirrors stimulation of the canonical Wnt axis, GSK3 must be inactivated during Wnt stimulation (Wu and Pan, 2010). And secondly, the stimulated complex of Frizzled/LRP5/6 and the Wnt ligand must be internalized (Blitzer and Nusse, 2006, Yamamoto et al., 2006). This is usually associated with the sequestration of a protein called Dishevelled (Dsh) and axin from the destruction complex to the plasma membrane surrounding the receptor complex (Bilic et al., 2007, Zeng et al., 2008). Classically, Dsh was thought to inactivate GSK3 by is N-terminal phosphorylation (Fig. 2.6).

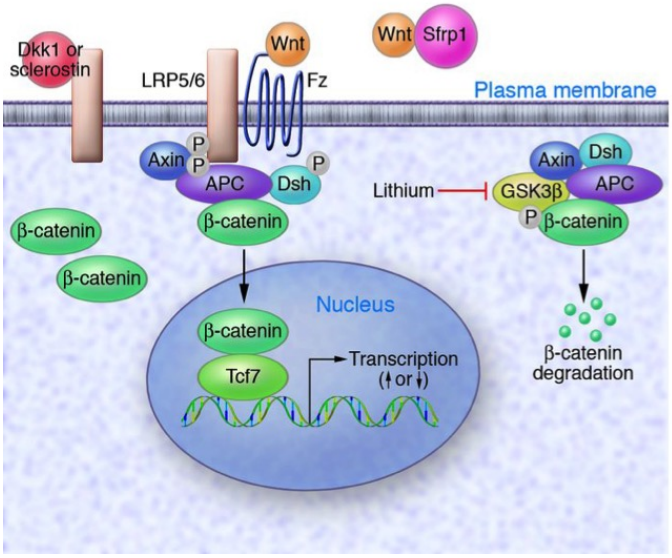


Figure 2.6: Canonical Wnt signaling leads to the stabilization of β -catenin and translocation to the nucleus, upon which it interacts with various LEF/TCF activators and the regulation of target genes.

2.4.3 CDK5 and Tau

Various studies were able to demonstrate how cdK5 is capable of phosphorylation of Tau epitopes that are of relevance in AD (Michel et al. 1998, Patrick et al. 1999, Alvarez et al. 2001, Lund et al. 2001, Gotz and Nitsch 2001, Bu et al. 2002, Hashiguchi et al. 2002 and Liu et al. 2002) and inhibition of cdK5 has been proven to reduce Tau phosphorylation and neuronal degeneration (Vincent et al., 2002). Another study described how overexpression of a cdK5 activator (p25) in mice is a key factor for Tau tangle formation in vivo (Noble et al. 2003). In the same study they found out that cdk5 activity is associated with increased Tau hyper phosphorylation and aggregation in mice overexpressing the Tau activator p25. Interestingly they also demonstrated how, not only cdK5 but also Gsk3 activity was increased in these p25 overexpressing mice, contributing to the Tau pathology and that GsK3 and cdK5 were co localized neurons (Noble et al., 2003).

Symptoms of AD and that include neurofibrillary tangles are not exclusively postulated for AD but other diseases as well, including post-encephalitic parkinsonism, posttraumatic dementia or dementia pugilistica, type C Niemann-Pick disease, progressive supranuclear palsy and amyotrophic lateral sclerosis/parkinsonism dementia complex of Guam. To date the occurrence of neurofibrillary Tau tangles remains unclear amongst all these diseases.

2.4.3.1 Neuroinflammation

Different mechanisms have been associated to drive neuroinflammation in the aging brain. In the case of AD it has been demonstrated that Aβ plaque occurrence is linked to microglial and astrocyte activation (McGeer et al., 1996). Because microglia are critical for Aβ phagocytosis, the microglial presence at the Aβ plaque can be interpreted as an attempt to clear this pathological deposit. Evidence for an important role of microglial phagocytosis comes from studies that show that restricting microglial Aβ uptake leads to increased cerebral Aβ levels (El Khoury et al., 2007; Lee and Landreth, 2010). However, once initiated, microglia can secrete pro-inflammatory cytokines, which may contribute independently to neuronal dysfunction and cell death. Inflammatory mediators may establish a self-perpetuating neurotoxic vicious cycle by increasing Aβ generation (Sastre et al., 2003, 2006). Therefore, in late stages of the disease, inflammation may be involved in creating further neurodegeneration.

Over the past decade, attention has been paid to the role of astrocyte activation during progression of neural pathologies and it has been suggested that these glial cells may also perpetuate the progression and severity of brain pathologies associated with chronic inflammation, such as diabetes (Nagayach et al, 2014) and AD (Akiyama et al, 2000). Astrocytes can release both pro- and anti-inflammatory factors, contributing crucially to inflammatory processes in the CNS.

2.4.3.2 Risk factors for AD

Additionally to the age of a person, various other risk factors associated to develop AD have been proposed. There are two types of risk factors. The first type includes the environmental factors (type two diabetes, brain trauma, history of vascular disease) and the second are genetic factors. The most famous genetic disposition to develop late-onset AD, suggested by a genome wide associated study (GWAS), is the APOE4 allele, which encodes Apoε4. The risk to develop AD for people carrying the APOE4 allele is increased by a factor of 3-5. Other genes associated with AD are familiar AD mutations, typical of early onset AD and that have been involved in the generation of Aβ, such as APP mutations.

2.4.4 The link between Alzheimer's disease and type 2 Diabetes

Alzheimer's Disease and metabolic disorders such as type 2 Diabetes seem to share common characteristics and various studies have shown that there is a higher risk of developing AD amongst people with type 2 diabetes (Arvanitakis et al., 2004, Leibson et al., 1997, Luchsinger et al., 2001 and Peila et al., 2002). The core defect in type 2 diabetes is insulin

resistance, which leads to hyper insulinemia as a compensatory response (Goldstein, 2002). Highest risk amongst diabetic patient to develop AD is for those carrying the Apo-ε4 allele. (Peila et al., 2002). Hyper insulinema has yet to be shown as a risk factor for AD in non-diabetic patients and also in patients lacking the (ApoE)-ε4 allele (Luchsinger et al., 2004), meaning that hyper insulinemia can independently of ApoE-ε4 increase the risk of AD. The fact that AD patients lacking ApoE-ε4 have higher fasting plasma insulin levels and that AD patients expressing ApoE-ε4 or normal individuals lacking ApoE-ε4 gives evidence for the peripheral insulin resistance in individuals with AD (Craft et al., 1998). These findings suggest that peripheral insulin resistance, in the absence of diabetes, may be sufficient to contribute to the development of AD in many cases.

Yet, it still remains unclear how peripheral insulin resistance can affect the brain in ways, which would be relevant to the pathology of AD. One idea is that insulin resistance could cause impaired insulin receptor signaling in neurons resulting in alterations in this signaling pathway. Studies in AD tissue and animals in which the insulin receptor signaling was inhibited in neurons lead to the proposal of neuronal insulin resistance as a model for sporadic AD (Hoyer et al., 2000). In fact, autopsies of AD patients versus control brains showed a strong decrease in insulin receptor mRNA levels in the hippocampus and frontal cortex (Steen et al., 2005). The same study showed also that mRNA levels of the Insulin like growth factor 2 were strongly decreased in AD cases (Steen et al., 2005). Diet-induced insulin resistance in the Tg2576 AD mouse model resulted in reduced neuronal insulin receptor signaling, increased Aβ levels as well as impairments in performance of the spatial water maze task (Ho et al, 2004). Additional studies in animals demonstrated that hippocampal and cortical insulin receptors are involved in synaptic plasticity, learning and memory (Zhao et al, 2004), suggesting that neuronal insulin resistance may play a part in the underlying mechanisms leading to cognitive dysfunctions in AD.

Another effect mediated by insulin levels is the up-regulation of IDE. As mentioned in the previous chapters, IDE degrades effectively monomeric Aβ but also insulin (Selkoe et al, 2001). It has been shown that IDE is up regulated by insulin in neuronal cells (Zhao et al, 2004).

and presenilin 1 and 2 mutations (Scheuner et al, 1996), which are typical of early onset AD cases.

2.4.5 Amyloid precursor protein (APP) processing

The proteolytic pathways causing Aβ generation from the amyloid precursor protein were well characterized by Selkoe in 2000. The membrane integrated APP protein is expressed in many tissues but more concentrated in the neuronal

synapses. It serves as the precursor molecule whose proteolysis generates Aβ ranging from 39-43 amino acids. The sequence is highly conserved (Sarkar et al., 2013) and various splicing isoforms have been discovered, some of them only being specifically expressed in neurons and changes in the ratio of these isoforms have also been associated with AD (Matsui et al., 2007). The membrane integrated sequence, coding for the Aβ is not very well conserved amongst other species and is not involved into its biological functions (Zheng et al, 2006). If the region in APP that is associated with Aβ exhibits mutations, the risk to develop AD can be increased as this can increase the production of Aβ (Citron et al., 1992). Oppositely, the mutation A673T in the APP gene has shown to have protective properties against AD as it can lower Aβ production around 40% (Jonsson et al., 2012). Two main proteolytic cleavage sites close to the membrane and one site within the trans membrane domain have been identified and, starting from the amino terminus of the protein, are termed β, α and γ cleavage sites. Each cleavage is catalyzed by separate enzymes referred to as β-, α- and γ-secretases, respectively. The α and β cleavages seem to be mutually exclusive events and each liberate a large extracellular domain of the protein, differing in size by only 17 amino acids at the carboxyl terminus (Sisodia, 1992).

Normally, APP gets transported to the surface membrane followed by protelytic cleavage of α-secretase but if they fail to get processed by α-secretase they are eventually internalized in recycling compartments such as the endosomes where they will be further processed (Koo et al, 1992; Choy et al., 2012). The internalized APP will lead to the generation of Aβ peptides. This process is initiated by β-secretase cleavage, producing a soluble, extracellular APP fragment (sAPPβ) and a trans membrane, C-terminal fragment with a length of 99 amino acids (C99) (Fig 2.6). This C99 fragment will be further processed by their ε-cleavage cleavage site by γ-secretase, producing two APP intracellular signaling domains (AICDs) with a length difference of 1 amino acid AICD 49-99 and AICD 50-99 (Sastre et al., 2001) and a subsequently second product of Aβ peptides of various length including Aβ42 which be eventually released into the extracellular space by the endosome (Greenfield et al., 1999).

Homologous proteins for APP have been identified amongst various such as the app1 in Drosophila, C. Apl-1 in C. elegans, and APP-like protein1 (APLP1) (Wasco et al., 1992) and APLP2 (Wasco et al., 1993; Slunt et al., 1994) in mammals. However, Aβ can only be generated from APP and all homologous proteins lack the Aβ domain, which only seem to be present in APP of humans and mice. APP is much less often cleaved by β-secretase in the mouse brain in comparison to the human brain, leading to the assumption that Aβ in mice plays a less critical role than in human (De Strooper et al., 1995).

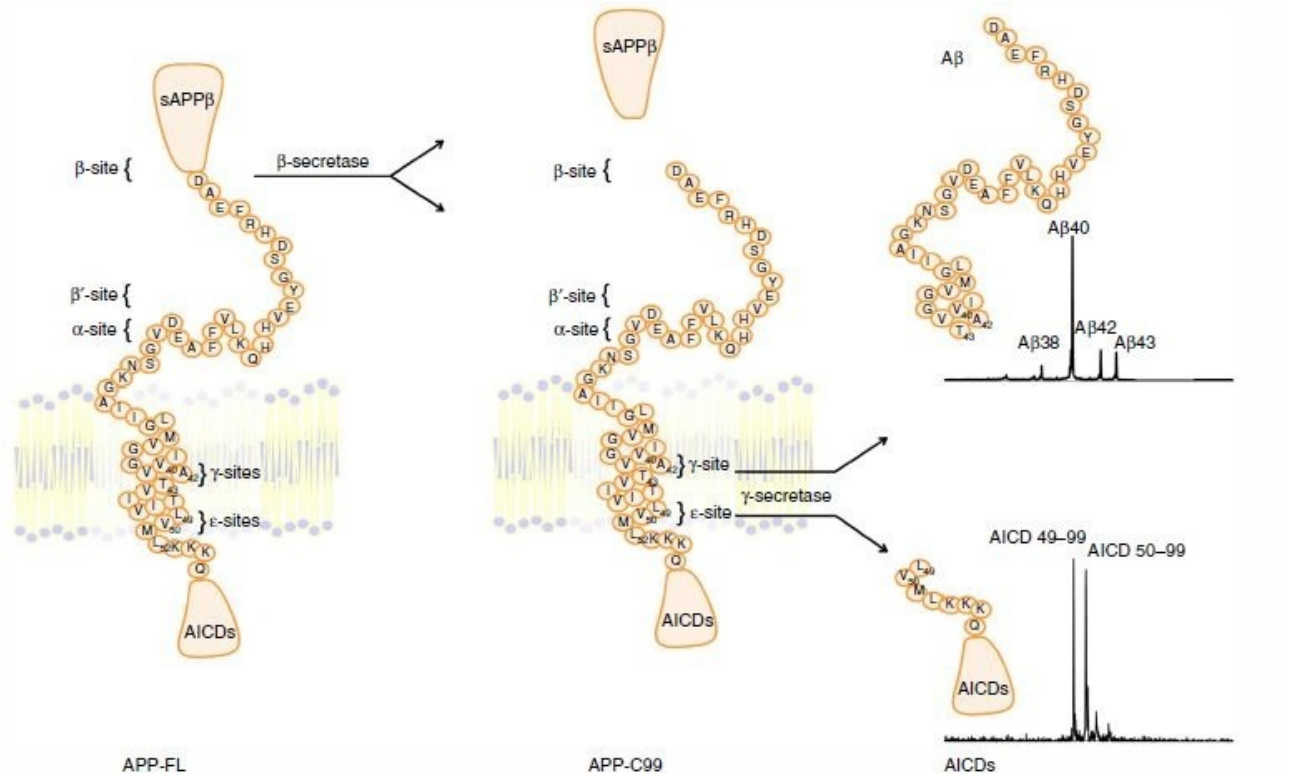


Figure 2.7: Amyloidogenic APP processing: After β-cleavage a soluble fragment (sAPPβ) is liberated and released into the extracellular space. A remaining membrane integrated 99 amino acid long fragment (C99) will be the second product of this cleavage. A further cleavage by γ-secretase of the C99 at γ- and ε-cleaving sites will finally release Aβ and second, c-terminal, trans membrane product called AICD (APP intracellular signaling domain), which can be either 49 or 50 amino acids long. The mass spectrometry above shows that these two AICDs are produce in a nearly equimolar ratio. The N-terminal fragment of this γ-cleavage will release the Aβ species of all different length to the extracellular space. Mass spectrometry of Aβ species showed that Aβ40 isoform is present in much higher levels than the more toxic Aβ42. (Taken from Dimitrov et al., 2013)

2.4.5.1 Biological functions of APP

Most of the research concerning the amyloid precursor protein has been focused on the deregulation caused by β-cleavage and the implicated Aβ toxicity; hence the biological functions of APP are still poorly understood. Evidence has accumulated over the past years that showed how APP is implicated in synapse formation and functions (Priller et al., 2006) neurogenesis (reviewed in Zouh et al., 2011), neuronal plasticity (reviewed in Turnera et al., 2003), neuronal transport and iron export (Duce, 2010). APP is a trans membrane protein exposing a large domain into the extracellular space with its N-terminus and a short C-terminal intracellular domain, which contains the Aβ region. Some of these domains have been identified by crystallography including the growth factor like domain (Rossjohn et al., 1999), the copper domain (Kong et al., 2007) and the E1 and E2 domains (Dahms et al., 2010; Wang et al., 2004) and it has been suggested that the released, soluble α-fragment of the C-terminal domain has neurotrophic functions. APP has at least three different isoforms resulting from alternative splicing of its mRNA and it is strongly post transcriptionally processed by glycosylation and specific proteolytic cleavage and the different products form this cleavage participate in various functions including neurotrophic and neuroproliferative activity, intracellular communication and membrane to nucleus signaling (Ruberti et al., 2010; DeStrooper et al., 2000). Similarities of the posttranslational processing of APP became subject to comparison with the surface receptor Notch. Interestingly, just like all other surface receptors, APP contains the same two-conserved motif in its C-terminal region, which is mainly responsible for it's trafficking (O'Brien et al., 2011). A similar fragment like the NICD (Notch intracellular domain) produced from Notch, will be generated through APP processing (called AICD), which gets just like the NICD trans located into the cell nucleus where it acts as a transcriptional regulator (Sastre et al., 2001; Cao, and Sudhof, 2001).

The expression of APP is found to be ubiquitous throughout all body tissues but exhibiting different ratios of its isoforms depending on the tissue type (Selkoe et al., 1988; Tanaka et al., 1989). Localization studies of APP demonstrated its abundance in various membranous structures such as the endoplasmatic reticulum, Golgi apparatus and the cell membrane (Schubert et al., 1991, Shigematsu et al., 1992, Caporaso et al., 1994 and Tomimoto et al., 1995) but Kirazov et al. showed in 2001 that APP can be detected preparations of synapses suggesting a an important function for APP at synapses. Indeed, mouse models overexpressing the human version of APP showed an increase in synaptophysin in the frontal cortex and oppositely the APP-null mutation model had decreased level of synaptophysin in neocortical and hippocampal neurons as well as reduced survival of hippocampal neurons (Mucke et al., 1994; Dawson et al., 1999; Phinney et al., 1999; Seabrook et al., 1999). These observations are possibly due to the neurotrophic

functions of the soluble αAPP domain one of the two products resulting from the α-cleavage induced by α-secretases including ADAM10 and ADAM17 (see section below: α-secretase processing). Additionally, the mouse model lacking APP has showed that mice are having only minor phenotypic effects like impaired long term potentiation and memory loss but no neuronal death (Matsuyama et al., 2007). Another study for this mouse model demonstrated how excitatory synaptic transmission in cultured hippocampal neurons is strongly enhanced and both, amplitude and frequency of synaptic currents were increased (Priller et al., 2006). As APP has shown to interact with cargo and kinesin, a protein involved in molecular transport within cells, it seems like APP is also affecting fast anterograde cellular transport (Satpute-Krishnan et al., 2006). This interaction between kinesin and APP is highly specific to the peptide sequence of APP mediated by a short peptide sequence of 15 amino acids at the C-terminal end of APP. Furthermore recent findings implicated that APP could function to influence proliferation of neural progenitor cells. Studies demonstrated that influence of neurogenesis by APP is conferred differently via its two separate domains, soluble secreted APPs (sAPPs, mainly sAPPα) and APP intracellular domain (AICD)(Zhou et al., 2011). The sAPPα was shown to be neuroprotective and important to neurogenesis, whereas AICD was found to negatively modulate neurogenesis (Zhang et al., 2014).

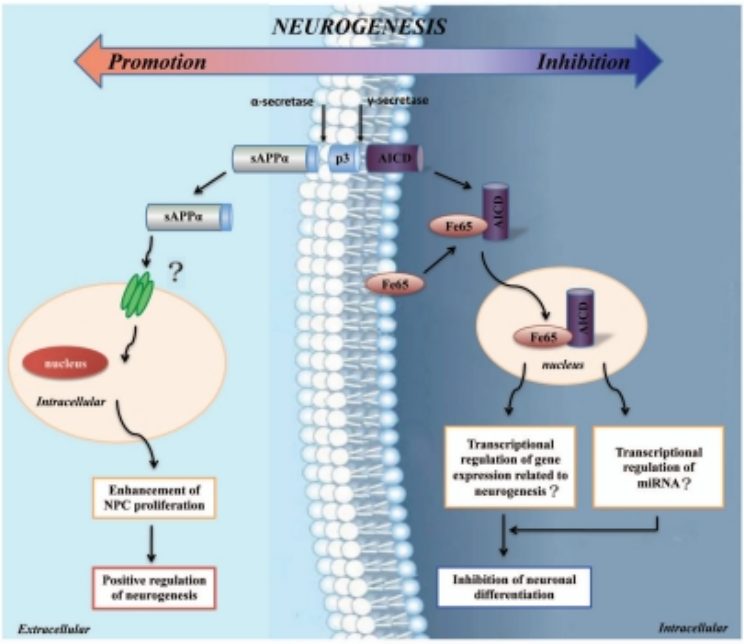


Figure 2.8: Influence of neurogenesis by sAPPα and AICD. sAPPα possibly functions on cells via binding with its specific receptors and positively stimulate neurogenesis by promoting neuro progenitor cell proliferation. Contrary, the release of AICD, which eventually forms a complex with Fe65, might act as a inhibitory regulator on neuronal differentiation by yet unknown mechanisms.

.

2.4.5.2 α-secretase processing

The α-secretase cleavage site is located close to the trans membrane domain between lys613 and leu614 within the critical Aβ peptide region and cleavage at this site precludes amyloid beta formation and is considered to be part of the non-amyloidogenic pathway in APP processing (Fig2.8). It produces a protein of 612 amino acids, the sAPPα. The α-cleavage is dependent on the secondary structure of APP rather than on a primary sequence (Sisodia, 1992). The main proteins are identified as alpha-secretases are ADAM10 and ADAM-17 or Tumor necrosis factor (TACE) (Black et al, 1997). TACE/ ADAM17 belongs to the family of disintegrin and metalloproteases. It releases tumor necrosis factor from its receptor form but it has also been shown to cleave other receptors including Notch (Black et al., 1997 Brou et al, 2000). Mice lacking TACE/ ADAM17 exhibited deficiencies in the secretion of sAPPα (Buxbaum et al., 1998), which supports the assumption that is indeed involved into APP cleavage.

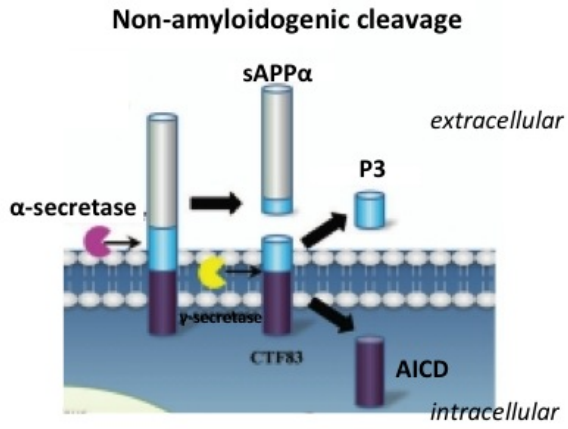


Figure 2.9: Non-amyloidogenic cleavage of APP by α.-secretases. The alpha secretase ADAM17/ TACE cleaves the APP protein within the Aβ region, preventing the generation of toxic amyloid-β species.

2.4.5.3 β-secretase processing

For long time, β-cleavage has been subject to intensive research in order to understand molecular mechanism of Aβ generation, hence a lot of knowledge about this pathway, its regulation and manipulation by mutations could be gathered. It has never been possible to get a full understanding why elevated beta cleavage seems to occur in AD. What researchers do understand is that this pathway, ending in the generation of amyloid beta, is initiated by β-site APP cleaving enzyme 1 (BACE1), a protein to be found having elevated level of abundance and activity in AD brains (Holsinger et al., 2002; Fukumoto et al., 2002). BACE was discovered by 5 different, independent groups around the same time (Vassar et al. 1999; Yan et al. 1999; Sinha et al. 1999; Hussain et al. 1999; Lin et al. 2000) and since then two major isoforms, BACE1 and BACE2, exhibiting high homology of 75% and identical sequence of 45%, have been identified (Sun et al., 2005; Benett et al., 2000). Expression of BACE1 is high in the brain and pancreas and low in

other organs (Vassar et al. 1999; Marcinkiewicz and Seidah 2000) while BACE2 expression is low in the brain.

BACE2 is believed to be enriched in astrocytes, whereas BACE1 is mostly expressed in neurons (Basi et al., 2003; Irzarry et al. 2001). Although BACE2 is also expressed in the brain, its potential role in AD has not been resolved. One study, examining this potential function found that BACE1 protein amount and activity indeed showed significant positive correlation with the amount of extractable Aβ but that BACE2 level and enzymatic activity in the human brain have not been changed in the frontal cortex of AD brains and were not related to Aβ concentrations (Ahmed et al., 2010). BACE2 is believed to be enriched in astrocytes, whereas BACE1 is mostly expressed in neurons (Basi et al., 2003; Irzarry et al. 2001). Although BACE2 is also expressed in the brain, its potential role in AD has not been resolved. One study, examining this potential function found that BACE1 protein amount and activity indeed showed significant positive correlation with the amount of extractable Aβ but that BACE2 level and enzymatic activity in the human brain have not been changed in the frontal cortex of AD brains and were not related to Aβ concentrations (Ahmed et al., 2010). BACE2 cuts APP in a different cleavage site as BACE1 and studies showed it cleaves APP around the alpha-secretase site (Farzan et al., 2000; Sun et al., 2005). Even though both isoforms, BACE1 and BACE2, compete for the same substrate it can be concluded that BACE1 is the responsible candidate for most of the production of Aβ, because its knockout completely abolishes Aβ generation (Luo et al., 2001).

BACE1 is a type I integral membrane protein with characteristics of an aspartyl-protease. Its main localization within the cell is the Golgi apparatus and late endosomes having optimal enzymatic activity at the low pH of these compartments (Vassar et al., 1999). Mice lacking BACE1 are not able to produce any Aβ, sAPPβ and CTFβ (Luo et al. 2001). It is possible that BACE2 might contribute to neurodegeneration in individuals with Down syndrome as it's located in the critical location on chromosome 21 (Acquati et al., 2000; Motonaga et al., 2002). Interestingly, a double knock out of BACE1 and 2 indicated a higher mortality than the BACE1 knock out alone (Yan et al. 2001; Cai et al. 2001; Luo et al. 2001; Dominguez et al., 2005).

APP gets cleaved by β-secretase between the residues of 596 and 597 at the N-terminus, releasing a soluble APP beta fragment (sAPPβ), which is 17 amino acids shorter than sAPPα (Fig. 2.6). The introduction of the so called swedish mutation in between the residues KM594 and 595NL in APP leads to a 10-fold higher cleavage rate by BACE1, being a much better substrate to this β-secretase than normal APP (Yan et al., 1999). Analyzing the Aβ cleavage products initiated by BACE1 it occurs that Aβ species 1-40/42 and 11-40/42 are increased (Vassar et al., 1999). Accordingly, amounts of β CTFs were also strongly increased in cells carrying the Swedish mutation.

It has been suggested that BACE1 is subject to transcriptional and/ or translational regulation (Rossner et al., 2006). Within its promoter region various binding sites for transcription factors have been discovered including Sp1, NF-Sp1, NF-ϰB, YY1, MZF1, HNF-3β and four GATA sites. Additionally, these binding sites are highly conserved between the species of mouse, rat and human (Lange-Dohna et al., 2003 and Christensen et al., 2004) meaning that regulation of BACE1 expressions are similar within species which makes both rodent species appropriate models to study and test therapeutic strategies for AD patients.

Although BACE1 expression level reach highest numbers in the brain tissue, it has to be kept in mind that it is globally expressed throughout the human body and that it serves physiological relevant functions in other tissue that could be harmed by its inhibition (see Fig. 2.9). In line with this, it was discovered that BACE1 knockout animals accumulated unprocessed neuregulin 1 (NRG1), an axonally expressed factor required for glial cell development and myelination. BACE1-/- mice displayed hypomyelination of peripheral nerves (Willem et al, 2006).

2.4.5.4 γ-secretase processing

β-cleavage may be the initiating event of the Aβ producing pathway but the actual toxic Aβ peptide is created by the follow up cleavage of the γ-secretase. It cleaves APP at the carboxyl terminal ending of the Aβ region, which is located in the APP trans membrane domain (reviewed in Wolfe et al., 1999). γ-secretase is in fact a is a multi-subunit protease complex, composed of several proteins that cleaves single-pass trans membrane proteins. The two prime candidates proposed to reconstitute γ-secretase activity are presenilin 1 and 2 (PS1 and PS2), which seem to contain the catalytic domain of the enzymatic complex. The γ-secretase complex furthermore contains three more individual proteins, nicastrin, anterior pharynx-defective1 (APH-1) and presenilin enhancer 2 (PEN2) (see review Kaether et al., 2006) (Fig 2.11).

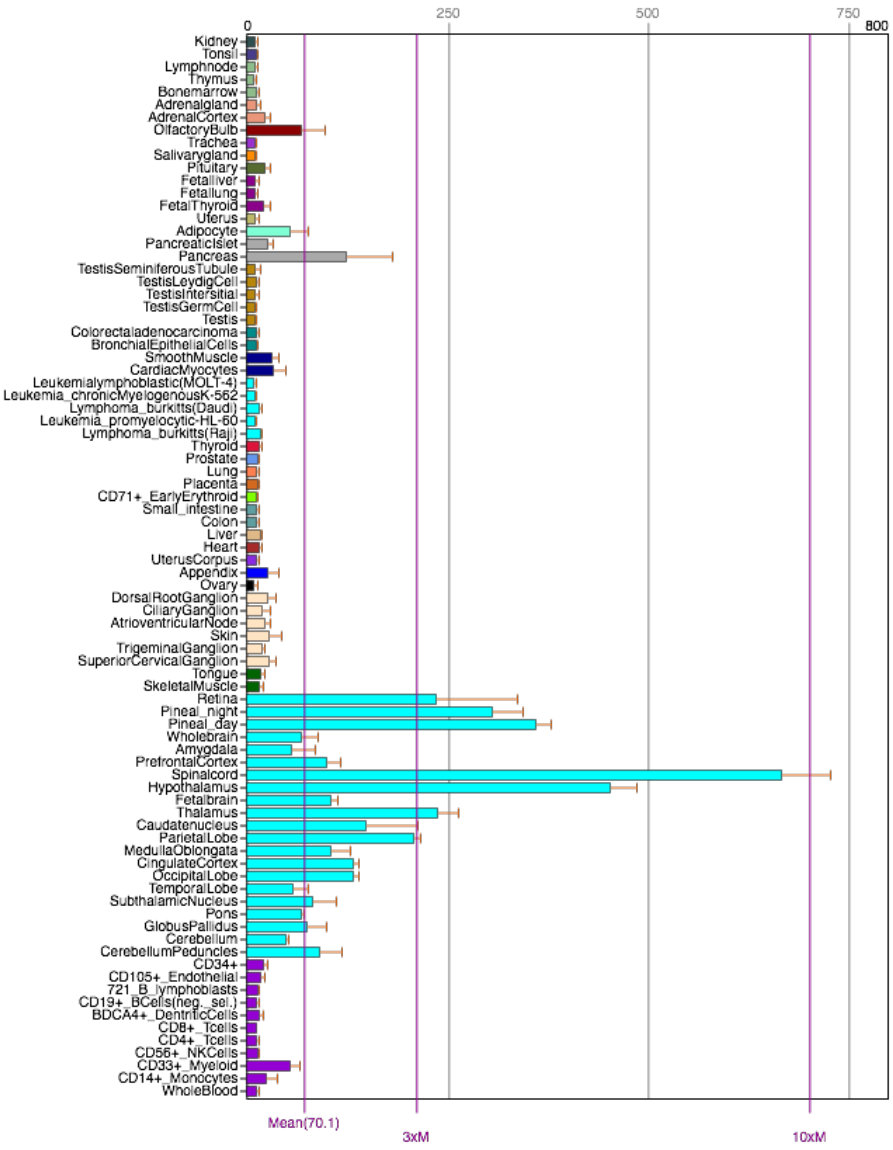


Figure 2.10: BACE1 gene expression profile in human tissues. The expression profile of BACE1 indicates that its expression is not exclusive to the brain but almost all other tissues where it appears with higher expression in the pancreas (Source: www. biogps.org).

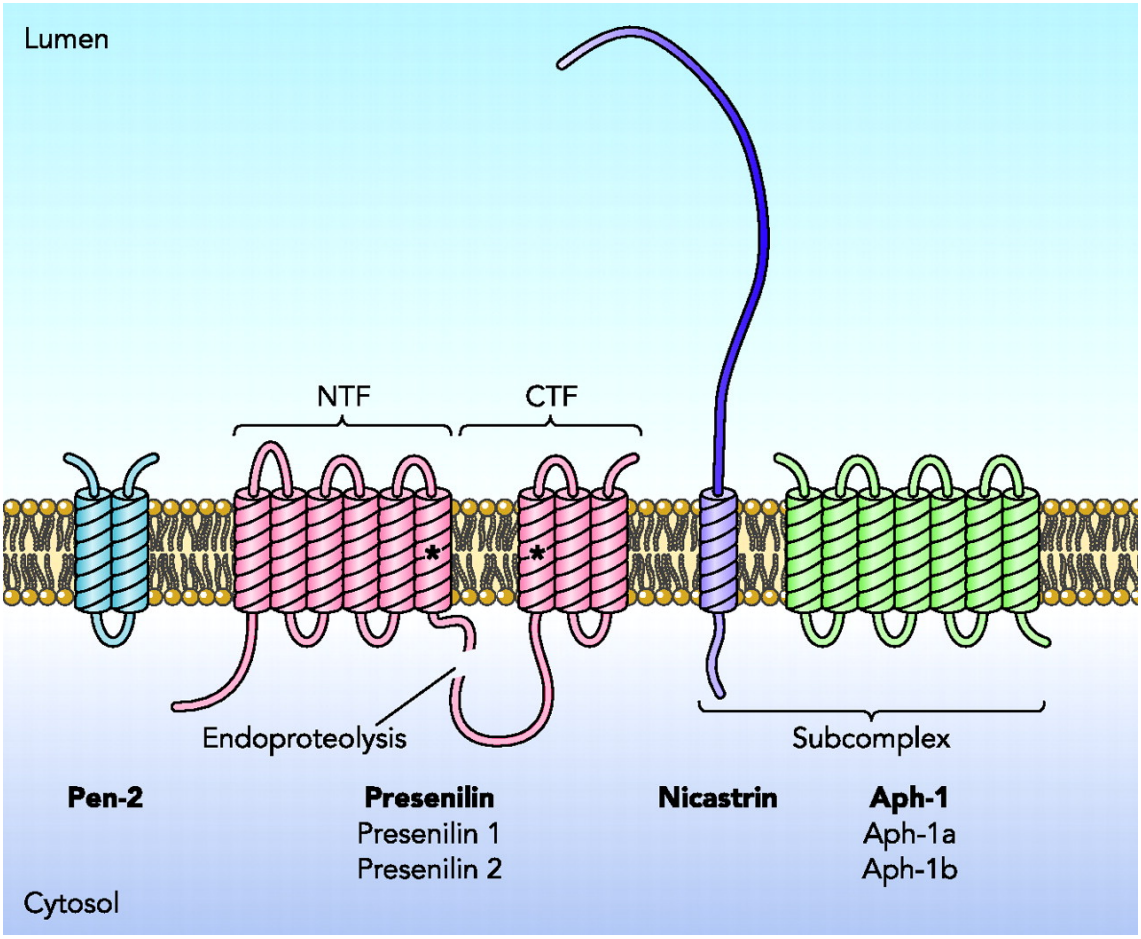


Figure 2.11: Schematic view of the γ-secretase complex. γ-secretase is a multi-subunit, intra membrane protease complex. It cleaves single-pass trans membrane proteins at residues within the trans membrane domain. It consists four individual proteins: presenilin, nicastrin, APH-1 (anterior pharynx-defective 1), and PEN-2 (presenilin enhancer 2). There are two known presinilin forms, 1 and two which expression is tissue specific and they are never expressed at the same time in the same complex. APH1 consits two isoforms, APH-1a and APH-1b (taken from Tomoko Wakabayashi, Bart De Strooper, 2008).

Two isoforms of each, presenilin and APH-1 have been identified in human, which gives at least six different possibilities of γ-secretase complex compositions which are probably specific to tissues and certain cell types (Shirotani et al., 2004). Interestingly, PS1 and PS2 are not found in the same complex but have distinct tissue specific expression, which can overlap (Saura et al., 1999) and are thought to contain the catalytic domain of γ-secretase. Presenilins are homologous polytopic membrane proteins having 9 passing points through the membrane. They were initially identified by screens for mutations with a high linkage to AD and are located on chromosomes 14 and 1 (Cruts et al.,

1995; Hutton et al., 1996). Additionally to this study, mouse embryonic fibroblasts (MEF) cells deriving from mice lacking PS1 had reduced γ-secretase activity, causing a decrease in Aβ peptides and p3 fragments but at the same time showed accumulations of CTFs of APP in the membrane, which arises from and α- and β-cleavage (De Strooper et al., 1998). Another study in which a double knock in was generated, mice expressing the human APP with swedish mutation and PSEN1 M146L mutants, animals exhibited increased AD pathology including Aβ accumulations and corresponding memory impairment and cognitive decline in a much stronger manner than the single APP knock in (Trinchese et al.,2004). A study using a conditional knock out in the postnatal forebrain for PS1 and 2 (PS cDKO mice) was able to show linked reduction in Aβ production (Beglopoulos et al., 2004). The γ-secretase complex is capable of producing the different fragments varying in length by cleaving APP at two different cleavage sites called ε, and γ (see figure 2.6). The sequential cleavage of APP CTF by γ-secretase at the ε-cleavage site, which is close to the membrane, produces larger peptides of Aβ with a size of 49 amino acids (Aβ49) (Sastre et al., 2001). The most prominent Aβ peptides, Aβ40 and Aβ42, result from the subsequent γ-cleavage, with Aβ40 being in large excess in comparison to Aβ42 (Dimitrov et al., 2013) (Fig. 2.6).

An additional cleavage site was described for γ-secretase. The ξ-cleavage occurs between ε- and γ-cleavage sites and generates longer Aβ forms within cells and in the brain, including Aβ43, Aβ45,Aβ46, and Aβ48 (Zhao et al., 2004). However, γ-secretase activity is regulated by nicastrin subunit, as activity assays of purified γ-secretase by affinity chromatography have previously demonstrated (Esler, et al., 2002). Nicastrin interacts with PS1 and PS2 and the CTF of APP (Yu et al., 2000). Deletion of highly conserved sequences of nicastrin prevented generation of Aβ while substitution of residues in the same region increased the production of Aβ. Nicastrin has four conserved cysteine residues close to its N-terminus and exhibits strong glycolisation. Furthermore it has been shown that trafficking and post-translational processing of nicastrin is affected in PS double knockout mice (Leem et al., 2002). Another interesting observation of the PS knock out mouse is its very strong similarity to the Notch knock out mouse (Conlon et al., 1995). In addition, γ-secretase has shown to process Insulin receptor and growth hormone receptor, which are like Notch type I trans membrane cell receptors (De Strooper et al, 1999). It has been shown that in the brain, γ-secretase is involved in synaptic contact maintenance by regulating the cleavage of neuronal adhesion molecules like cadherins and neurexins (Bot et al, 2011; Uemura et al., 2006).

2.4.6 Mechanisms of Aβ degradation

Aβ can be removed via enzymatic degradation by specific peptidases insulin degrading enzyme (IDE) and neprylisin or can be cleared and exported out the brain by direct binding to LRP or first binding to LRP chaperones APoE and α2- macroglobuline (reviewed in Tanzi et al., 2004). As indicated above, Aβ can be also internalized and degraded by microglia.

2.5 Peroxisome proliferation activating receptors

Peroxisome proliferating receptors (PPARs) are transcription factors of the steroid hormone family, which can be activated through specific ligands. They are involved in various physiological processes such as lipid homeostasis (Keller et al., 2007), energy metabolism (Desvergne and Wahli, 1999), inflammation (Delerive et al., 2001) and cellular differentiation and proliferation. The first description and discovery of PPARs took place in mice and Xenopus and later in humans (Dreyer et al., 1922; Zhu et al., 1993; Sher T, 1993). So far, three different isoforms, PPARα, PPARβ/δ and PPARγ could be identified (Chen et al., 1993). The N-terminal domain is only poorly conserved between the different PPAR subtypes and is responsible for the differences of their biological functions. The DNA binding domain (DBD) consisting two zinc finger motifs exhibits high homology in all three isoforms while the ligand binding domain shows less homology, causing the specificity for ligand binding of each subtype (Glass, 1994). PPAR's are regulating gene expression by forming an activated heterodimer complex with the retinoid x-receptor (RXR)(Fig.2.12), which then binds to specific recognition sites in the DNA (Kliewer et al., 1992). These recognition sites have been named PPAR-response elements (PPRE). The first identified PPRE has been found in the Acyl-CoA oxidase gene promoter (Tugwood et al., 1992). Additionally, the active heterodimer recruits co-activators and/or releases co-repressor molecules from the transcriptional start site, leading to regulation of transcription of target genes.

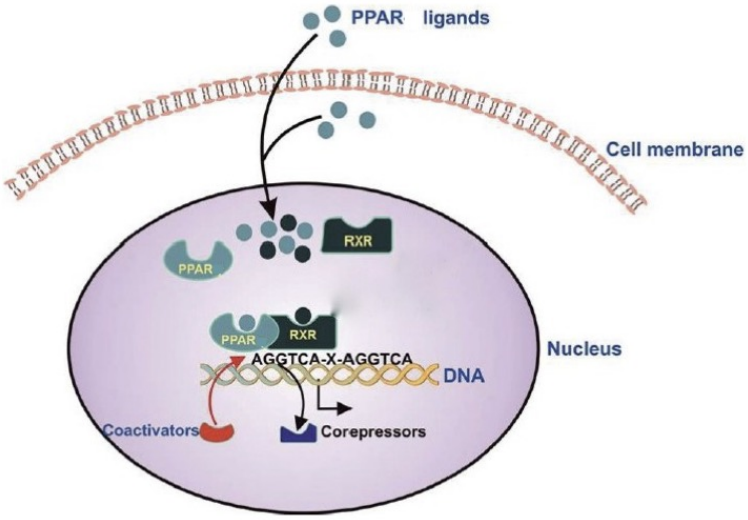


Figure 2.12: General mechanism of PPARs. PPAR's belong to the nuclear receptors, hence their localization within the nucleus. Specific PPAR ligands of extracellular and intracellular origin will bind to the PPAR ligand binding domain and allow dimerization with the RXR. RXR is also abundant in the nucleus and activated by its own specific ligands form within the nucleus. The activated heterodimer complex will then bind to the PPRE. The active complex is further regulated by recruitment and de-recruitment of co-activators and co-repressors of PPAR.

2.5.1 Discovery of PPARs

The name peroxisome proliferating receptors goes back to the firstly observed effects of PPAR ligands on the number of peroxisomes. In 1965, the treatment with ethyl cholorphenoxy-isobutyrates, a substance that later has been demonstrated to be a PPAR activator (Lalloyer and Staels, 2010), showed a massive increase in the peroxisome number in the liver of rats (Hess and Staubli, 1965). It was only 25 years later when the first receptor for the corresponding ligand was cloned, which caused the proliferation of peroxisomes (Issemann and Green, 1990). This effect was further investigated and a treatment with hypolipidemic compounds like clofibrate lead then to an increase of peroxisome number, volume and density in rat livers. Simultaneously, the expression of peroxisomal enzymes involved in β-oxidation such as actetyl-CoA oxidase, enoyl-CoA hydratase-hydroxy-Acyl-CoA dehydrogenase and 3-ketoacyl-CoA thiolase was increased (Latruffe et al., 2000).

2.5.2 Isoforms

Different PPAR isoforms exhibit specific expression patterns, assuming they may have different functions in different cell types (Braissant et al., 1996). During embryonic development in rat brains, all three isoforms are expressed and only get regulated post natal The expression of PPARα and PPARγ within the brain declines postnatal, while PPARβ/δ expression remains constant throughout adult stages (Krey et al., 1997).

2.5.2.1 PPARα

PPARα expression is particularly high in liver, heart, kidney, gut and adipose tissue (Keller et al., 2000). Fatty acids are the natural activators for this receptor, which also functions as a lipid sensor. Stimulation of fatty acid- and cholesterol catabolism in liver tissue as well as gluconeogenesis are PPARα mediated processes (Reddy and Hashimoto, 2001). It has been demonstrated that through PPARα stimulation, transcription of enzymes involved into lipid metabolism was elevated after treatment with fenofibrate, a specific PPARα ligand (Latruffe and Vamecq, 1997). Fibrates and its derivatives to which fenofibrate pertains belong into the group of hypo lipodaemic substances and count as synthetic ligands of PPARα. Originally they have been developed to normalise the amounts of cholesterin and triglycerides in blood plasma (Thorp and Warning, 1962). It was later postulated that fibrates act as specific PPARα ligands (Issemann, Green, 1990). In addition to their lipid lowering properties fibrates exhibit anti-inflammatory, anti- oxidative properties (Staels et al., 1998; Escher and Wahli, 2000). In particular, fenofibrate has been recently proven to have under inflammatory conditions neuroprotective properties in cortical neurons (Gray et al., 2011). In cells of human origin, a much shorter splice variant of PPARα with dominant repressive function was detected (Gervois et al., 1999). This variant is a C terminal truncated version, which gets initiates through an early stop codon and alternative splicing. The shorter variant is lacking the entire ligand binding domain and if it is trans located into the cell nucleus it will act as a repressor on the trans activating function of the complete PPARα transcript (Gervois et al., 1999).

2.5.2.2 PPARβ/δ

PPARβ/δ is ubiquitously expressed, however certain tissues including the brain, adipose tissue and skin exhibit elevated level of PPARβ/δ mRNA (Amri et al., 1995; Braissant et al., 1996). PPARδ is the most abundant PPAR in the brain (Heneka et al., review). Notably, increased PPARβ/δ expression was detected in the developing neuronal tube (Krey et al., 1997). Like PPARα, PPARβ/δ controls various physiological functions including lipid and glucose homeostasis,

inflammation and cell proliferation and differentiation (Barish et al., 2006). Mice with a PPARβ/δ deficiency disclosed disturbances in myelin, forming the white matter of the brain of the corpus callosum (Peters et al., 2000). PPARβ/δ is the only PPAR isoform for which so far repressive activity could be reported whilst being bound to DNA. It could be demonstrated that non ligand bound PPARβ/δ is acting as a transcription repressor leading to a repression of the trans- activation of the other PPAR isotypes (Shi et al., 2002; Krogsdam et al., 2002). The fact that PPARβ/δ expression is ubiquitous it can be assumed that it has an additional repressing role for PPRE target genes. It seems like that PPARβ/δ has auto regulatory functions as well, which is supported by the discovery of a 5' untranslated exon as well as few 5' UTR's of PPARβ/δ mRNA transcripts. Those could have an influence on the translation efficiency. Additionally, the expression of a 3'splice variant of human PPARβ/δ has been found, which acts as a potential dominant negative regulator for PPARβ/δ (Lundell, 2007). Some of the known ligands to specifically bind and activate PPARβ/δ are natural ligands like fatty acids and eicosanoids and synthetically ligands like bezafibrate (Krey at al., 1997), furan conjugated linoleic acid metabolites (Moya-Camarena et al., 1999), GW0742 and GW501516. Treatment of mice with GW0742 with experimental autoimmune encephalomyelitis (EAE) showed beneficial effects and a decrease of the neurological damage. The stimulation of PPARβ/δ with GW0742 increased the expression of myelin associated genes and affected the maturation of oligodendrocytes. Interestingly, the amount of mature oligodendrocytes in PPARβ/δ null mice was significantly lower than in wild-types (Vittoria Simonini et al., 2010). Recently, it was also demonstrated that PPARβ/δ has anti-inflammatory and metabolic effects and activation of this receptor may also regulate different aspects of AD (Schnegg et al., 2011). There have been already two studies showing that PPARβ/δ agonists can be neuroprotective in AD (In fact, two studies have reported that PPARβ/δ agonists can be neuroprotective in AD (Madrigal et al., 2007; Kalinin et al., 2009). The findings of the most recent study of PPARβ/δ null mice in AD demonstrated that PPARβ/δ null mice exhibited cognitive impairment, increased BACE1 level and Tau hyper phosphorylation (Barroso et al., 2013).

2.5.2.3 PPARγ

PPARγ (also called NR1C3) is the best investigated PPAR isoform which natural functions are regulation of lipid and carbohydrate homeostasis and showing anti-inflammatory effects in the central- and peripheral-nervous system (Heneka et al., 2007; Bernado, 2008). Abundance of PPARγ has been proven in neurons as well as in glial cells (Braissant et al., 1996). This distribution pattern reflects the effects of PPARγ activity like lipid storage, adipocyte differentiation and

the regulation of glucose metabolism (Rosen, 1999; Desvergne et al., 2004; Strauss et al., 2007). PPARγ expression within the central nervous system (CNS) could be demonstrated in various cell types including neurons, astrocytes, microglia and oligodendrocytes (Minghetti et al., 2008; Cullingford et al., 1998; Moreno et al., 2004). Immunostaining for PPARγ in neuronal cells appeared mainly in the nucleus of the cell (Moreno et al., 2004; Imini et al., 2005) and higher level have been found in the piriform cortex, olfactory tubercle, basal ganglia, rhomboid, centromedial and parafascular thalamic nuclei, the reticula formation and the stellate cells of cerebellar cortex (Moreno et al.,2004). Constant expression of PPARγ was exhibited in microglial cells where its levels are dependent on the microglial activity state and are strictly regulated (Bernado et al., 2000). Human PPARγ contains nine exons , which can be translated into the different mRNA forms of PPARγ1, PPARγ2, PPARγ3 and PPARγ4 (Knouff and Auwerx, 2004), with PPARγ1 being the most abundant form. Evidence has been given that PPARγ regulates the expression of certain inflammatory cytokines such as TNFα, COX and iNOS (Heneka et al., 2000; Park et al., 2003). Ligands of PPARγ have been identified as neuroprotective substances (Kaundal and Sharma, 2010) and in vivo studies demonstrated that treatment with PPARγ ligands can reduce the strength of the pathology of certain neurodegenerative diseases for example AD (Yan et al., 2003) and Parkinson's disease (Shintu et al., 2009). Activating ligands for PPARγ are thiazolidinedione's such as the synthetic agonists pioglitazone, rosiglitazone and troglitazone. Natural ligands are fatty acids, eicanosides and 15d-prostaglandin J2. Similar as described for PPARα, human PPARγ also has a N-terminal truncated version which is also generated through alternative splicing and functions as a dominant negative regulator as well (Kim et al., 2006).

2.5.2.4 Neuroprotective functions of PPARγ

The fact that PPARs are also expressed in almost all CNS cell types, raised the possibility of exploring the neuroprotective efficacy of their agonists in several neurodegenerative disorders (Woods et al. 2003; Bordet et al. 2006; Heneka and Landreth 2007). Various reports during recent years demonstrated neuroprotective properties for PPARγ, most likely to be mediated by its activation. Treatment with pioglitazone and rosiglitazone can lower the neuronal damage by preventing inflammation and oxidative stress and apoptosis (Border et al., 2006, Heneka and Landreth, 2007). Both drugs can also prevent neuronal damage, myelin loss and neuropathic pain (McTigue et al., 2007, Park et al., 2007). Different studies using a model of Parkinson's disease (PD) were able to show that TZDs have neuroprotective functions (Ridder et al., 2012). Parkinson's disease (PD) is a chronic neurodegenerative disease characterized by progressive

loss of dopaminergic neurons in the substantia nigra and there is evidence that points the involvement of oxidative stress and inflammation (Gupta et al., 2008). Pioglitazone administration into the MPTP (1-methyl-4-phenyl-1,2,3,6-tetrahydropyridin) model of PD could completely block dopaminergic neurodegeneration (Breidert et al., 2002; Dehmer et al.,2004). These studies suggested that the neuroprotection in response to pioglitazone is mainly mediated through its anti-inflammatory effects. However another study showed that Pioglitazone is likely to inhibit the monoaminoxidase B (MAO-B, an enzyme that converts MPTP to its active form 1-methyl-4-phenyl-pyridium (MPP+). MTPT is a substance used to induce clinical symptoms of PD. Because Pioglitazone reduced this conversion, this results point out that this could be another mechanism associated to its neuroprotective effects (Quinn et al., 2008).

Rosiglitazone has further reported neuroprotective effects in global cerebral ischemia (Cornio et al., 2008) and treatment demonstrated preservation of cell viability of CA1 hippocampal region (Al Roqa et al., 2013). Here the suggested mechanism responsible for the neuroprotection was also suggested to be associated to the anti-oxidant, anti-inflammatory effects of rosiglitazone.

Lastly, the administration of pioglitazone was also able to improve motor performance, attenuate motor neuron loss and extend survival of animals of a transgenic amyotrophic lateral sclerosis (ALS) model (Kiaei et al., 2004). It has been suggested that inflammation may also play a major part in ALS and level for certain inflammatory factors were reduced in the same mouse model due to pioglitazone treatment.

2.5.2.5 PPARγ in AD

PPARγ levels have been found reduced in the brain of AD patients as well as in animal models of AD (Sastre et al., 2006). The mechanisms by which PPARγ activation could be beneficial in AD are based on its anti-inflammatory properties as well as in its capacity to regulate APP processing. Demonstrations of the anti-inflammatory effects of PPARγ were reported using in vivo treatment of transgenic APP mice with pioglitazone, which resulted in reductions on microglia and inflammatory mediators, such as iNOS (Heneka et al., 2005). In addition, it was recently shown that pioglitazone treatment can enhance in mice the microglial uptake of Aβ in a PPARγ dependent manner (Yamanaka et al., 2012). In that study, the combined treatment with agonists for the RXRs showed additive enhancement of the Aβ uptake. Another specific PPARγ agonist, rosiglitazone, has been shown to regulate hippocampal expression of PPAR-target genes and restores ERK/MAPK signaling in AD transgenic mice (Denner et al., 2012). The observation of reduced Aβ pathology due to PPARγ treatment could also be caused by the ability of PPARγ to affect Aβ homeostasis. It has

been reported that PPARγ activation inhibits Aβ production stimulated by inflammatory cytokines. The investigators of this study postulated that the decrease in Aβ generation is mediated by the suppression of BACE1 expression likely through PPARγ dependent repression of the BACE1 gene promoter (Sastre et al., 2003, 2006). Furthermore PPARγ activation can act at an earlier step of APP processing, by affecting cellular APP levels through ubiquitin mediated degradation of APP leading to a subsequent Aβ decrease (d'Abramo et al., 2005).

Pedersen et al. (2006) showed interesting effects caused by oral rosiglitazone administration that were not only lowering Aβ42 level, without affecting amyloid deposition, but also exhibited better spatial learning and memory abilities during behavioral testing on a Tg2576 Alzheimer mouse model. A preliminary, clinic trial using rosiglitazone, was also able to detect a mild cognitive improvement relative to the placebo group at 4 and 6 months (Watson et al., 2005).

In addition, Treatment with PPAR agonists has also been beneficial in Tau models. Treatment with the pan-PPAR agonist bezafibrate significantly decreased Tau hyper phosphorylation and caused behavioral improvement, as evidenced by reduced hyperactivity and inhibition in P301S mice (Dumont et al, 2012). In addition, 3xTg-AD mice treated with pioglitazone for four months showed improved learning, decreased hippocampal amyloid-β and Tau deposits, and enhanced short- and long-term plasticity (Searcy et al, 2012). Furthermore, pioglitazone significantly increased memory scores in patients with AD in recent clinical trials (reviewed in Sastre and Gentleman, 2010).

We hypothesize here that PPARγ could be the link between type-2 diabetes and AD, because insulin sensitivity has been associated with the down-regulation of PPARγ and PPARγ is also involved in the transcriptional regulation of genes involved in AD. The primary effects of PPARγ on gene transcription were initially described in adipose tissue, where it is most abundantly expressed, which ultimately lead to improved insulin action in muscle and liver (Moller et al., 2001). Activation of PPARγ using artificial high affinity ligands such as TZDs is widely used to increase peripheral insulin sensitivity leading to decreased plasma glucose level (Wagstaff and Goa, 2002). It is there for not surprising that PPARγ has become the predominant molecular target for insulin-sensitizing thiazolidinedione (TZD) drugs (Wilson et al., 2000; Moller et al., 2001). However, TZDs only show a modest efficiency accompanied by several side effects resulting in the expansion of research for improved PPARγ ligands and treatments as potential drugs and targets.

Interestingly, loss of function mutations of PPARγ leads to severe insulin resistance and type 2 diabetes in mice (Barroso et al, 1999). A very recent study demonstrated that PPARγ activation in the brain ameliorates diabetes induced cognitive dysfunction and improves brain-derived neurotrophic factor (BDNF) expression hippocampal neuronal

cells (Kariharan et al., 2015).

PPARγ has also been shown to suppress expression of pro-inflammatory genes in myeloid lineage cells, such as microglia and macrophages (Daynes et al., 2002).

PPARs inhibit pro-inflammatory gene expression by a mechanism of transcriptional trans repression, which is not mediated by their binding to PPREs. They suppress the action of other transcription factors like NFκB, AP-1 and STAT1 (Daynes et al., 2002). Similarly, suppression of TNF-α gene expression by PPARγ in adipose tissue has been reported. TNF-αa is also a cytokine involved in systemic inflammation and potential systemic mediator of insulin resistance.

Another model suggests that trans repression of PPARγ is co-factor dependent. Under basal conditions NFκB-regulated inflammatory genes are maintained in a repressed state by the PPARγ cofactor N-Cor (nuclear co-repressor) containing co-repressor complexes. When exposed to pro-inflammatory stimuli this N-Cor containing complex is dismissed and gene expression is initiated, which can be prevented by sumoylated PPARγ. PPARγ agonist complexes stabilize N-Cor complexes at the promoters of NFκB-regulated genes, thus preventing inflammatory gene expression (Ghisletti et al., 2007; Ogawa et al., 2005). This observation points out an important potential role of PPAR regulation by co-factors and not only ligands alone. Taken this together, it can be assumed that the specific modification of inflammatory factors might also alter insulin resistance. The observation that PPARs are able to suppress the inflammatory response in peripheral macrophages and in several models of human autoimmune diseases, lead to the idea that PPARs might be beneficial for CNS disorders possessing an inflammatory component. Inflammatory factors such as C-reactive protein, interleukin-6 and TNF-α are also elevated in type 2 diabetes (van de Ree et al., 2003).

2.5.2.6 Stiumlation of PPARγ: agonism vs antagonism

Pioglitazone Pioglitazone The most widely used synthetic ligands for PPARγ are members of a class of ant diabetic agents known as thiazolidinedione's (TZDs), including rosiglitazone, troglitazone, and pioglitazone. Two TZD drugs rosiglitazone (Avandia™) and pioglitazone (Actos™) are potent activators of PPAR-γ and are approved by the US Food and Drug Administration for the treatment of type II diabetes. Pioglitazone belongs to the group of insulin sensitizing drugs, currently used to treat diabetes type II. It triggers the sensitivity of the tissue to insulin, which can then lower the level of sugar in the blood. Although Pioglitazone has been shown to be highly effective for the treatment of diabetes type II, evidence has emerged, reporting severe side effects for these drugs including fluid retention, weight

gain, bone loss and congestive heart failure (Kahn et al., 2008, Nesto et al., 2004).

Pioglitazone has been used as a highly selective, ligand for the activation of PPARγ (Peroxisome proliferation activated receptor, subtype γ) but does also bind with a certain affinity to the subtype α. Within the cells body, it activates PPARγ inside the nucleus, regulating genes involved in various mechanisms for carbohydrate and fatty acid metabolism. The activation increases the insulin sensitivity of liver, muscle and adipose tissue. Fatty acids and glucose uptake into these cells is improved when PPARγ is stimulated with pioglitazone. Recently, it was shown that many PPARγ-based drugs have a separate biochemical activity, blocking the obesity-linked phosphorylation of PPARγ by cdk5. This action is completely independent of classical receptor transcriptional agonism (Choi et al., 2010) and it seems that the inhibition of PPARγ phosphorylation in obese patients by TZDs is very tightly associated with the anti-diabetic effects of these drugs.

Pioglitazone can cross the blood brain barrier (Kiyota et al. 1997), while there are controversial reports on blood brain barrier permeability by rosiglitazone (Pedersen and Flynn 2004; Watson et al. 2005; Risner et al. 2006; Strum et al. 2007).

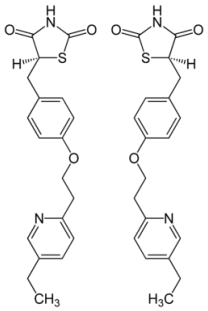


Figure 2.13: Chemical structure of (S)- (left) and (R)- (right) Pioglitazone. The pioglitazone molecule exhibits chirality with one stereo centre leading to the two enantiomer forms of (S)- and (R)- pioglitazone. The available pharmalogical drug contains a racemic mixture of both forms as a hydochloride (taken from wikipedia.org).

T0070907 In 2002, Gary Lee et al. described a novel, non TZD artificial, PPARγ ligand with high binding affinities, using a variety of biochemical and cellbased assays. They demonstrated that T0070907 is functioning as an effective PPARγ antagonist of cellular and biochemical activities. They have shown that T0070907 inhibited the agonist-induced recruitment of coactivator-derived peptides to PPARγ and induced recruitment of the transcriptional corepressor NCoR to PPARγ. Further on, T0070907 is capable of displacing [3H]rosiglitazone with an apparent Ki of 1 nM as shown in Fig

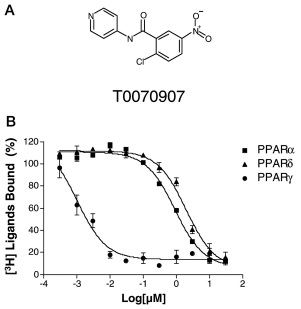


Figure 2.14: Chemical structure of T0070907 (A) and analysis of its binding to different PPAR subtypes (B). The affinities of T0070907 for the various PPAR subtypes were determined using an SPA assay. [3H]GW2433 (5 nM) was used as a ligand for PPARα and PPARδ, and [3H]rosiglitazone (5 nM) was used for PPARγ. T0070907 Is a non-TZD ligand for PPARγ, binding PPARγ with high affinity and being capable of displacing [3H]rosiglitazone with an apparent Ki of 1 nM. (Gary Lee et al., 2002).

2.6 PPARγ Cofactors

The implications of PPARγ in neurodegenerative diseases such as AD and the severe side effects of substances for PPARγ activation have increased demands to investigate further the regulation of PPARγ. The precise spatial and temporal regulation of transcription by nuclear receptors requires the recruitment of intermediary factors, which are characterized as co-regulators or co-factors. Activation of nuclear receptors such as PPARγ can be induced by ligand binding or by ligand-independent pathways. The function of NRs such as PPARs is regulated by recruitment of co- activators in the presence of agonists and release of co-repressors, resulting in transcriptional activation. Transcriptional trans repression can be achieved by diverse mechanisms (see review Katsouri et al, 2012). In vitro studies have demonstrated other mechanisms of transcriptional regulation, such as transcriptional interference (termed as „squelching“), which can occur when one nuclear receptor represses the transcriptional activity of another nuclear receptor by sequestering. Therefore, the density of different cofactors in certain brain areas would be a limiting factor on the transcription of genes (Nishihara E et al., 2004). One of the main co-regulators of PPARγ is the PPARγ co-activator-1α (PGC-1α). Other PPARγ cofactors include the receptor-interacting protein 140 (RIP140), and NR co-repressor (NCoR)/silencing mediator for retinoid and thyroid hormone receptor (SMRT) (see review Katsouri et al., 2012).

2.6.1 Receptor interacting Protein 140 (RIP140)

The receptor interacting Protein 140 (RIP140), also known as nuclear receptor interacting protein (NRIP), was identified as a cofactor for nuclear receptors and found to function as a co-repressor for a number of nuclear receptors (NR) that regulate metabolic pathways, namely estrogen-related receptors (ERRs), liver X receptor (LXR) and PPARs (Leonardson et al., 2004; Seth et al., 2007; Christian et al., 2006) and it has been proposed that it even may interact with most if not all NR (L'Horset et al., 1996). So far, very limited knowledge about RIP140s potential role in the brain exists while PPARs, some of the main interacting partners of RIP140, have been extensively studied in this tissue. RIP140 is widely expressed throughout the body and controls various physiological processes. When discovered, it was identified as a modulator of estrogen receptor activity in breast cancer cells (Cavailles et al., 1994). Two obvious phenotypes from mice lacking RIP140 were female infertility and impaired energy homeostasis, arising from the observation of RIP140s essential role in the ovary for ovulation (White et al., 2000). Furthermore, studying these RIP140 deficient mice revealed that it plays an essential role in the glucose and lipid metabolism of adipocytes, muscle and liver tissue (Leonardsson et al., 2004; Herzog et al., 2007; Seth et al., 2007). Additionally, studies of not only RIP140 knockout but also transgenic mice demonstrated roles for this co-factor in the heart tissue (Fritah et al., 2010), macrophages (Zschiedrich et al., 2008), mammary gland (Nautiyal et al., 2013) and brain (Duclot et al., 2012).

RIP140 is ubiquitously expressed throughout the human body but with expression levels highest in the uterus, parts of the brain and immune cells (Fig. 2.15). High expression level in the uterus can be linked to fertility problems described in the RIP140 knock out mice before, however less is known about the role of RIP140 in the brain. ISH hybridization of RIP140 in the mouse brain confirms the high expression level in this organ, being particularly high in the Hippocampus and area that is highly affected during AD (Fig.2. 16)

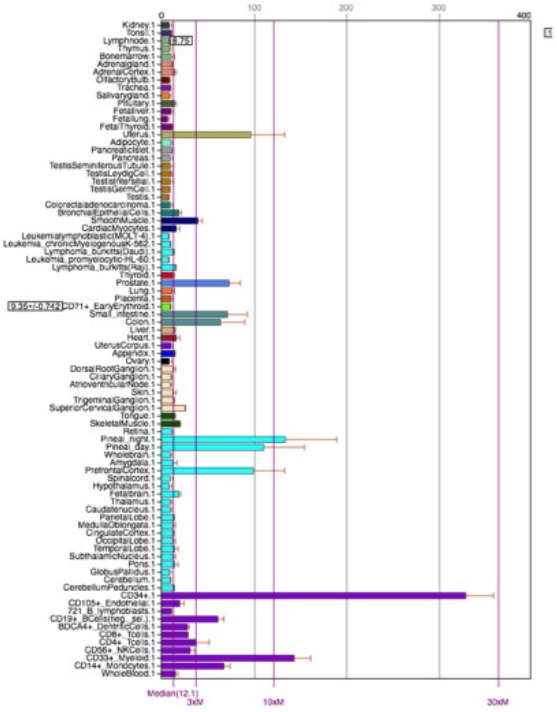


Figure 2.15: Expression of RIP140 in human tissue. RIP140 expression was detected in all tissues tested. Expression levels were particularly high in the uterus, certain areas of the brain and in CD positive immune cells.

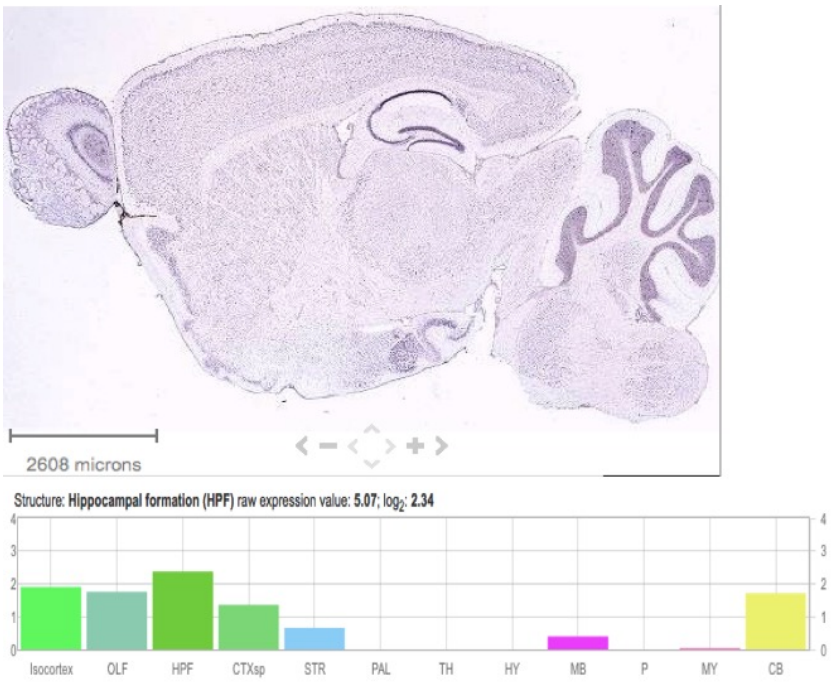


Figure 2.16: In situ hybridization for RIP140 in the mouse brain. ISH of RIP140 indicates further that RIP140 seems specifically expressed in the brains of mice. Interestingly, within the brain expression seems highest in the Hippocampus an area that has been strongly linked to AD (taken from brain explorer; Allen brain atlas; ISH data for RIP140 (http://mouse.brain-map.org/experiment/show?id=740)).

It was initially thought that the RIP140 gene was monoexonic, but a study characterizing the human RIP140 found via sequencing analysis that the mRNA is actually containing 4 exons, indicating the existence of alternatively splice variants (Fig. 2.14). They also tested the mRNA for the presence of promoters and found only one promoter within the first exon. The search for transcription factor binding sites revealed several putative response elements for transcription factors (Augereau et al., 2006).

2.6.2 Regulation of RIP140 Activity

RIP140 can be regulated by posttranslational modification, however not much is known about the implications of such modifications (Christian et al., 2006). RIP140 is subject to ubiquitination, sumoylation (Rytinki et al., 2008), acetylation, phosphorylation, and methytylation, and a number of these modifications have been shown to affect its function (Mostaqul et al., 2008).

Being a cofactor for nuclear receptors, it is widely assumed that RIP140 will be localised in the nucleus but truth is that its localisation seems to be subject to regulation of alternative signaling pathways. Sumoylation of RIP140 leads to recolocalisation from small nuclear foci to a more diffuse nuclear distribution (Tazawa et al., 2003; Rytinki et al., 2008). Additionally it has been shown that co-expression of RIP140 and PGC-1α affects the distribution pattern of PGC-1α to a granular, nuclear distribution through co-localizing with RIP140 (Rytinki et al., 2009). Interaction of PGC-1α and RIP140 is further modulated by sumoylation of PGC-1α.

RIP140 is also subject to protein arginine N-methyltransferase-1 (PRMT1) mediated methylation which leads to the export of RIP140 from the nucleus, preventing its repressive properties (Mostaqul et al., 2006). This re-localization may inhibit the repressive functions of RIP140 and nuclear export has been shown to be elevated in adipocytes by phosphorylation followed by methylation (Gupta et al., 2008a).

RIP140 null mice fail to accumulate fat and reintroduction of a mouse model with phosphorylation deficient RIP140 was able to rescue this defect (Gupta et al,. 2008b) and the idea has been suggested that RIP140 cytoplasmic localisation may be a supplementary mechanism to move RIP140 away from target promoters and there for enables the expression of genes implicated in fatty oxidation (review Fritah et al., 2010). But the fact that RIP140 gets re-localized to the cytoplasm led to further investigations of potential cytoplasic roles of this cofactor by the group of Wei. They demonstrated that RIP140 interacts with the Rab GTPase-activating protein AS160, leading to its phosphorylation or inactivation by the protein kinase Akt. This leads to inhibition of glucose metabolism by reducing insulin-stimulated glucose transporter type 4 (GLUT4) trafficking and glucose uptake (Wei et al., 2009) (Fig2.17).

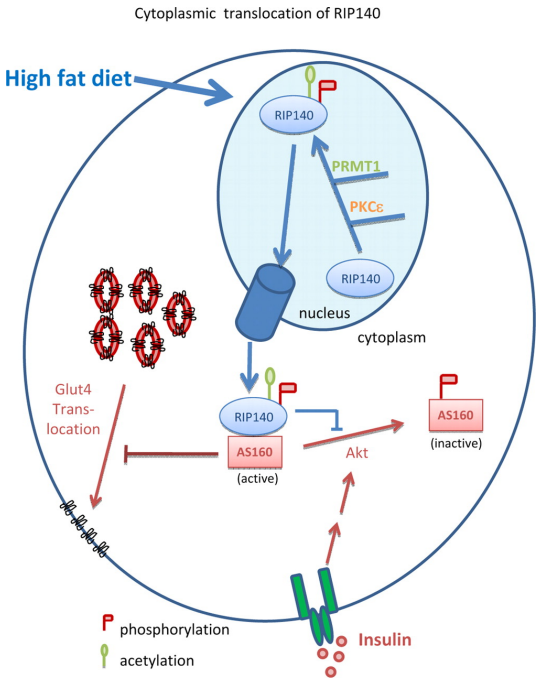


Figure 2.17: Cytoplasmic functions and effects on glucose metabolism by RIP140. A high fat diet will eventually lead to phosphorylation by PKCε or methylation by PRMT1 and subsequent re-localization of RIP140 from the nucleus to the cytoplasm. A Rab GTPase-activating protein, AS160 can interact in the cytoplasm with RIP140 causing inhibition of GLUT4 translocation. Further on The RIP140 AS160 complex can inhibit the Akt inactivation, normally mediated by insulin, which is up taken by the cell.

The same study demonstrated that a high fat diet leads to cytoplasmatic localization of RIP140 in epididymal white adipocytes and it provides first insights into potential mechanisms by which RIP140 impairs glucose metabolism and promotes insulin resistance.

2.6.3 Corepressor vs. Coactivator

Despite the long established understanding of RIP140 acting as a co-repressor, there is now emerging evidence that RIP140 does not only displays inhibitory functions but can also act as a co-activator. In fact RIP140 seems to be remarkable in its ability to function either as a co-repressor or co-activator following its recruitment to target genes. In the liver it has been demonstrated that RIP140 promotes activating function for liver x receptor (LXR) dependent regulation of the transcription factor sterol regulatory binding-protein-1c (SREBP-1c) (Herzog et al., 2007). LXR is a NR that regulates lipogenesis through modulation the SREBP-1c but also forms the active heterodimer complex

structure with PPARs.

Several studies have described RIP140 as a co-activator for various other transcription factors and many cellular responses (Nautiyal et al., 2010; Zschiedrich et al., 2008). RIP140 acts as a transcriptional co-activator for cAMP-response element binding protein, (CREB)-binding protein (CBP) via the N-terminal domain of RIP140, causing up-regulation in the expression of amphiregulin in granulose cells. Interestingly, RIP140 null mice exhibit a deficiency in amphiregulin expression with subsequent failure of ovulation causing the described female infertility (Nautiyal et al., 2010; Tullet et al., 2005; White et al., 2000).

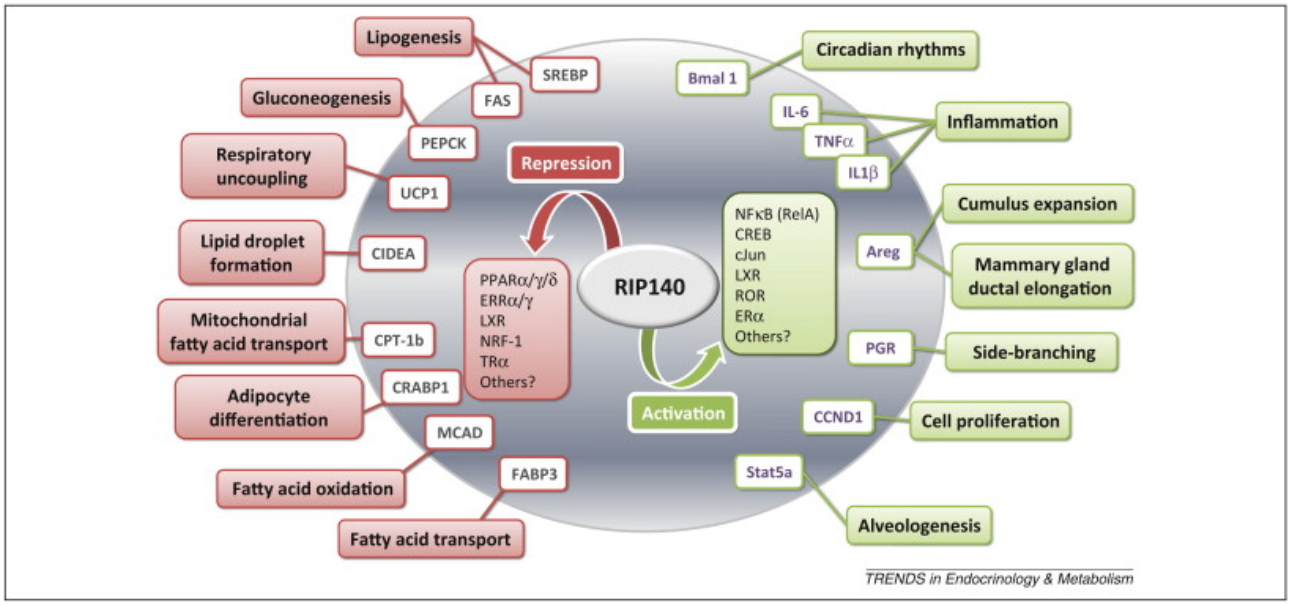


Figure 2.18: Processes and gene targets regulated by RIP140. RIP140 acts both as a co-activator and co-repressor in conjunction with several NRs and other transcription factors; indicated by upwards and downwards arrows, respectively. The inner periphery of the ellipse shows gene targets which are repressed by RIP140 (in red) and those that are activated (in green) against which are mentioned the processes which are affected by these gene targets. Abbreviations: Areg, amphiregulin; Bmal1, brain and muscle aryl hydrocarbon receptor nuclear trans locator (ARNT)-like; CCND1, cyclin D1; CIDEA, cell death activator; Cpt1b, carnitine palmitoyltransferase Ib; CRABP1, cellular retinoic acid binding protein; FABP3, fatty acid binding protein 3; FAS, fatty acid synthase; IL1β interleukin-1β; IL6, interleukin 6; MCAD, medium-chain acyl coenzyme A dehydrogenase; PEPCK, phosphoenolpyruvate carboxykinase; PGR, progesterone receptor; SREBP, sterol regulatory element-binding transcription factor; Stat5a, signal transducer and activator of transcription 5A; TNFα, tumor necrosis factor-alpha; UCP1, uncoupling protein 1 (taken from Nautiyal et. al, 2010).

2.6.4 Effects of RIP140 on the transcription of Inflammatory genes

Inflammatory responses represent a hallmark of numerous pathologies including AD. Zschiedrich et al., studied RIP140s implication on gene expression in macrophages and found that genetic as well as acute deficiency of RIP140 leads to the inhibition of the pro-inflammatory program in macrophages. RIP140 displays this effect by promoting the activity of the nuclear factor ϰ light-chain enhancer of activated B cells (NFϰB) and increases expression of the pro-inflammatory factors tumor necrosis factor α (TNFα) and interleukin-6 (IL6) and interleukin 1β (IL1β) (Zschiedrich et al., 2008). They demonstrated that the RIP140 n-terminal domain interacts directly with a subunit RelA or CBP of NF-ϰB. Importantly, genetic as well as acute deficiency of RIP140 led to the inhibition of the pro-inflammatory program in macrophages. The pro-inflammatory RIP140 action in macrophages and other cell types contributes to insulin resistance susceptibility by triggering cellular cytokine production and release under insulin-resistant or obese conditions, when adipose tissue is characterized by a relative increase in invading macrophages (Zschiedrich et al., 2008).

In line with this, Ho and colleagues found that lipopolysaccharide (LPS) stimulation of kinase Syk-mediates tyrosine-phosphorylation of RIP140 and interaction of the NF-ϰB subunit RelA with RIP140. These events resulted in more recruitment of the E3 ligase SCF to tyrosine-phosphorylated RIP140, which degraded RIP140 to inactivate genes encoding inflammatory cytokines. This shows that under endotoxin tolerance conditions, the degradation of RIP140 results in a loss of RelA binding, which contributes to the alteration of NF-ϰB transcriptional activity on the promoters of several pro-inflammatory cytokines (Ho et al., 2012). Therefore, our aim in this chapter was to define potential alterations in genes involved in AD and inflammation in the brain of RIP140 knockout animals.

2.7 Aims of the thesis

Our hypothesis is that RIP140 affects the progression of AD through the regulation of transcription factors such as PPARγ, which have been found to play an important role in the inflammatory processes linked to AD pathology. The role of RIP140 in the brain is almost unknown. RIP140 may be neuroprotective by affecting Aβ generation and reducing neuroinflammation, since PPARγ affects BACE1 transcription and has a role regulating inflammatory genes. Although the underlying mechanisms are unknown, further preliminary data reveal RIP140 is down regulated in human AD brain.

Together, there is a strong rationale for the urgent investigation of a role for RIP140 as a key regulator of APP

processing and neurodegeneration through regulation of the activity of transcription factors such as PPARγ or NFκB and their effects on inflammation or on the transcription of proteins as BACE1. Therefore, our aims are:

1. Determination of the effects of RIP140 over-expression or knockdown in a neuronal cell-line on the processing of APP, in particular on the expression of BACE1

2. Revealing possible regulation of genes involved or affected by Alzheimer's Disease in a mouse model lacking or over-expressing RIP140

Chapter 3

Materials and Methods

List of primary antibodies

Name	Target Species	Company	Antigen	Application	Dilution
6D7	mouse	Kind gift from Mark Christian	mouse RIP140 protein	WB	1:250
6E10	mouse	Covance	Aβ1-16	WB	1:1000
4G8	mouse	Covance	Aβ17-24	IP	1:100
ApoE	goat	Santa Cruz	ApoE	WB	1:1000
ß-Actin	mouse	Abcam	Actin	WB	1:2000
BACE 1	rabbit	Cellsignal	BACE1	WB	1:1000
CD10	mouse	Santa Cruz	Neprilysin	WB	1:1000
CP13	mouse	kind gift from Peter David	phosphorylated tau	WB	1:1000
p- GsK3	rabbit	Cellsignal	phosphorylated GsK3	WB	1:1000
GSK3	mouse	Invitrogen	GSK3α/β	WB	1:500
Iba1	rabbit	DAKO	activated microglia	IHC	1:500
IDE	rabbit	Abcam	IDE	WB	1:1000
NeuN	mouse	Millipore	neuronal cells	IHC	1:500
R1-57	rabbit	kind girft from	carboxy-terminus of full length APP	WB	1:1000

List of secondary antibodies

Name	Target Species	Company	Application	Dilution
Goat anti mouse IgG	mouse	Jackson Immuno	WB	1:1000- 1:10,000
Goat anti rabbit IgG	rabbit	Jackson Immuno	WB	1:1000
Fluorescent Alexa Flour 488	rabbit	Life technologies	IHC	1:500
Fluorescent Cy5 A105	rat	Life technologies	IHC	1:500
Biotinylated antibody	mouse	Vector laboratories	DAB stain	1:400

In vitro methods

3.1 Cell culture

3.1.1 Neuronal cellline N2a (N2a sw)

The cell line used for the in vitro work of this thesis was a murine neuroblastoma cell line called N2a (sw) which was stably transfected with the APP.695 Swedish mutation [Aminoacidlocation in the polypeptide chain: K594N/M595L]). The original cloning of this gene fused with a c-Myc tag and was inserted into a pCB6 vector (Lo et al, 1994). Selection with 0.4mg/ml geneticin/ G-418 generated the stable cell-line N2a (sw). The cells were maintained in a selective and undifferentiated state using the antibiotic G-418 at a final concentration of 0.2mg/ml in Dulbecco's Modified Eagle's Medium (DMEM) and OPTI-MEM (GIBCO, US), supplemented with 5% fetal bovine serum and penicillin/streptomycin. Cells were grown in a 5% CO2 incubator at 37^{o}C. This cell line was a kind gift from Dr Gopal Thinakaran at the University of Chicago.

N2a cells cultured on sterile 10cm dishes were passaged in ratio's 1:5 - 1:20 every 2 (1:5) - 4 (1:20) days. After washing twice with PBS (137 mM NaCl, 2.7 mM KCl, 10.1 mM Na2HPO4, 1.7 mM KH2PO4, pH 7.4), 500 µL of 0.05% Trypsin EDTA (GIBCO,US) was added on the cells and incubated for 2 minutes at RT. Trypsination was stopped by adding 5 ml DMEM and cells were collected and spun down at 1000g for 5 min. The supernatant was discarded and cell pellet re-suspended. Cell suspension was put on to a fresh culture dish, containing fresh cell culture medium.

3.1.2 Transfections and treatments

3.1.2.1 Transfections

24 hours after cells were seeded, transfections with either cDNA, shRNA or siRNA constructs (table 3.3) were performed.

3.1.2.2 Transfection and cell lysis for Western blot analysis

To transfect RIP140 cDNA (V5-tagged) we used the transfection reagent FuGENE® 6 in a 6:1 ratio (6µL FuGENE® 6:1µL cDNA). Control constructs were used at the same concentration as the RIP140 cDNA plasmid (GFP cDNA insert or empty pcDNA3 vector). Cells were seeded on 6 well plates on day 0 in a ratio of 1:6 from one confluent 10cm dish after (described as above). 24 h after seeding, transfection was performed. FuGENE reagent was pre-incubated in Optimem at RT for 5 minutes. After this incubation, cDNA was added and incubated for another 40 minutes at RT before adding the total mixture to the cells.. 24 h after transfection, the medium was replaced with media containing different PPARγ ligands or vehicle control at different concentrations (see above). 40 hours later, medium was collected for Aβ and APPs analysis and after washing with PBS, cells were harvested in 1x RIPA lysis buffer and medium collected for further analyses. Successful transfection efficiency was estimated by immunocytochemistry and by visualization of the GFP control under a fluorescent microscope. In addition, RIP140 overexpression was confirmed by Western blot using a V5 antibody.

For siRNA transfections, Lipofectamine transfection method was used (Invitrogen). All siRNA's were used at a final concentration of 50nM per well of a 6 well plate, containing 2ml Optimem medium. Prior to mixing the siRNA to form the complex, the Lipofectamine™ 2000 reagent was equilibrated in the OPTI-MEM medium for 5mins. Once mixed with the siRNA, the complex is stable for up to 45mins but was added to the plate after 20mins in a drop-wise fashion. Silencing of the mRNA lasted up to 48hrs upon which protein or mRNA was harvested as detailed elsewhere.

Prior to the experimental in vitro work, endogenous RIP140 and APPsw expression and co-localisation within the N2aSw cell line was determined by Immuocytochemistry, showing that the cells were overexpressing APPsw in the cytosol and that RIP140 was mainly expressed in the nucleus (Fig. 1.1). It is noteworthy, that not all cells were still overexpressing APPsw and that nuclear RIP140 was not detected in every cell nucleus.

Construct name	Source	Application	Assay
GFP cDNA	Dr. Mark Christian (University of Warwick)	control transfection to estimate transfection effiiciancy	Western Blot, fluoresence microscopation
pcDNA3	Dr. Efrat Levy (NYU)	non coding control transfection constructs	Western Blot, qPCR, Luciferase reporter, Aß and CTF quantification
RIP140 cDNA	Dr. Mark Christian and Prof. Malcolm Parker University of Warwick& Imperial College London)	transient over expression of the human RIP140 gene in the N2a celline	Western Blot, qPCR, Luciferase reporter,Aß and CTF quantification
shRNA control	Dr. Mark Christian University of Warwick)	non coding control for silencing endogenous RIP140 in N2a cells	Luciferase reporter
shRNA RIP140	Dr. Mark Christian (University of Warwick)	silencing endogenous RIP140 in N2a cells	Luciferase reporter
non coding siRNA	Gene Pharma	non targeting, scrambled siRNA for silencing endogenous RIP140 in N2a cells	Western Blot, qPCR
siRNA RIP140	Gene Pharma	silencing endogenous RIP140 in N2a cells	Western Blot, qPCR
Rat BACE1 promoter cDNA	Steffen Rossner (University Lepizig)	Overexpression of endogenoys BACE1 promoter combined with luciferase tag	Luciferase assay
PPRE cDNA	Gary Landreth (Cape Western Reserve University)	Overexpression of endogenoys PPAR response element combined with luciferase tag	Luciferase assay

3.1.2.3 Transfections and treatments for qPCR analyses

Transfections and treatments fro qPCR analyses were performed as decribed above for Western Blot analyses. Treatment with Pioglitazone was stopped after 16h and cells were harvested in Trizol reagent. RIP140 overexpression was confirmed by use of special designed human RIP140 Primer, picking up the transfected construct by mRNA expression level. The sequences of used Primer were as followed: Forward Primer: 5'-TTGGAGGGAGGCTTCATCTG-3' Reverse Primer: 5'-GCTTTCGTTTCTGCAG-3'. These primers were designed to produce a template of 81bp in the exon 5 of the human RIP140 gene. RIP140 knock down by siRNA was confirmed using specific RIP140 mouse primer, producing a template that spans the coding sequence and partially the untranslated region of the gene. This way contaminations of the construct used for overexpression and unwanted backround reading could be avoided. The sequences for the Primers were: 5'-CTTCTCGCCCACACAGTACA-3' (forward) and 5'-AAATTTTAAAAAGACCCAAAGTGG-3' (reverse).

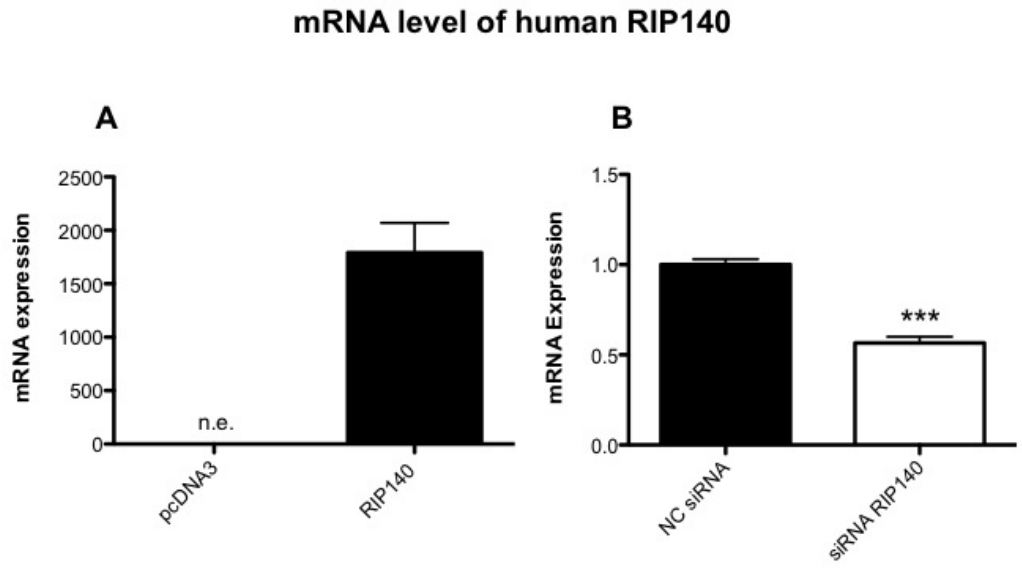


Figure 3.1: Validation of RIP140 overexpression or silencing via qPCR. The cDNA construct used for RIP140 transfection encoded for the human RIP140 gene and primers were designed to pick up overexpressed RIP140 only and no endogenous mRNA. The expression of human RIP140 was around a 1700 fold higher than in cells transfected with control pcDNA3 (A). Transfection with a siRNA targeting RIP140, mRNA expression was lowered for around 50% (B).

3.1.2.4 Confirmation of the efficiency of Transfections by qPCR analyses

Transfections and treatments for qPCR analyses were performed as described above for Western Blot analyses. Treatment with Pioglitazone was stopped after 16h and cells were harvested in Trizol reagent. RIP140 overexpression was confirmed by use of special designed human RIP140 Primer, picking up the transfected construct by mRNA expression level. The sequences of used Primer were as followed: Forward Primer: 5'-TTGGAGGGAGGCTTCATCTG-3' Reverse Primer: 5'-GCTTTCGTTTCTGCAG-3'. These primers were designed to produce a template of 81bp in the exon 5 of the human RIP140 gene. RIP140 knock down by siRNA was confirmed using specific RIP140 mouse primer, producing

a template that spans the coding sequence and partially the un-translated region of the gene. This way contaminations of the construct used for overexpression and unwanted background reading could be avoided. The sequences for the primers were: 5'-CTTCTCGCCCACACAGTACA-3' (forward) and 5'-AAATTTTAAAAAGACCCAAAGTGG-3' (reverse).

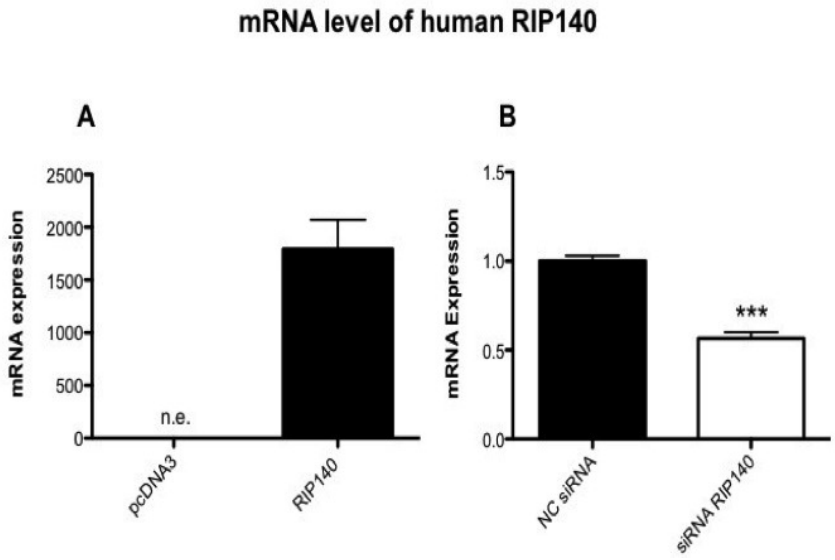


Figure 3.2: Validation of RIP140 overexpression or silencing via qPCR. The cDNA construct used for RIP140 transfection encoded for the human RIP140 gene and primers were designed to pick up overexpressed RIP140 only and no endogenous mRNA. The expression of human RIP140 was around a 1700 fold higher than in cells transfected with control pcDNA3 (A). Transfection with a siRNA targeting RIP140, mRNA expression was lowered for around 50% (B).

3.1.2.5 Transfections and treatments for Luciferase assays

Cells for promoter activity analyses using a firefly luciferase assay system were seeded on 24well plates in a ratio of 1:3. Transfection was performed as described above for Western Blot analyses, but with adjusted volumes and concentrations for 24wells. cDNA concentration per well was not supposed to exceed 0.2[lg and two constructs had to be co-transfected for each well with a concentration of 0.1[lg. Each well received either RIP140 or pcDNA3 and an additional construct for the BACE1 promoter and firefly Luciferase. A 1:100 diluted RLX construct was also added

to the transfection mix in 1:100 ratio (0.2µL per well). The RLX construct was used as a reference in the following luminescence measurement. Each well received 20 µL of the transfection master mix. 24h after the transfection, cells were treated over night (approx. 16 hours) with pioglitazone or PPARγ antagonist T0070907, both at a final concentration of 20µM.

3.2 SDS page and Western Blot analyses

Two different types of SDS pages were used to separate proteins of either whole cell lysates, membrane preparations or Aß peptides. 10% self-made Tris-Glycine polyacrylamide gel were used to separate proteins of whole cell lysates sized between 42 and 140 kD and precast NuPAGE® Novex® 4-12% Bis-Tris Protein Gels (life Technologies), to separate proteins sized 4 to 100kD.

3.2.1 Harvesting methods

3.2.1.1 Harvesting of cells for total protein expression assay

At the end of the treatment, 6 well plates containing cells were kept on ice and medium was collected for Aβ and APPs analysis. Cells were washed once with 1ml PBS. PBS was aspirated and 1ml fresh PBS was added to each well. Using a cell-scraper, cells were collected in PBS from each well and the cell suspension was transferred into a 1.5ml reaction tube and placed on ice. A 10min centrifugation at 6rpm in a bench-top centrifuge was performed to collect cells in a pellet. The PBS was discarded and the cell pellet was re-suspended in 200µL of radioimmunoprecipitation assay buffer (RIPA) (1% Triton X-100, 1% sodium deoxycholate, 0.1% sodium dodecyl sulfate [SDS], 150 mM NaCl, and 50 mM Tris-HCl, pH 7.2) lysis buffer containing Roche Complete® protease inhibitor cocktail, followed by a 10 min incubation on ice. A final 10 min centrifugation at maximum speed was performed after which the supernatant was collected and the pellet discarded.

Bradford analyses Bradford assay protein content of the cell lysates was measured using a commercial 1x Bradford reagent (Bio-Rad). A protein standard containing Bovine serum albumin (BSA) of the specific concentrations of 0, 0.2, 0.4, 0.6, 0.8 and 1[lg /µL was prepared in dd water and used to prepare a standard curve. 10 of each standard was dissolved in 500µL Bradford reagent and 2.5µL of each cell lysate sample. For a duplicate reading, 200 of each solution were transferred into 2 wells of a clear 96well plate. A Molecular Devices plate reader and the softMaxPro

10% separation gel		stacking gel	
Reagent	Volume	Reagent	Volume
Water	4.85ml	Water	1.9ml
Tris-HCL ph 8.8	2.5ml	Tris-HCL ph 6.8	315µL
Acrylamide	2.5ml	Acrylamide	250µL
10% SDS	100µL	10% SDS	25µL
APS	50µL	APS	12.5µL
TEMED	5µL	TEMED	2.5µL

Table 3.2: Compounds and Volumes to cast one 10%SDS Mini gel (Biorad), 1.5mm spacer and volumes for relating stacking gel.

software were used to measure protein concentration using the settings for Bradford assay. Only readings with standard curve R square value of 0.97 or higher was used to measure protein concentration of the samples. 4 to determine final protein concentration multiplied values for the sample readings.

3.2.1.2 Subcellular fractionation for C- terminal fragment expression assay

Cells were washed and collected in PBS as described above. Instead of RIPA, 500µL hypertonic buffer (10mM Tris-HCl, 1mM EDTA, 1mM EGTA) containing Roche Complete® protease inhibitor cocktail and left on ice for 10min. Passing mechanically ruptured the cells through a 0.6ml gauge needle for 15 times. A centrifugation at 6000 rpm for 10 min at 4^{o}C was performed to pellet the nuclear fraction. The supernatant containing the membrane and cytosol was transferred to a fresh tube and subsequently centrifuged at 13 000 rpm for 45 min at 4^{o}C. The pellet containing the membrane fraction was taken for further for measuring APP CTFs. The pellet was finally re-suspended in 2X NuPAGE® sample buffer (Invitrogen). All steps of procedure were carried out on ice.

3.2.2 SDS page and Western Blot immunoblotting

To quantify the levels of proteins in either cell lysates or brain lysates, proteins were separated in order of their size using a 10% polyacrylamide or NuPAGE® Novex® 4-12% tris-tricine gels. 10% polyacrylamide gels were casted according to the instructions in table 3.4. To quantify Aß peptides and CTF's, pre-casted NuPAGE® Novex® 4-12% Bis-Tris gels were used.

Between 40-60[lg of cell lysates and between 30-40[lg of brain lysates were loaded. A 2x SDS sample buffer (50mM Tris-HCl pH 6.8, 2% sodium dodecylsulfate, 10% glycerol and few grains of bromophenol blue made up in ddH20) containing 10% ß-Mercaptoethanol was added to each sample with the identical volume of the sample volume . The ß-

Mercaptoethanol was added freshly each time before adding to the samples and sample buffer was not reused. Samples were boiled for 5 min at 95°C, loaded into the wells and run for 10 min at 85V, mA at constant voltage to let the samples gently enter into the gel. Once the entire samples had entered the stacking gel, the voltage was increased to 120 V and gels were left until the front reached the end of the gel. 10% acrylamide gels were run in a standard, Tris-Glycine buffer (25 mM Tris-Cl/250 mM glycine/0.1% SDS). NuPAGE® Novex® 4-12% Bis-Tris gels were run in commercially available MES buffer (life science technologies) . The separated proteins on the SDS page were transferred to either PVDF or Nitrocellulose membrane, both with 0.45 pore size. For most of the proteins isolated from cells or brain homogenates PVDF membranes were used; however, for Aß, CTFs and Neprilysin gels were transferred to Nitrocellulose membranes. The transfer was performed in Tris Glycine buffer containing 20% freshly added methanol at constant 400mA for one hour. After the transfer, membranes were blocked in 5% semi skimmed milk in TBS-T or 5%BSA in TBS-T and left on a rocker for one hour at RT. Membranes were washed 3 times with TBS buffer (50 mM Tris-Cl, pH 7.5. 150 mM NaCl) containing 0.05 % Tween 20 reagent (TBS-T) and then incubated with primary antibodies. All primary antibodies were diluted in 1%BSA containing 0.1% sodium acid in TBS. The incubation took place at 4ºC on a 8-roller with incubation times varying between overnight and three days. Weak antibodies such as Neprilysin, BACE1, p-GsK3 and 6E10 were incubated for a whole weekend. Following this, the first antibody was washed 3x with TBS-T buffer and then incubated with secondary HRP antibody diluted generally 1:3000 in 5% milk-TBS-T for 1 hour at RT, shaking on a rocker. Other three washing steps for 10 min were performed before membranes were incubated with ECL and then developed using a Image Quant LAS 4000 developer machine (GE healthcare life sciences). Two different types of ECL solution were added to the membranes and incubated between 1 and 5 min, depending on the strength of the signal. ECL super signal was used for weak antibodies like BACE1, p-GsK3- Neprilysin, and 6D7 and incubated for 5 min on the membrane at RT. For all other membranes, a "standard" ECL was used and incubated for 1 min. Both ECL were purchased from Thermo Scientific (SuperSignal West Pico Chemiluminescent Substrate and Pierce ECL Western Blotting Substrate). To further test other primary antibodies with the same membranes, the blots were stripped by incubating with ReBlot Plus Strong Antibody Stripping Solution (Millipore) for 20 minutes at room temperature, followed by washing for 3x 10 minutes with TBST and blocked with milk for 1 h. New primary antibody could then be added to the blot and the procedure for development repeated. Digital images were quantified by densitometry using ImageJ software and normalized to total protein level using β-actin as a loading control. Every single band was framed with the square selection and the same sized square was

moved from band to band for measurement. The integrated density was measured of each individual bands and their relating background. The background was then subtracted from the band measurement and the number was then divided through the integrated density of each band from the corresponding actin Western Blot image. The actin bands have been measured in the same way.

3.3 Analyses of Ribonucleic Acids (RNA)

RNA was isolated to estimate mRNA level for different genes of interest. Total RNA was harvested and transcribed into cDNA and used for real time PCR analyses.

RNA from N2a (sw) cells and hippocampus sections and frontal cortex sections of the mouse RIP140 transgenic and RIP140 knock out mouse lines was prepared using a Trizol-Chloroform extraction (TRI Reagent®, Sigma). Cells and tissue were directly lysed with Trizol. N2a (sw) cells, were grown on a 6well plate, washed twice with RNAse free PBS and lysed with 1ml Trizol on the well for 5min at RT. Brain tissues were homogenized in 1 ml Trizol using a Ultra-thorax homogenizer at maximum speed for 30-60sec and left on ice for 20min. RNA Isolation followed immediately after lysis.

3.3.1 RNA Isolation

During the whole preparation, samples were kept on ice and all centrifugation steps took place at 4^{o}C only. All tubes and tips were RNAse free, all surfaces and pipets were wiped with RNaseZAP™(Sigma) and gloves were permanently worn and changed regularly. Trizol reagent was stored at 4^{o}C and chloroform, 75% Ethanol and Isopropanol were all stored and pre-chilled at -20^{o}C. To each 1ml Trizol sample lysate, 200µL of ice cold Chloroform was added. Tubes were mixed by inverting them 15 times and incubated at RT for 10 min, followed by 30 min centrifugation in a bench-top centrifuge at maximum speed. After this step the sample will have subdivided into 2 phases, the upper clear phase containing RNA and the lower pink phase with a white intermediate layer on top. The upper clear phase, around 500µL, were transferred into a fresh Eppendorf tube. The equivalent volume of ice-cold isopropanol was added and after 15 sec. vortex mixing the samples were left at RT for 15 min for precipitation. Another 30 min centrifugation at maximum speed was performed to pellet the precipitate. The entire supernatant was carefully removed and discarded. The small, white pellet was washed in 1ml 75% ethanol for 30 min centrifugation at maximum speed. The entire ethanol supernatant was discarded and samples were spun for another 20 sec to collect ethanol remains to collect and

discard them so that the pellet could be left as dry as possible. The tubes were left with open lids under a fume hood for another 10 min to allow the pellets to dry properly. Depending on the pellet size, pellets were re-suspended in between 10 and 50μL of RNAse free DEPC water. RNA yield was measured using a nano-drop spectrophometer. The 280/260nm ratio lay at 2.00 highest and lowest allowed lay at 1.87. 1[lg of RNA was used for the up following procedures.

3.3.2 Digestion of genomic DNA with DNAse

Digestion of genomic DNA was perform to remove possible DNA remains or contaminations from the RNA isolation (DNase I Amplification Grade, Sigma). During the real time PCR, genomic DNA would give a false background reading and the result would not be representative.

1μg RNA was topped up with RNAse free water to a total Volume of 4μL. 0.5μL of DNAse enzyme and 0.5 of the 10x reaction buffer were added to each tube individually, followed by a 15 min incubation at RT. The reaction was stopped with 0.5 μL EDTA stop solution and incubated at 60^{o}C for 10 min in a thermocycler. Samples were put on ice and transcription into cDNA was performed immediately.

3.3.3 Reverse Transcription Polymerase Chain Reaction (RT PCR)

In order to perform real time PCR, RNA samples had to be transcribed into cDNA. Two master mixes were prepared separately and added to each RNA sample. The first one contained dNTP's and random hexamers and 4.5μL Master mix were added to each sample and incubated in a thermocycler for 10 min at 70^{o}C (table 1.2), followed by a 2 min incubation on ice. The second master mix contained the revers transcriptase enzyme and 10μL of it were added to each sample. Reverse transcription took place in a thermocycler with a specific program as described in table 1.2. The total reaction volume at the end of the reaction was 20μL and was topped up with 180μL DEPC water. Reagents for reverse transcription were purchased from Sigma (M-MLV Reverse Transcriptase Kit).

Reagent	concentration	1x Volume in µL
dNTPs	10mM	1
Random Hexamers	10mM	1
Water	-	2.5
RNA sample	-	5.5
total Volume per reaction	-	10

Table 3.3: Master mixes used for reverse transcription PCR. After the genomic DNA digestion, 4.5µL of the first Master mix, containing dNTPs and random Hexamers, were added to the DNAse treated RNA sample. After pre-annealing of the first master mix for 10 min at 70^{o}C in a thermocycler, 10µL of the second master mix containing the reverse transcriptase enzyme were added to each tube and reverse transcription was performed.

Reagent	concentration	1x Volume in µL
MMLV buffer	10x	2
MMLV reverse Transcriptase	200U	1
Water	-	7
total Volume per reaction	-	20

3.3.4 Quantitive Real time Polymerase Chain Reaction (qPCR)

To evaluate mRNA of specific genes level in N2a (sw) and brain tissue samples, qPCR was performed from the obtained cDNA as described above. 4µL of each cDNA sample were used for one well in a 96well plate and duplicates for each sample were pipetted. A master mix was prepared according to the instructions in table 1.3.. For each gene, a seperate master mix was prepared adjusted to the number of samples, containing a specific set of primer for the selected gene. Primer were designed using the NCBI primer design tool (http://www.ncbi.nlm.nih.gov/tools/primer-blast/). The qPCR was performed in a thermocycler from life technologies (StepOnePlus™ Real-Time PCR Systems) which also supplied the software for data analyses. Data was further analysed with Exel software. All genes were normalized to houskeeping genes which were in our case GAPDH, Actin and L19.

reagent	concentration	1x Volume in µL
SYBR mix	-	10
ROX reference dye	25mM	0.2
Forward Primer	20µM	0.3
Reverse Primer	20µM	0.3
Water	-	5.4
total Volume		20

Table 3.4: Master mix mixture for quantitive real time PCR. All volumes are shown for one reaction (1x) and the number was multiplied by the number of samples plus one for the negative control.

Step	Temperature in ^{o}C	Time in min	cycle repeat
1	94	2:00	1
2	94	0:15	40
3	60	1:00	
4	72	1:00	

Table 3.5: Cycling conditions for quantitive real time PCR

Direction	Gene	Sequence 5'–> 3'
Forward	ApoE	GGGACAGGGGGAGTCCTATAA
Reverse		ATTGGCCAGTCAGCTCCTTC
Forward	BACE1	CTCAAGATGGACTGCAAGGAG
Reverse		AATGTTCCAAGGGGTCGTGC
Forward	BACE2	TGGTGGCCCAAGCAAAGATT
Reverse		CCCACCCAGGACAAGACTAC
Forward	cdK5	AGAAGATTGGGGAAGGCACC
Reverse		TCATCATCCAGCCTGACACG
Forward	GAP43	CTGAGGAGGAGAAAGACGCTG
Reverse		AGGCATGTTCTTGGTCAGCC
Forward	GsK3	TTGGACAAAGGTCTTCCGGC
Reverse		AGCTTCCAGTGGTGTTAGCC
Forward	IDE	CCAAGGAGCAGCTTGGCTAT
Reverse		TGAAGCGCAAGCCTTGGATA
Forward	IgF2	CTTCGCCCGCTGTTCGG
Reverse		GGATCCCCATTGGTACCTGGAAG
Forward	Mtap1	AGCAAAGTTCAGTCAAGATGTGG
Reverse		TTTGTACATTTCCGCCCCCA
Forward	Mtap2	TTAACCAACCACTGCCGGAC
Reverse		AGTAACAATTTGTACCTGACCCC
Forward	Neprilysin	GCCGAAACTACAAGGAGTCCA
Reverse		TGACGTAGTTAGCACACCGT
Forward	RIP140	GCTTTCGTTTCTGCAG
Reverse		TTGGAGGGAGGCTTCATCTG

Table 3.6: List of qPCR primer. The following primer was used to evaluate gene ex- pression of the indicated genes. Forward and reverse primer was designed with the NCBI primer design tool in 5'–> 3' direction. (http://www.ncbi.nlm.nih.gov/tools/primer-blast/index.cgi?ORGANISM=10090&INPUT_SEQUENCE=NM_173440.2&LINK_LOC=nuccore)

3.4 Luciferase Promoter Activity Assay

In this assay a firefly luciferase gene has been used as a reporter gene to assess the activity of a specific promoter, which was in our case either a promoter for BACE1 or a PPARγ-Response element. The reporter gene was attached directly to the promoter, which allowed assessment of the activity of the promoter. Each time a promoter was read, the luciferase reporter gene was transcribed into mRNA and translated into the protein. This protein contains luciferin, a light-emitting compound, found in many firefly (Lampyridae) species. The activity of the BACE1 promoter was determined by measuring luciferase activity in a luminometer. N2aSw cells were transfected with the rat BACE1 promoter fused to the Firefly luciferase reporter gene and co-transfected with the CMV-Renilla luciferase normalising construct in a 400:1 ratio. The 1.5kb BACE1 promoter region was originally cloned from a highly conserved region upstream of the rat BACE1 coding region. Homologous sequences from rat, mouse and human are highly conserved and contain multiple putative binding sites for transcriptional regulators (Lange-Dohna et al., 2003). Therefore this luciferase construct is and has been a reliable method for assaying BACE1 promoter activity in both mouse and human cells and has done so before (Sastre et al., 2006a, Bourne et al., 2007). BACE1 promoter activity and TOP/FOP flash reporter assays were carried out on a luminescence reader following the protocol for the Promega dual reporter assay®. The data was normalised to the Renilla luciferase expression to allow for varying transfection efficiencies. The chemical reaction catalyzed by firefly luciferase takes place in two steps:

1) luciferin + ATP → luciferyl adenylate + PPi

2) luciferyl adenylate + O2 → oxyluciferin + AMP + light

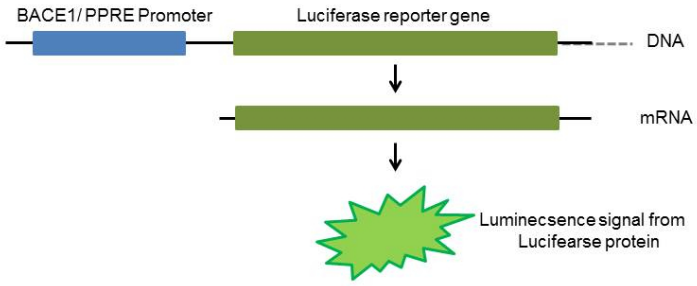


Figure 3.3: The luciferase reporter gene has been put under the control of a specific BACE1 promoter so that expression of the Luciferase protein represents how often the BACE1 promoter was read. After protein translation a biochemical reaction of lucefrin, which is part of the luciferase protein will induce a light signal, which can be measured. A higher light signal indicates a higher promoter activity.

The light signal at the end of the reaction is measured with and taken as an indicator for the promoter activity. To measure the luminescence light signal, samples were read in a plate promega plate reader using a pre set up protocol for luciferase assays.

3.5 Immunocytochemistry

The subcellular localization of RIP140 and APP was detected in N2a cells overexpressing APPsw and RIP140 grown to 70% confluence on sterilized coverslips. Cells were washed once in sterile 1X PBS and then fixed and permeabilized in 100% methanol for 10 mins at -20^{o}C. The cells were then rehydrated with PBS and blocked in 10% bovine serum albumin (BSA) made up in PBS for 10 minutes at RT. Cells were washed 3x in PBS. Primary antibodies were prepared in 1% BSA in PBS. A monoclonal mouse anti RIP140 was used at 1/500 and full length APP was detected by R1-57 at 1/100. Cells were incubated with the primary for 1 hour at 37^{o}C in a humid chamber to prevent coverslips from

drying out. Secondary Anti-Rabbit Alexa Fluor 488® (Invitrogen, US) and an anti-mouse Alexa Fluor 594® were used at 1/200 for 1hr at 37C. The coverslips were mounted onto glass slides using Vectashield mounting medium with a DAPI counterstain (Vector Laboratories, Burlingame,CA) and observed under confocal microscope.

3.6 ELISA

The levels of Aβ40 and Aβ42 were determined in the media of N2asw cells using a kit from Millipore. Concentrations were quantified according to the manufacturer's instructions.

In vivo methods

3.7 Animal work

3.7.1 RIP140 Mouse lines

N-RIP knock out line

The complete coding sequence and 3' un-translated sequence of Nrip1 is contained in a single exon, and this genomic organization is conserved among vertebrate species; the relative positions and specific sequences of the nine leucine motifs are also highly conserved in human and mouse and in chicken. Mouse Nrip1 was deleted by homologous recombination in embryonic stem cells. The complete coding sequence was replaced with a cassette containing an internal ribosome entry site and a lacZ−neo fusion gene (IRES GEO), except for the first 27 amino acids, which allowed both selection of recombinant clones and analysis of the expression of -galactosidase as a marker for Nrip1 expression. Homologous recombination was verified by analysis of genomic DNA (Fig 3.2 b) and established two lines of Nrip1-null mice (called RIP knockout (RIPKO)) from independent clones of embryonic stem cells.

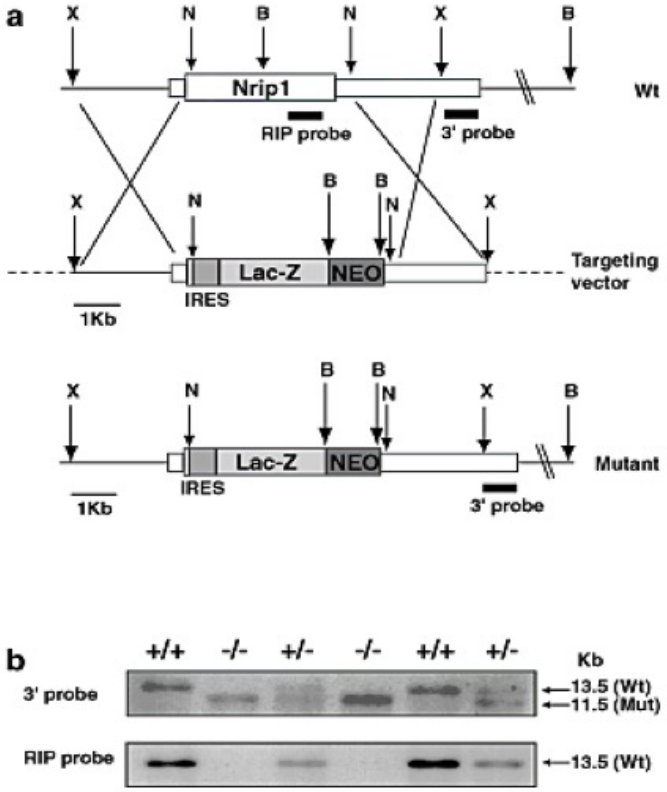


Figure 3.4: Genomic organization of mouse Nrip1. A 3.6-kilobase fragment containing the complete open reading frame of Nrip1, with the exception of the first 27 amino acids, was removed using NsiI and was replaced with an IRES NEO cassette to generate the targeting vector. Short thick black horizontal lines, positions of the 3' probe outside the targeted region and the RIP140 probe. B, BamHI; N, NsiI; X, XbaI; Kb, kilobase; Wt, wild-type. b, Southern blot analysis of DNA samples from wild-type (+/+), heterozygous (+/-) and RIPKO (-/-) mice, digested with BamHI. Wt, wild type; Mut, mutant. Right margin, molecular sizes (taken from White et al., 2000)

Mice used in this study were backcrossed eight generations to C57BL/6J background. Animals were maintained under standard conditions, with controlled light and temperature, and fed a chow diet ad libitum. Only males were used and sacrificed at 9 months of age, except the two used for the expression array, which were two males at the age of 2 months. Animal's gender and ages were used as followed:

For Immuno: -WTs:3 males, 9 months old -Heterozygous 3 Females 9 months old -Knockouts: 3 Females 9 months old

For Western: -WTs: 4 Males 9 months old -knockouts: 5 Males 9 months old

N-RIP transgenic line

RIP140 transgenic mice were generated by inserting human RIP140 (hRIP140; NRIP1 – Human Gene Nomenclature Database) in FVB/N background using a pCAGGS-hRIP Vector (Fritah et al., 2010; Nautiyal et al., 2013). The Vector was modified by changing a XhoI site (1726 nucleotides) to a Spe I site and a Hind III site (2275 nucleotides) to a Sal I site. The human RIP140 sequence was inserted at 1726 nucleotides using the Spe I site. The pCAGGS-hRIP vector was then digested using Sal I and the fragment containing the CMV enhancer, beta actin promoter and hRIP cDNA and β-globin polyA sequence was injected into the male pronuclei of a one-cell stage blastocyst. Transgenic mice were identified by PCR using primers 5'- CGCCGCCGTCCCCTTCTCCAT-'3 and 5'-TTGTCAACGGCAGTACCTGA-'3. The mice generated had access to food pellets ad libitum and were kept on a 12-hour light and dark cycle. Primers used to determine the expression of human RIP140 are as follows: forward primer 5'-ACA TTTGGAGGGAG-GCTTCA T-3', reverse primer 5'- GCTTTCGTTTCTGCAGTAGGAAGTA-3'. Primers used to detect both mouse and human RIP140 (total RIP140) are as follows: forward primer 5'- ACTCATGGAGAAGAGCTTGG - 3', reverse 5'-AATGACTGAAGCAAAGAGGC-3' . FVB/N wild-type (WT) littermates were used as controls. All animal studies were carried out in accordance with the UK Home Office guidelines. Animals gender and ages were as followed: For Immuno: -WTs: 6 females, 5 months old -Tg:3 females, 5 months old

For Western: -WTs: 6 males, 5 months old -Tgs:5

3.7.2 DNA extraction from mice ear snips

Ear snips were incubated with 500μL of a digestion buffer (50mM Tris-HCL ph 8.0; 100mM EDTA; 100mM NACl; 1% SDS) containing proteinase K at 55^{o}C overnight in a eppendorf shaker with continuous shaking. The next day, samples were spun down and the supernatant transferred into a new tube. To precipitate DNA, 600 μL of chloroform, stored at -20^{o}C, was added to the tube, vigorously shaken and spin precipitated for 10 min in a bench top centrifuge at maximum speed. The supernatant was discarded and NaCl oversaturated solution ($>$ 6M) added. Two volumes of ice cold Ethanol (stored at -20°C) were added and the sample were stored for one hour at -20^{o}C. After a final centrifugation at maximum speed for 10 min, the supernatant was carefully removed, the pellet dried in a speed vac at medium drying rate for not longer than 10 min and re-suspended in 100μL DEPC treated water.

Reagent	concentration	1x Volume in µL
Buffer	10x	2.5
dNTPs	0.5	100mM
Forward Primer	20µM	1
Reverse Primer	20µM	1
DNA Polymerase	1unit/µL	1
Water	-	17
Total Volume	-	25

Table 3.7: Master mix for genotyping PCR

3.7.3 Genotype Polymerase chain reaction for RIP140 knock down animals (genotype PCR)

To determine the genotype for each animal a PCR with two sets of primer was performed. The possible outcomes were:

- homozygous knockout
- heterozygous
- wild-type

As previously described, the LacZ gene has been used as a knock in to replace the RIP140 gene and primer designed for LacZ will show heterozygous or knockout specific expression of it. For each sample, two master mix were prepared (table 3.8), one containing primer for LacZ (LacZNeo forward 3'-CCGGTCGCTACCATTACCAG-5'; LacZNeo reverse 3'-CCGATTGTCTGTTGTGCC-5') and the second one containing primer for RIP140 (RIP140 forward 3'-GAGTCATCCCATCCCGCA-5'; RIP140 reverse 3'-GCAAGTCTTTCGCTTGCC-5'). To each mix, 2.0uL of ear snip prepared DNA was added and cycled under conditions as listed in table 3.9 10 uL of the reaction was separated on a 1.5% agarose gels at 120V. Bands for LacZ could be found at the size of 150 base pairs (bp) and for RIP140 at

250 bp. If a sample had one band for LacZ and one for RIP140 it was heterozygous and with two bands for LacZ a homozygous knockout. Genotyping for the transgenic mouse line was not required as they were genotyped previously by Jenny Steel. The genotype of RIP140 null and transgenic mice was determined by genotyping.

3.7.4 Harvesting, dissectioning and storage of brain tissue

Animals were anesthetized and transcardially perfused with ice-cold phosphate-buffered saline (PBS) (0.1 M, pH 7.4). Brains were rapidly removed, and the right hemisphere was immersion fixed in 4% paraformaldehyde in PBS (0.1

Step	Temperature in ^{o}C	Time in sec	cycle repeat
1	94	180	-
2	94	45	35
3	55	45	
4	72	30	
5	72	300	

Table 3.8: Cycling conditions for genotying PCR. Master mix mixture for quantitive real time PCR. All volumes are shown for one reaction (1x) and the number was multiplied by the number of samples

M, pH 7.4) for 48 hours and then cryoprotected in 20% sucrose in PBS (0.1 M, pH 7.4). The left hemispheres were dissected in different areas (including cortex and hippocampus), snap frozen, and stored at -80 °C until protein or RNA isolation (Katsouri et al, 2014).

3.7.5 ELISA assays

Total brain homogenates from the hippocampal and frontal cortex areas were used for all the ELISAs. For the endogenous mouse Aβ1-40 and Aβ1-42 ELISAs (Millipore) we analyzed 200 mg per well and for the interleukin (IL)-1β and the tumor necrosis factor IL-6 ELISAs (Preprotech) 50 mg per well. Concentrations were quantified according to the manufacturer's instructions

3.7.6 Immunohistochemistry (IHC)

Brain serial sagittal sections (40 [lm) were collected with a vibratome (Leica VT-1000S) and kept in Tris-buffered saline (TBS) pH 8.0 supplemented with 0.05% sodium azide. Briefly, sections were treated for 20 minutes with 0.6% H2O2 in TBS, permeabilized in TBS Triton X-100 0.25% (TBS-Tx) for 30 minutes, and blocked for 1 hour with 10% fetal bovine serum (FBS) in TBS-Tx 0.1%. For Ab staining, an additional step of antigen retrieval was performed before permeabilization with 98% formic acid for 5 minutes. All the antibodies were incubated overnight at 4 °C (anti- NeuN, 1:500; anti-GFAP 1:500, anti-IBA1 1:500) in 1% FBS in TBS-Tx 0.02%. The following day, the sections were incubated with the appropriate secondary antibodies (1:200; Vector), followed by enhancement with avidin-biotin complex (ABC; Vector). The staining was visualized using diaminobenzidine (DAB; Sigma). Images were acquired with a Leica DM2500 microscope connected to a camera (Q-Imaging Micropublisher 3.3 RTV) using the Q-capture Pro software (Katsouri et al, 2014).

3.7.7 Quantification of NeuN, GFAP, and IBA1 staining

GFAP and Iba-1 staining's were quantified using the ImageJ software (National Institutes of Health) as previously described (Katsouri and Georgopoulos, 2011). Briefly, the images were converted to 16-bit grayscale images, thresholded within a linear range, and the percentage of the area covered by Iba-1 or GFAP staining was calculated separately for the hippocampus and the cortex. The mean intensity of the staining was estimated in at least 4 sections per animal. The neuronal density was quantified in the subiculum area of the hippocampus. The NeuN-positive cells were quantified in the CA3 area in 6 independent sections (240 mm apart) for each animal (n $\frac{1}{4}$ 5) using the Image Pro-Plus software (Media Cybernetics). Because of the high density of neurons in the Dentate Gyrus (DG), CA1 and subiculum, the thickness was quantified as the area covered by NeuN cells using Image J (National Institutes of Health) (Gomez-Nicola et al., 2014; Turner et al., 2011).

3.7.8 Human post mortem samples

Human brains were obtained from routine autopsies at the Huddinge Brain Bank in accordance with the laws and the permission of the ethical committee. The control group included frontal-cortex from subjects who died either of non-neurological diseases or traffic accidents and had no history of long-term illness or dementia (76yrs ±6: 4F, 2M). The sporadic AD group included the frontal-cortex samples from patients with clinically and pathologically confirmed AD (81yrs ±2: 5F, 2M). The frozen tissue was crudely fractionated to give a nuclear, membrane and cytosolic fraction. Samples were kept at -80°C until used.

3.8 Statistical analyses

Data were analyzed with GraphPad prism, using unpaired Student t tests or 1-way analyses of variance (ANOVA), and followed by Tukey post hoc analysis. Probability values less than 0.05 were considered significant. All data are expressed as mean± standard error of the mean.

Chapter 4

Results I: Effects of RIP140 expression on APP processing in vitro

4.1 Introduction

According to the amyloid hypothesis, proposed by Hardy and Selkoe (Hardy and Selkoe, 2002) accumulation of Aβ deriving from the "miss-cleavage" of APP in the brain is the primary influence driving AD pathogenesis. A lack of understanding why this occurs and which are the factors triggering this event have been disclosed during the past decades. One of the hypotheses is that elevation in BACE1 protein expression and its increased activity found in AD brains (Ahmed et al, 2010) puts this gene into a position for a prime target to regulate Aβ pathology. Approaches to inhibit BACE1 function were made suggesting that blocking Aβ production by inhibiting the first protease required for its generation, may be the next step in blocking AD progression. However some of the results obtained during clinical trials raised some criticism as side effects, such as liver damage, occurred (May et al, 2013). Although BACE1 expression level reaches high values in the brain tissue, it has to be kept in mind that it is globally expressed throughout the human body and that it serves physiological relevant functions in other tissue that could be harmed by its inhibition. Some of its biological functions are also relevant within the brain, as BACE1 has recently shown to be involved in Neuregulin 1 (NRG1) cleavage with an impact on myelination of neuronal fibers (Velanac et al., 2012). Inhibiting BACE1 seems therefor risky and a regulative strategy affecting its relative expression and activity level rather than

losing all of its biological function may appear more sensible.

BACE1 transcription is regulated by various transcription factors (Rossner et al., 2006). The nuclear receptor PPARγ was described to modulate mRNA, protein and promoter activity level of BACE1 (Sastre et al., 2006). A cell line lacking PPARγ was used to determine if and how promoter activity was possibly regulated and it was demonstrated that cells lacking PPARγ have increased BACE1 promoter activity. This effect was reversible through PPARγ cDNA transfection, suggesting the specificity of the action of PPARγ on BACE1 promoter activity. Interestingly they discovered that within the BACE1 promoter region lays a PPAR response element (PPRE) and it is likely that PPARγ suppressive actions works through binding to this element. During the same study it was established that PPARγ expression in post mortem brains of AD patients is lower that healthy individuals. Another study by Heneka et al. could also demonstrate that administration of artificial and highly selective PPARγ agonist Pioglitazone lowered glial inflammation and Aβ42 levels in a mouse model of AD (Heneka et al., 2005).

Our group recently demonstrated that the beneficial effects of PPARγ stimulation by drug treatment on Aβ generation are also observed by transfection with co-factors such as PGC-1α (Katsouri et al., 2011). PGC-1α has co activating effects on PPARγ and we found that overexpression of PGC-1α lead to an efficient decrease of Aβ and BACE1 transcription in N2aSW cells. This result has also been confirmed by the group of Giulio Pasinetti (Wang et al., 2013). Additionally, we found out that PGC-1α levels are reduced in the brains of AD patients, just like what happens with PPARγ, Not much is known about RIP140, another co factor for PPARγ, regarding its potential beneficial effects on APP processing. So far, only one study in the brain could show that mice lacking RIP140 had cognitive and memory impairments (Duclot et al, 2012). Therefore, one of the aims of this study was to investigate whether RIP140 has potential effects in the processing of APP, as it happens with other co-activators of PPARγ. For this purpose, we analysed the expression of RIP140 in the brain of AD patients and determined if and how APP processing could be affected by RIP140, using the same in vitro cell model and the same approach as previously carried out in our group for studies analyzing the role of the PGC-1α

4.1.1 Determination of RIP140 levels in the post-mortem brain from AD patients

We determined whether the expression of RIP140 was altered in AD patients, comparing brain samples from AD patients with age-matched healthy control brains. We performed IP/Western blotting experiments with antibody 6D7 in nuclear extracts from brain cortex from 7 AD cases and 6 controls. The results indicate that RIP140 expression is

reduced in AD patients compared to healthy controls.

4.2 Results: RIP140 affects APP processing *in vitro*

Because RIP140 seems to be down regulated in AD brains, our objective was to determine whether changes in its expression may modify the processing of APP, in particular BACE1 transcription.

4.2.1 Human RIP140 localizes to the nucleus and can efficiently be transfected into N2a cells

RIP140 has been described to either have activating or repressive functions in various cell types and tissues. Its activation status seems linked to its localization within the nucleus of the cell, since it is a transcriptional regulator. RIP140 has not been investigated in neuronal cultures in vitro, therefore it was crucial for us to be able to induce human RIP140 expression using an expression vector and if expressed, to determine its localization. When transfecting a human construct of RIP140 into the neuronal N2aSw cell line we demonstrated that its localization was exclusively nuclear (Fig.4.3). The cell line N2aSW has previously been stably transfected with human APP carrying the Swedish mutation, because it secretes enough Aβ to be detected by Western blot. We showed that cells stably transfected with APPsw do take up the newly introduced hRIP140 cDNA and express both proteins simultaneously but in different cell compartments, in the cytosol (APPsw) and nucleus (RIP140). DAPI (blue) was used to stain nuclei of all cells, indicating that not all cells were overexpressing RIP140 and/ or APPsw. In fact, some cells were overexpressing RIP140 or APPsw alone (data not shown) while some cells did not express enough levels of those proteins to be detected by immunocytochemistry.

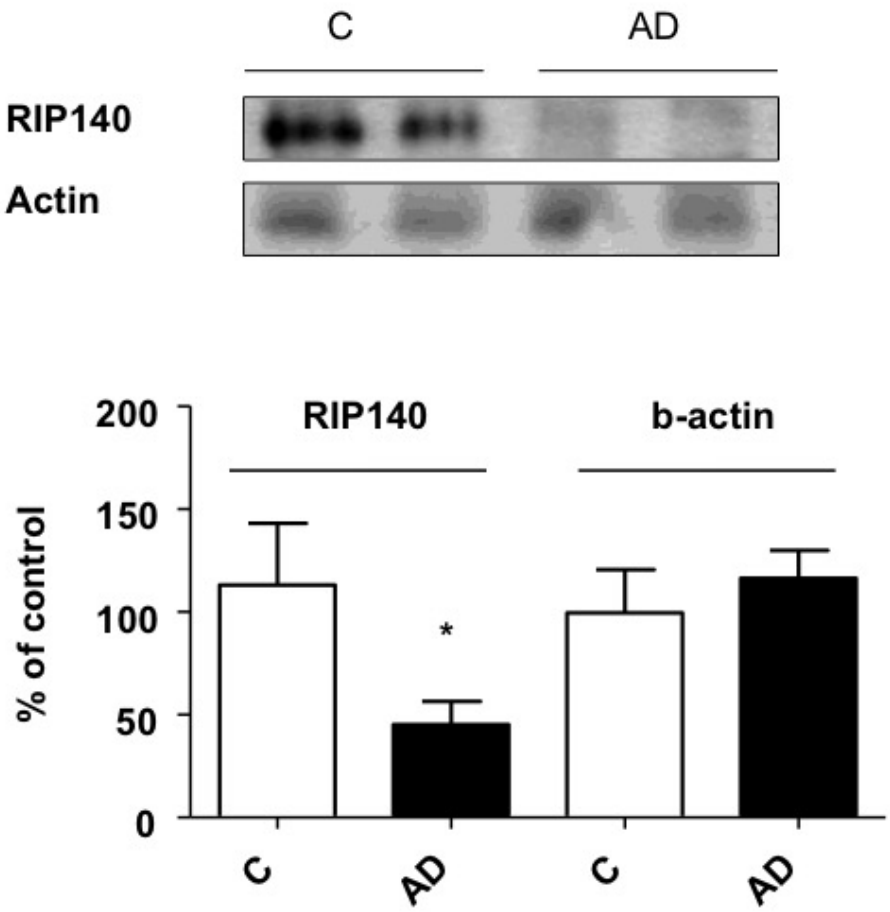


Figure 4.1: RIP140 is decreased in AD post-mortem brains. Representative Western blot and quantification of RIP140 levels. As control for protein loading we used β-actin. Values are expressed as mean±SEM; *P<0.05, Student's t test. (This experiment was performed preliminary to the PhD project and the figure is the courtesy of Dr. Magdalene Sastre).

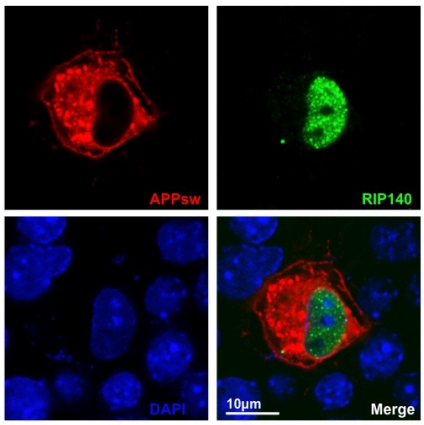
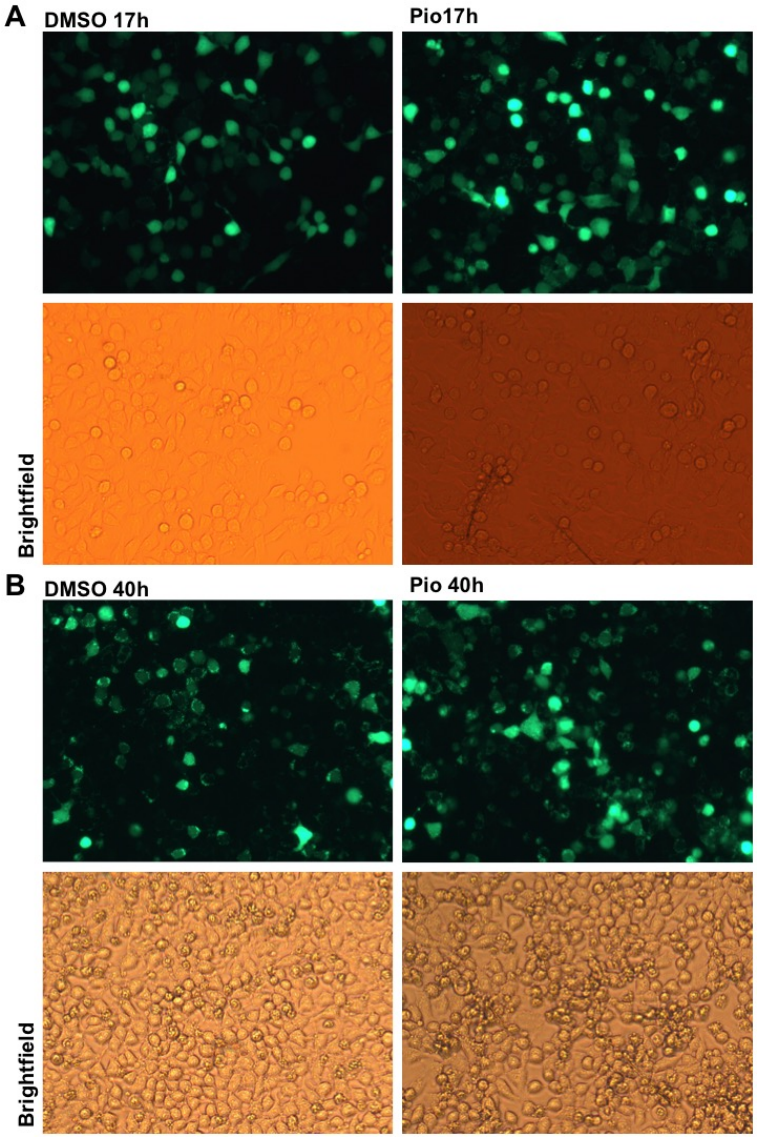


Figure 4.2: Localization of RIP140 in vitro. Immunofluorescence labeling with the 6D7 antibody against RIP140 protein (green) shows its localization, strictly restricted to the cell nucleus. The 6E10 antibody was used to detect full length APP (red). Cells were prior stably transfected with APP cDNA construct carrying the Swedish mutation. APP expression was detected in the cytoplasm and plasmatic membrane. Nuclear staining with DAPI (blue) was used a s a control and detected all cells.

In addition to the localization of hRIP140 overexpression by immunocytochemistry it was also important to validate the efficiency of transfection. Because RIP140 seems to require the presence of an agonist (such as pioglitazone) to affect PPARγ activity, we also analysed if RIP140 still can be efficiently expressed over a certain time period to allow the treatment with a PPARγ agonist. Initial experiments indicated that the treatment with the PPARγ agonist pioglitazone (Pio) is more efficient on changes in BACE1 protein expression if applied over a longer period of time (40 hours post transfection) rather than overnight treatment only (17 hours) (Fig. 4.3, B). It was crucial that transfection efficiency remained high during this treatment and we managed to optimize conditions in a way to reach a transfection efficiency of cells up to 90%, which remained stable over the longer treatment period of 40 hours and was unaffected by Pio (Fig.4.3, A). Additional confirmation of successful and specific RIP140 overexpression was obtained by detection with antibody for V5. V5 is a small peptide sequence that had been attached to the human RIP140 in the vector used to transfect and was used to detect the transfected human RIP140 (Fig.4.3, C). Although it seemed that this overexpression was lower after the longer treatment in comparison to overnight treatment (B) RIP140 expression remained stable, abundant and unaffected by Pio treatment when detected for 40-hour treatment only (C).


A
DMSO 17h
Pio17h
Brightfield
B
DMSO 40h
Pio 40h
Brightfield

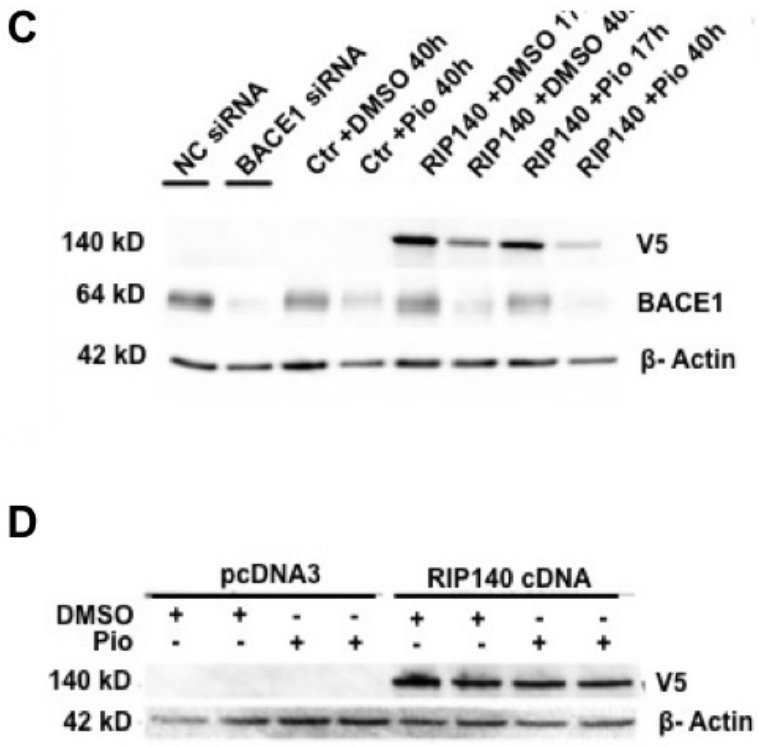


Figure 4.3: Evaluation of transfection efficiency and subsequent effects on BACE1 expression. A+B: Controls of GFP transfected cells showing a high transfection rate ($>$ 60%) of N2aSw cells. The expression of RIP140 was not affected by during the duration of the treatment time from 17h to 40 hours or the treatment with the PPARγ ligand Pioglitazone in comparison to vehicle DMSO alone. C: knock down of BACE1 protein by using a siRNA revealed the specificity of the antibody. Treatment with 20 μM pioglitazone alone or in cells transfected with RIP140 resulted in a decrease in BACE1 protein level with strongest effects at the long treatment (40h). The V5 antibody was used to detect the transfected RIP140, which was tagged with the V5 peptide. RIP140 level seemed to be lower after 40 hour post transfection in comparison to 17 hours but remained stable when compared to cells with the same time treatment (D). Previous experiments revealed that no changes in BACE1 protein expression were accomplished within the 17-hour treatment time span (data not shown).

4.2.2 RIP140 overexpression decreases extracellular Aβ42 peptides and AICD levels in a ligand dependent manner

Our group has previously demonstrated that the PPARγ cofactor PGC-1α reduces the generation of Aβ in N2acells by a PPARγ-dependent mechanism. We wanted to find out if RIP140 overexpression also affects Aβ generation in a

similar way as PGC-1α, and whether RIP140 acts as a co-activator for PPARγ. It has been described that RIP140 binds to PPARγ in a ligand activated dependent manner; this is why we had to stimulate cells with the synthetic PPARγ agonist Pioglitazone while simultaneously overexpressing RIP140. As a control we used cells transfected with empty vector cDNA (pcDNA3) and treated it with dimethylsulfidoxide (DMSO) as a vehicle treatment, as Pioglitazone had to be dissolved in this reagent. A further treatment pcDNA3 with Pio alone was performed as well, to determine the effect of this drug by itself (see Figure legend 4.5). Additional experiments to evaluate effects of RIP140 depletion were performed using siRNA against RIP140 and a non-coding (NC) siRNA control. Transfection of siRNA had to be performed using Lipofectamine, which caused some cell death.

The maximal activity and specify of various PPAR ligands has been studied by Seimandi et al. including the specify of Pioglitazone to PPARγ (Table 4.1). It shows that Pio induces almost 100% activity with PPARγ only but much lower activity of 5% for PPARδ and 18% for PPARα (Seimandi et al., 2005).

Maximal activity and EC_{50} and IC_{50} values of various ligands obtained with PPARα, PPARδ, and PPARγ reporter cell lines

Compound	PPARα			PPARδ			PPARγ		
	Percentage of activity	EC_{50} (nM)	IC_{50} (nM)	Percentage of activity	EC_{50} (nM)	IC_{50} (nM)	Percentage of activity	EC_{50} (nM)	IC_{50} (nM)
DMSO	7±2	—	—	3±1	—	—	20±3	—	—
GW7647	100±2	6±1	—	50±2	942±266	—	100±2	350±53	—
WY-14643	20±0.4	—	—	4±0.3	—	—	26±0.2	—	—
L165041	86±0.5	—	—	100±1	110±37	—	94±3	1905±155	—
GW501516	66±2	—	—	100±4	1.8±0.4	—	75±4	—	—
BRL49653	26±3	—	—	25±2	—	—	100±3	18±2	—
Ciglitazone	17±4	—	—	4±1	—	—	72±3	—	—
Pioglitazone	18±1	—	—	5±1	—	—	99±0.1	261±62	—
GW9662	33±2	26±9	188±43	10±2	—	471±84	29±1	—	3.8±1.3
BADGE	8±1	—	—	9±2	—	—	27±3	—	—

Figure 4.4: The EC50 values were derived from dose–response curves using the Cheng–Prusoff equation, with values representing the means and standard deviations calculated from three dose–response curves. The IC50 values were derived from inhibition curves at constant GW7647 (30 nM), L-165041 (200 nM), and BRL49653 (20 nM) concentrations for PPARα, PPARδ, and PPARγ, respectively, using the Cheng–Prusoff equation, with values representing the means and standard deviations calculated from three inhibition curves (taken from Seimandi et al., 2005).

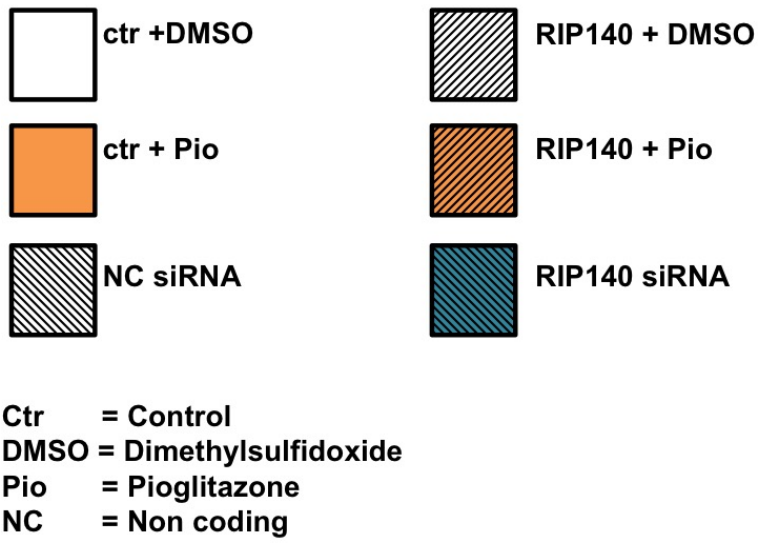
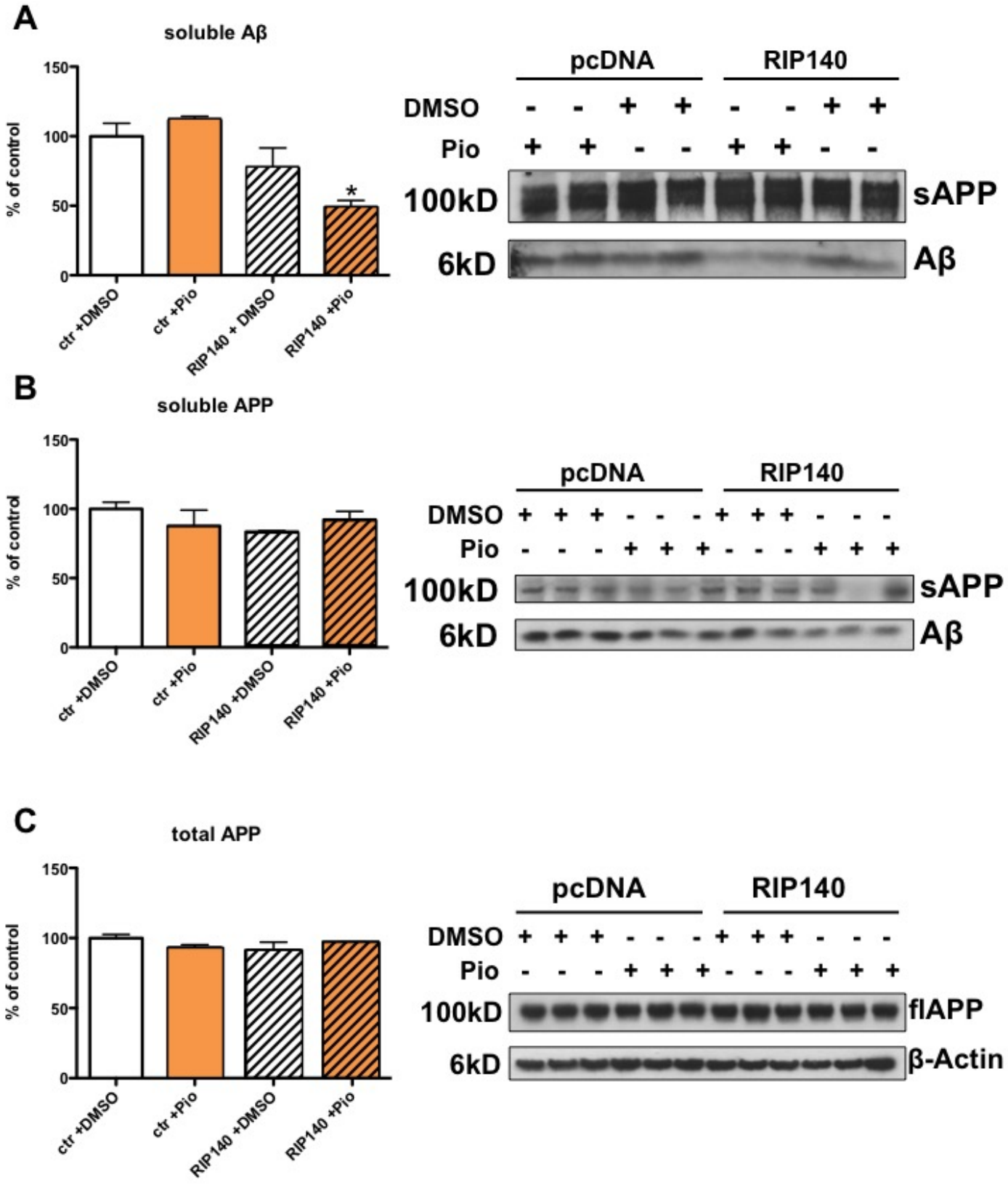


Figure 4.5: Legend of treatments. N2aSw cells were transfected with RIP140 cDNA to induce overexpression or siRNA to silence RIP140. Additionally, cells overexpressing RIP140 received treatment with the synthetic PPARγ agonist Pioglitazone (Pio) which was dissolved in Dimethylsulfideoxide (DMSO) hence 3 different controls had to be performed: cells transfected with pcDNA3 (scrambled control DNA) + DMSO and pcDNA3 + Pio alone for the RIP140 overexpression experiments and cells receiving non coding siRNA as a control for siRNA experiments.

To evaluate the effects of RIP140 overexpression on Aβ production, cells were transfected with a plasmid carrying the human RIP140 cDNA and 24 hours later, conditioned medium was replaced with medium containing the PPARγ ligand Pio at a final concentration of 20 μM during 40 hours. Because Aβ peptides are secreted, conditioned medium was collected and analysed for Aβ and APPs. The cells were scraped off the plate, lysed and the concentration of proteins was determined by Bradford assay. The volume of medium used was adjusted to protein concentrations measured from the total lysate of the corresponding cells. Each sample was then immunoprecipitated with 4G8 antibody, since the levels of Aβ were too low to be detected straight by Western blot. Proteins in the conditioned medium were separated by a 4-12% gradient gel, allowing detection of 4kD Aβ and the corresponding soluble APPs using antibody 6E10. We were able to show that Aβ was reduced in cells overexpressing RIP140 (Fig. 4.6., A and C,D = representative western blots). This effect seemed to be enhanced when cells were stimulated with pioglitazone, showing significant reductions in Aβ while APP stayed relatively steady (B). Cell lysates were separated on a different 8% SDS page gel showing that full length APP was unaffected by the treatment (E, F=representative western blot).


A
soluble Aβ
% of control
150
100
50
0
*
ctr +DMSO
ctr +Pio
RIP140 + DMSO
RIP140 +Pio
pcDNA
RIP140
DMSO - - + + - - + +
Pio + + - - + + - -
100kD
sAPP
6kD
Aβ
B
soluble APP
% of control
150
100
50
0
ctr +DMSO
ctr +Pio
RIP140 +DMSO
RIP140 +Pio
pcDNA
RIP140
DMSO + + + - - - + + + - - -
Pio - - - + + + - - - + + +
100kD
sAPP
6kD
Aβ
C
total APP
% of control
150
100
50
0
ctr +DMSO
ctr +Pio
RIP140 +DMSO
RIP140 +Pio
pcDNA
RIP140
DMSO + + + - - - + + + - - -
Pio - - - + + + - - - + + +
100kD
flAPP
6kD
β-Actin

We further validated the data by a more quantitative method to determine Aβ concentration, using a commercial ELISA assay, which allowed determining the relative amount of Aβ species. We were able to validate the effect of the Western blot experiment above, in which we observed the PPARγ activated-dependent reduction in total Aβ levels by RIP140 overexpression. In this case, we detected a reduction in the Aβ42 isoform (Fig.4.7, A). However, no changes for Aβ40 were observed (B) and the ratio Aβ40 to Aβ42 remained unaffected (C). The Aβ40/42 ratio has been suggested to be critical for Alzheimer's disease pathogenesis. Small alterations in the molecular composition of Aβ, reflected in the Aβ40/42 ratio, can substantially affect Aβ aggregation kinetics, and synaptic function. γ-secretase cleavage results in variable 38- to 43-amino-acid Aβ peptides, with Aβ40 and Aβ42 constituting the two most common isoforms. The biophysical and biochemical properties of Aβ vary strongly with its length. While Aβ42 aggregates faster, less of it is produced. We also wanted to examine if depletion of RIP140 in N2aSw cells can reverse the effect of overexpression and possibly increase the production of Aβ42, however that was not the case for conditioned medium of cells treated with siRNA for RIP140 (D).

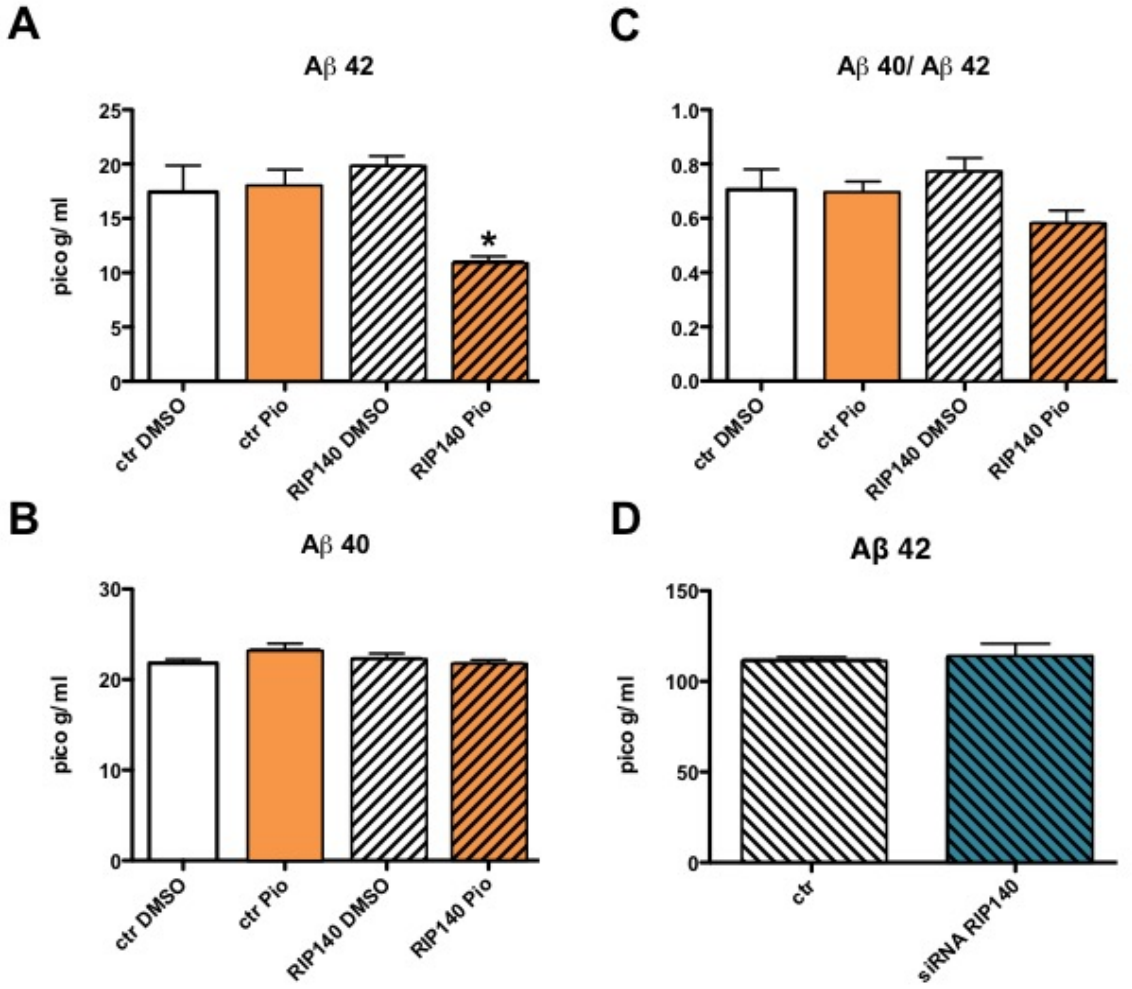


Figure 4.7: ELISA for Aβ40 and Aβ42 secreted in conditioned medium from N2aSw cells. Cells overexpressing RIP140 alone do not show any difference in amounts of Aβ42 (A) or Aβ40 (B) but if stimulated with pioglitazone, Aβ42 species were significantly lower in comparison to the control group. The ratio taken of Aβ40 to Aβ42 does not show any differences (C).Knock down of RIP140 did had no effect on Aβ42 level in vitro. (n=2 with 3 biological samples per group. Values shown in graphs represent the mean value ±SEM and are expressed as a percentage of control. Statistical analysis included one-way ANOVA with a post Tukey test, *P<0.05 for A, B and C and students t-test for D).

The cleavage of γ-secretase at the ε-site produces a membrane-integrated product termed AICD (APP intracellular domain). The quantification of this fragment can give an idea of the γ-secretase activity. Because we observed reductions in Aβ levels by RIP140 overexpression, we investigated whether this could be due to a reduction in γ-

secretase. We isolated membranes of N2aSw cells, which were treated in the same way as described above, and separated the different fragments on a 4-12% gradient gel. AICD fragments appeared to be significantly reduced in cells treated with pioglitazone alone and cells that were overexpressing RIP140 and treated with Pioglitazone (Fig.4.8, A, B= representative western blot). Full length APP remained unaffected and stable (C) and was used as internal loading control.

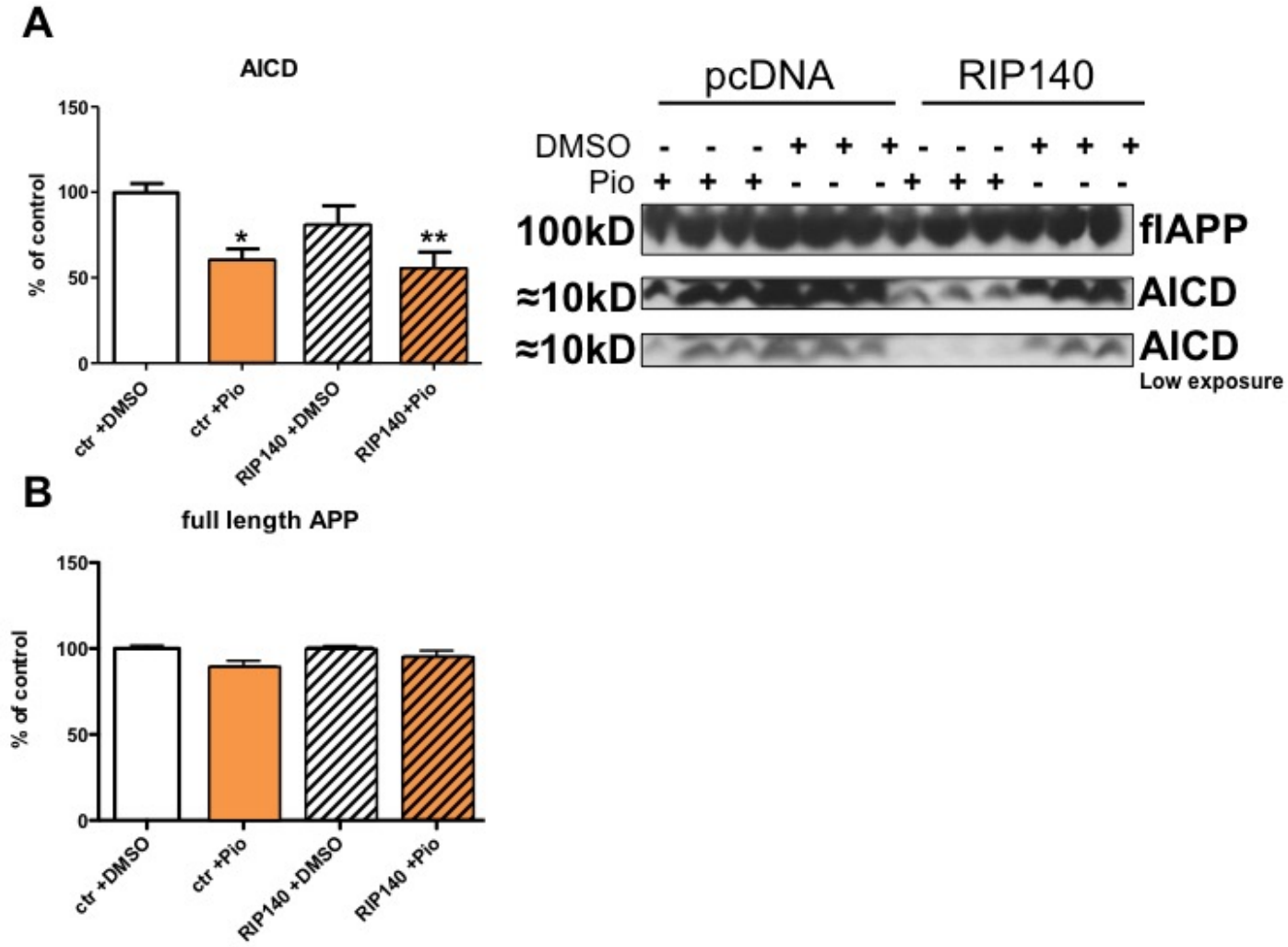


Figure 4.8: Effects of RIP140 overexpression on AICD level in membrane preparations of N2aSw cells overexpressing RIP140. Pioglitazone alone and combination of overexpression of RIP140 and pioglitazone treatment decreased amounts of AICD significantly (A, with representative western blot) while full length APP remained unchanged. (n=3 with 3 biological samples per group. Values shown in graphs represent the mean value ±SEM and are expressed as a percentage of control. Statistical analysis included one-way ANOVA with a post Tukey test, **P<0.01).

4.2.3 BACE1 protein and mRNA levels are affected by the expression status of RIP140

β-cleavage is the initiating step to induce amyloidogenic cleavage, causing the generation of Aβ peptides. The β-secretase BACE1 has been reported to be increased in AD patients. It is therefore of importance to evaluate the

effect of RIP140 on the relative amounts of BACE1, as PPARγ is involved in its transcription (Sastre et al., 2003, 2006). We did so by measuring protein and mRNA level of this enzyme. The specificity of the antibody for BACE1 is shown in figure 3.4, using specific siRNA for BACE1. We used two different experimental approaches, one involving cells overexpressing RIP140 and receiving PPARγ stimulation with pioglitazone and the second using cells that are lacking RIP140, by transfection with RIP140 siRNA or RIP140shRNA. The cells which have been stimulated with Pio (20 μM) exhibited a significant decrease in BACE1 protein expression, independent of RIP140 overexpression. But also, overexpression of RIP140 by itself appeared to be effective in reducing BACE1expression. The combined treatment of both factors showed to have an accumulative effect, with the highest significance in lowering BACE1 protein expression (Fig 4.9,A). The V5 antibody validated the successful overexpression of exogenous human RIP140 which was absent in the untransfected controls. Conversely, cells that were treated with RIP140 siRNA exhibited an increase in BACE1 protein level (B), showing the specificity of the effect of RIP140 on BACE1 expression. Although the antibody for detection of endogenous RIP140 could not pick up any differences for cells treated with siRNA against RIP140 compared to control cells, control cells overexpressing RIP140 did show increased RIP140 expression, indicating that endogenous RIP140 may be too low to detect differences in RIP140 depleted and control cells.

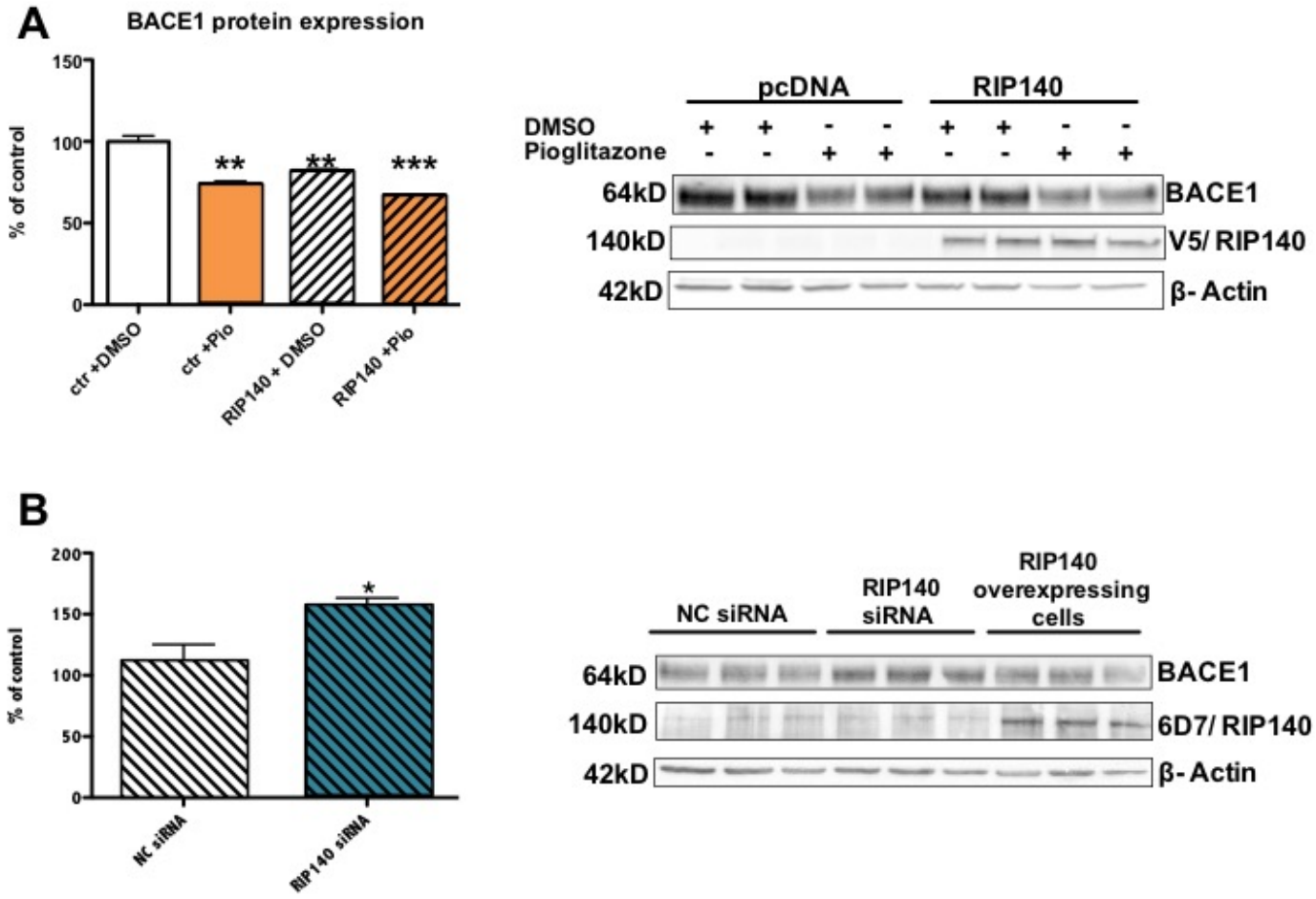


Figure 4.9: Effects of RIP140 on BACE1 protein expression in vitro. Pioglitazone treatment and RIP140 overexpression can independently lower BACE1 protein level significantly and have a cumulative effect when combined together (A). Silencing of RIP140 increases BACE1 protein expression (B) . Differences in endogenous RIP140 expression using the 6D7 antibody were not detected for cells treated with RIP140 siRNA in comparison to control, but showed an increase using cells overexpressing exogenous RIP140 as a control. (n=3 with 2-3 biological samples per group for RIP140 overexpression and n=1 with 3 biological samples per group for RIP140 silencing. Values shown in graphs represent the mean value ±SEM and are expressed as a percentage of control. Statistical analysis included one-way ANOVA with a post Tukey test, **P<0.01 ***P<0.001 for A and students t-test for C *P<0.05).

We carried out qPCR analyses to determine whether RIP140 levels were reduced by transfection with RIP140 siRNA. Using specific primers against the endogenous RIP140 we validated if knock down of RIP140 using siRNA

was successful. Cells treated with a siRNA targeting RIP140 showed a reduction up to 50% of RIP140 mRNA levels (Fig.4.10, D). We also showed that the overexpression of RIP140 in cells transfected with RIP140 cDNA was up to a 5000 fold higher than in untransfected cells, varing from values of 2000fold (B). We then investigated whether.the effects of RIP140 overexpression on BACE1 protein expression were due to changes in BACE1 transcription. Our results indicate that cells transfected with RIP140 and incubated with pioglitazone or with vehicle showed a reduction in BACE1 mRNA in comparison to the untreated control (Fig. 4.10 A). Only the reductions caused by Pio mediated PPARγ stimulation and the combined treatment were significant.

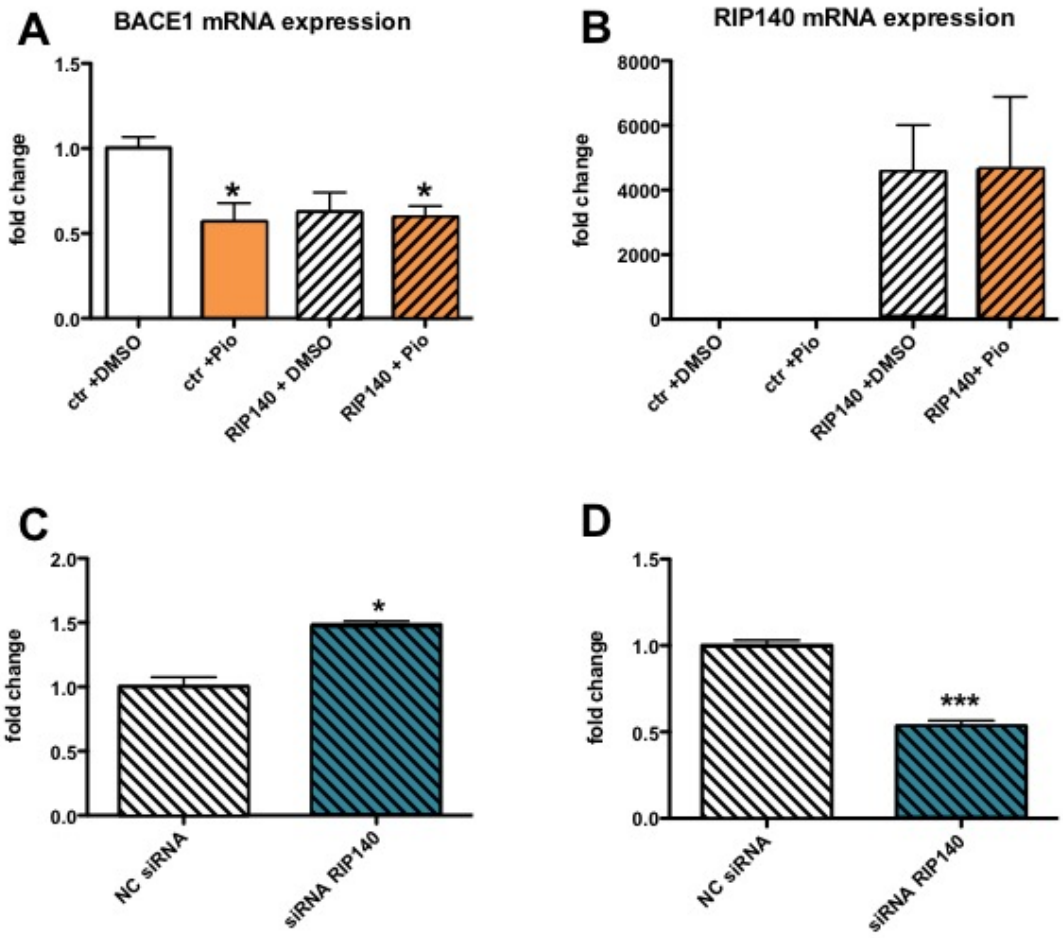


Figure 4.10: Effects of RIP140 on BACE1 mRNA expression in vitro. Pioglitazone treatment and RIP140 overexpression can both lower BACE1 mRNA level but only pioglitazone alone and combined treatment (RIP140 overexpression + pioglitazone) in a significant manner (A). Expression level of exogenous human RIP140 were around a 4000 fold higher than RIP140 untransfected cells in which no RIP140 expression was detected (B). Silencing of RIP140 increases BACE1 mRNA expression significantly (C). A 50% silencing rate of endogenous RIP140 was reached using RIP140 siRNA (D). (n=3 with 3 biological samples per group for RIP140 overexpression (A and B) and RIP140 silencing (C and D). Values shown in graphs represent the mean value ±SEM and are expressed as a fold change in comparison to the normalized control. Statistical analysis included one-way ANOVA with a post Tukey test, *P$<$0.05 for A and students t-test for C and D *P$<$0.05, ***P$<$0.001).

4.2.4 Alterations of BACE1 promoter activity are induced by PPARγ agonism and linked to RIP140 expression changes

Previous work in our group had demonstrated that PPARγ has a response element in the BACE1 promoter DNA sequence to which it can bind specifically . In the same context it was shown that expression of PPARγ in N2a cells can lower the the activity of the BACE1 promoter, indicating that it may act as repressor for BACE1 transcription.

Our results form above indicate that RIP140 co activates PPARγ lowering BACE1 protein amounts. There for we tried to find out if overexpression of RIP140 alone and together with PPARγ stimulation affects the activity of the BACE1 promoter. To do so, we used a Luciferase promoter activity assay. It occurs that RIP140 overexpressioon alone can strongly decrease BACE1 promoter activity but alos together with PPARγ stimulation through pioglitazone (Fig. 4.11). We then checked how absence of RIP140 in N2a cells would affect BACE1 promoter activity and interestingly the opposite effect of overexpression was observed meaning that silencing RIP140, using a shRNA construct, strongly increased the activity of the BACE1 promoter.

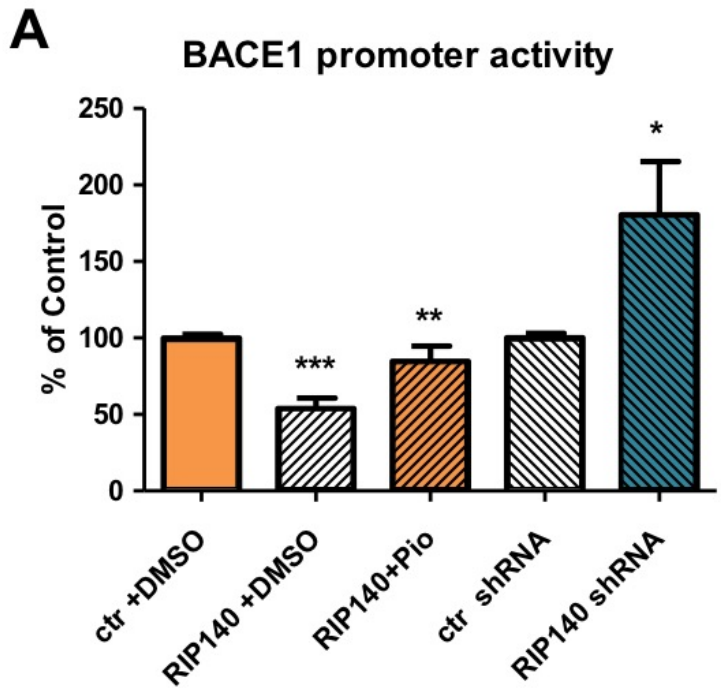


Figure 4.11: BACE1 promoter activity. BACE1 Promoter activity was decreased when RIP140 was overexpressed alone or combined with pioglitazone treatment (white colums). Silencing of RIP140 strongly increased BACE1 promoter activity (blue colum). (n=3 with 3 biological samples per group for RIP140 overexpression and RIP140 silencing. Values shown in graphs represent the mean value ±SEM and are expressed as a fold change in comparison to the normalized control. Statistical analysis included one-way ANOVA with a post Tukey test, *P<0.05, **P<0.01,***P<0.001).

4.3 Discussion

In this part of the project, we have found that RIP140 overexpression reduces Aβ levels in a neuroblastoma cell line, in particular the Aβ42 subtype and seems to require the activation with pioglitazone. This effect appears to be mediated by a reduction in BACE1 transcription. This coincides and supports the previous work in our lab regarding the effect of activation of PPARγ on BACE1 which has shown to reduce BACE1 protein and activity level together with a reduction in Aβ level (Sastre et al., 2003, 2006).

Therapies aimed to reduce BACE1 levels are currently under investigation. New drugs on the market such as the Astra Zeneca's β-secretase (BACE) inhibitor AZD329, seem to have promising effects. In the Phase I trial, the AZD3293 lowered Aβ production in humans by up to 75% (Nature Reviews Drug Discovery | AOP, published online

17 October 2014). However, because BACE1 knockout mice do not seem to have relevant side effects, it seems that targeting BACE1 is a better option than inhibiting γ-secretase. It has to be taken into account that Amyloid deposition is a very early event in the pathogenesis of this disease, so the treatment for BACE1 inhibition might be more sensible during early stages of AD.

In the present study we have found that RIP140 appears to behave as a co-activator for PPARγ. It has been established that RIP140 acts as a transcriptional co-repressor for NR in metabolic tissue whilst PPARγ co-activator-1α (PGC-1α) can be seen as the main co-activator, stimulating mitochondrial biogenesis (Puigserver et al., 2003). This goes along with the observation that most genes that are repressed by RIP140 can be activated by PGC-1α (Christian et al., 2005; Herzog et al., 2007) putting them into antagonistic roles towards each other. Interestingly, RIP140 has shown to directly interact with PGC-1α suppressing its activity (Hallberg et al., 2008).

4.3.1 RIP140 acts possibly as a co-activator for PPARγ in the transcriptional regulation of BACE1 in vitro

Our in vitro results indicate that RIP140 is likely to act as a co activator of PPARγ. The reduction in Aβ levels and BACE1 was demonstrated previously in our group with a similar approach overexpressing PGC-1α in N2a cells (Katsouri, Parr, et al, 2011) or by incubation with a PPARγ agonist pioglitazone (Sastre et al., 2003, 2006). Additional data showing that PPARγ binds to a specific response element within the BACE1 promoter and inhibiting its transcription, contributes to this hypothesis. RIP140 binds to PPARγ in a ligand-activated dependent manner, enhancing PPARγ's regulatory functions leading to lower BACE1 mRNA, protein and activity levels. Furthermore the decrease in BACE1 expression and function seems to impair the amyloidogenic cleavage, reducing Aβ. Some recent results from our lab have shown that indeed this effect on BACE1 expression is mediated through PPARγ, since transfection with PPARγ siRNA reversed the effects.

On the other hand, we have also observed that RIP140 is able to reduce the levels of AICD fragments if cells were treated with Pioglitazone at the same time; however this effect may not be exclusive to the RIP140 overexpression because the administration of Pioglitazone by itself can also reduce AICD levels by 50%. It is likely that this observation could be linked to an increase in PPARγ activity only or to an off-target effect of pioglitazone.

In the past pioglitazone treatment has shown to induce proteolytic subunits of caspase-3 and caspase-9 in macrophages in a dose- and time-dependent manner whilst pretreatment with a PPARγ inhibitor, GW9662, prevented pioglitazone

induction of the apoptotic pathway (Bodles et al, 2006). Caspase-3 has been shown to directly and efficiently cleave APP (Gervais et al., 1999; LeBlanc, 1995; Weidemann et al., 1999; Zhang et al., 1997). This caspase-3 cleavage was shown to take place mainly at the C-terminus of APP and Aβ peptide formation as a consequence and additional literature supports the formation of Aβ induced by caspases (Lu et al, 2003; Ayala-Grosso et al, 2002; Stone et al, 2002). Because caspase cleaves the C-terminus, it may be possible that Pioglitazone induced caspase in our experiments causing a further cleavage of the C-terminal domain of APP. Therefore, the cleavage by γ-secretase would produce a smaller fragment which would not be detected by Western blot with our antibody. This would appear as reduction of AICD just like we saw it, but would be independent of RIP140 or PPARγ activities. To confirm this, we could use a caspase inhibitor and determine if the effect of pioglitazone is reversed.

On the other hand, it could be possible that PPARγ activation may modify γ-secretase and reduce AICD and Aβ levels. To prove this hypothesis, a γ-secretase in vitro assay could be performed using membrane preps from cells that have been transfected with a 100kD C terminal fragment (C100) and RIP140. These membranes could be incubated with pioglitazone and we could detect if AICD levels have changed or not. Interestingly, it was previously shown that pioglitazone does not affect γ-secretase activity in vitro (Sastre et al., 2003).

4.3.2 Silencing RIP140 in vitro reverses the effects on BACE1 transcription and may contribute towards amyloid pathology

In this chapter we have shown that exogenous expression of RIP140 reduced BACE1 transcription so we hypothesized that silencing of this co-factor may result in the opposite effects. By transfecting RIP140 siRNA into N2a cells we achieved a 50% knock down of RIP140, confirmed by qPCR. Despite this incomplete knock down, we observed strong effects in the levels of BACE1 mRNA and protein expression, all being significantly higher than in control cells. This confirms the importance of RIP140 regulating the amyloidogenic pathway. A complete knockout may give even more insight into how severe the effects might be. Therefore, in the next chapter we aim to confirm the results using an animal model lacking RIP140. This will be more relevant, since we will investigate the significance of RIP140 ablation in vivo.

In addition, evaluation of basal RIP140 expression levels in the human brain of AD patients demonstrated that RIP140 is reduced compared with healthy individuals. This possibly indicates that the decreased levels of this transcriptional regulator may contribute to the increased amyloid pathology observed in these patients. It is still not clear

why the expression of RIP140 is reduced in AD brain. This could be consequence of factors associated with the AD pathology such as Aβ deposition and inflammation, or already an early change in the AD brain. We have previously shown that PPARγ expression is modulated by inflammation in neuroblastoma cell lines (Sastre et al., 2006). Others have also shown that inflammatory cytokines and oxidative stress decrease PPARγ mRNA in adipocytes (Xing et al, 1997), and thiazolidinedione's reverse this effect (Gimble, et al, 1996). We do not know yet whether inflammatory cytokines modulate RIP140 levels or it's binding to transcription factors. This is something that we plan to investigate in the future.

Chapter 5

Results II: Study of the brain of RIP140 knock out mice

5.1 Introduction

5.1.1 RIP140 in the brain

The role of RIP140 in the brain is not fully understood but it has been demonstrated that it is expressed in the cortical and hippocampal areas and a connection has been made for its implications in cognition and memory (Duclot et al, 2012). In addition, RIP140 levels seem to be highly expressed during neurodevelopmental stages and reduced during aging (see review Katsouri et al., 2012). Phenotypic analysis of RIP140 null mice has shown that while this cofactor is not essential for embryonic or tissue development it has profound effects on cell function, in particular with regard to the physiological activity of metabolic tissues including adipose and skeletal muscle. In addition, RIP140 null mice suffer from memory and learning impairments and display an increased response to stress in comparison to wild types (Duclot et al., 2012). RIP140 knockout animals do not appear to have significant differences in brain structure. The effects of RIP140 on memory could be mediated through the regulation of RIP140 by nuclear receptor transcriptional activities involving cognitive plasticity. For instance, hippocampal ERα has been involved in memory formation (Fugger et al . 1998, 2000; S'anchez-Andrade & Kendrick 2011).

Interestingly RIP140 is located on chromosome 21 within the same region causing Down Syndrome, a condition that has been linked to a higher risk of developing AD because it also contains the APP gene. Patients with Down syndrome also showed higher expression level of RIP140, correlating with certain metabolic and developmental pathways altered in those patients. It has also been shown that the brain tissue expresses a novel splice variant of RIP140, which is targeted in the 5'UTR by the microRNA mir-346 (Tsai et al., 2008). When this mir-346 is expressed, RIP140 protein level will be elevated, accompanied by increased RIP140 co-repressive activity but without affecting mRNA level of RIP140. The gene encoding glutamate receptor ionotropic delta generates mir-346 in the brain and has been shown to be implicated in schizophrenia and inflammation (Zhu et al., 2009).

5.2 Results

5.2.1 RIP140 is located mainly in the hippocampus of mouse brain

Our aim was to study RIP140 if mice express RIP140 in the brain and also what areas show stronger or specific expression of this cofactor.

In situ hybridization using primers against a specific exon of RIP140 showed that within the mouse brain the hippocampus area is highly expressing RIP140 (Fig. 5.1). In situ hybridization of sagittal slices also revealed that RIP140 is highly expressed in the cerebellum and to some extend in the frontal cortex area. Both the hippocampus and frontal cortex area are associated with AD pathology. Therefore we chose to focus our research on these two areas in RIP140 knockout and transgenic mice.

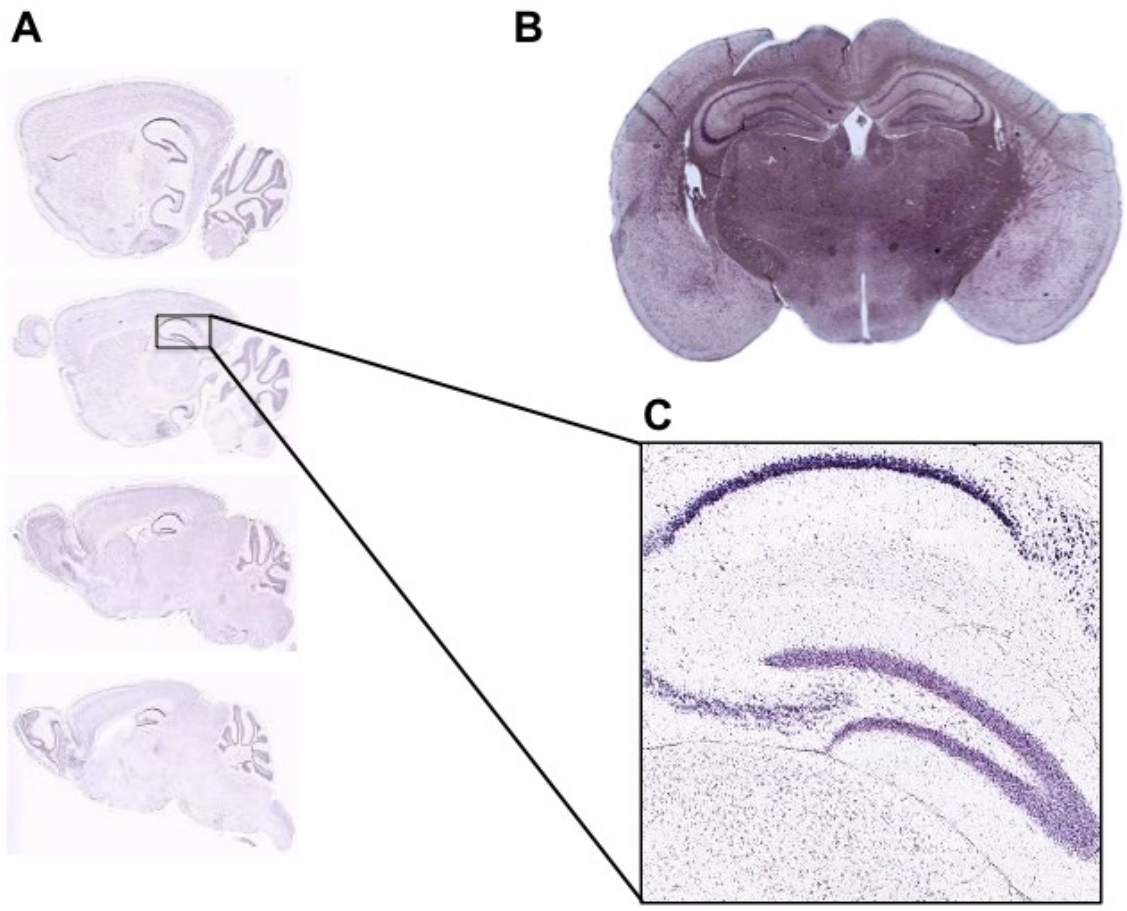


Figure 5.1: Localization of RIP140 in the mouse brain. In situ hybridization, using specific primer designed to detect the RIP140 transcript exhibited specific RIP140 labeling within the hippocampus area (C) on sagittal (A and C) and coronal (B) brain sections of wild-type mice. The cerebellum and olfactory bulb also showed enhanced RIP140 labeling throughout the sections for cerebellum and more inside the brain for the olfactory bulb and frontal cortex area. (Images A and C taken from: http://mouse.brain-map.org, Image B: courtesy of Dr. Jenny Steel, Imperial College London)

Another way to determine the distribution of RIP140 was performing β-Galactosidase staining to detect LacZ gene expression in sections of RIP140 knockout mice. Because RIP140 gene was replaced by the LacZ sequence in the generation of RIP140-KO animals, β-galactosidase transcription is driven by the RIP140 promoter and therefore mirrors the expression of the endogenous RIP140 gene in wt mice. LacZ staining confirmed the localization of the RIP140 gene in the nucleus of cells from hippocampus and cortical areas of the brain, two areas highly involved in AD pathology (Fig. 5.2). These experiments were carried out in collaboration with the group of Professor Parker and the

image above is the courtesy of Dr. Jenny Steel. Some information on ISH data was obtained using the Allen Brain Atlas database (www.mouse.brain-map.org).

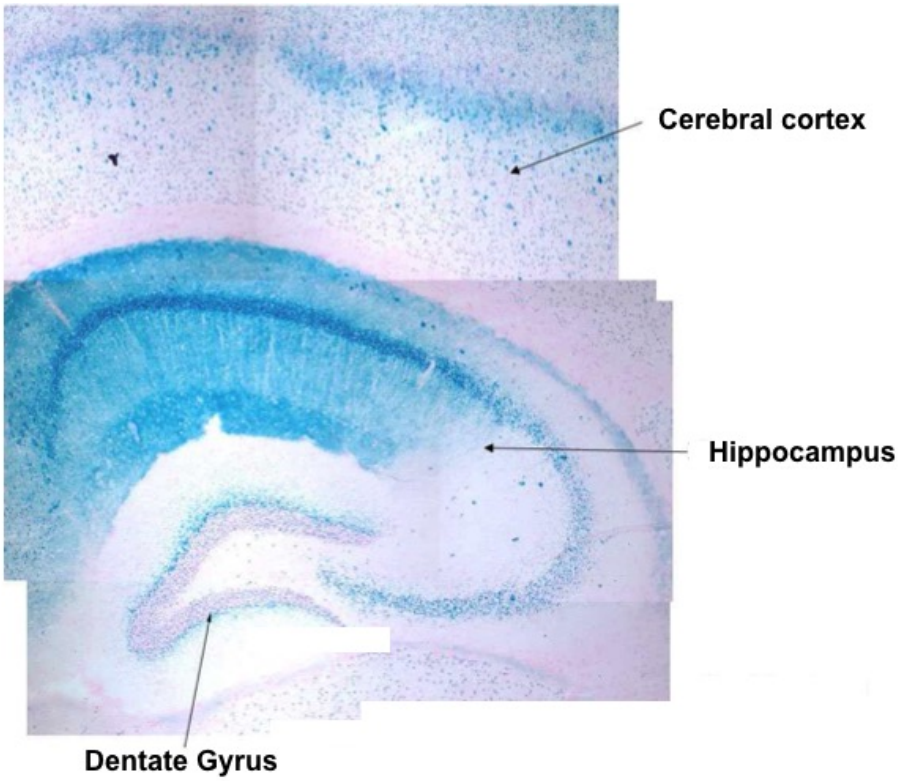


Figure 5.2: LacZ staining of RIP140 deficient mice. Mice lacking RIP140 had the gene replaced by a LacZ gene. β-Galactosidase staining shows where LacZ is expressed in the RIP140 ko brain serving as an indirect marker with expression in the dentate gyrus and cerebral cortex and highest in the hippocampus. Image is the courtesy of Dr. Jenny Steel.

5.2.2 Effects of RIP140 depletion on expression level of various genes implicated in AD

Because we have seen in vitro that RIP140 seems to modulate genes such as BACE1, we were interested in the possibility that other genes that have been involved or associated with Alzheimer's Disease would be altered in RIP140 knockout mice. We performed a qPCR based array (Qiagen) specific for 90 genes involved in AD using mRNA extracts from hippocampus tissue of two young male mice lacking RIP140 and 2 matching wild-type controls.

This array gave us some insight on what genes involved in the AD pathology are affected in the absence of RIP140.

The results are illustrated in figure 5.4 Bars with changes above the baseline 1 are interpreted as up-regulations and below the baseline as down-regulations in comparison to wild-type expression of the gene (Fig.5.3). The data analyses and graph were made using the supplied online software from Qiagen. We decided then to select some of the genes showing the strongest alterations by RIP140 gene depletion. Genes of interested that appeared to be up regulated were: ApoE, BACE1, BACE2, cdK5, GAP43, Igf2 and Mtap (green arrows). Genes down regulated were GsK3β and IDE (red arrows). We proceeded then to design primer for these genes to run validation qPCRs on the same samples again (Fig.5.3). The data analyses and graph were made using the supplied online software from Qiagen.

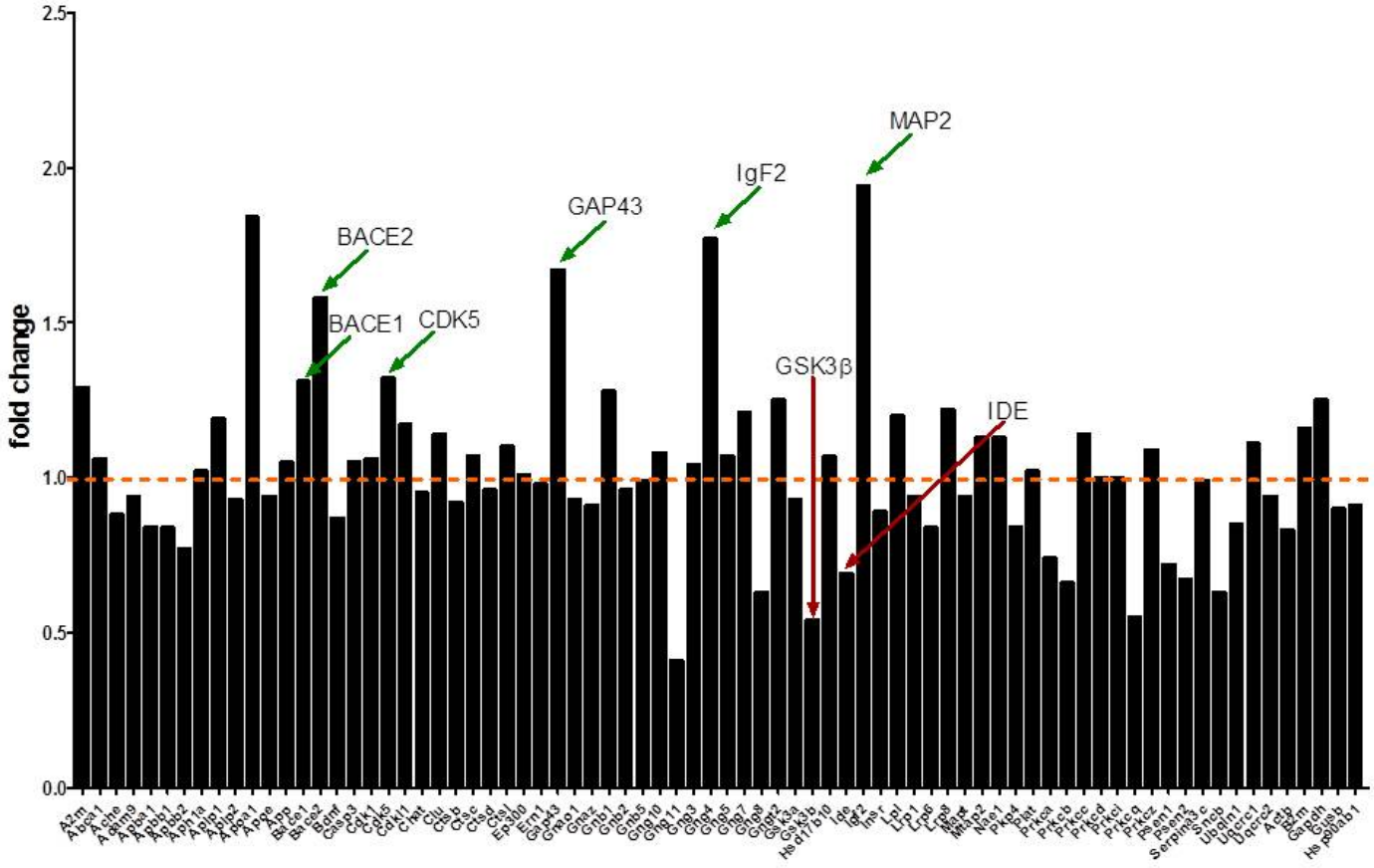


Figure 5.3: RT2 Profiler qPCR array. A Qiagen Alzheimer's Disease qPCR profiler array specific for mouse was used to screen a wide range of genes, implicated in AD in RIP140 knockout mice. Hippocampus mRNA samples of 2 young (2 months) knock out and wild-type mice were analysed and expression differences are expressed in fold change to the baseline 1. Green arrows highlight genes exhibiting overexpression and have been selected for further analyses. Red arrows show genes down-regulated and have been selected for further analyses. (n=2, no statistical analyses on n of 2)

Additionally, we aimed to validate these data by qPCR using self-designed primers and adding some genes not present on the array but of relevance for us, such as Neprilysin and L-PGDS and direct targets of RIP140 including estrogen related receptor γ (Esrrγ), cell death activator (CIDEA), Pyruvate dehydrogenase lipoamide kinase isozyme 4 (PDK4), PGC-1α and PPARγ (Fig. 5.4).

We were able to validate some of the effects observed in the array, such as the slight up regulation of cdK5 and the much stronger ones of Igf2 and Mtap. IDE expression remained lower as well. However, we did not detect an up regulation in BACE1 or BACE2 with the new primers and contrary to the observed above, GsK3 was strongly up regulated using our new primers in RIP140 knockout mice. Unexpectedly, none of the RIP140 direct targets showed any response, suggesting that RIP140 signaling may regulate other pathways in the brain than previously described for other tissues. L-PGDS showed a strong induction of gene expression in mice lacking RIP140 and Neprilysin level seemed slightly lower than in the wild type. Again, this preliminary screen was performed with a number of 2 animals per group no statistical analyses was performed, therefore more samples should be analysed in order to confirm these results.

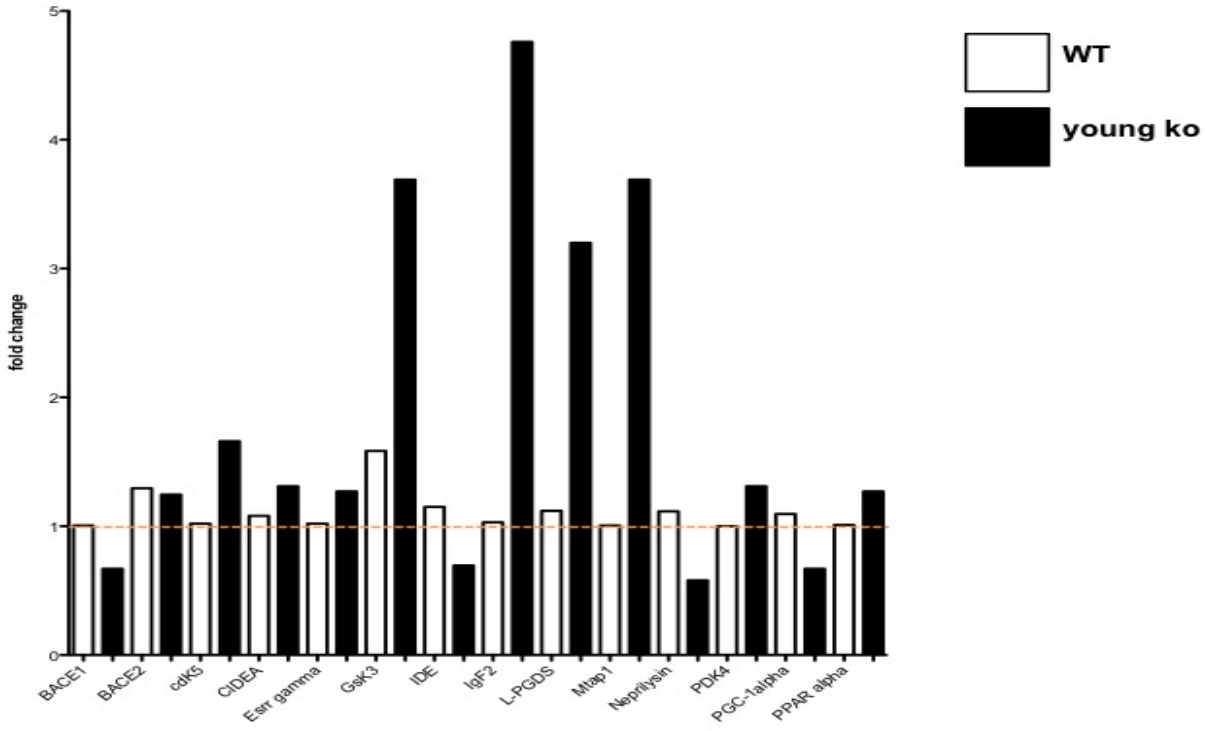


Figure 5.4: Validation of the qPCR values of the array with new primers. The same samples used in the array (Fig. 5.3) were used for further confirmation by qPCR using self-designed primer of the selected genes. Additionally, genes known to be direct targets of RIP140 were examined as well, including CIDEA, ESRR-γ, PDK4, PGC-1alpha and PPAR-α. Wild-types (white bars) have been plotted next to ko samples (black bars) for each gene. Effects observed on some genes remained the same as in the array, such as strong up-regulations in IgF2 and Mtap1, slight up-regulation of cdk5 and down-regulation of IDE. Contrary to the array data, BACE1 and GsK3 appeared down-regulated. None of the target genes of RIP140 showed any strong response to the knockout of it. The n= number remains the same as in the array above (2) and therefor no statistical analyses could have been performed

Because these results were obtained in only 2 animals per group, we proceed to investigate further the effect of RIP140 in some of the genes that we found altered in the array this time using brain samples from a group of 9 months old RIP140 knockout mice and their control wild-type littermates (n=5-6 per group). We categorized the selected genes into different groups depending on which process they are involved in AD (Tab.5.1). As there are two transcript variants for Mtap we decided to investigate changes for both variants 1 and 2. In total we assigned all genes into five groups:

1. APP Processing

2. Aβ degradation

3. Memory and cognition

4. Tau pathology

5. Inflammation

All gene groups were evaluated for two brain areas, the hippocampus and frontal cortex as both showed elevated RIP140 expression in the in situ hybridization assay and both areas are affected in AD.

Gene	Name	Process linked to AD
ApoE	apolipo protein E	Aβ degradation
BACE1	beta-site APP cleaving enzyme 1	APP Processing
BACE2	beta-site APP cleaving enzyme 2	APP Processing
cDK5	cyclin dependent kinase 5	Tau pathology
GAP43	growth associated protein 43	Memory and cognition
Gsk3	glycogen sythase kinase 3	Tau pathology
IDE	insulin degrading enzyme	Aβ degradation
IgF2	insulin like growth factor 2	Memory and cognition
Mtap1	microtubulin assosiated protein 1	Tau pathology
Mtap2	microtubulin assosiated protein 2	Tau pathology
Neprilysin	Neprilysin	Aβ degradation

Table 5.1: List of selected genes potentially affected by RIP140. Initial analyses of the qPCR array revealed changes in some genes that could be potentially regulated by RIP140 and they have a link to AD. Selected genes have been subdived into groups with similar context such as: APP processing, Aβ clearance, memory and cognition and Tau pathology. 9 genes have been selected form the initial array data and 2 more have been added that weren't present on the array, including: Mtap1 and Neprilysin.

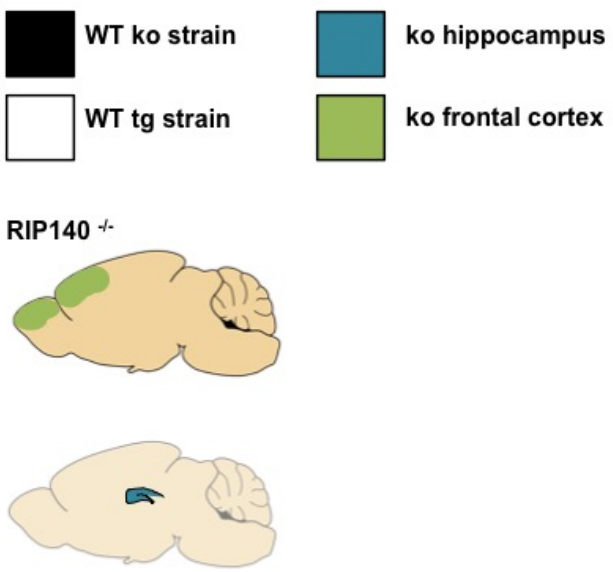


Figure 5.5: Protein homogenates and mRNA extracts of two brain areas and mouse lines were studied. A mouse line lacking (knockout) RIP140 and its corresponding wild-type strain (black) were studied using hippocampus (blue) and frontal cortex (green) areas of each animal. Dissections of hippocampus and frontal cortex areas of the right hemisphere were used to extract RNA for subsequent mRNA analyses via qPCR and left hemisphere dissections were lysed to produce protein homogenates for subsequent analyses of protein expression level via Western blot.

5.2.3 Mice lacking RIP140 show higher BACE1 mRNA expression in the Hippocampus

Our in vitro experiments have shown that either RIP140 overexpression or its absence can alter the level of BACE1 protein, mRNA and its promoter activity. BACE1 accounts as one of the key enzymes involved in APP processing. Importantly it is the first secretase to initiate the amyloidogenic cleavage pathway that can lead to the pathology of AD. Initial analyses of young mice lacking RIP140 indicated that not only BACE1 but also BACE 2 are potentially up regulated in their hippocampus areas. Much less is known about BACE2 but it appears to be a close homologue of BACE1 and it is also with involved in pathways that can lead to the cleavage of APP. We next aimed to validate the

preliminary results from the young RIP140 knock out mice (see array in Fig. 5.3) with a higher n numbers and older mice. Brain dissections of 5 months old RIP140 null mice were prepared and hippocampus and frontal cortex areas were subject to qPCR and/ or Western Blot analyses.

Interestingly, in the group of 9 months old RIP140 null mice, BACE1 mRNA level were significantly elevated in the hippocampus region whereas BACE2 level seemed slightly, but not significantly higher than in wild-type mice (Fig. 5.6 A+B). BACE1 and BACE2 mRNA expression did not seem to be affected in the frontal cortex area of RIP140 null mice (Fig.5.6 C+D).

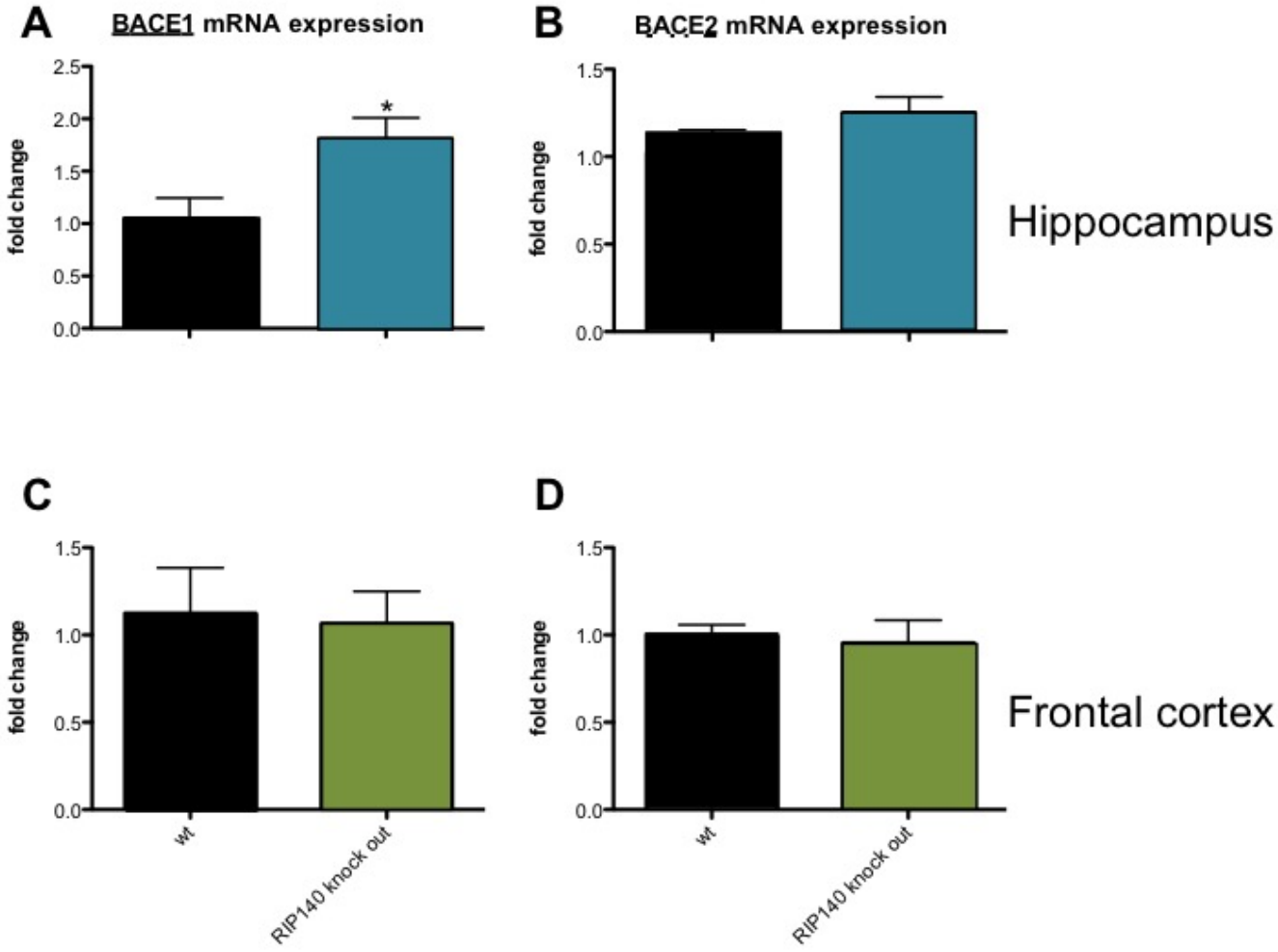


Figure 5.6: BACE1 and BACE2 mRNA expression. RNA preparations of 9 months old RIP140 null mice hippocampus and frontal cortex were analysed for changes in BACE1 and BACE2 mRNA expression. Mice lacking RIP140 in the Hippocampus showed a significant increase in BACE1 mRNA level in comparison to wild-type animals (A) and a mild but non-significant increase in BACE2 mRNA expression in the same area (B). Expression level of BACE1 and 2 mRNA in the frontal cortex region appeared to be unchanged (C+D).). (n=4 for RIP140 null mice and n=4 of corresponding wild-type. Values shown in graphs represent the mean value ±SEM and are expressed as a fold change in comparison to the normalized wild-type control. Statistical analysis included students t-test *P$<$0.05).

To confirm that the changes on BACE1 mRNA are present at the level of protein expression, we prepared homogenates of the left hemisphere of the same animals and performed Western Blot analyses with a BACE1 antibody. Neither hippocampus nor frontal cortex homogenates from RIP140 knockout mice exhibited any changes for BACE1

protein expression (Fig. 5.7).

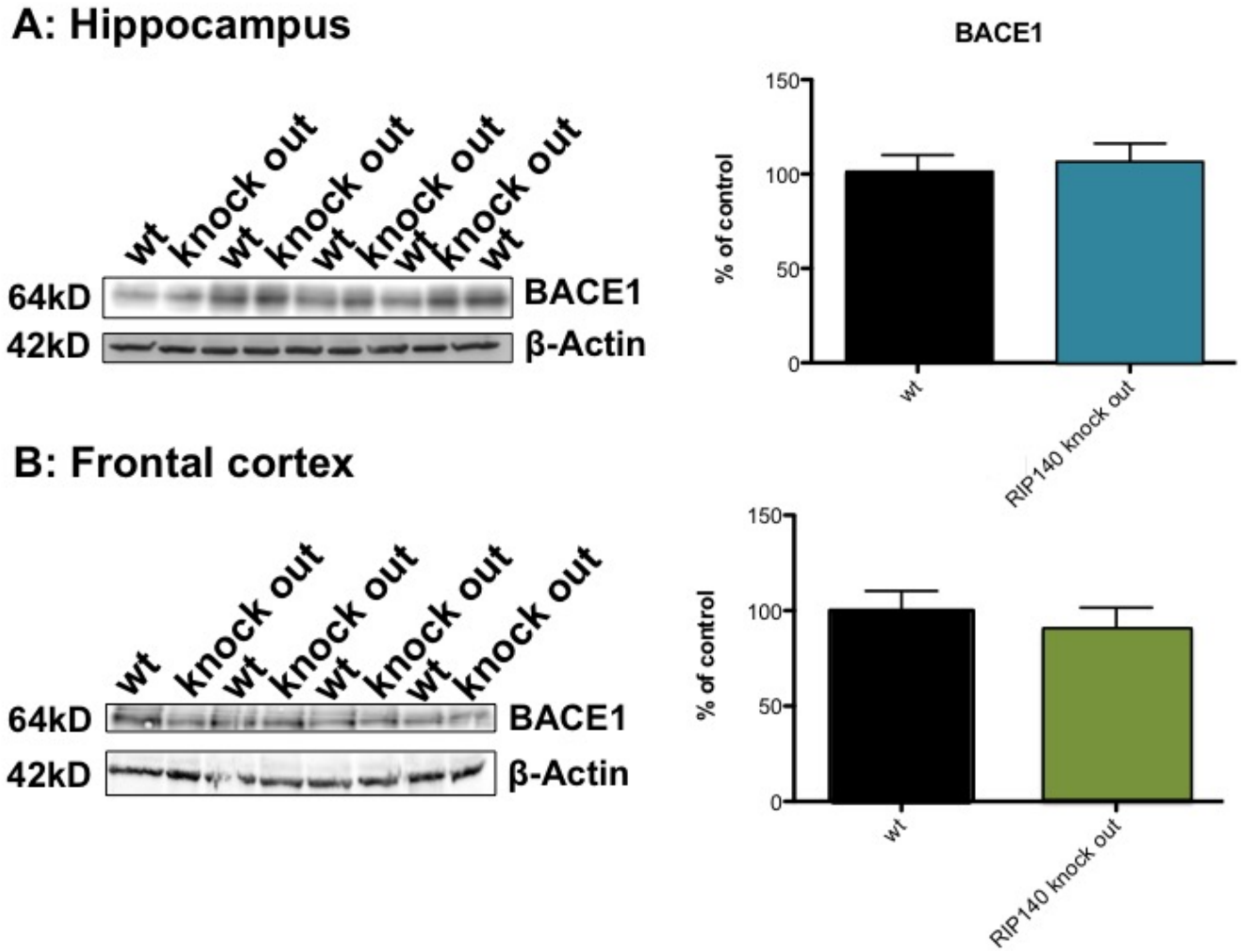


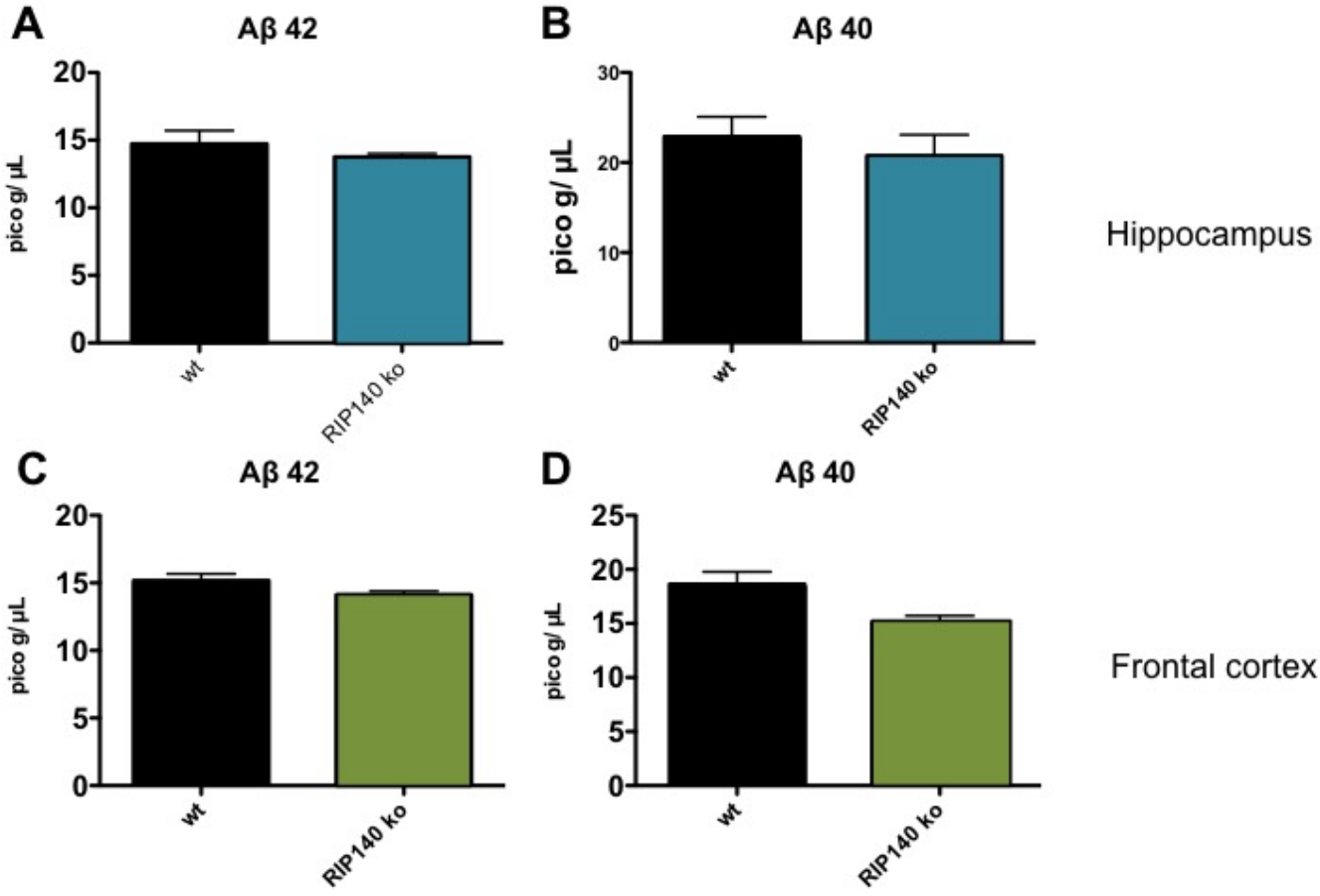
Figure 5.7: Western Blot analyses for BACE1 protein level. Protein expression of BACE1 in RIP140 null mice in Hippocampus and frontal cortex area showed no changes in comparison to matching wild-type expression (A+B). BACE1 expression was normalized to β-actin level. (n=4, RIP140 mice and n=5 matching wild-type animals for hippocampus, n=4 RIP140 null mice and matching wild-type for frontal cortex. Values shown in graphs represent the mean value ±SEM and are expressed as a fold change in comparison to the normalized wild-type control. Statistical analysis included student's t-test)

Although some of the effects of a RIP140 knock down in vitro could be validated in our RIP140 mouse model, showing that the lack of RIP140 can increase the mRNA expression level for BACE1, this observation seems to be limited to the Hippocampus area and the stage of mRNA expression rather than protein level. Even it has been

discussed that BACE2 has been described as homologues protein to BACE1 and we have seen to be up-regulated in our preliminary mRNA expression data, (see above, Fig. 3.13) we were not able to validate this observation in older mice using a higher n number.

5.2.4 Endogenous Aβ40 and 42 are not significantly altered by absence of RIP140 expression

In the previous chapter, using a neuronal cell line we were able to demonstrate that RIP140 overexpression leads to a reduction in Aβ42, resulting from the pathological cleavage of APP initiated by BACE1. This decrease seemed to be consequence of the observation that RIP140 overexpression was also able to decrease BACE1 strongly, suggesting that Aβ generation was blocked at the early stage of β-secretase cleavage in vitro. However, when RIP140 was silenced in vitro, we were unable to detect any changes in Aβ level. Our observation of BACE1 mRNA level was elevated in mice lacking RIP140, led us to find out whether RIP140 null mice could present changes in Aβ as well. We used two ELISA kits detecting the two mouse endogenous Aβ species Aβ42 and Aβ40 in brain homogenates of Hippocampus and frontal cortex areas. Similar to what found in vitro, the depletion of RIP140 did not affect Aβ levels (Fig. 5.8) despite an increase of BACE1 mRNA in the same area. Figure 5.8 shows that neither Aβ42 nor Aβ40 levels are affected by the depletion of RIP140 and that the ratio of Aβ42 to Aβ40 remains unchanged too. This was the case for both brain areas, hippocampus and frontal cortex.


A
Aβ 42
pico g/ µL
20
15
10
5
0
wt
RIP140 ko
B
Aβ 40
pico g/ µL
30
20
10
0
wt
RIP140 ko
Hippocampus
C
Aβ 42
pico g/ µL
20
15
10
5
0
wt
RIP140 ko
D
Aβ 40
pico g/ µL
25
20
15
10
5
0
wt
RIP140 ko
Frontal cortex

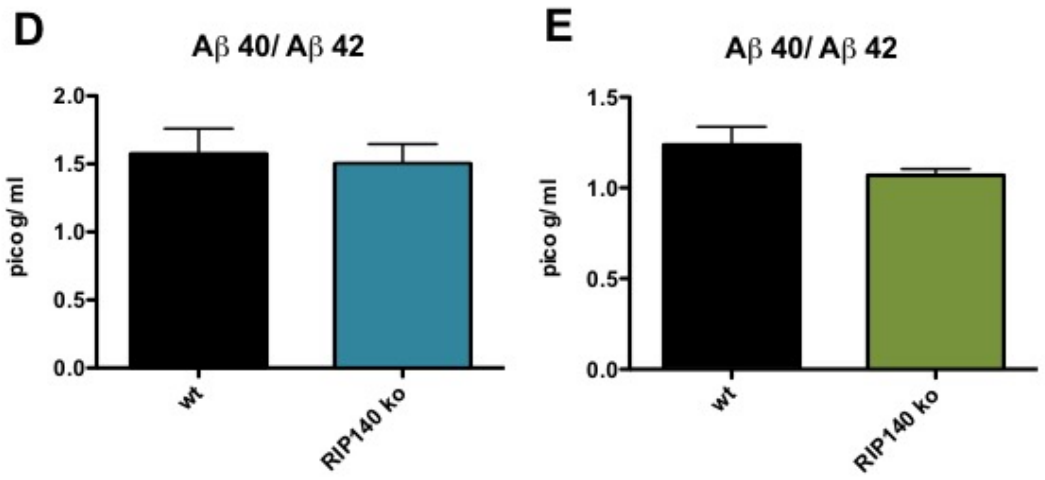


Figure 5.8: Endogenous level of the two Aβ species of 40 and 42 amino acids in RIP140 mice. ELISA assays with antibodies against either Aβ42 (A+C) or Aβ40 (B+D) were used to evaluate these species in brain lysates from hippocampus (A+B) and frontal cortex (C+D) of RIP140 knockout and wild-type mice. Comparison of RIP140 ko mice revealed no significant differences in either Aβ40 or 42 level and no changes in the ratio of Aβ42 to Aβ40 (D+E). (n= 3 for both wild-type and RIP140 ko. Values shown in graphs represent the mean value ±SEM and are expressed as a picogram per µL. Statistical analysis included student's t-test).

5.2.5 Genes involved in Aβ degradation

Although we could not observe any significant decrease in Aβ species in brains of RIP140 null animals, we wanted to investigate whether enzymes involved in the degradation of this toxic peptide may be altered. One of the best

known candidates for Aβ clearance is Neprilysin (or neutral endopeptidase (NEP)), that functions as a zinc-dependent metalloprotease with the ability to cleave peptides at the amino side of hydrophobic residues. Mice globally lacking NEP exhibit high level of Aβ depositions in the brain and AD like behavioral impairments (Madani et al., 2006). Another well described enzyme known to lead to lower amounts of Aβ is the insulin degrading enzyme (IDE). Like NEP, IDE acts as a zinc- dependent metalloprotease and is thought to be capable of Aβ degradation (Kurochkin and Goto, 1994). Similar to what is described for the ko mouse model of NEP, a mouse model lacking IDE exhibited a 50% lower Aβ degradation leading to a higher accumulation of the peptide (Farris et al., 2003).

We determined mRNA expression level of NEP and IDE in Hippocampus and frontal cortex (NEP only) regions. We observed almost 20% reduction in the hippocampal NEP mRNA expression (Fig. 4.9, A). IDE mRNA and protein expression appeared to be unaltered in Hippocampus and frontal cortex areas in comparison to wild-type expression (Fig. 5.9, B+E; Fig. 5.10, A). Examination of expression level of L-PGDS in our initial array appeared promising, however we could not confirm these changes as L-PGDS expression remained unaltered in the brains of old RIP140 ko mice (Data not shown).

We next evaluated the expression of the protein levels of Neprilysin and IDE and found that Neprilysin in RIP140 null mice showed a roughly 20% decrease in comparison to matching wild-type expression in the frontal cortex area, however this change has not shown to be significant (Fig.5.10, B). IDE expression was found unchanged.

Taken together these findings may indicate a trending decrease in Neprilysin mRNA and protein expression if RIP140 is knocked out in the mouse brain. These finding vary between the hippocampus and frontal cortex brain area.

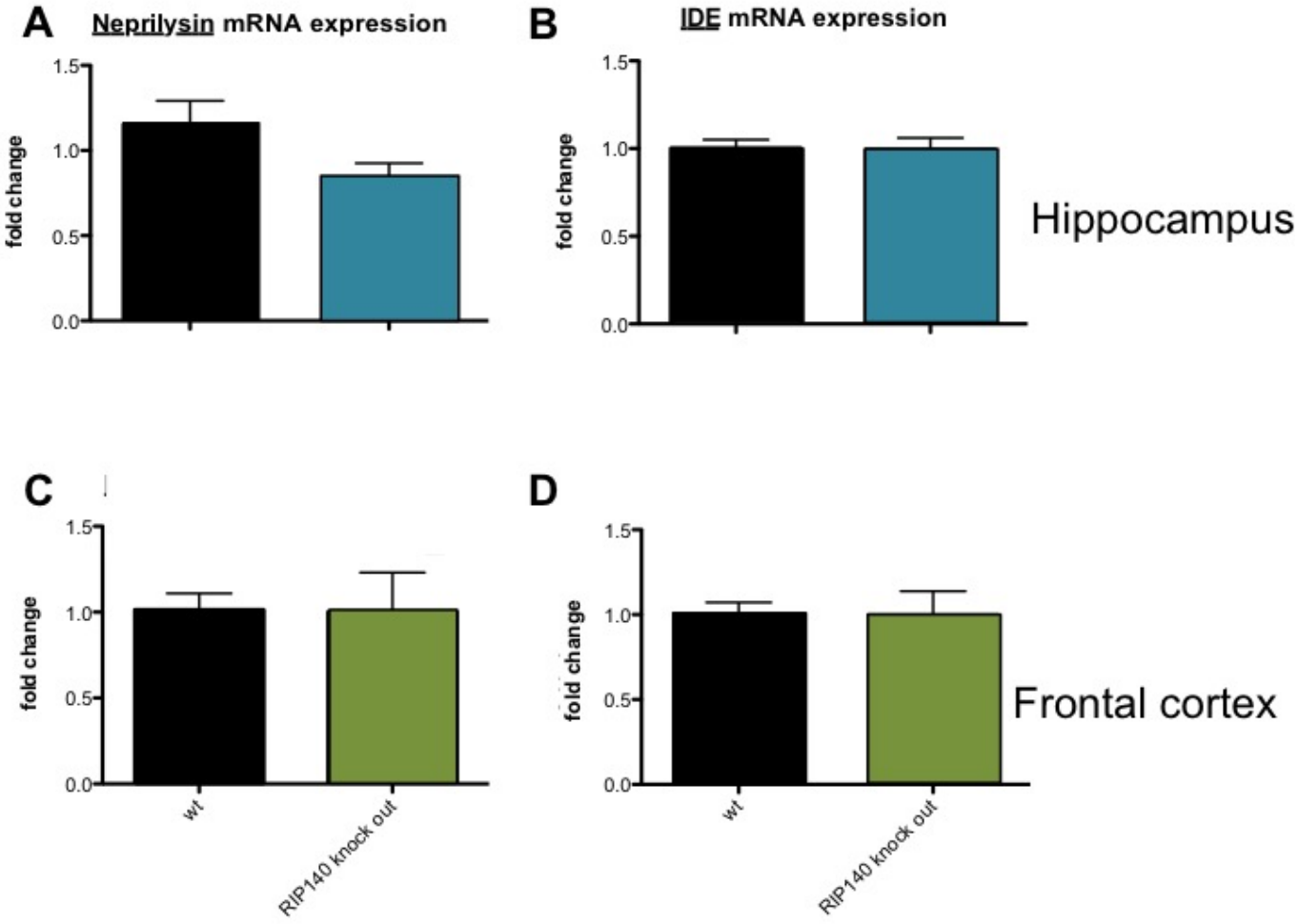
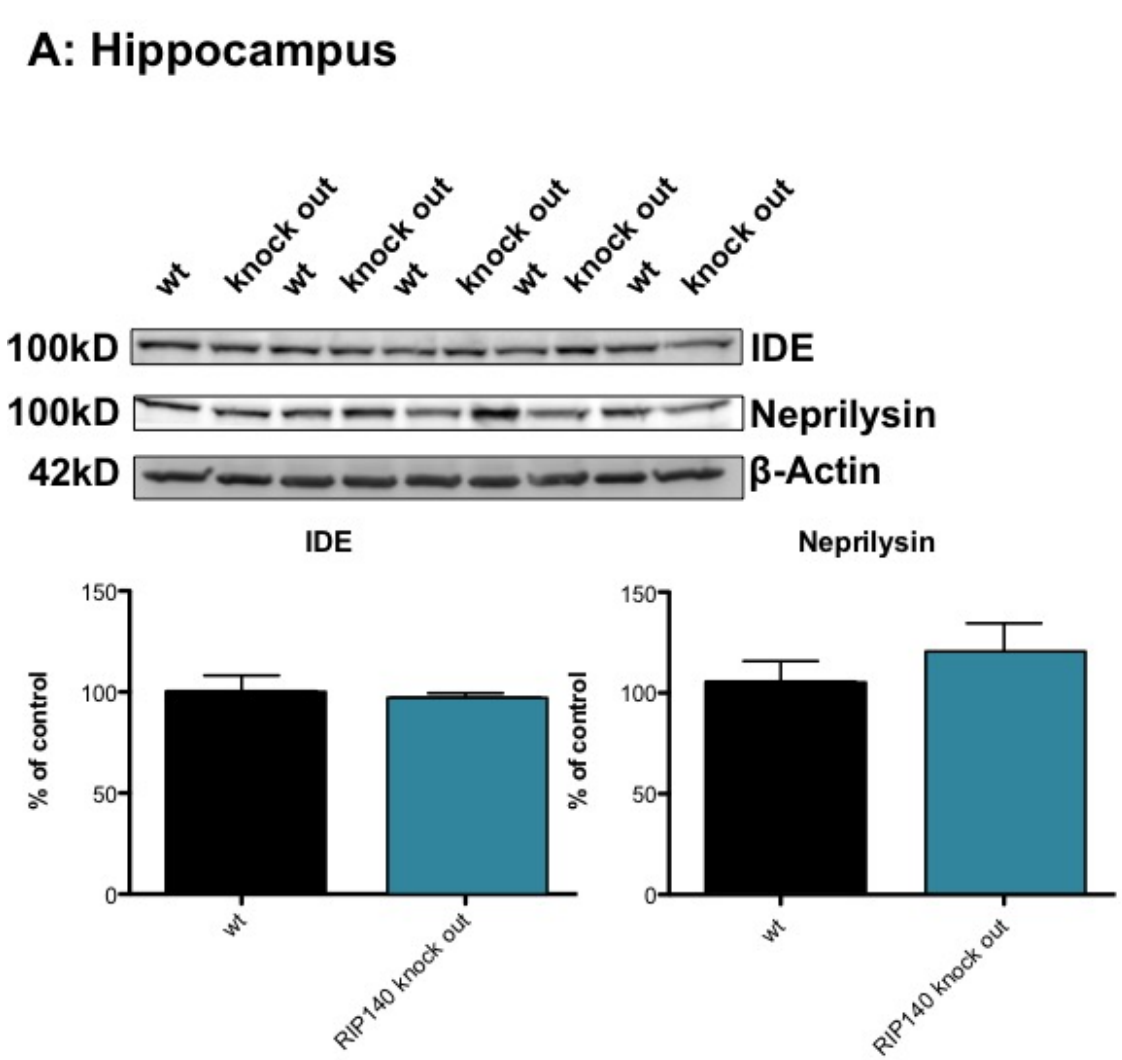


Figure 5.9: Neprilysin and IDE expression in RIP140 knockout mice. mRNA samples from hippocampus and frontal cortex obtained from 9 months old RIP140 null mice were analysed for changes in Neprilysin and IDE mRNA expression. Mice lacking RIP140 in the Hippocampus showed a decrease in Neprilysin mRNA level in comparison to wild-type animals (A). IDE hippocampal mRNA expression remained unchanged (B).Expression level of Neprilysin and IDE mRNA in the frontal cortex region appeared to be unchanged (C+E). (n=4 for RIP140 null mice and n=4 of corresponding wild-type). Values shown in graphs represent the mean value ±SEM and are expressed as a fold change in comparison to the normalized wild-type control. Statistical analysis included student's t-test).


A: Hippocampus
wt
knock out
wt
knock out
wt
knock out
wt
knock out
wt
knock out
100kD
IDE
100kD
Neprilysin
42kD
β-Actin
IDE
Neprilysin
% of control
150
100
50
0
wt
RIP140 knock out
% of control
150
100
50
0
wt
RIP140 knock out

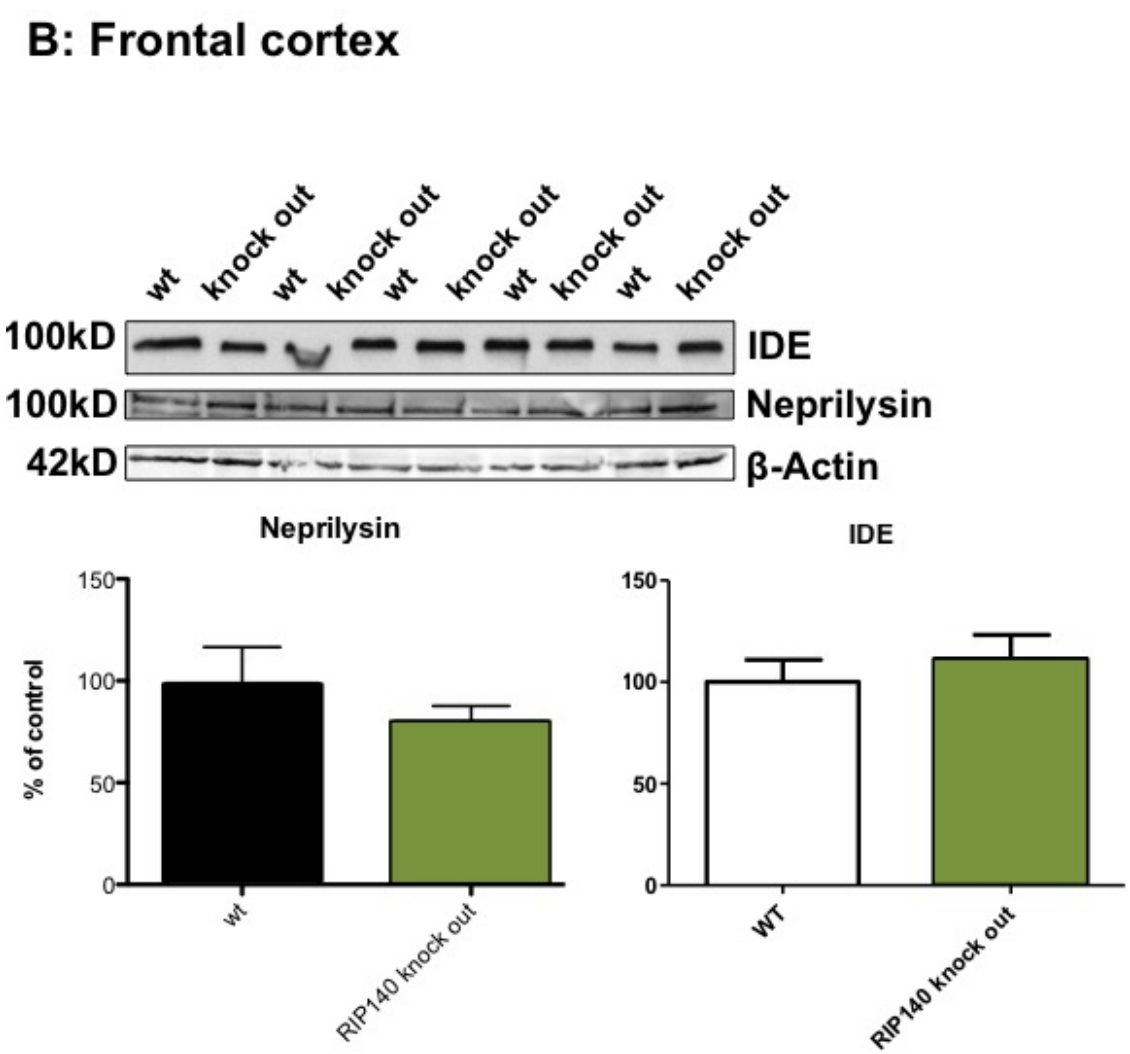


Figure 5.10: Western Blot analyses for Neprilysin and IDE protein level. Protein expression of Neprilysin in RIP140 null mice showed a roughly 20% decrease in comparison to matching wiltype expression in the frontal cortex area (B) but not in the hippocampus (A). IDE protein expression was unchanged in the hippocampus (A).Neprilysin and IDE expression were normalized to Actin level. (n=5, RIP140 mice and matching wiltype animals for both, hippocampus and frontal cortex. Values shown in graphs represent the mean value ±SEM and are expressed as a fold change in comparison to the normalized wiltype control. Statistical analysis included students t-test)

ApoE (Apolipoprotein E) genetic variant 4 (The E4 allele) is an important risk factor for late-onset AD. The normal function of ApoE in the brain is to enhance the clearance and proteolytic breakdown of Aβ by direct protein-to-protein interaction and facilitating Aβ trafficking outside the brain. The ApoE-ε4 allele is less active than the

ApoE-ε3 or ApoE-ε2 normal isoforms, and as such results in a reduced Aβ clearance. We were interested in this gene in particular, because ApoE expression is transcriptionally induced through the action of PPARγ and liver X receptors in coordination with retinoid X receptors (RXRs) (Mandrekar- Colucci, et al., 2012). It should be noted that mice do not carry the E4 allele and all experiments carried out in our mice will refer to ApoE-ε3 or ApoE-ε2, which are actively clearing Aβ.

The analysis of the ApoE mRNA levels in the hippocampus revealed a reduction in ApoE expression in RIP140 knockout mice compared to wild-type controls (Fig.5.11, A); however the ApoE protein expression remained unchanged in the Hippocampus (B) and frontal cortex (C). Unfortunately, we did not have tissue available to determine ApoE mRNA expression in the frontal cortex. These data demonstrate that mice that do not express any RIP140, express less mRNA levels of ApoE, therefore suggesting reduced Aβ clearance, and These changes were not paralleled with alterations on ApoE protein.

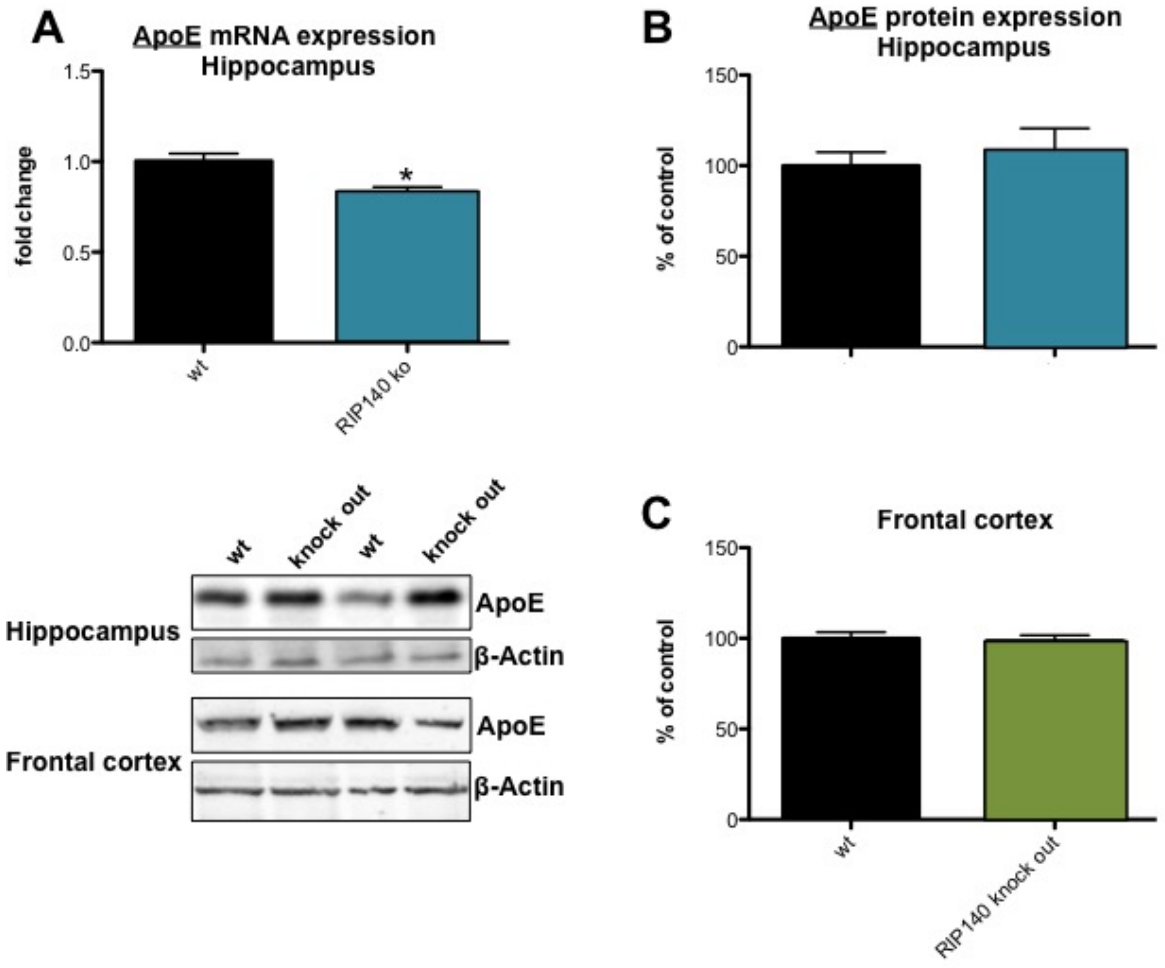


Figure 5.11: ApoE mRNA and protein expression in RIP140 ko mice. ApoE mRNA levels are significantly decreased in the Hippocampus of RIP140 ko mice (A). Protein levels are unaltered in both Hippocampus (B) and frontal cortex(C). (n=4, RIP140ko mice and n=5 for matching wild-type animals for both, hippocampus and frontal cortex. Values shown in graphs represent the mean value ±SEM and are expressed as % of wild-type control. Statistical analysis included students t-test, *$p<0.05$)

5.2.6 Genes involved in memory and cognition

Mild cognitive and memory impairment are some of the earliest indicators for Alzheimer's Disease, often appearing before a diagnosis has been done. The early death of neurons and synaptic loss often remains undetected. The expression status of molecular factors involved in these impairments could possibly help to detect or prevent progression

at earlier stages. Interestingly, during our preliminary examination of RIP140 ko mice with the RT-Profiler array, two candidates stood out that have currently been linked to play a role in both memory and cognition in mice. Growth Associated Protein 43 (GAP43) is expressed at high level during neuronal development, neuronal growth and axonal regeneration (Aigner et al, 1995; reviewed by Benowitz and Routtenberg, 1997; Doster et al, 1991). Additionally, it appears to be phosphorylated after learning and long term potentiation. The lack of GAP43 has shown to be lethal only few days after birth. One study investigating a heterozygous GAP43 knock out model showed that these mice suffer hippocampal dependent memory impairment (Rekart et al., 2005).

The second candidate is Insulin-like growth factor 2 (IgF2), getting its name from the structural similarity to insulin. It is a hormone and acts as a neutral peptide and is secreted by the liver and circulates in the blood. A recent study found that systemic administration of IgF2 leads to memory enhancement and prevents forgetting (Chen et al., 2011; Stern et al., 2014). A group studying an APP transgenic AD mouse model was even able to demonstrate that delivery of a IgF2 expression vector to the hippocampus was able to reverse AD dependent memory deficits (Pascual-Lucas, et al., 2014). In the following section we evaluated the mRNA expression status of both candidates, GAP43 and IgF2 in the hippocampus and frontal cortex of mice that do not express RIP140.

IgF2 expression seemed lower in hippocampus of RIP140 ko mice compared to wt animals, but due to high variability in the wild-type group these changes were not significant (Fig.5.12, A). Conversely, IgF2 expression appeared up-regulated in the frontal cortex area of RIP140 null mice, but this change was also not significant.

Expression level of hippocampal GAP43 mRNA appeared strongly and significantly elevated in RIP140 ko. mice compared to WTs (Fig. 5.12, A) whereas GAP43 mRNA expression in the frontal cortex remained unaltered (D).

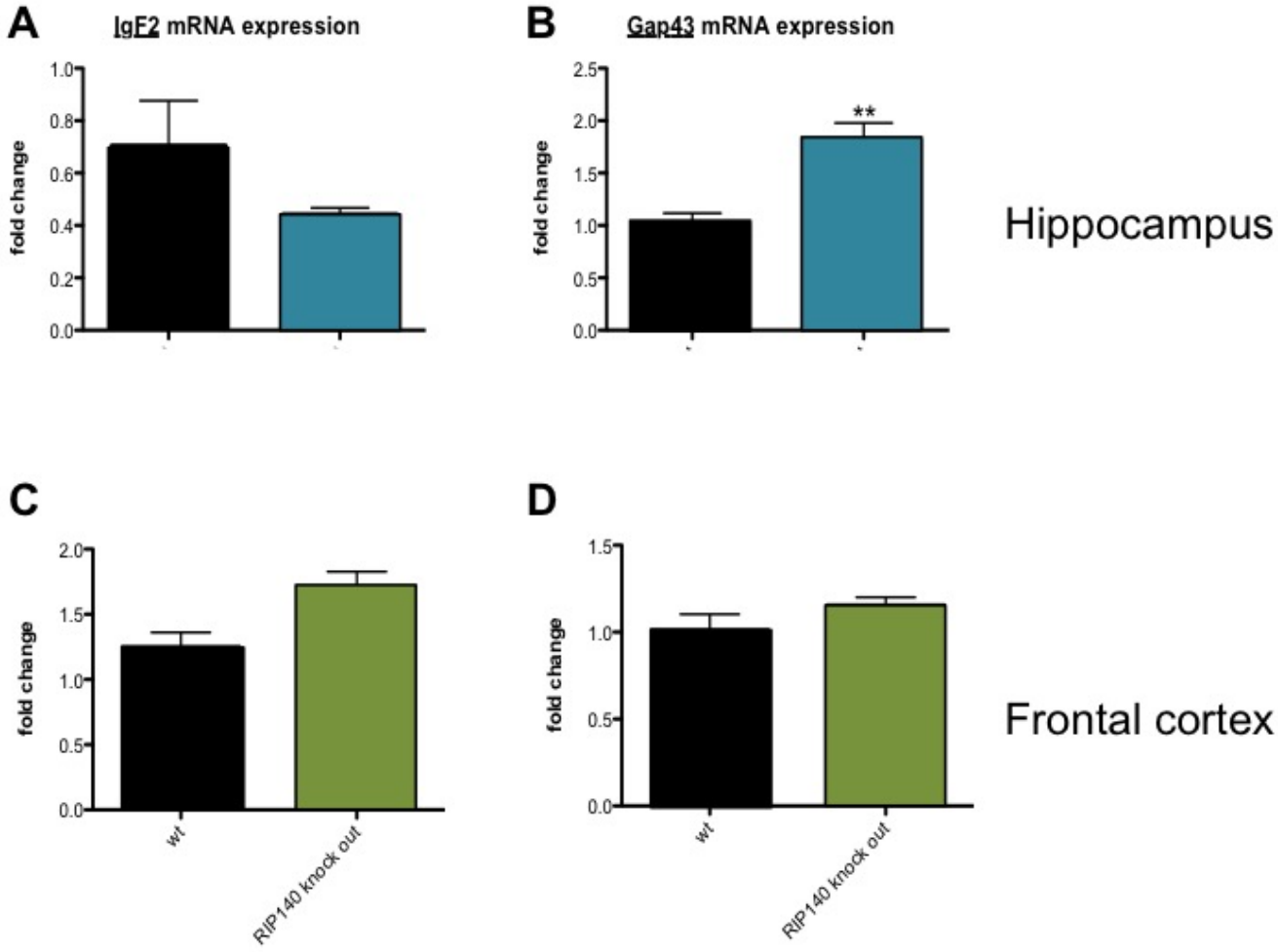


Figure 5.12: IgF2 and GAP43 mRNA expression in RIP140 ko mice. RNA extractions in hippocampus and frontal cortex of 9 months old RIP140 null mice brain were analysed for changes in IgF2 and GAP43 mRNA expression. Mice lacking RIP140 in the Hippocampus showed a non-significant decrease in IgF2 mRNA level in comparison to wild-type animals(A) and a strong, significant increase of GAP43 mRNA expression in the same area (B). Expression level of IgF2 and GAP43 mRNA in the frontal cortex region appeared to be unchanged (n=4, RIP140 mice and n=5 matching wild-type animals for hippocampus, n=4 RIP140 null mice and matching wild-type for frontal cortex). Values shown in graphs represent the mean value ±SEM and are expressed as a fold change in comparison to the normalized wild-type control. Statistical analysis included student's t-test **$p<0.01$).

5.2.7 Genes involved in the tau pathology

So far our studies have mainly focused on the pathology around the Aβ peptide, because it is the main trigger of AD, according to the amyloid hypothesis. However, NFT have also been found to be modified by PPARγ treatment in animal models of AD. Part of the pathology of AD results from the hyper phosphorylation of Tau proteins, causing the aggregation of Tau, which no longer stabilize microtubule properly, leading to axonal dysfunction and neuronal death. Tau proteins are produced by alternative splicing from the MTAP gene (Goedert et al, 1988). Microtubule-associated proteins (MAPs) of the MAP2/Tau family include the vertebrate proteins MAP2, MAP4, and Tau and homologs in other animals. MAP2 and Tau are found in neurons, whereas MAP4 is present in many other tissues but is generally absent from neurons. In our array we found the Mtap2 or also called MAP2 gene, a version of Tau to be altered in young RIP140 knockout mice, suggesting that it would be interesting to further investigate these changes in a larger population of older mice.

The array data obtained from the young RIP140 ko mouse indicated strong expression changes for the MAP2 gene. Interestingly, we here demonstrate that MAP2 mRNA levels are over a threefold higher expressed in the Hippocampus of the group of 'old' RIP140 ko mice compared with wt controls (Fig. 5.13 B+D). Two other candidates were also examined connected to the Tau pathology were found altered in the mRNA array, glycogen synthase kinase 3 (GsK3) and cycling dependent kinase 5 (CDK5), both having been linked to Tau pathology because they are kinases involved in Tau phosphorylation.

While cdK5 expression appeared unchanged in the frontal cortex of RIP140 ko mice (F), we observed a highly significant increase in the hippocampus region (E). These results demonstrate that two key proteins being involved in the Tau pathology have higher mRNA expression level in the hippocampus of mice that do not express any RIP140. These two proteins are involved in the production of Tau protein (MAP2) and Tau phosphorylation and tangle formation (CDK5).

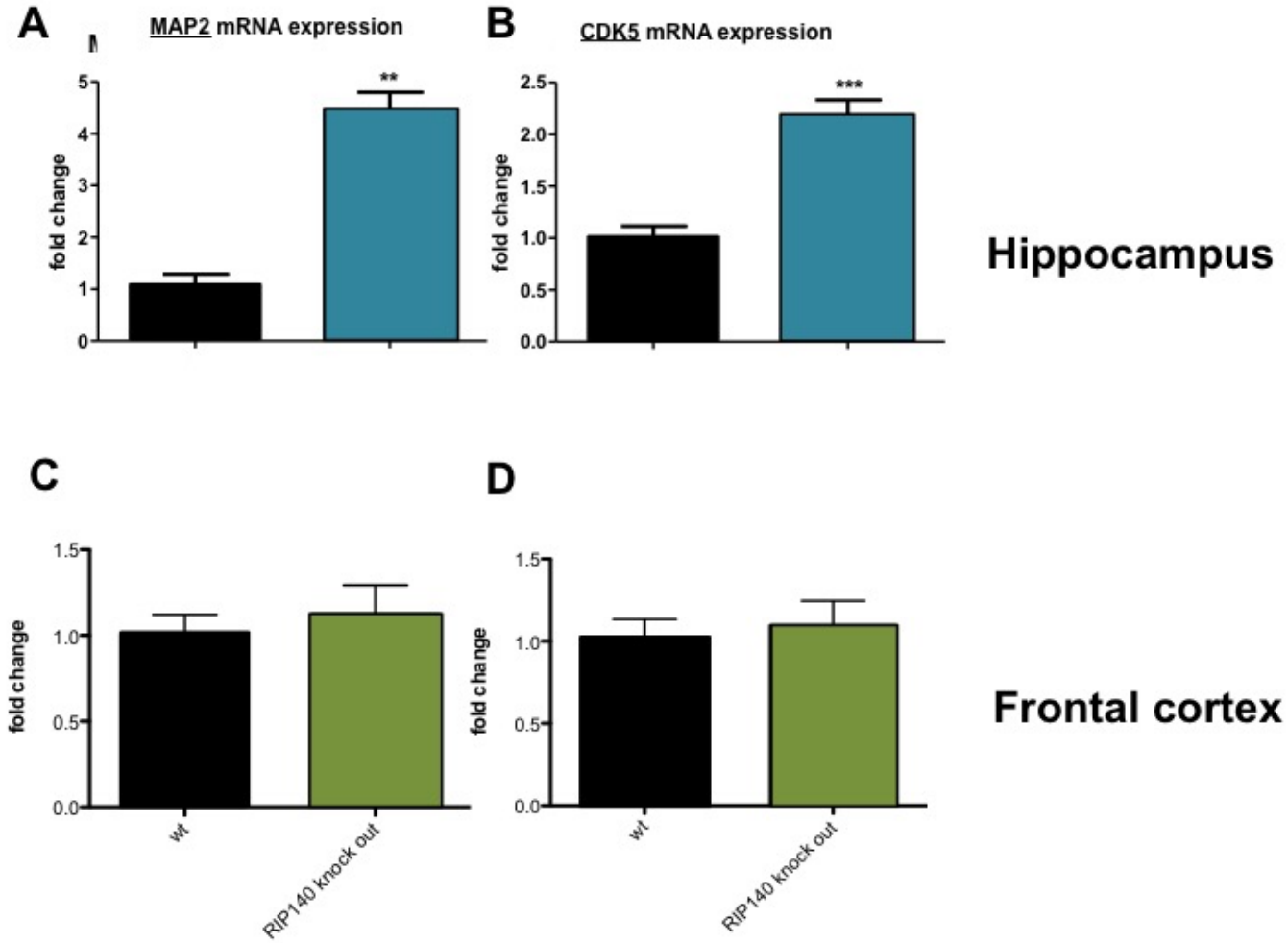


Figure 5.13: MAP2 and CDK5 mRNA expression. RNA preparations of hippocampus and frontal cortex from 9 months old RIP140 null mice were checked for changes in MAP2 and CDK5 mRNA expression. Mice lacking RIP140 in the hippocampus showed a significant increase in MAP2 (A) and cdK5 (B) mRNA level in comparison to wild-type animals but no differences for these genes were observed in the frontal cortex (C,D). (MAP2: n=4 for ko animals and n=2 for matching wt. cdK5: n=4 for ko animals and n=3 for matching wt. Values shown in graphs represent the mean value ±SEM and are expressed as a fold change in comparison to the normalized wild-type control. Statistical analysis included students t-test **p=0.01, ***p=0.001)

GSK3 is a proline-directed serine/ threonine kinase with permanent activity. It is involved in various physiological processes including glycogen metabolism and gene transcription. Additionally, GSK3 has been linked to the pathology of AD in both familial and sporadic forms of the disease. This lead to the 'GSK3 hypothesis of AD,' which implies

that

GSK3 over activity is responsible for memory impairment, increased β-amyloid level, microglial inflammatory responses but also Tau hyper phosphorylation. Two genes of GSK3 exist, producing GSK3β and GSK3α and both versions are ubiquitously expressed but partially involved in different processes (Mukai et al.,2002; Schaffer et al.,2003). Both versions, GSK3β and GSK3α can lead to hyper phosphorylation of Tau. Only GSK3α knockout mice have been shown to be viable whereas GSK3β knock-out mice die in utero (MacAulay et al. 2007; Hoeflich et al. 2000). Transgenic mice overexpressing GSKβ showed a hyper phosphorylation of Tau followed by neurodegeneration. This was reversed when these mice were treated with a GSK3 inhibitor and it could prevent Tau driven NFT formation (Lucas et al., 2001). GSK3 is negatively regulated by kinases that directly inhibit GSK3 by phosphorylating a regulatory N-terminal serine of GSK3 known as Ser9 (S9) of GSK3β (Jope and Johnson, 2004). Given that GSK3 is involved in many aspects of AD pathology we aimed to explore this enzyme in the brain of the RIP140 knockout mice. For the mRNA expression level for GSK3 we observed an 2 fold increase of GSK3 level in the hippocampus of RIP140 ko mice, however due to high variability this increase could not be proven significant (Fig 5.14, E). The frontal cortex region also seemed to have slightly higher GSK3 level but like in the hippocampus these changes were not significant (B).

In addition to the mRNA data, we assessed changes in protein level of GSK3 via western blotting, being able to detect and quantify the protein expression of both subtypes GSK3β and GSK3α as well as the phosphorylated version (pGSK3). Fig. 5.15).

The results of the Western blot experiments using an antibody that selectively recognizes the inactive phosphorylated form of GSK3β at position S9 revealed a decrease in the Hippocampus of RIP140 knockout mice, which appeared to be non-significant (A); no changes were observed for pGSK3 in the frontal cortex area (B). GSK3α was significantly up regulated in the frontal cortex of RIP140 mice (E) but unchanged in the Hippocampus (C). GSK3β protein levels were increased in the Hippocampus and frontal cortex (D+F) of RIP140 ko mice and in both of these changes were statistically significant.

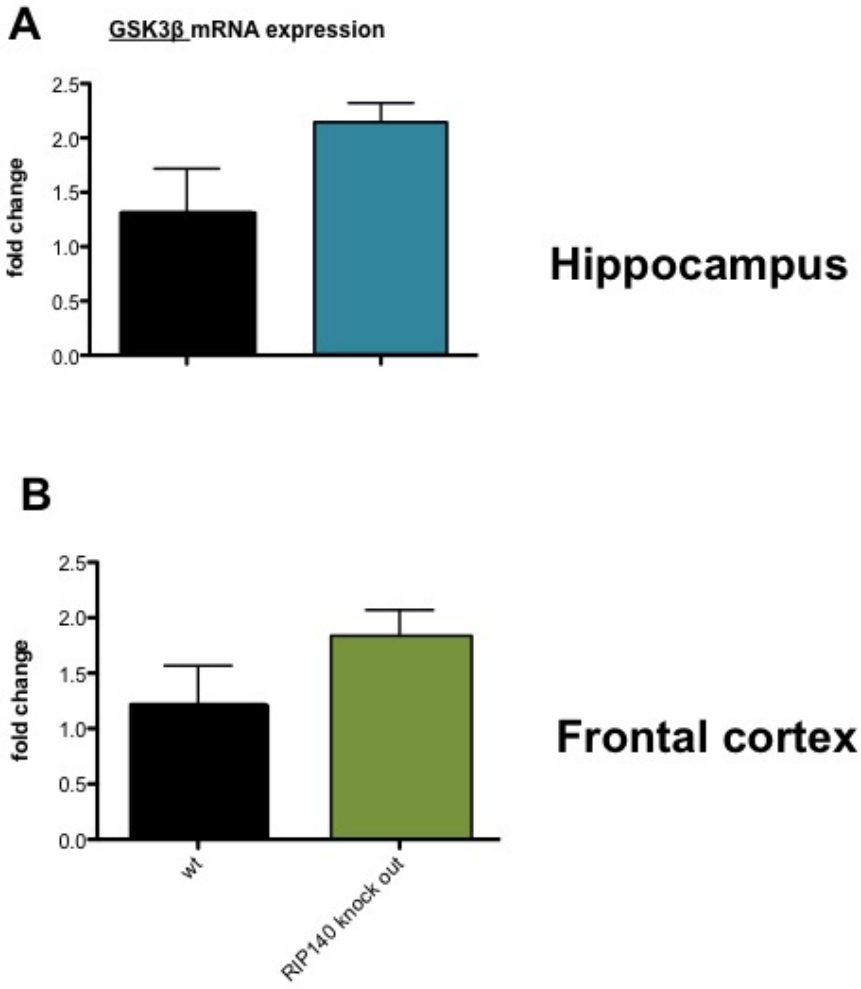
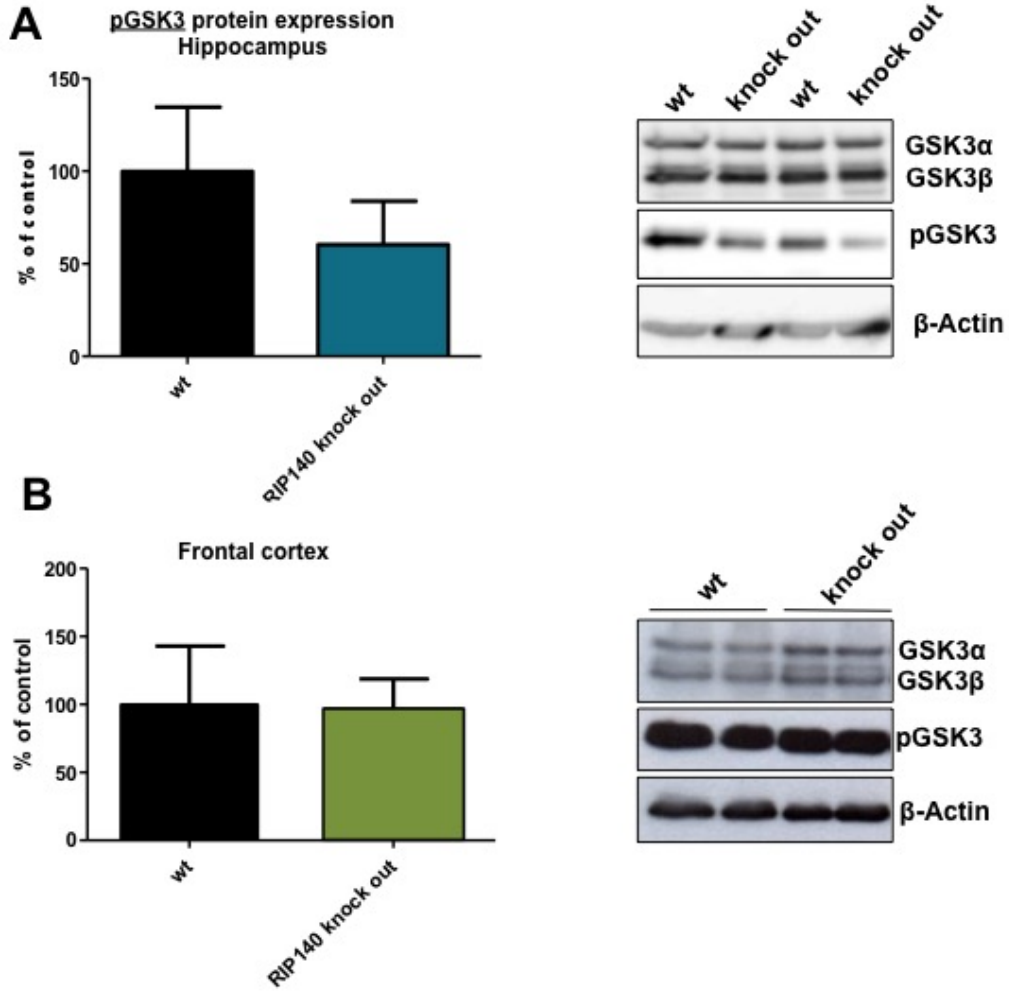


Figure 5.14: GSK3β mRNA expression. GSK3β mRNA seemed increased in the hippocampus and frontal cortex, however not significant in either case (A+B). GSK3β: n=4 for ko and wt animals. Values shown in graphs represent the mean value ±SEM and are expressed as a fold change in comparison to the normalized wild-type control. Statistical analysis included student's t-test.



5.2.8 5.2.8 Effect of RIP140 knock out on the levels of inflammatory mediators in the brain

Progression and increased inflammation in the brain is a major characteristic of the aging process and is associated with age-related diseases such as AD. Neuroinflammation contributes to the formation and aggregation of Aβ plaques and Tau tangles and is involved in Aβ toxicity (see review Sastre, Klockgether and Heneka, 2006).

Inflammation therefore is an early and relevant event for the progression of the pathology of AD, rather than just being a consequence of the other hallmarks (Zhang et al. 2013). Various pro-inflammatory factors have been described

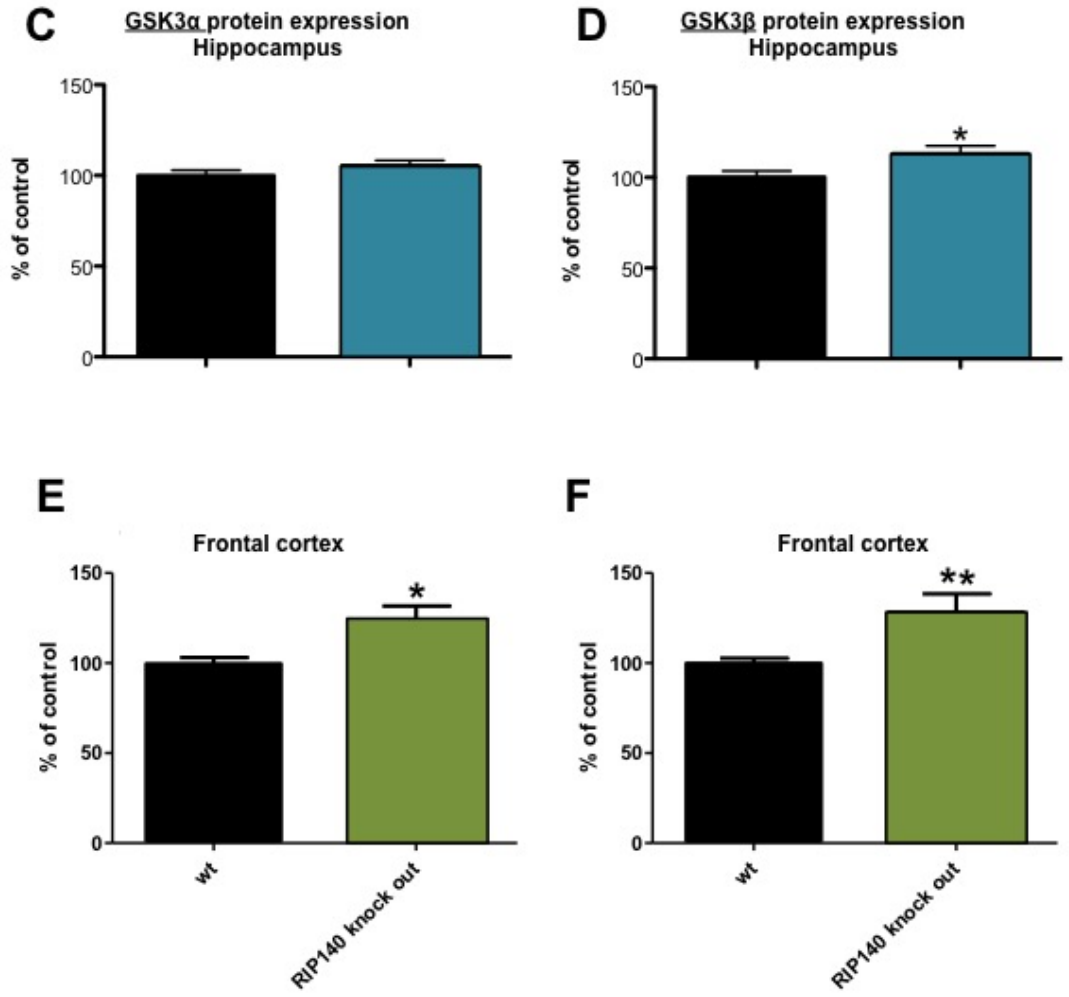


Figure 5.15: GSK3 protein expression in RIP140 knockout mice. Representative Western blot and quantification of different GSK3 subtypes (α and β) and phosphorylated GSK. No significant changes were observed for pGSK3 in cortex and hippocampus of RIP140 knockout mice(A, B). GSK3α was higher in the frontal cortex of RIP140 ko mice (E) but not the Hippocampus (C). GSK3β was up regulated in the Hippocampus (D) and frontal cortex (F) of RIP140 ko mice. (n=5, RIP140 mice and matching wild-type animals for both, hippocampus and frontal cortex). Values shown in graphs represent the mean value ±SEM and are expressed as % of wild-type control. Statistical analysis included student's t-test. *$p<0.05$, **$p<0.01$).

and linked to the progression of AD pathology, ranging from short peptides to enzymes. Interleukins are a group of cytokines and their receptors are present on astrocytes and microglia in the brain and are also known to be involved in the development of spatial memories in mice (Menachem-Zidon et al. 2010).

Interleukin 1 (IL1) is a pluripotent, pro-inflammatory cytokine involved in the regulation of inflammatory events. It belongs to a family consisting of three related proteins, IL1α, IL1β and IL-1 receptor antagonist (IL-1ra), all encoded by separated but related genes. IL-1α and IL-1β are isoforms and share some homology as well as affinities for IL-1 receptors, biological activities and regulatory factors (Murzin et al., 1992, Auron et al., 1994). One of the main differences between IL-1α and IL-1β is that while IL-1α is active in its precursor and mature form, IL-1β can only be active in it mature form. IL-1 cytokines are expressed at low level in adult healthy brains (Vitkovic et al., 2000). Overexpression of IL-1β in Alzheimer brain was first shown by Griffin et al. in 1989. AD is a prime example for overexpression of IL-1β and it has been associated into initiation as well as the progression of the disease.

Another Interleukin, interleukin 6 (IL-6), is an interleukin that may act as a pro-inflammatory cytokine or an anti-inflammatory myokine. A study conducted in 1996 by Hul and Bauer examined post mortem brain from AD patients for IL-6 level and compared them to healthy brains (Hul et al., 1996) They found that IL-6 was consistently higher expressed in people with AD than in healthy persons. Interestingly they could also link the location of IL-6 expression to neuritic Aβ plaques. This co localization was found to appear before neuritic pathology has not yet developed (Fig. 5.16) and the authors hypothesized that this could indicate that the appearance of interleukin-6 may precede neuritic changes and is not just a consequence of neuronal degeneration.

Some of the factors we have previously evaluated can also be linked to the inflammatory aspect of AD, including GsK3 (Jope et al., 2007). GsK3 has been shown to drive inflammation in dendritic cells and to increase level of IL-6 (Rodionova et al., 2007).

To find out whether the lack of RIP140 may affect the expression of cytokines IL-1β and IL-6 we then determined by ELISA changes in IL-1β and IL-6 in homogenates of hippocampus and cortex of RIP140 mice. It appears that in the frontal cortex, both IL-1β and IL6 seem present in higher levels in RIP140 KOs than in control animals (Fig 5.17 C+D), however in the case of IL-1β this increase seems to be just below statistical significance ($p=0.057$). There was high variability between the values of IL-6, due to the lower number of samples used for these experiments.. There were no obvious changes in the level of IL-1β or IL-6 in hippocampus of RIP140 mice in comparison to wild-types (A+B).

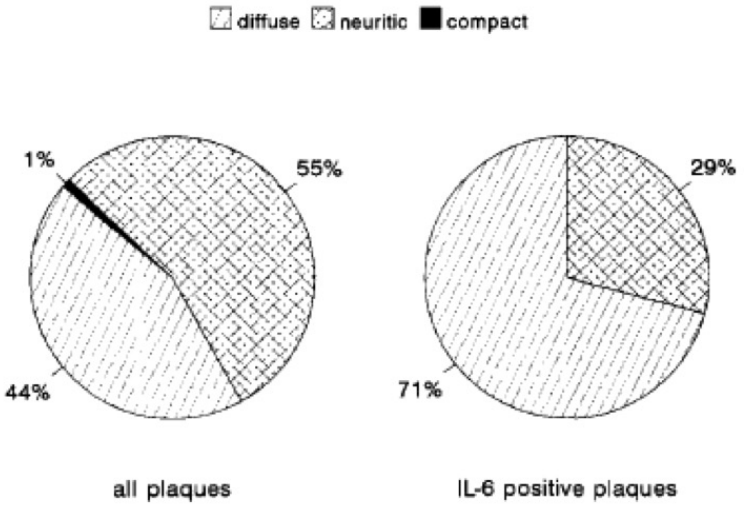


Figure 5.16: Comparison between the distribution of all plaques and IL-6 positive plaques. Plaques were measured according to the morphology in the brains of AD patients. More than 50% of plaques have characteristic neurotic signs (left). More than 70% of all plaques are diffuse plaques (right). Taken and modified from Hul et al, 1996.

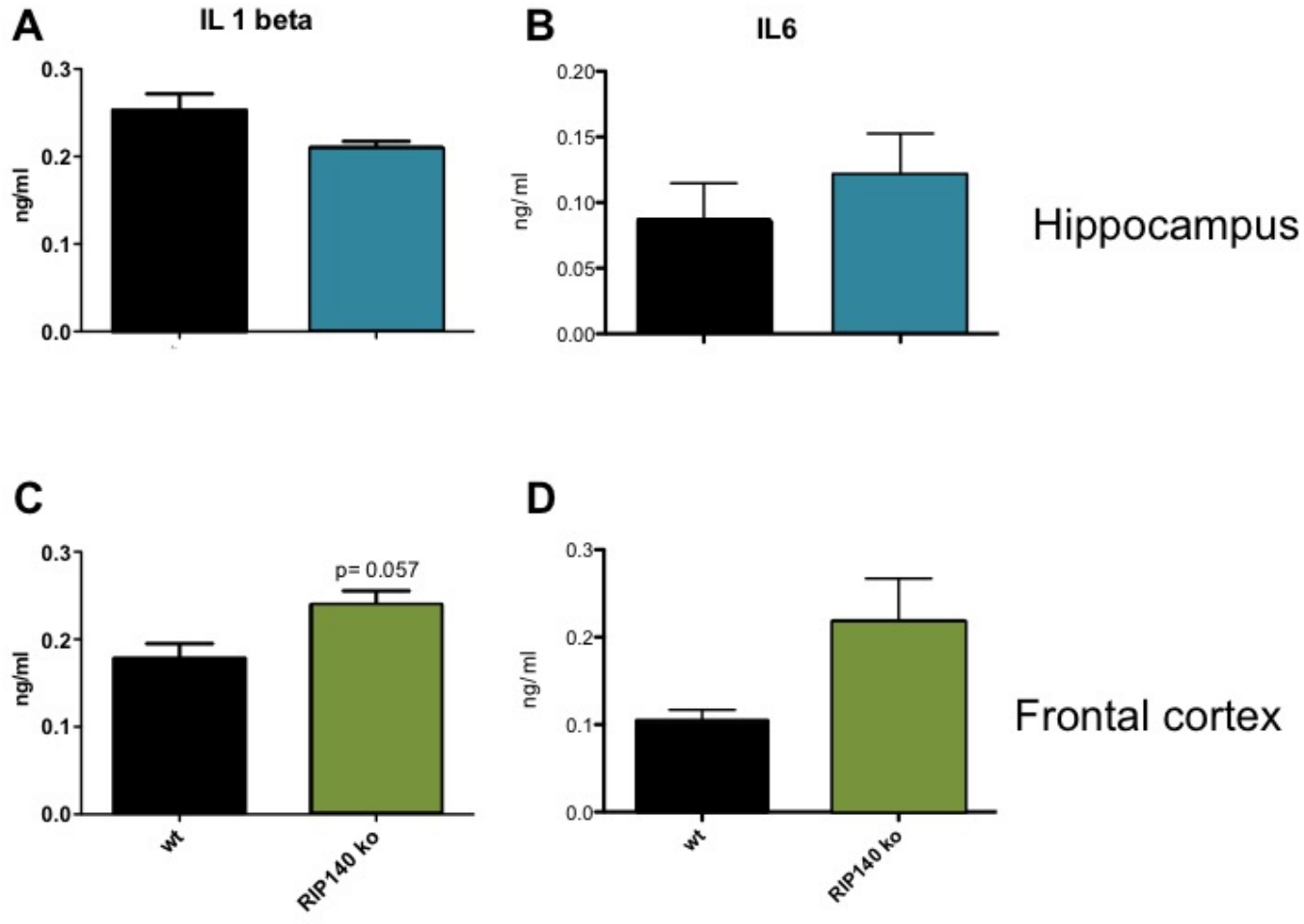


Figure 5.17: ELISA assays for interleukin expression. Homogenates of hippocampus and frontal cortex were tested

In AD brains, the deposition of Aβ can provoke activation of microglia cells alongside with an increase of pro-inflammatory molecules. The ionized calcium-binding receptor adaptor molecule 1, also known as allograft inflammatory factor 1 (AIF-1) (Iba-1) is specifically expressed in microglia cells and is increased when these cells are activated.

These expression changes in Iba-1 allow discrimination between activated and surveilling microglia cells.

To determine whether there were changes in microglia activation in RIP140 knockout mice, we obtained brain sagittal sections from those animals and stained them with an IBA-1 antibody (Fig.5.18).We quantified then Iba-1 staining in hippocampus and frontal cortex. We observed a non-significant increase in IBA-1 staining in the hippocampus, of RIP140 knockout animals compared with wt controls (A, C). There was no change for IBA1 positive cells in the cortex (B, D).

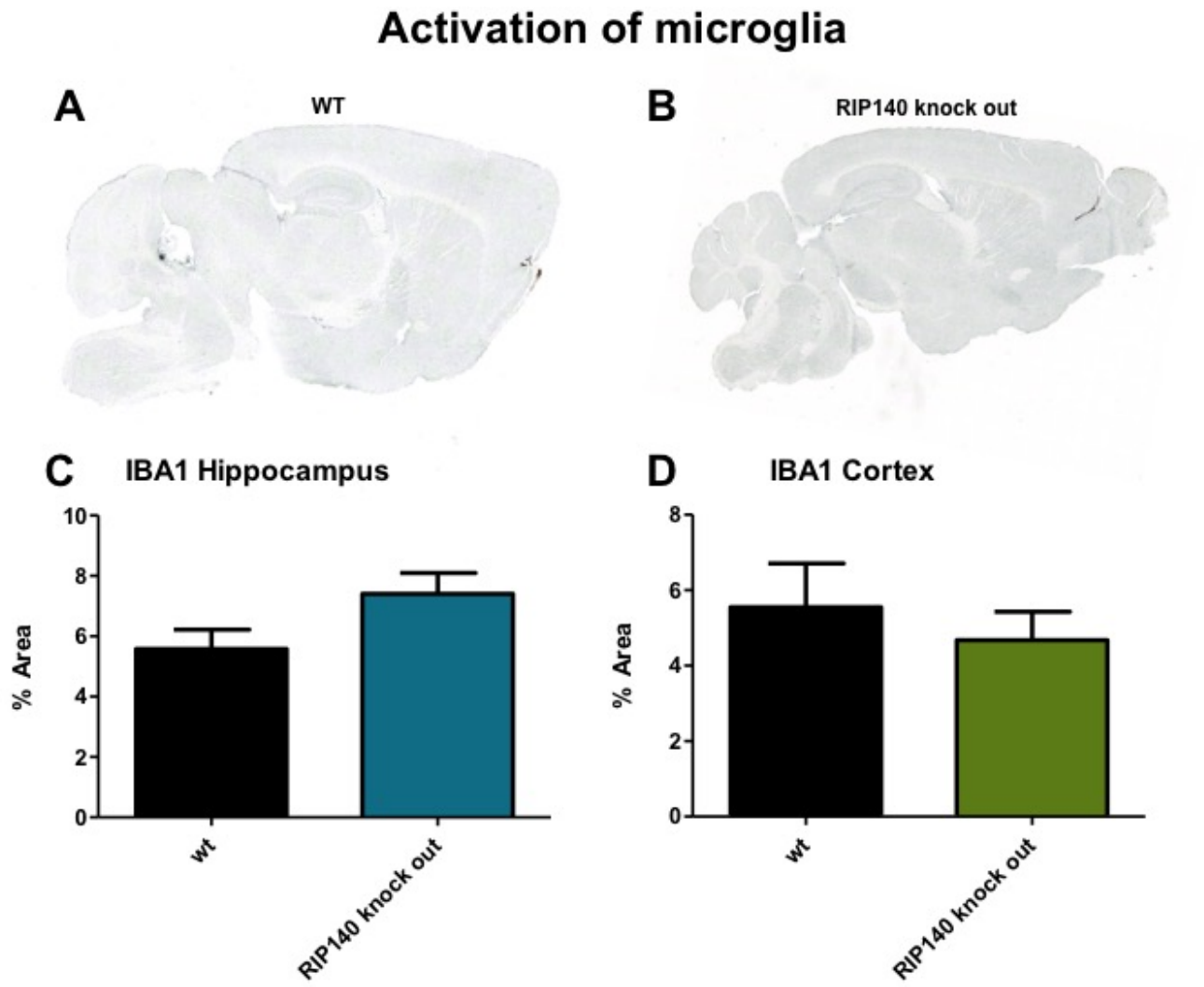


Figure 5.18: Microglial activation in RIP140 ko brain sections. Sections of 40µMwere prepared and immunohistochemistry using a stain against IBA1 was performed to detect activated microglia cells. Areas of Hippocampus (A, C) and Cortex (B, D) were quantified, but none of them revealed a significant difference. Values shown in graphs represent the mean value ±SEM and are expressed as % area of wild-type control. Statistical analysis included student's t-test. Staining, quantification and analyses were performed by Mr. David Morrow).

In human brain tissue from patients with AD, activated astrocytes were closely associated with amyloid plaques (Wegiel et al, 1991). Astrocytes might be activated by human Aβ (DeWitt et al, 1998) indicating a correlation between this protein and subsequent alterations in astrocyte function.

Glial fibrillary acidic protein (GFAP) is a protein that is expressed in astrocytes and once activated, astrocytes

show elevated GFAP expression. Astrocytes can also accumulate neuron-derived amyloid material from local dying neurons. Once these debris accumulate within the astrocytes, they themselves might undergo cell death, resulting in the formation of GFAP-positive amyloid plaques (Nagele et al, 2004).

Following this, we stained sagittal brain slices using a GFAP antibody to determine changes in astrocyte activation in either the Hippocampus or Cortex of RIP140 knockout mice. We observed an increase of GFAP positive staining in the Hippocampus of RIP140ko mice (Fig. 5.19, A) but no change in the Cortex in comparison to wild-type animals (B).

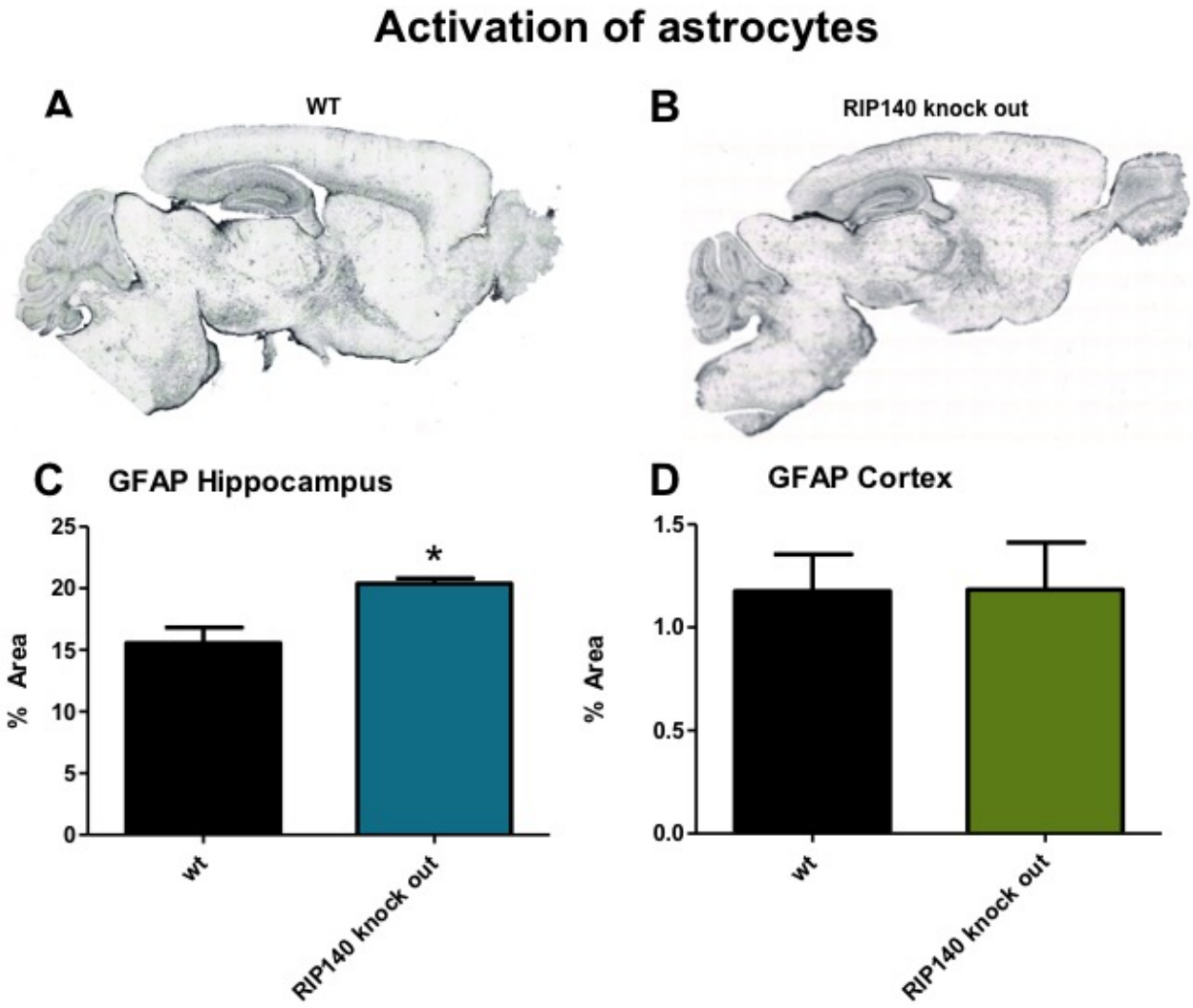


Figure 5.19: Astrocyte activation in RIP140 knockout brain sections. Immunohistochemistry was performed on fixed 40µMbrain sections using an anti GFAP antibody. Hippocampi of RIP140 KO mice exhibit higher level of reactive astrocytes (A). No changes were seen in the cortex (B). Values shown in graphs represent the mean value ±SEM and are expressed as % area of wild-type control. Statistical analysis included student's t-test. *$p<0.05$. Staining, quantification and analyses were performed by Mr. David Morrow).

5.3 Neuronal density in RIP140 knock out mice

The study of Duclot et al in 2012 described how the loss of RIP140 impairs memory and cognitive functions. The Hippocampus region is a well-known area to be responsible the storage of long term memories and spatial functions.

Our staining showed previously (Fig.5.1) that RIP140 is highly expressed in this brain region. We aimed then to find out, if the loss of memory described by Duclot could possibly be linked to a loss of neurons in the Hippocampus of RIP140 ko mice. We prepare brain sagittal sections of 40µMof RIP140 knockout and wt mice and stained them

with NeuN antibody, which stains specifically the nucleus of the neurons (Fig. 5.20, A 1-7). At the layer where the Hippocampus and its sub regions were visible (B), we counted or measured neuronal density in different hippocampal sub regions. We divided into the sub regions as previously done by Ramon and Cajal (C). In the less dense CA3 region we counted single cells whereas in the CA1 and Dentate Gyrus we were only able to determine the intensity in an area per [l square meter ([lm2), since the density of neurons is very high on those regions.

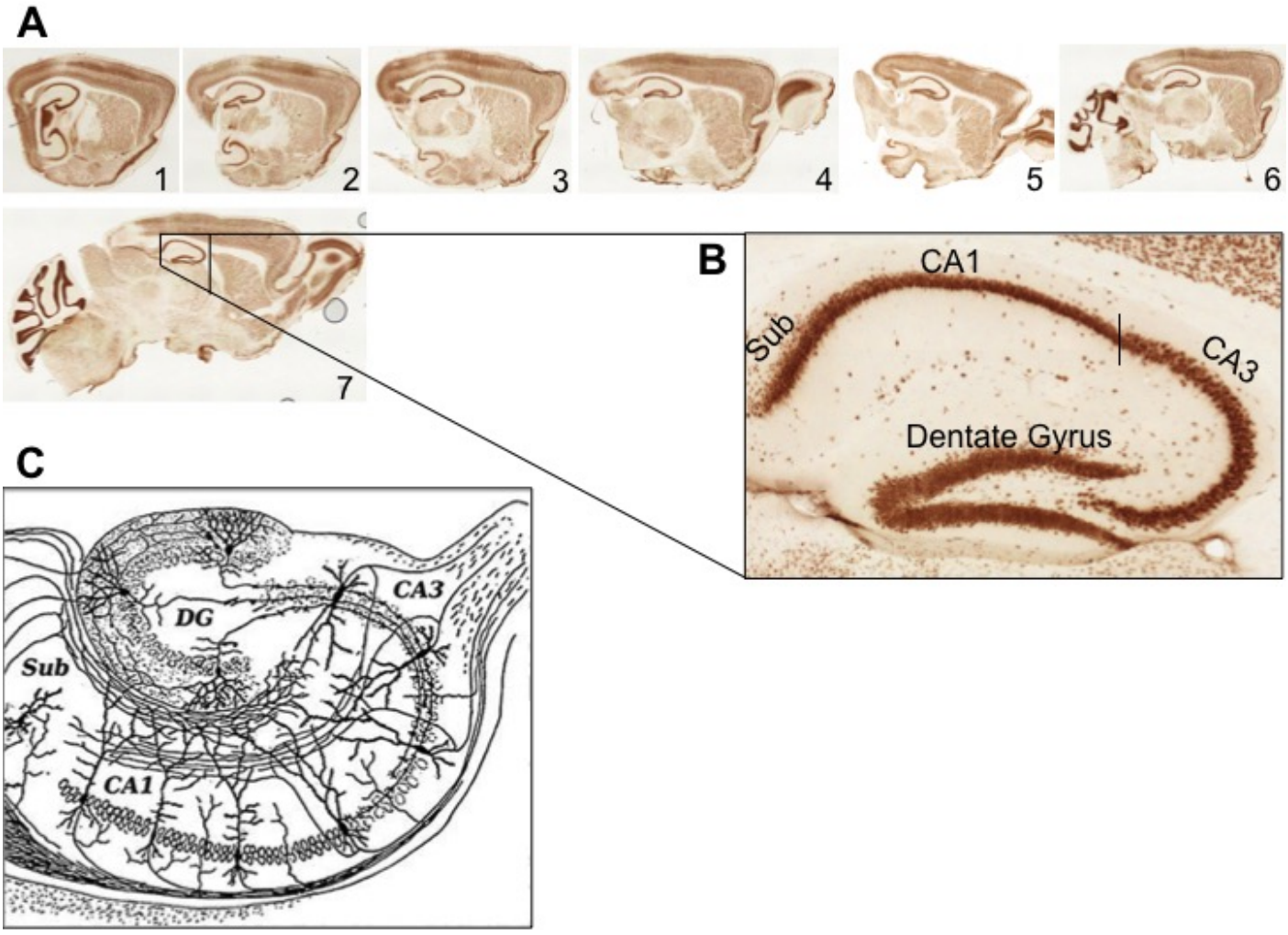


Figure 5.20: Brain dissections stained with NeuN antibody. Fixed sections were stained with a NeuN antibody to determine neuronal density. Each hemisphere was cut into 40µMsections and layers that started to show the Hippocampus (A,1) were used. We quantified the density of neurons in Subiculum, CA1, CA3 and dentate Gyrus (B), quantification of neuronal density was done either using a cell count tool (CA3 region) or the intensity per µM square meter area was measured. The sub sectioning was performed according to the description of the Hippocampus by Ramon and Cajal (C).

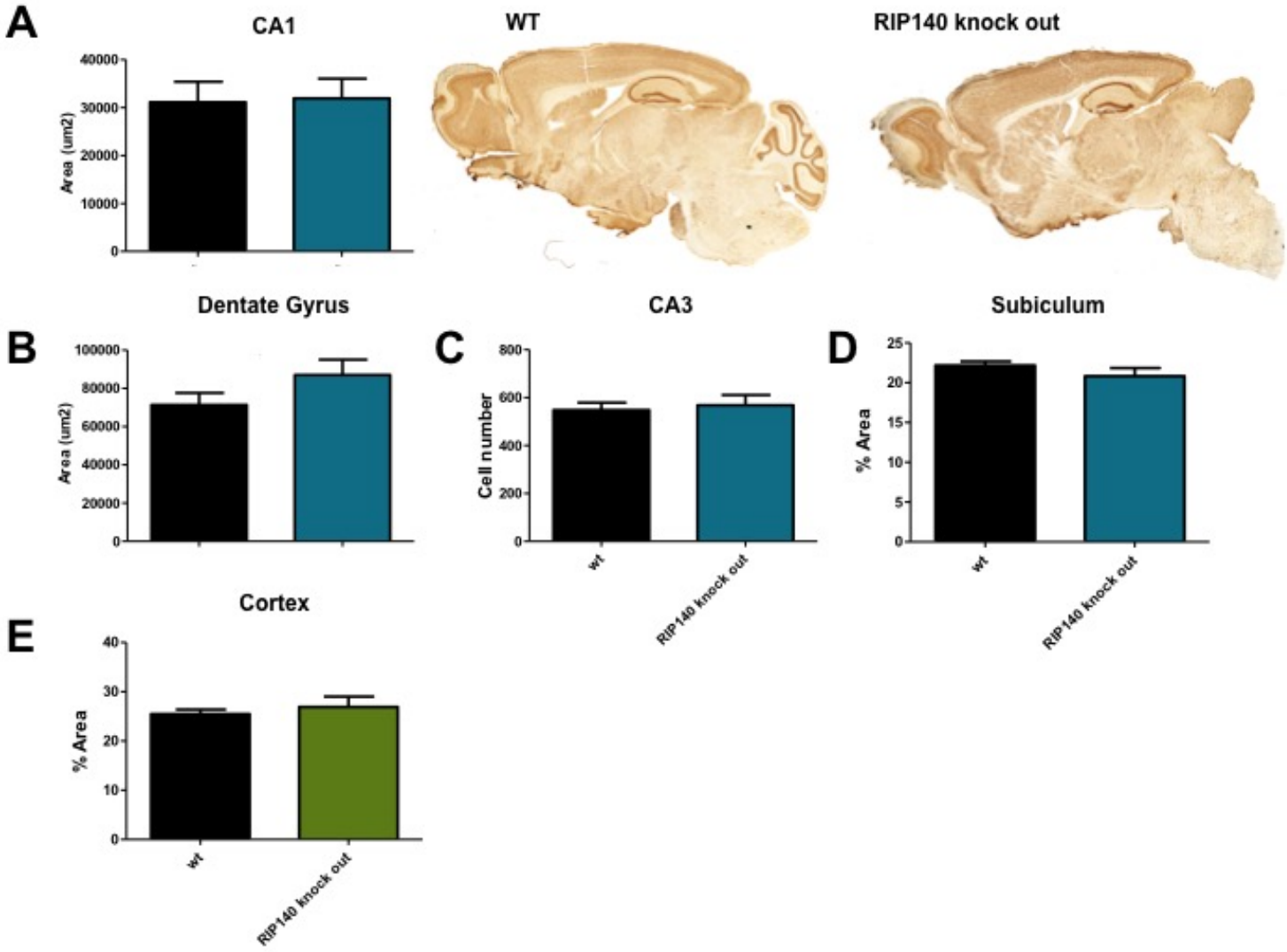


Figure 5.21: Neuronal density in the brains of RIP140 ko mice. The hippocampal sub regions CA1 (A), Dentate Gyrus (B), CA3 (C) and Subiculum (D) did not show any changes in neuronal density or cell number in RIP140 mice in comparison to wild-types. No differences were observed in the Cortex region (E). Values shown in graphs represent the mean value ±SEM and are expressed as % Area of wild-type control. Statistical analysis included student's t-test. Quantification and analyses were performed by Mr. David Morrow).

5.4 Discussion

This chapter shows for the first time how changes in the expression of the nuclear receptor co factor RIP140 in the brain has implications on AD. So far only very few studies had a look at this cofactor in the brain and never before a connection to AD was made.

The study of the role and distribution of PPARγ in the brain is also very recent (Heneka and Landreth, 2007) due to the lack of reliable antibodies. In addition, most of the research on this transcription factor and its cofactors had been carried out in tissues related to metabolic disease, such as the adipose tissue, muscle and pancreas. We here report how relevant is the role of RIP140 in the regulation of the expression patterns of genes involved in AD, by using a knockout model of RIP140. In the previous chapter, we gained insight into the potential consequences of RIP140 depletion in vitro, showing how it can affect BACE1 expression and consequently Aβ generation.

Interestingly the study of the distribution of RIP140 in the mouse brain revealed how its levels are highest in the hippocampus, but also in the frontal cortex two areas being strongly affected during AD.

5.4.1 Implications on APP processing

In the previous chapter, we were able to show that knock down of RIP140 in a neuronal cell line can elevate BACE1 mRNA, protein and activity level. Assessment of BACE1 mRNA expression level in the Hippocampus of RIP140 knockout mice confirmed this observation, confirming the hypothesis that RIP140 regulates the amyloidogenic pathway via inhibiting β-secretase cleavage. However, the mRNA levels of BACE1 in frontal cortex did not exhibit such changes and it is unclear if the involvement of BACE1 in this area is relevant. Unexpectedly, BACE1 protein levels were unchanged in the Hippocampus of RIP140 knockout mice. It may be difficult to detect changes in BACE1 protein expression, as this step naturally appears later and undergoes further regulatory processes such as post-translational changes (Rosnner et al, 2006). However, it would be worth in the future to investigate changes in BACE1 activity in those tissues. In AD it is still not clear why BACE1 is elevated and yet unknown deregulations or disturbances of biochemical pathways may be the ultimate cause. Interestingly, it was published that inflammation is an important factor, leading to an increase in BACE1 levels (Sastre et al, 2003). BACE1 promoter contains binding sites for transcription factors involved in inflammation, such as PPARγ and NFκB (Sastre et al, 2006; Rossner et al, 2006). There are evidences that pathologies with an inflammatory component can drive AD pathology, in particular by enhancing BACE1 expression and consequently Aβ generation. This has been reported for traumatic brain injury

cases, metabolic disease, infection, etc. (Sastre et al., 2011).

In this study, we investigated the effect of RIP140 knockout in mouse endogenous proteins involved in AD, such as BACE1 and mouse Aβ. The brain of the RIP140 knockout that we used does not replicate several features present in AD brains, such as amyloid plaques, neuronal death and neuroinflammation. We did not crossed a RIP140 ko with an APP transgenic mouse. Consequently, perhaps the effects of RIP140 knockout on BACE1 and Aβ would have been stronger if investigated in APP/RIP140ko mice. For the same reasons, it may have been impossible to detect actual changes in Aβ levels as generation of this peptide is the latest step during APP processing and the RIP140 knockout mice may have not had enough Aβ production in the first place. Most animal models of AD contain a double if not triple transgenic variation to cause Aβ plaque generation, meaning that basal Aβ are simply too low to detect any changes as a cause of any changes or treatments. In addition, BACE1 has stronger affinity for APP containing the Swedish mutation than for wild-type APP, which is the form expressed in the mice that we investigated. In any case, we would expect to find an increase of Aβ species in the absence of RIP140, but as described above we were not able to detect any changes in endogenous Aβ species in RIP140 ko mouse brains.

The homologue BACE2 was unaltered in both brain regions and it is possible that the PPRE domain present in thee BACE1 promoter,, is not present within the BACE2 promoter and therefore this gene is not affected by either RIP140 or PPARγ.

5.4.2 RIP140 affects the levels of the Aβ clearing enzyme ApoE but not IDE or Neprilysin

Previous studies from Espuny-Camacho (2005, 2010) showed that PPARγ may be involved in the clearance of Aβ. They found that PPARγ activation modulates a cell surface metalloprotease that can be inhibited by metalloprotease inhibitors. However, they were unable to identify what enzyme was, although the metalloprotease profile of the Aβ-degrading mechanism was surprisingly similar to insulin-degrading enzyme (IDE). Enzymes like Neprilysin and IDE have been described as metalloproteases involved in Aβ degradation and appear to be down regulated during the development of AD, consequently leading to greater Aβ accumulation. However, we did not detect any changes in the expression of these enzymes in RIP140 knockout brains.

We found that in the RIP140 knock out mouse line, the animals exhibited lower mRNA level of ApoE in the Hippocampus.

One possibility is that the effect of RIP140 on ApoE could be mediated through another transcription factor, such as the estrogen related receptor alpha (ERRα). Both RIP140 and ApoE are regulated by estrogen related receptor alpha (ERRα) and liver X receptor (LXR) (Laffitte et al, 2001). ERRα is also one of the direct targets of RIP140 (Debevec et al, 2007). There are evidences that indicate that ApoE expression is regulated through EERα stimulation (Nichol et al, 2006, Srivastava et al, 1997). Our results suggests therefore that in the absence of RIP140, ApoE mRNA expression is lowered, possibly due to the lack of stimulation of ERRα by RIP140.

Although one study suggest that estrogen treatment can also induce Neprilysin expression (Liang, et al, 2010) through ERRα or the other isoform ERRβ we can not conclude that RIP140 would affect Neprilysin through this pathway. It is also possible that ApoE is not only regulated only through ERR by RIP140 but additionally by LXR dependent regulations, which do not affect Neprilysin or IDE. It was previously demonstrated that PPARγ agonists are able to increase ApoE expression in adipocytes. They reported that the liver receptor X (LXR) response element within an ApoE gene downstream enhancer is required for the ApoE response to PPARγ agonists. Prior work from Gary Landreth has also shown that PPARγ and LXR agonists improve Aβ pathology and symptoms in AD mice (Jiang et al., 2008; Heneka and Landreth, 2007). One study revealed that the RXR agonist beratoxene promotes degradation of soluble Aβ42 in a PPARγ-, LXR-, and ApoE-dependent manner in both primary microglia and astrocytes but at the same time found that the levels of IDE and Neprilysin were unchanged with beratoxene treatment (Cramer et al, 2012). This is because ApoE expression is transcriptionally induced through the action of PPARγ and liver X receptors in coordination with retinoid X receptors (RXRs) (Mandrekar- Colucci, et al., 2012). This could explain that absence of RIP140 may affect ApoE expression by failing to activate PPARγ or the LXR.

5.4.3 RIP140 alters the expression of GAP43

Studies of Duclot et al, (2012) using this knockout models revealed that these mice suffer from memory and learning impairments and display an increased response to stress in comparison to wilt types. We found that some proteins related to memory are transcriptionally modified in RIP140 knockout mice.

GAP 43 has been found to play a role in hippocampal dependent memory because its absence causes memory impairment (Rekart et al., 2005). Interestingly we found that GAP43 mRNA levels were only changed in this region but not the frontal cortex in RIP140 knockout mice.

GAP 43 is also well known to appear reduced in the brains of AD patients (de la Monte et al, 1991), just like

PPARγ and RIP140. Conversely, we found it fairly strongly up-regulated in RIP140 null mice. It is arguable if this may be secondary to other effects caused by the RIP140 knock out. RIP140 null mice exhibit increased insulin sensiviity, which can be linked to overall lower insulin level. In addition to that, these mice are lean and show low body fat content, which will also result in lower insulin level. Decreased insulin, increases the nerve growth factor (NGF) (Gezginci-Oktayoglu et al, 2012). This is interesting, because NGF stabilizes GAP 43 mRNA level and the higher the NGF level, the higher the GAP 43 mRNA level will be.

Therefore, if would be interesting to study the effects of RIP140 on GAP43 in either a conditional neuronal RIP140 knock out or using a cell line transfected with RIP140 siRNA, to avoid secondary effects of RIP140 knockout in other tissues.

5.4.4 RIP140 affects the expression of genes involved in the Tau pathology

Tau protein is a highly soluble microtubule-associated protein (Mtap/ MAP), which is subdivided into various splice variants of which we found MAP2 strongly induced in the hippocampus of RIP140 animals, but not in the frontal cortex, indicating again RIP140 importance within this brain area. This result also indicates that in the absence of RIP140, expression of this major Tau pathology contributor is elevated.

An increase of Tau protein itself would not lead to the formation of NFT's resulting in Tau pathology, as this only happens when Tau proteins get hyper phosphorylated. A mouse line overexpressing human mutant Tau showed that Tau was hyper phosphorylated whilst overexpressing an activator for cdk5, suggesting that cdk5 initiates a major impact on Tau pathology progression (Noble et al, 2003). Interestingly, we detected also an increase in cdK5 in the hippocampus of RIP140 mice, alongside with the increase of MAP2. Therefore, it can be assumed that lack of RIP140 promotes the development of hyper phosphorylated Tau and tangle formation.

Another important kinase involved in Tau phosphorylation is GSK3. GSK3 activity is increased in the frontal cortex of AD patients and its expression is up regulated in the hippocampus (Blalock et al. 2004). It co-localizes with degenerating neurites and NFTs (Yamaguchi et al. 1996; Imahori and Uchida 1997; Pei et al. 1997) and active GSK3 appears in neurons with pre-tangle changes (Pei et al. 1999). We found that RIP140 ko mice showed statistically elevated mRNA levels of the active versions of GSK3, α and β in the frontal cortex, and GSK3β additionally in the Hippocampus compared to wt mice while the inactive phosphorylated version was unchanged in both regions. This indicates that lack of RIP140 affects expression level of active GSK3 and therefore may contribute to the Tau

pathology. It would be therefore interesting to determine whether the GSK3 promoter contains consensus binding sites for transcription factors regulated by RIP140. Another possible explanation for this may be found in the effects of the insulin signaling pathway on GSK3. Impairment of insulin signaling in the brain has been linked to Tau phosphorylation. As mentioned before, RIP140 ko mice exhibit high insulin sensitivity resulting in lower insulin plasma level due to their lower fat body content and higher insulin degradation. Insulin signaling activates the PI13-kinase, which activates Akt8 a factor known to phosphorylate GSKα and β at two serine residues (Saltiel and Kahn 2001; Lizcano and Alessi 2002). This serine phosphorylation leads to prevention of the enzymatic activity of GSK3. In fact, neuronal insulin receptor knockout mice present reduced pGSK3 levels (which is less active) and increased Tau hyper phosphorylation (Schubert et al., 2004). This could also mean that regulations seen in GSK3 expression in our mouse model could be consequence of whole body RIP140 knock out on the insulin pathway rather than a transcriptional regulatory effect of RIP140 itself. Excessive administration of insulin to RIP140 knockout mice, maybe directly to the brain, could show if this observation is reversible and insulin-mediated.

5.4.5 Inflammation in the RIP140 ko brain

RIP140 effects in the transcription of pro-inflammatory mediators suggest that RIP140 acts as a co-activator rather than repressor. It was shown that RIP140 interacts with the nuclear factor ϰ light-chain enhancer of activated B cells (NF-ϰB) subunit RelA or cAMP-response element binding protein (CREB)-binding protein (CBP) to induce the expression of the cytokines IL-6, TNFα, and IL-1β in macrophages (Zschiedrich et al, 2008). We were interested to investigate if RIP140 was also able to regulate cytokine expression in the brain. We observed that, in contrast to what was reported in macrophages, there is a trend for IL1-β and IL-6 expression to be increased in the brain in absence of RIP140, suggesting that RIP140 may have anti-inflammatory effects in the brain. It is possible that in this case RIP140 is not affecting cytokine expression through NFkB but through activation of PPARγ, which is something that needs to be investigated in future studies. Because cytokines in the brain are mainly secreted by glial cells, we aimed to determine whether there were changes in microglia activation in the brain of RIP140 knockout mice. However, we did not detect any increase in microglial activation by IBA-1 staining. Immunostaining of hippocampal sections however, showed an increase in reactive astrocytes. It is possible that the increase in cytokines we have observed may not have reached significance as we used whole homogenates of the Hippocampus which contains a larger and mixed population of cell types and only a small, more accurately measured GFAP positive Hippocampus fraction seems to contain the

reactive cell type that may be responsible for this increase.

Chapter 6

Study of the brain of RIP140 transgenic mice

6.1 Introduction

RIP140's biological role as a metabolic co-regulator became clear through the analysis of a RIP140 knockout mouse model. However, to determine the potential of RIP140 as therapeutic agent it has been important to develop a RIP140 transgenic mouse. Some secondary effects of RIP140 overexpression have emerged after the generation of a RIP140 overexpressing mouse model.

The group of Prof. Malcolm Parker characterized the RIP140 transgenic phenotype and described how there were reduced survival rates for both male and female animals. They investigated the effects of elevated RIP140 expression in the cardiac muscle and found that it results in cardiac hypertrophy and impaired cardiac function (Fritah et al. 2010). It occurred that RIP140 transgenic mice have cardiac issues including hypertrophy of the cardiac muscle and increased calcification of the arteries. In addition, RIP140 overexpression in the heart resulted in alterations in mitochondria membrane potential and oxygen consumption. These animals presented more than 50% reduced expression of genes involved in mitochondrial activity and fatty acid metabolism, many of which are known targets for nuclear receptors, including peroxisome proliferator-activated receptors PPARα and PPARδ and estrogen-related receptors ERRα and ERRγ. A recent paper from the same group has revealed the role of RIP140 in the mammary gland development by promoting the generation of key mitogenic signals, such as amphiregulin (Areg), the progesterone receptor (Pgr) and signal transducer and activator of transcription 5a (Stat5a) (Nautiyal et al., 2013).

As we hypothesize that RIP140 co-activation function may induce beneficial effects in the pathology of AD brains, we were curious to see how RIP140 overexpression in vivo may affect the expression of certain genes we have found to be regulated in the RIP140 ko mouse model. Our vitro results using a RIP140 expression vector to induce overexpression of the cofactor in neurons gave a first insight and evidence of how RIP140 may actually affect APP processing at various stages.

In this chapter we aimed to find out if the data we have generated in vitro culture of a neuronal cell line are reproducible in vivo. Furthermore we wanted to find out if some of the in vivo data we have obtained from the RIP140 knockout model were possibly conversed in the RIP140 transgenic mouse line. We postulate that RIP140 acts as a co-activator in cerebral tissue and may have beneficial effects by changing expression patterns of enzymes that are responsible for the pathology of AD.

6.2 Results

In the previous chapter we have investigated the effects of RIP140 depletion on a variety of genes that have been implicated with AD. The RIP140 ko mouse has previously been shown to display some alterations in the brain, including changes in memory and cognition. The RIP140 transgenic mouse model emerged much later and has been less investigated. There is nothing known about RIP140 overexpression in the brain so far. The previous chapters of this thesis have indicated that RIP140 overexpression in a neuronal cell line can affect the transcription of genes involved in the process of AD pathology and have a beneficial effects by reducing Aβ load. Additionally we also learned that in vivo, the absence of RIP140 can have some adverse effects on the same genes. In this chapter, we repeated the same experiments performed in vivo on the RIP140 ko mouse model in the RIP140 tg model to see if overexpression of RIP140 in the mouse brain will reciprocate our previous observations. We examined again the hippocampus (Fig. 6.1 orange) and frontal cortex (red) areas of RIP140 transgenic brains and evaluated changes in mRNA as well as protein expression for the same genes analyzed in the previous chapter.

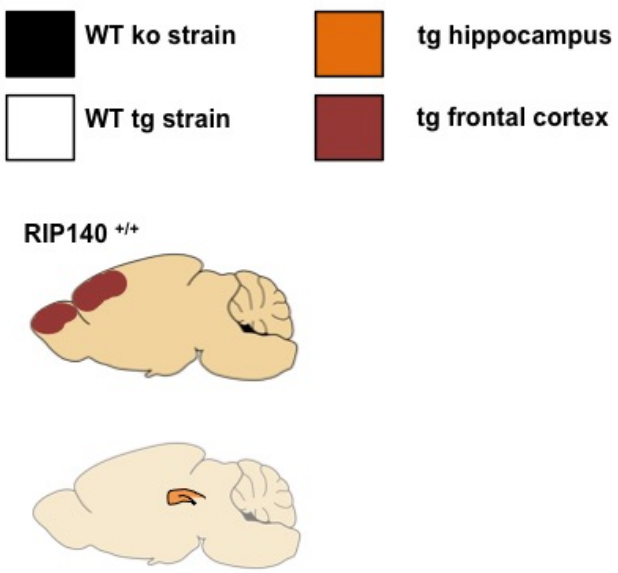


Figure 6.1: Legend for brain areas and mouse lines studied in the follwoing chapter. A mouse line overexpressing (transgenic (tg)) and its corresponding wiltype strain (white) were studied using hippocampus (orange) and frontal cortex (red) areas.

Effects of RIP140 overexpression on expression level of various genes implicated in AD

We evaluated the same genes that appeared changed in the initial mRNA expression array of RIP140 knockout mice (Fig 5.3) in the RIP140 transgenic brains, to determine whether the opposite effects were observed.

6.2.1 Genes involved in APP processing

We previously reported changes in the mRNA and protein levels of BACE1 when RIP140 was overexpressed in vitro (see chapter 4). We tried to verify these observations in hippocampus and frontal cortex in vivo using transgenic RIP140 brains and their wt littermates. mRNA was obtained from dissections of the right hemisphere and protein lysates from the left hemisphere. We have also evaluated the mRNA expression level for BACE2 as this gene was modified in the initial screen in the RIP140 ko mouse hippocampus. However, we did not detect any changes in BACE1 or BACE2 mRNA levels in the hippocampus of RIP140 Tg mice (Fig6.2 A+B) and only a very mild decrease in the frontal cortex (Fig. 6.2 C+D).

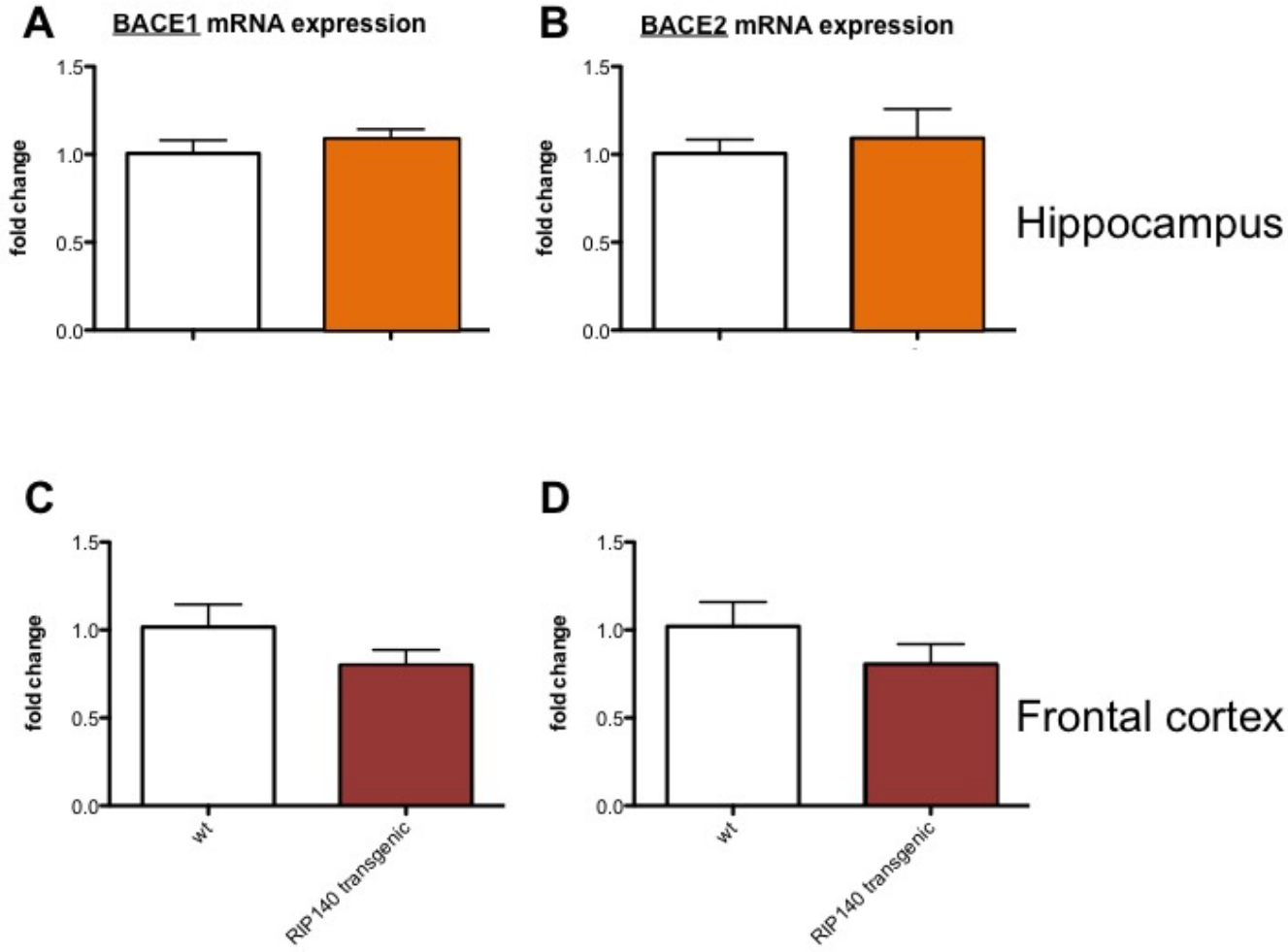


Figure 6.2: BACE1 and BACE2 mRNA expression levels in RIP140 Tg mice. Evaluation of expression level of, BACE1 and BACE12 in hippocampus (A-B) and frontal cortex areas of RIP140 Tg mice (C-D). RIP140 transgenic mice showed mild but not statistical significant reductions of BACE 1 and BACE2 in cortex but no changes in the hippocampus (A, B).(BACE1: n=5 for tg animals and n=3 for matching wt. BACE2: n=5 for tg animals and n=3 for matching wt.). Values shown in graphs represent the mean value ±SEM and are expressed as in fold change of control. Statistical analysis included student's t-test, * $p<0.05$).

Protein lysates of the same animals revealed a strong reduction in BACE1 protein levels in the frontal cortex of RIP140 transgenic mice compared to wt littermates (Fig 6.3 B). Similar to the values obtained for the mRNA expression, BACE1 protein levels in the Hippocampus of RIP140 Tg mice appeared unchanged (A).

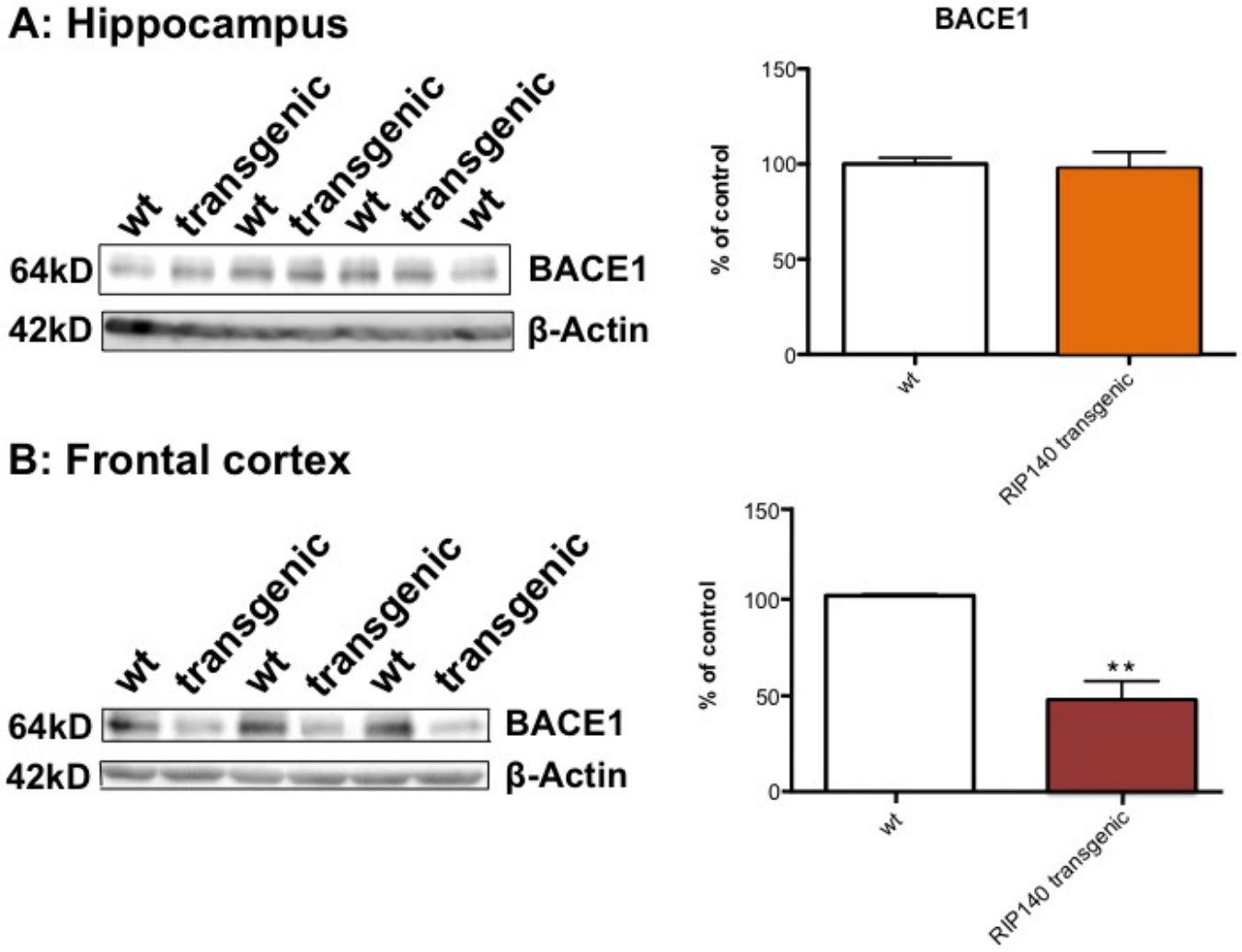
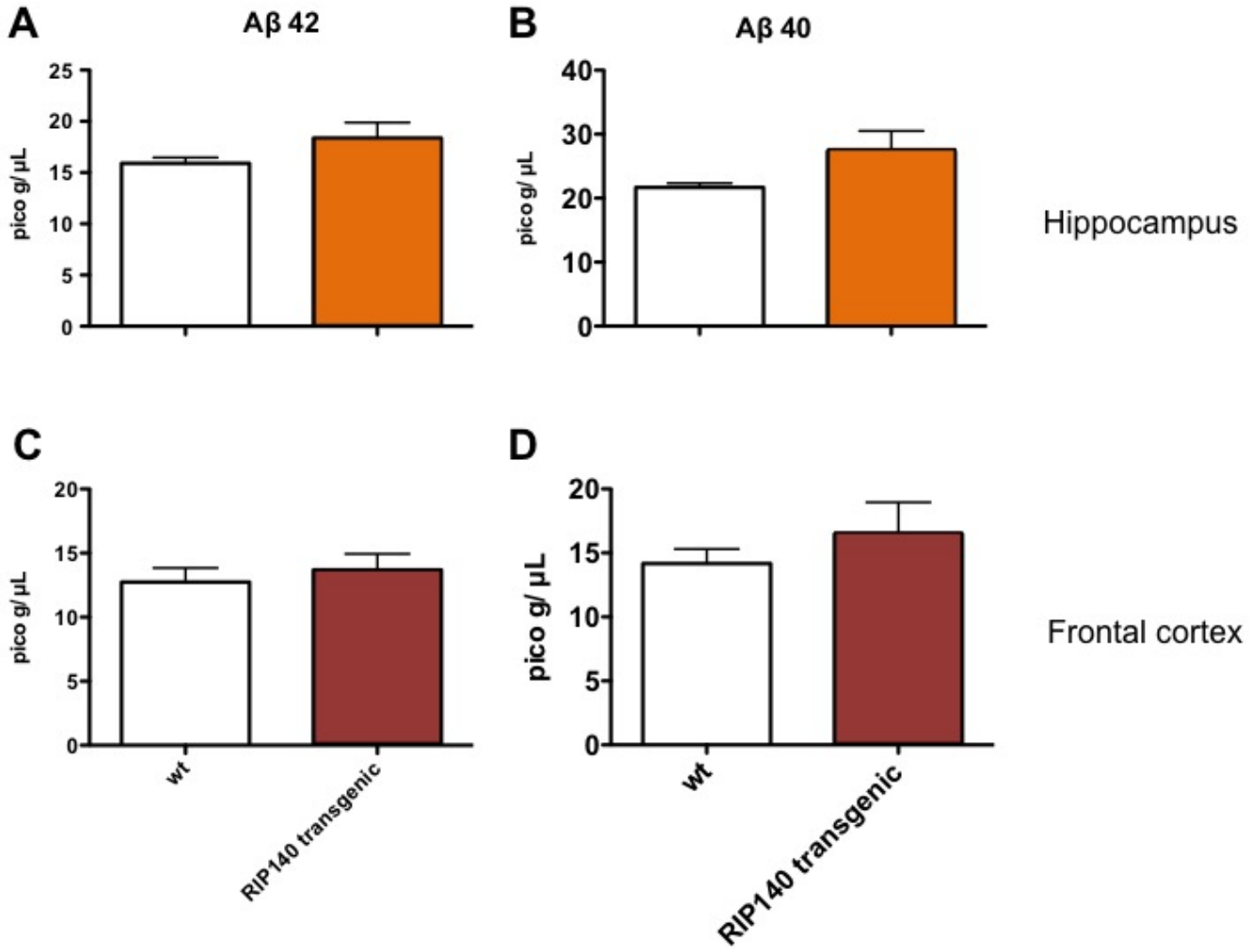


Figure 6.3: BACE1 Protein expression in RIP140 transgenic mice. BACE1 protein levels were found significantly reduced in RIP140 transgenic mice in the frontal cortex area (B), but no effect was observed in the hippocampus of the same animals (A). (Hippocampus: n=4 for Tg animals and corresponding n=5 wt, n=3 for tg animal and corresponding wt n=4; frontal cortex: n=4 for Tg animal and corresponding wt, n=3 for tg animals and corresponding wt). Values shown in graphs represent the mean value ±SEM and are expressed as in fold change of control. Statistical analysis included students t-test, **$p < 0.001$).

6.2.2 Endogenous expression of Aβ42 and Aβ40 are not affected by RIP140 overexpression in vivo

Our results on Aβ quantification in vitro suggested that RIP140 overexpression reduces the generation of this peptide. Now we aimed to validate these results in vivo, using a transgenic RIP140 mouse line. Using a highly specific ELISA assay, we were able to determine changes for mouse endogenous Aβ42 and Aβ40 and determine if the ratio of those two peptides was also affected. We did not observe any significant differences for either Aβ42 or Aβ40 in cortex or hippocampus, hence the ratio remained unaffected as well (Fig. 6.4 A-F). However, slight differences for Aβ40 were observed, indicating a slightly increased level for Aβ 40 in RIP140 transgenic mice. It has to be noted that for the ELISA assays, we only used a small number of animals.



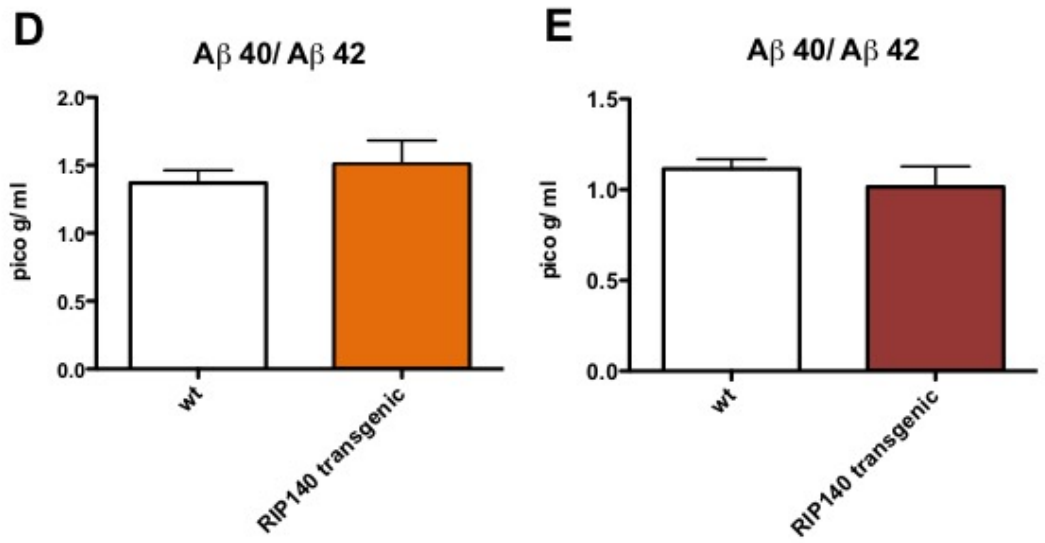


Figure 6.4: ELISA of endogenous Aβ40 and Aβ42 in RIP140 transgenic mice. Whole brain lysates were loaded on an ELISA plate to detect Aβ40 and Aβ42 in hippocampus and frontal cortex of a RIP140 transgenic mouse line. The reduction in Aβ42 level observed in cells overexpressing RIP140 could not be validated in the hippocampus (A) and frontal cortex (C) of RIP140 transgenic mice. No changes were also observed for Aβ40 in both brain regions(B, D) and subsequently, no differences in the Aβ40/Aβ42 ratio were detected (E,F). (n=3 for tg animal and corresponding wt). Values shown in graphs represent the mean value ±SEM and are expressed as in pico gram per milliliter of control. Statistical analysis included student's t-test.

Like in the in the previous chapter for RIP140 knock out mice, we evaluated the same genes that appeared changed in the initial mRNA expression array (Fig 5.3) and divided them into the same sub groups.

6.2.2.1 Effect of RIP140 overexpression on genes involved in Aβ degradation

Neprilysin and IDE were genes found modified in the first mRNA screening in RIP140 knockout brains. However, we did not find significant changes in the expression of those enzymes when we performed Western blots assays in the brains of a larger group of older RIP140 ko mice. In RIP140 tg mice we noticed a small increase in Neprilysin mRNA in the Hippocampus and frontal cortex (Fig 6.5 A+C) and the same effect was detected for IDE but only in the Hippocampus (B). None of these observations appeared to be statistically significant.

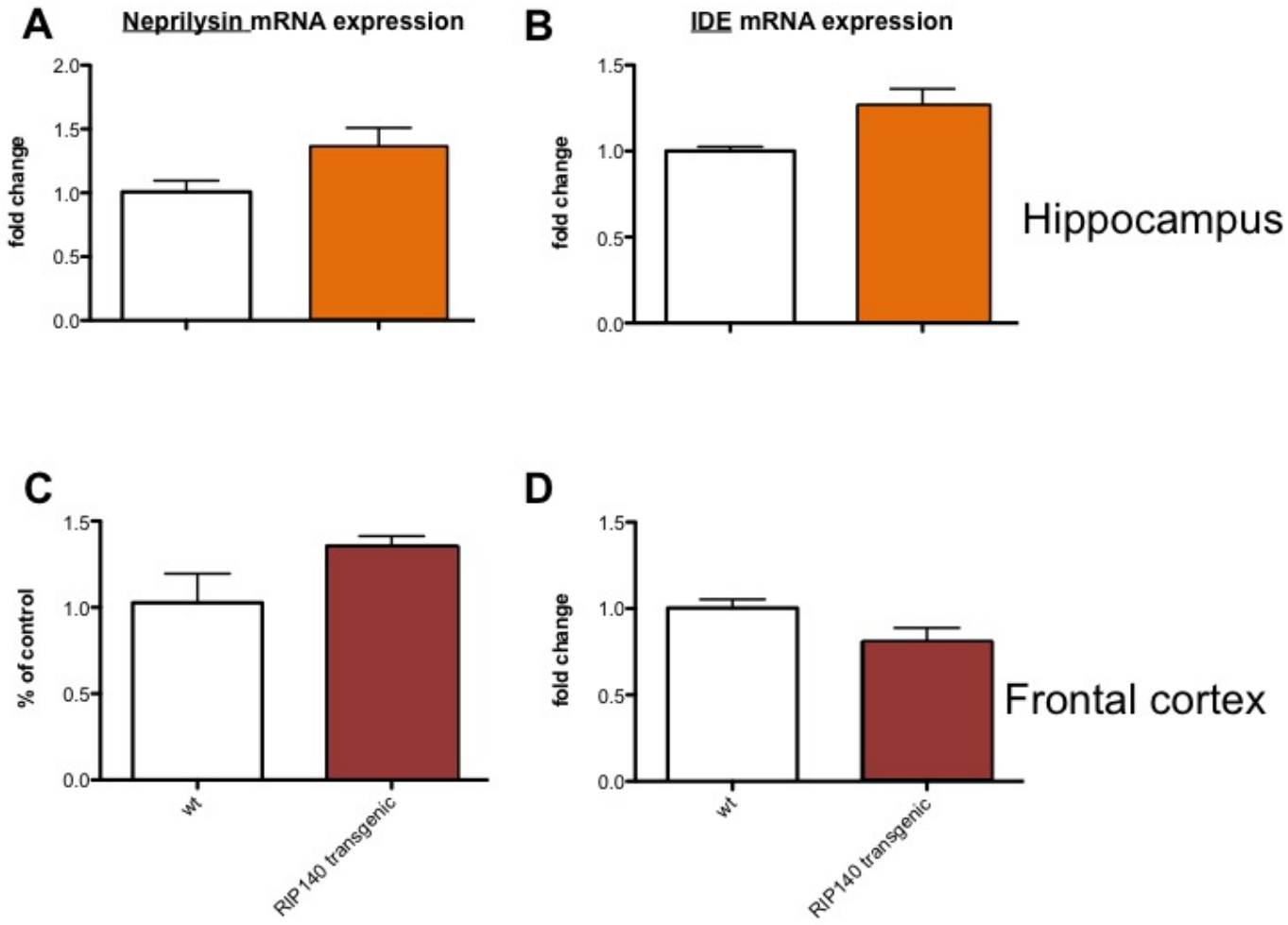
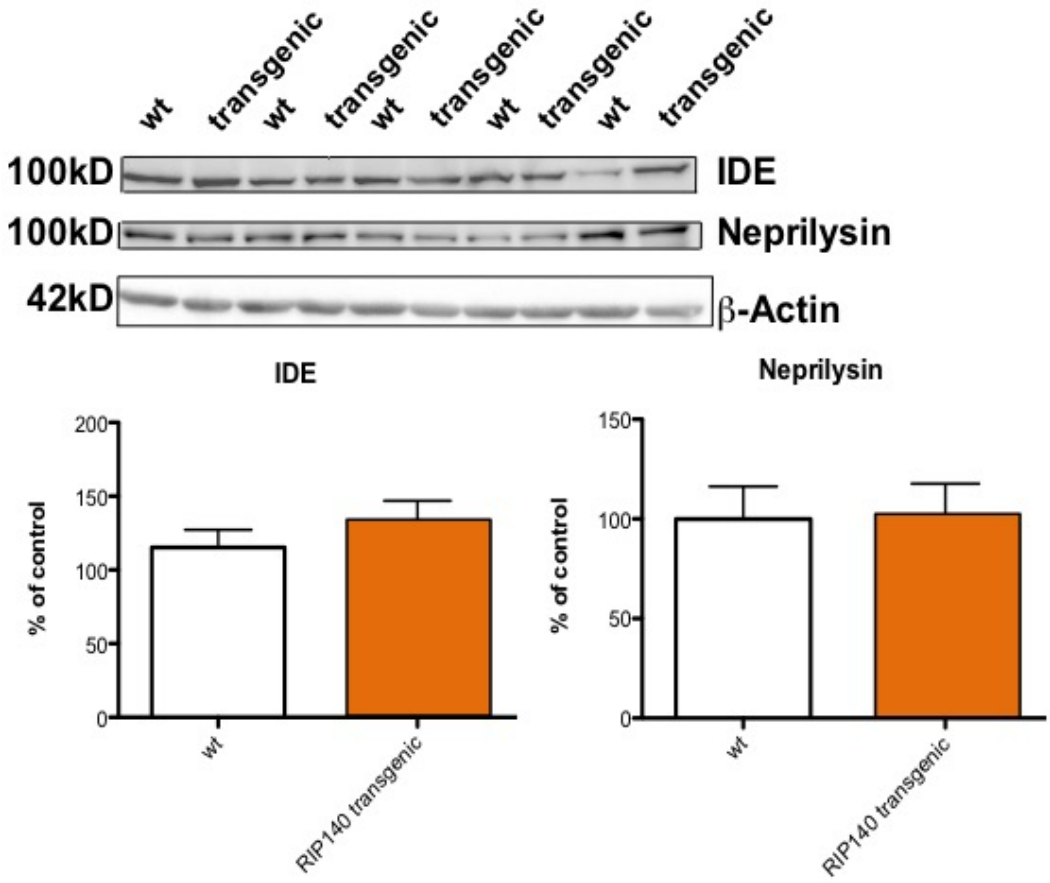


Figure 6.5: Neprilysin and IDE mRNA expression level in RIP140 tg mice. Evaluation of expression level of Neprilyisin and IDE in Hippocampus (A,B) and frontal cortex areas (C,D) of RIP140 tg. Neprilysin expression appeared slightly higher in the hippocampus of mice overexpressing RIP140 (A) as well as IDE expression (B). Neprilysin seemed higher in the frontal cortex but not statistically significant due to high variability in the wt group (C). No changes were observed for IDE in the frontal cortex area (D).(NEP: n=5 for tg animal and n=3 corresponding wt, IDE: n=5 tg and n=3 wt animals). Values shown in graphs represent the mean value ±SEM and are expressed as in fold change of control. Statistical analysis included student's t-test).

We then assessed if there were any changes for these two genes in their protein expression (Fig 6.6) We were unable to detect any changes on Neprilysin expression in the hippocampus (A) or frontal cortex (B). IDE protein expression also appeared unaltered in the Hippocampus (A) and frontal cortex (B).


A: Hippocampus
wt
transgenic
wt
transgenic
wt
transgenic
wt
transgenic
wt
transgenic
100kD
IDE
100kD
Neprilysin
42kD
β-Actin
IDE
% of control
200
150
100
50
0
wt
RIP140 transgenic
Neprilysin
% of control
150
100
50
0
wt
RIP140 transgenic

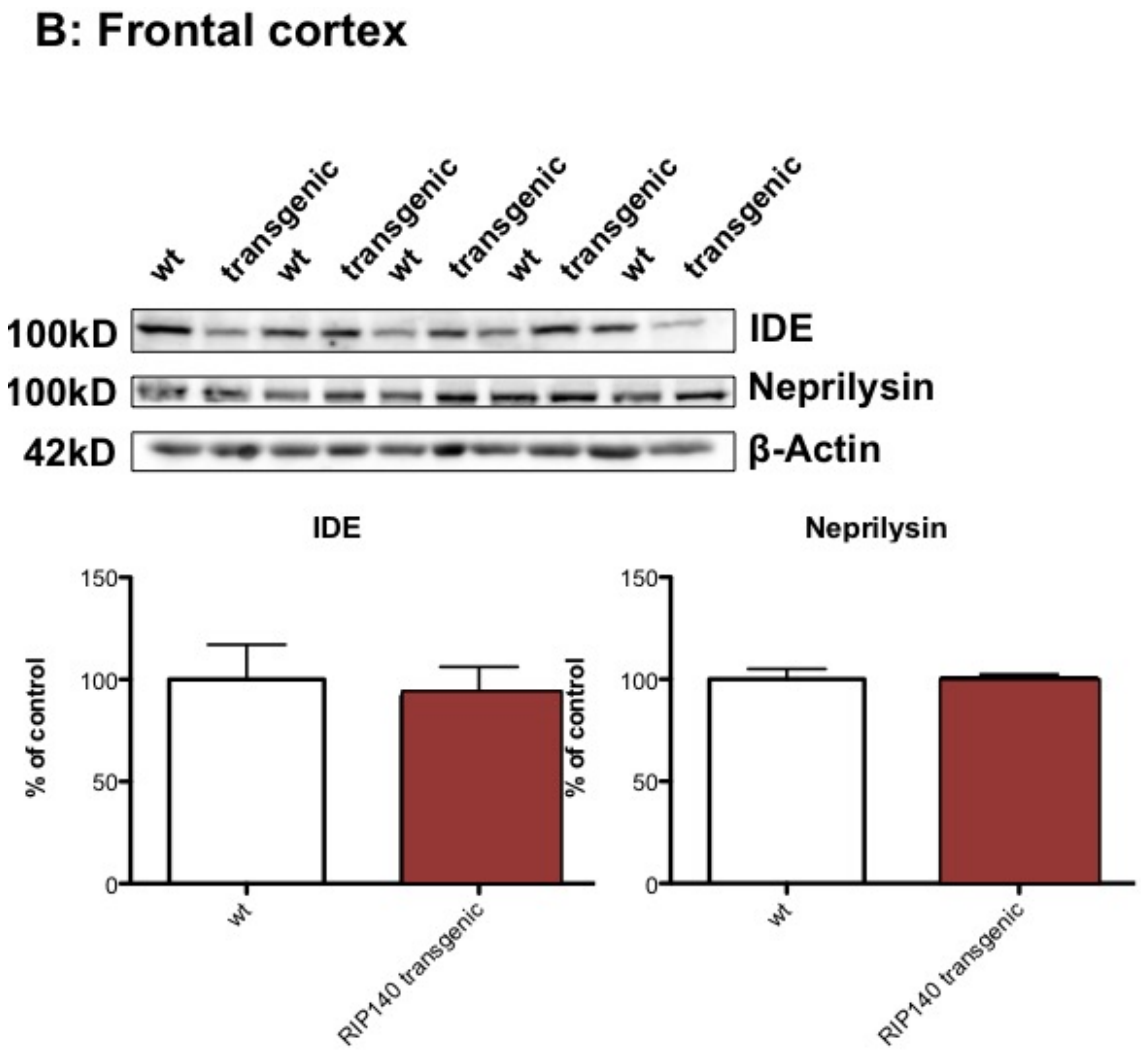
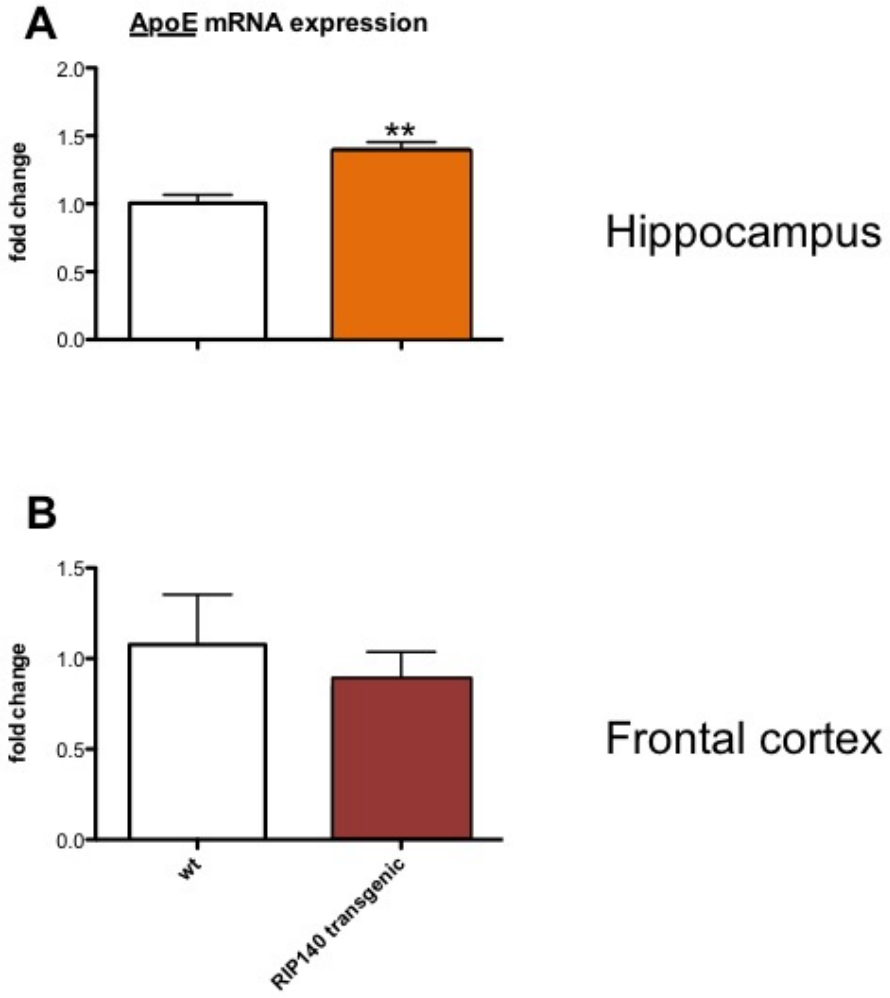


Figure 6.6: Neprylisin and IDE protein expression in RIP140 transgenic mice. Neprilysin protein levels were unchanged in the hippocampus (A) and frontal cortex (B) of RIP140 Tg mice compared to WTs. IDE protein level of RIP140 tg animals were also unchanged in comparison to wt animals in the hippocampus (A) and frontal cortex (B). (Hippocampus: n=5; frontal cortex: n=5.) Values shown in graphs represent the mean value ±SEM and are expressed as in % change of control. Statistical analysis included student's t-test).

We also analysed the expression of ApoE in RIP140 Tg mice. Interestingly, ApoE mRNA was significantly higher in the Hippocampus of RIP140 transgenic animals (Fig. 6.7, A), showing the opposite effect observed in the RIP140 ko animals. However, ApoE mRNA expression level was unchanged in the frontal cortex region of RIP140 tgs (B). Western Blots for the ApoE protein could not confirm the changes seen in mRNA expression level of the Hippocampus

(C) and remained unaltered in the frontal cortex region (D).



6.2.3 Effect of RIP140 overexpression on genes involved in memory and cognition

The effects of RIP140 ablation on memory and cognition have been previously studied (Duclot et al, 2012) however similar type of studies have not been performed in the RIP140 transgenic mouse model. As already mentioned in the previous chapter, IgF2 and GAP43 have not only been linked to AD but also have beneficial effects on memory and

learning processes if expressed at higher levels. In our initial array in RIP140 ko mice, both of these genes appeared to be both highly up-regulated (chapter 5, Fig 5.3). In the follow up data we verified this observation for GAP43, which was about 2, fold increased in mice lacking RIP140 (chapter 5, Fig 5.12).

In the transgenic RIP140 hippocampus, we observed a strong increase in IgF 2 mRNA level that could not reach statistical significance (Fig 6.8, A) and also an increase in GAP43 which was about 1.5 fold higher than wild-type level but not significant either (B). In the frontal cortex area the increase in gene expression for and GAP43 could not reach any significance due to high variability in the single groups (C+D).

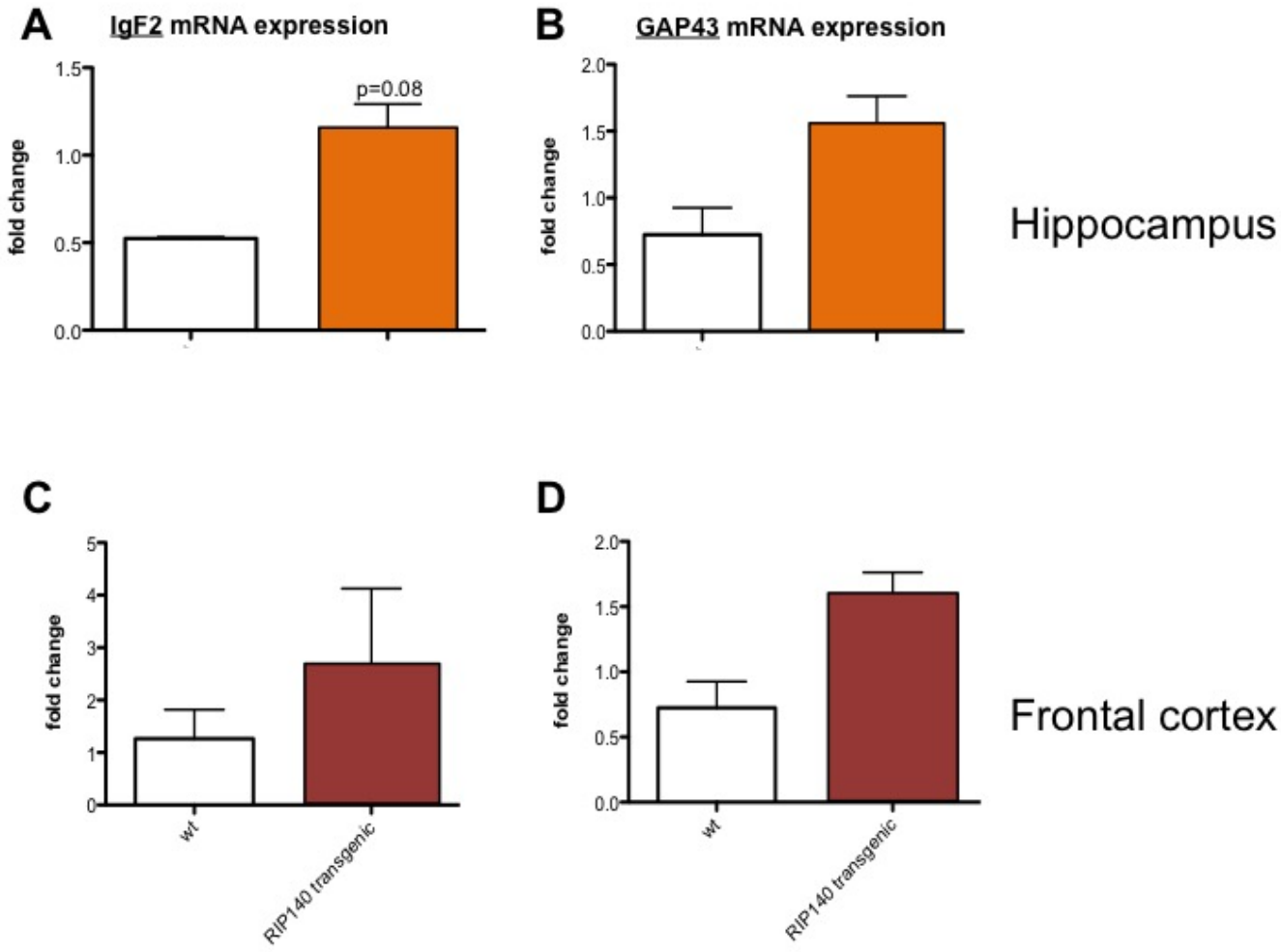


Figure 6.8: IgF2 and GAP43 mRNA expression level in RIP140 transgenic mice. Evaluation of expression level of IgF2 and GAP43 in hippocampus (A,B) and frontal cortex areas (C,D) of RIP140 tg. IgF2 expression appeared higher in the hippocampus of mice overexpressing RIP140 reaching a p value of 0.08, there for remaining insignificant (A). GAP43 expression appeared higher but not statistically increased than wt expression level (B). IgF2 seemed higher in the frontal cortex but not statistically significant due to high variability (C) GAP43 expression is increased in the frontal cortex area, although did not reach significance (D) .(IgF2: n=4 for tg animals and n=3 corresponding wt, GAP43: n=3 tg and wt animals). Values shown in graphs represent the mean value ±SEM and are expressed as in fold change of control. Statistical analysis included student's t-test *$p<0.05$).

6.2.4 Effect of RIP140 overexpression on genes involved in Tau pathology

In the previous chapter we described how the lack of RIP140 in knockout animals alters the expression of the Tau pathology related genes MAP2 and CDK5 in the Hippocampus (Chapter 5. Fig 5.13). Both genes were strongly up-regulated compared to wild-type expression level; therefore we aimed to determine how overexpression of RIP140 would affect the expression of these genes. In this section, we analysed whether the expression of MAP2, GSK3 and CDK5 were affected by RIP140 overexpression in frontal cortex and hippocampus. MAP2 appeared to be down-regulated in the frontal cortex of RIP140 transgenic mice (Fig. 6.9), however it was up regulated in the Hippocampus (Fig. 6.9, B). On the other hand, CDK5 expression was found to be up-regulated in the Hippocampus (Fig. 6.9 E) but not the frontal cortex (Fig. 6.9 F).

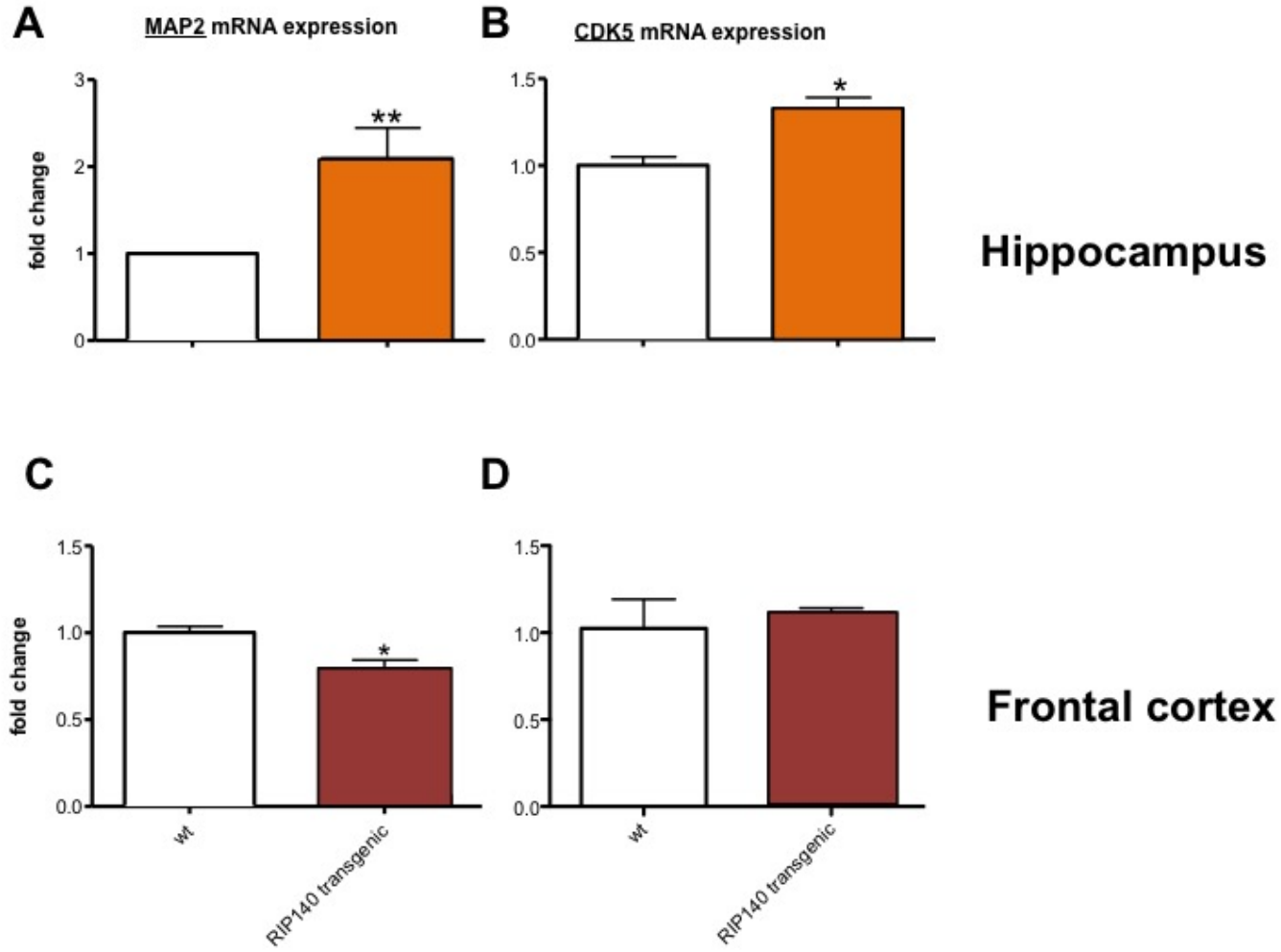


Figure 6.9: MAP2 and CDK5 expression level. MAP2 was up regulated in the Hippocampus (A) but decreased in the frontal cortex (C). CDK5 level were higher in the Hippocampus but unchanged in the frontal cortex (B,D).(CDK5 : n=5 for tg animal and n=3 corresponding wt, MAP2: n=3 tg animals and matching wt). Values shown in graphs represent the mean value ±SEM and are expressed as in fold change of control. Statistical analysis included students t-test, *$p<0.05$, **$p<0.01$).

We also checked expression level for GSK3β mRNA and found no differences in the expression of GSK3β mRNA in either Hippocampus or frontal cortex of RIP140 transgenic mice (Fig 6.10).

Estimation of the protein expression of the phosphorylated form of GSK3 (pGSK3)showed that is strongly reduced by 50% in mice overexpressing RIP140 (Fig 6.11, A). The frontal cortex region showed a similar reduction in pGSK3, but was not significant due to high variability in the wild-type group. Evaluation of the protein expression of the

different isoforms of GSK3 showed a non-significant reduction in the levels of GSK3α in hippocampus and cortex (Fig. 6.11 ,C+E) and no changes in GSK3β in RIP140 Tg mice (6.11 D, F).

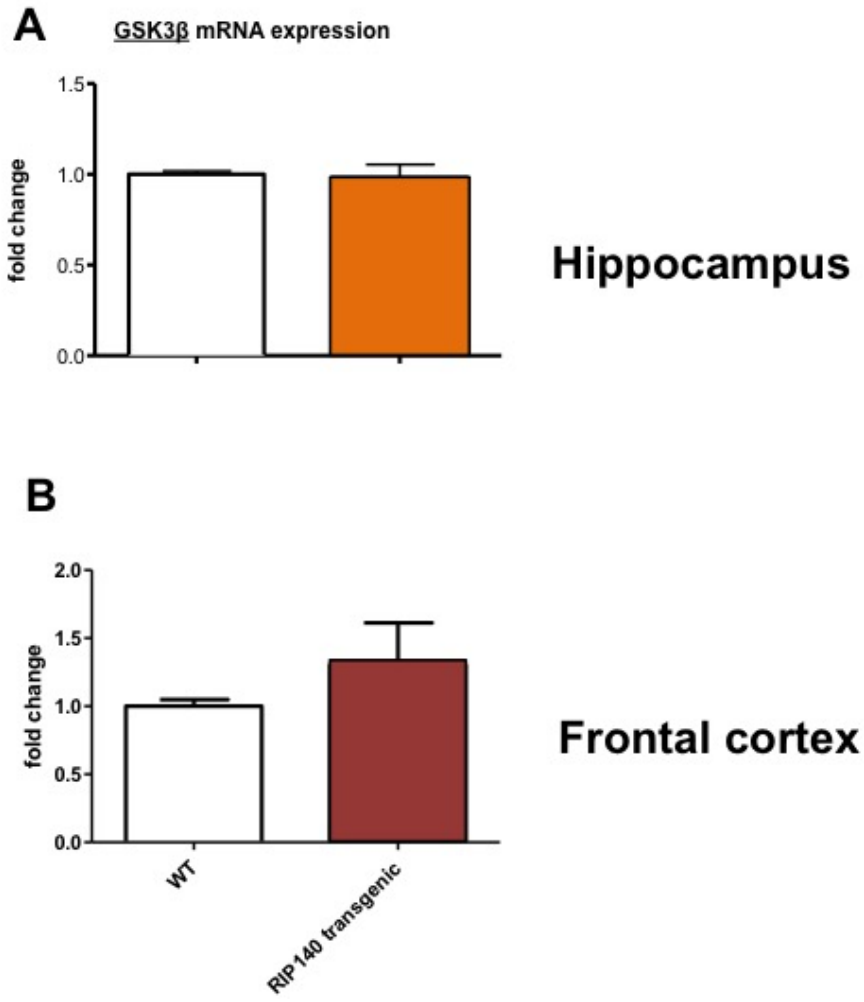
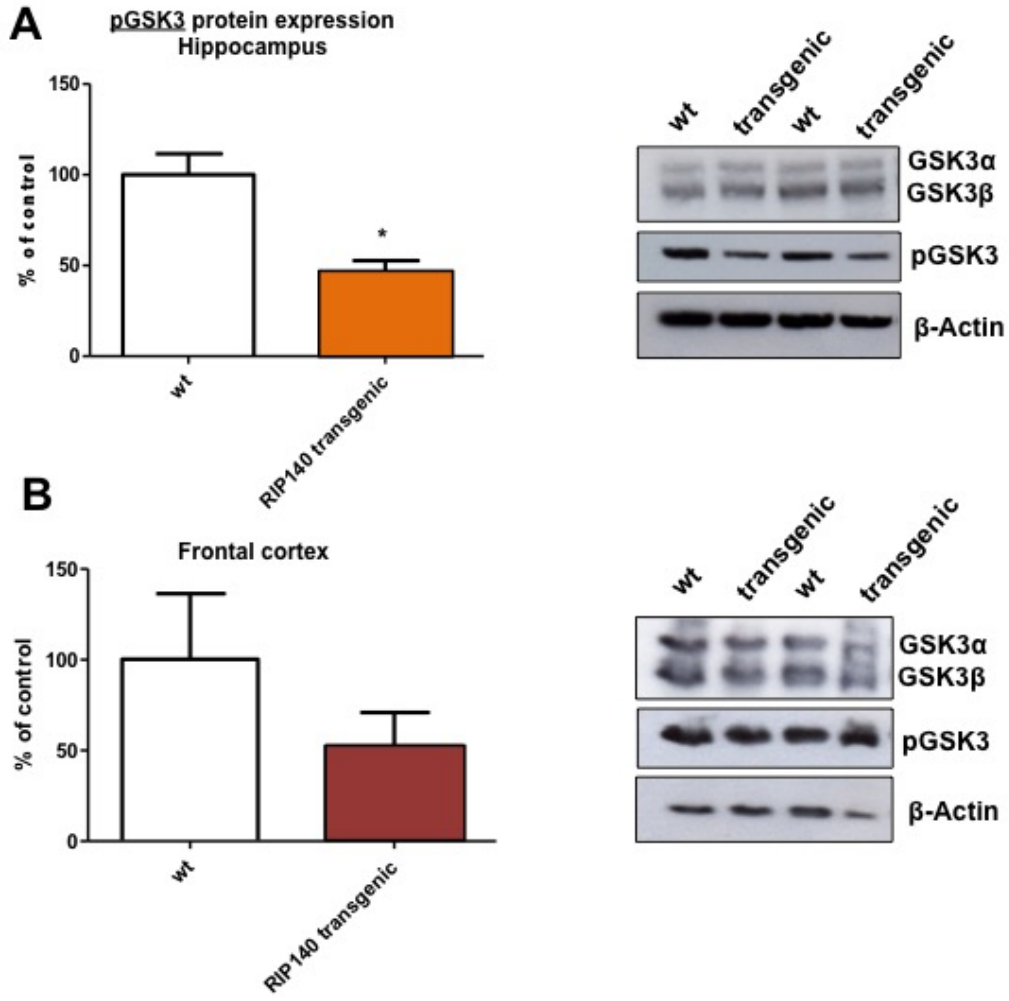


Figure 6.10: GSK3β mRNA expression level. GSK3β expression level were unaltered in both Hippocampus (E) and frontal cortex (G), (n=5 for tg animal and n=3 corresponding wt, Mtap2: n=3 tg animals and matching wt). Values shown in graphs represent the mean value ±SEM and are expressed as in fold change of control. Statistical analysis included student's t-test.


A
pGSK3 protein expression
Hippocampus
% of control
150
100
50
0
*
wt
RIP140 transgenic
wt
transgenic
wt
transgenic
GSK3α
GSK3β
pGSK3
β-Actin
B
Frontal cortex
% of control
150
100
50
0
wt
RIP140 transgenic
wt
transgenic
wt
transgenic
GSK3α
GSK3β
pGSK3
β-Actin

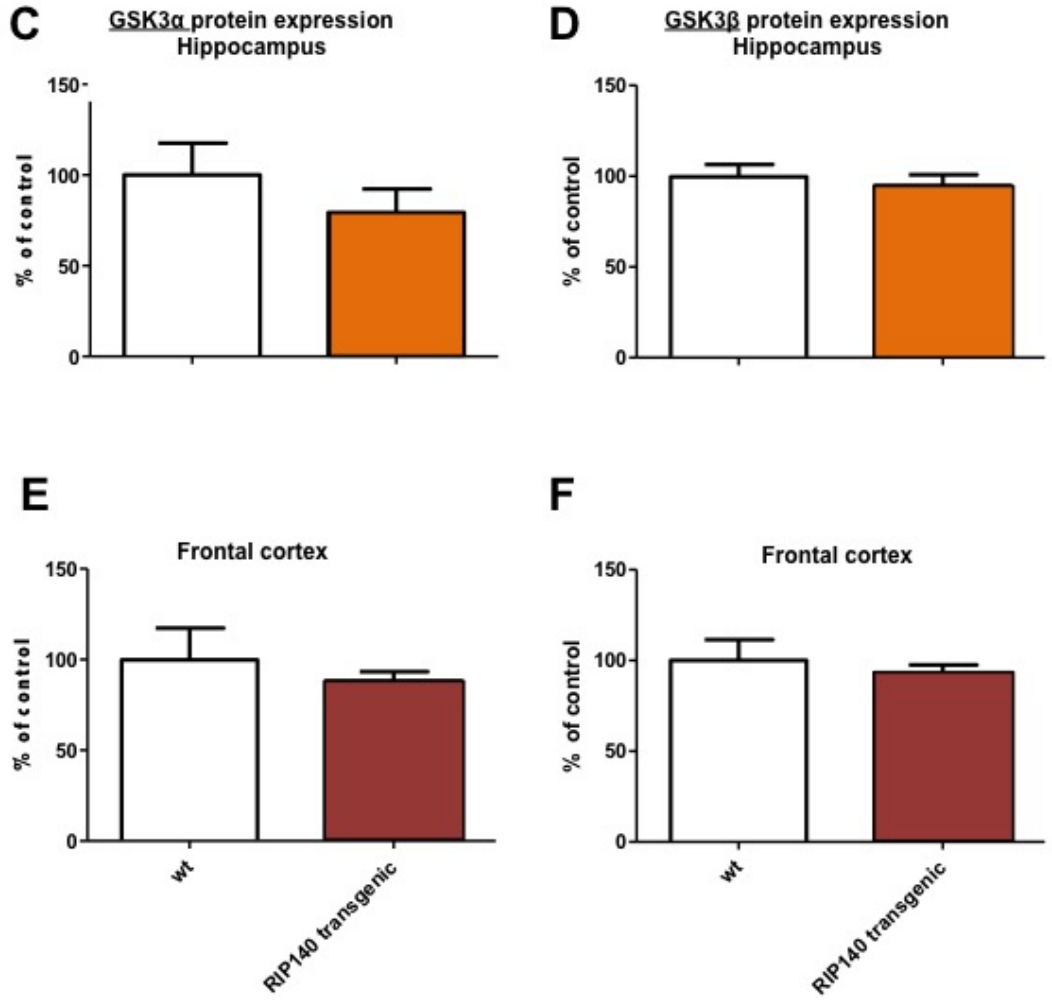


Figure 6.11: GSK3 protein expression in RIP140 transgenic mice. Representative western blot and quantification of different GSK3 subtypes (α and β) and phosphorylated GSK3 protein levels in Rip140 transgenic. a 50% decrease was observed for pGSK3 in the Hippocampus (A) but no changes of pGSK3 in the frontal cortex (B) of RIP140 tg mice. GSK3α was reduced but not significantly in the frontal cortex of RIP140 ko mice (E) and the Hippocampus (C). GSK3β was unchanged in the Hippocampus (D) and frontal cortex (F) of RIP140 ko mice. (n=5, RIP140 mice and matching wild-type animals for both, hippocampus and frontal cortex). Values shown in graphs represent the mean value ±SEM and are expressed as % of wild-type control. Statistical analysis included student's t-test. *$p<0.05$).

6.2.5 Effect of RIP140 overexpression on inflammatory mediators

We then sought to detect whether there were differences in the levels of pro-inflammatory cytokines in the brains of RIP140 transgenic mice. We detected the expression of Interleukins 1β and 6 using an ELISA assay. Interestingly we

observed a reduction on IL-1β expression in the Hippocampus of RIP140 transgenic mice in comparison to wild-type (Fig. 6.12, A). In the frontal cortex, IL-1β levels remained unaltered (C). Due to limitations of the amounts of sample we analysed IL-6 in the Hippocampus only, where levels of this peptide in RIP140 transgenic mice showed no difference with the ones secreted in wild-types (B). The level of Interleukins were expressed in nano gram per milliliter and the basal secretion lies around 0.15 ng/mL in the Hippocampus and 0.2 ng/ ml in the frontal cortex.

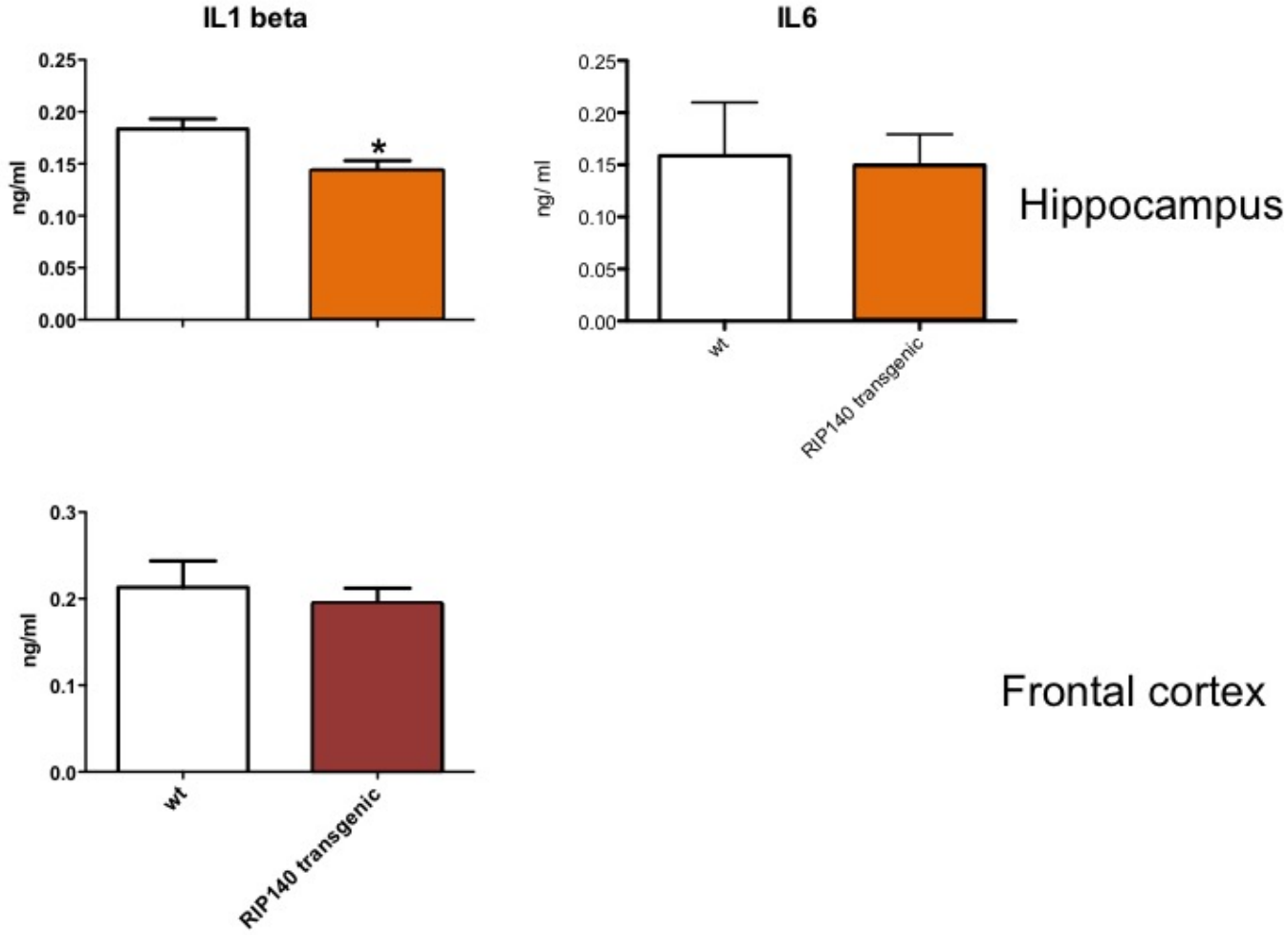


Figure 6.12: ELISA assays for cytokine expression in RIP140 transgenic. Homogenates of hippocampus and frontal cortex were by ELISA for IL-1β or IL-6 and levels of IL-1β or IL-6 were compared between RIP140 transgenic and wild-type animals. c IL-1β levels were reduced in the hippocampus of RIP140 Tg mice (A) but not in cortex (C). However, IL-6 were found unchanged between the different strains (B) (IL-1β and IL-6: n=4 for tg animals and =3 for matching wt. Statistical analyses included student's t-test *$p<0.05$).

Assessment of IBA1 expression in brain slices for microglial activation revealed no differences between Hippocampus or Cortex region of RIP140 transgenic mice and wild-types (Fig 6.13, C+D).

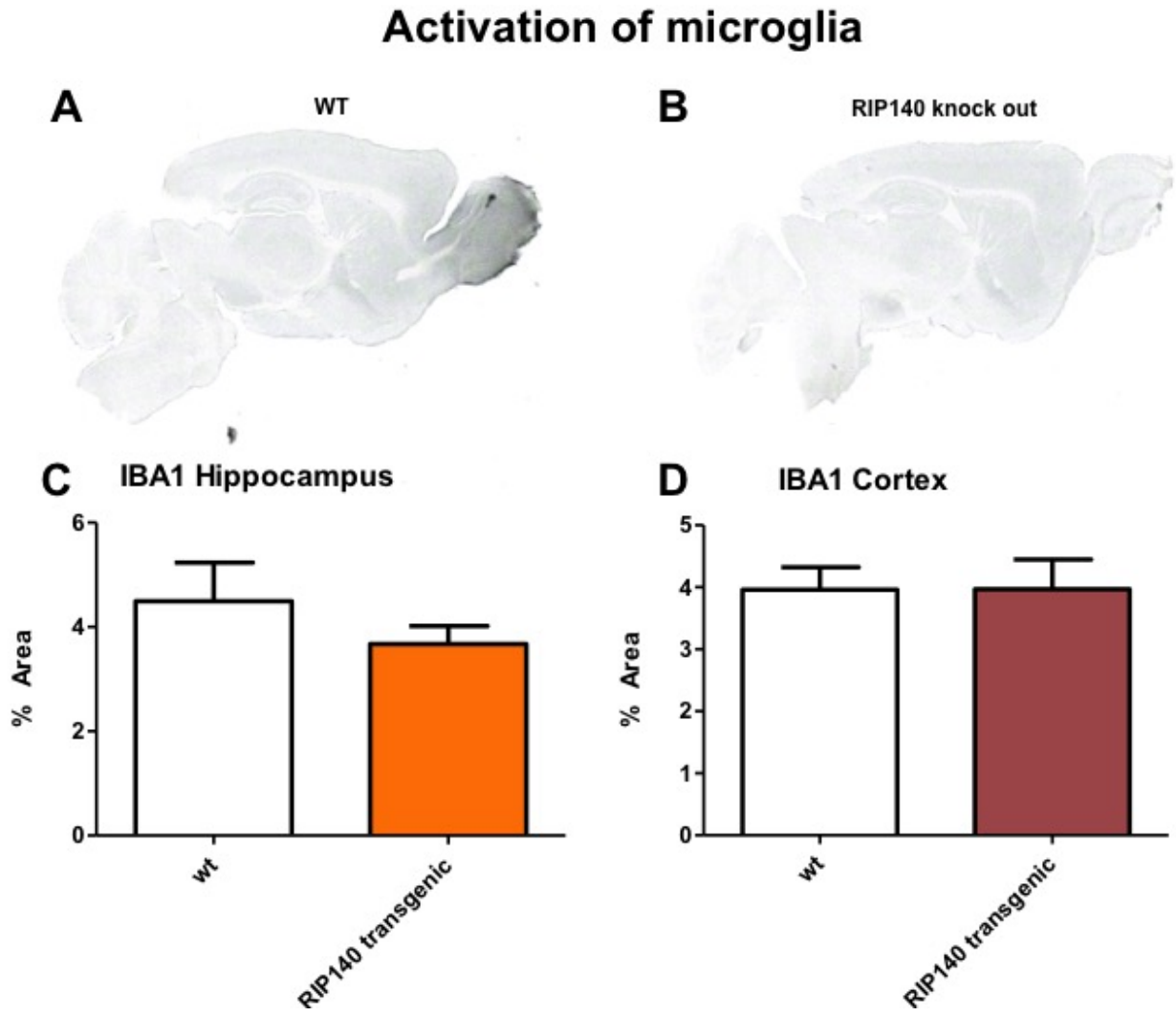


Figure 6.13: Microglial activation in RIP140 tg brain sections. Sections of 40µMwere stained using an antibody against IBA1 to detect activated microglia cells. Areas of Hippocampus (C) and Cortex (D) were quantified, but none of them revealed a significant difference. Values shown in graphs represent the mean value ±SEM and are expressed as % area of wild-type control. Statistical analysis included student's t-test. Staining, quantification and analyses were performed by Mr. David Morrow).

Likewise, GFAP staining for reactive astrocytes did not show any differences between wild-type and RIP140 tg brain slices in the Hippocampus or Cortex region (Fig. 6.14 C+D).

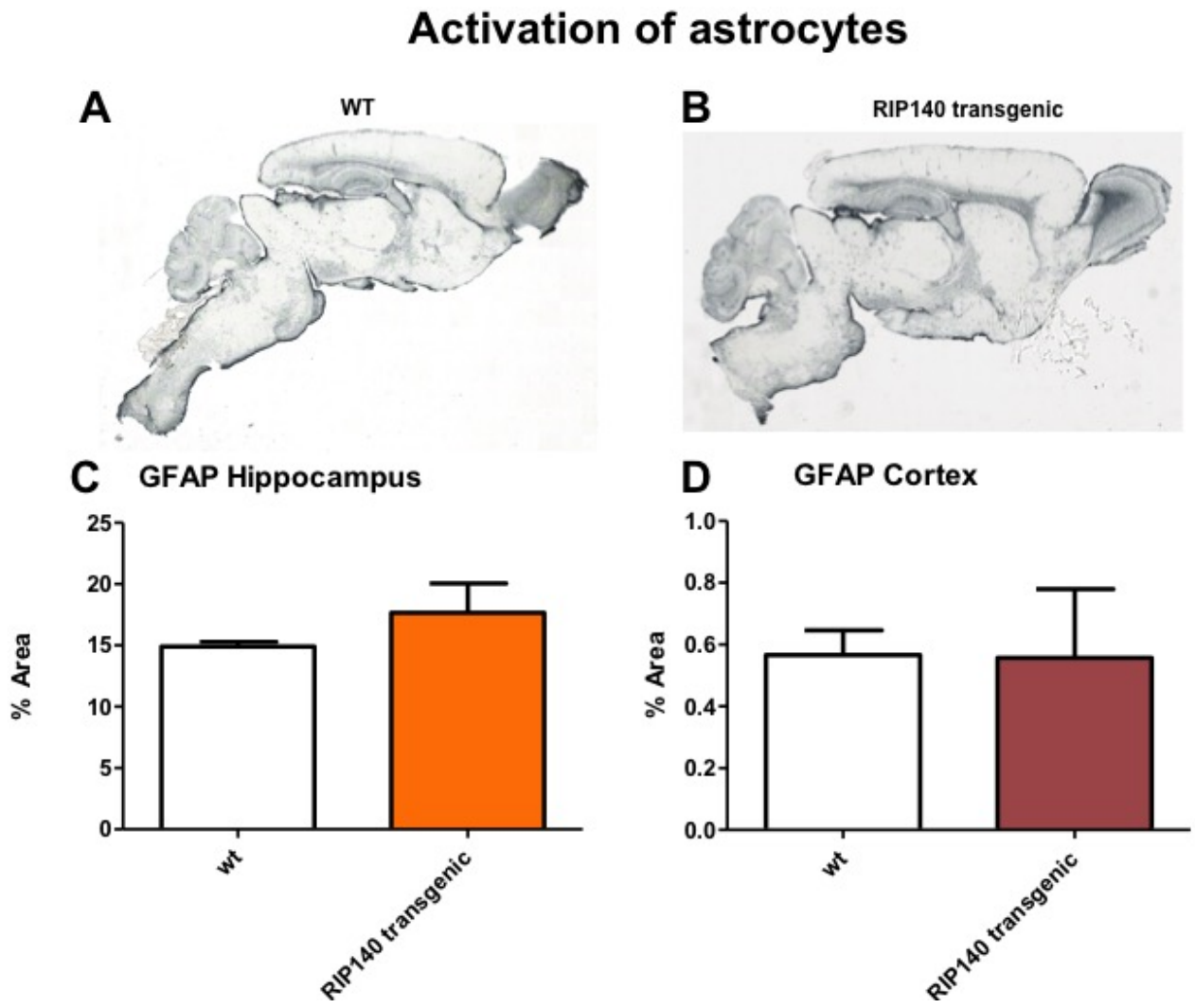


Figure 6.14: Astrocyte activation in RIP140 transgenic brain sections. Immunohistochemistry was performed on fixed 40µMbrain section using an anti GFAP antibody. No changes were seen in the Hippocampus (A) or Cortex (B). Values shown in graphs represent the mean value ±SEM and are expressed as % area of wild-type control. Statistical analysis included student's t-test. Staining, quantification and analyses were performed by Mr. David Morrow).

6.3 Neuronal density in RIP140 trangenic mice

Although we were unable to detect any differences in neuronal density in RIP140 ko mice, we wondered if perhaps overexpression of RIP140 could possibly drive an increase of neuronal cells. We carried out the neuronal quantification

using NeuN staining in sagittal sections containing the Hippocampus area and the Cortex as well, because these are the areas involved in short term memory, spatial memory and working memory, which are affected by AD (Fig. 6.15).

The Dentate Gyrus showed an increase in the area of NeuN positive cells indicating a higher cell number in this area in RIP140 transgenic mice compared with wt controls (Fig. 6.15, B). However, in other areas of the hippocampus the increase was not significant, such as in the CA1 and CA3 (Fig. 6.15.A and C). We did not see any changes in density or cell number in the subiculum area of the Hippocampus (6.15 D) or the Cortex (E).

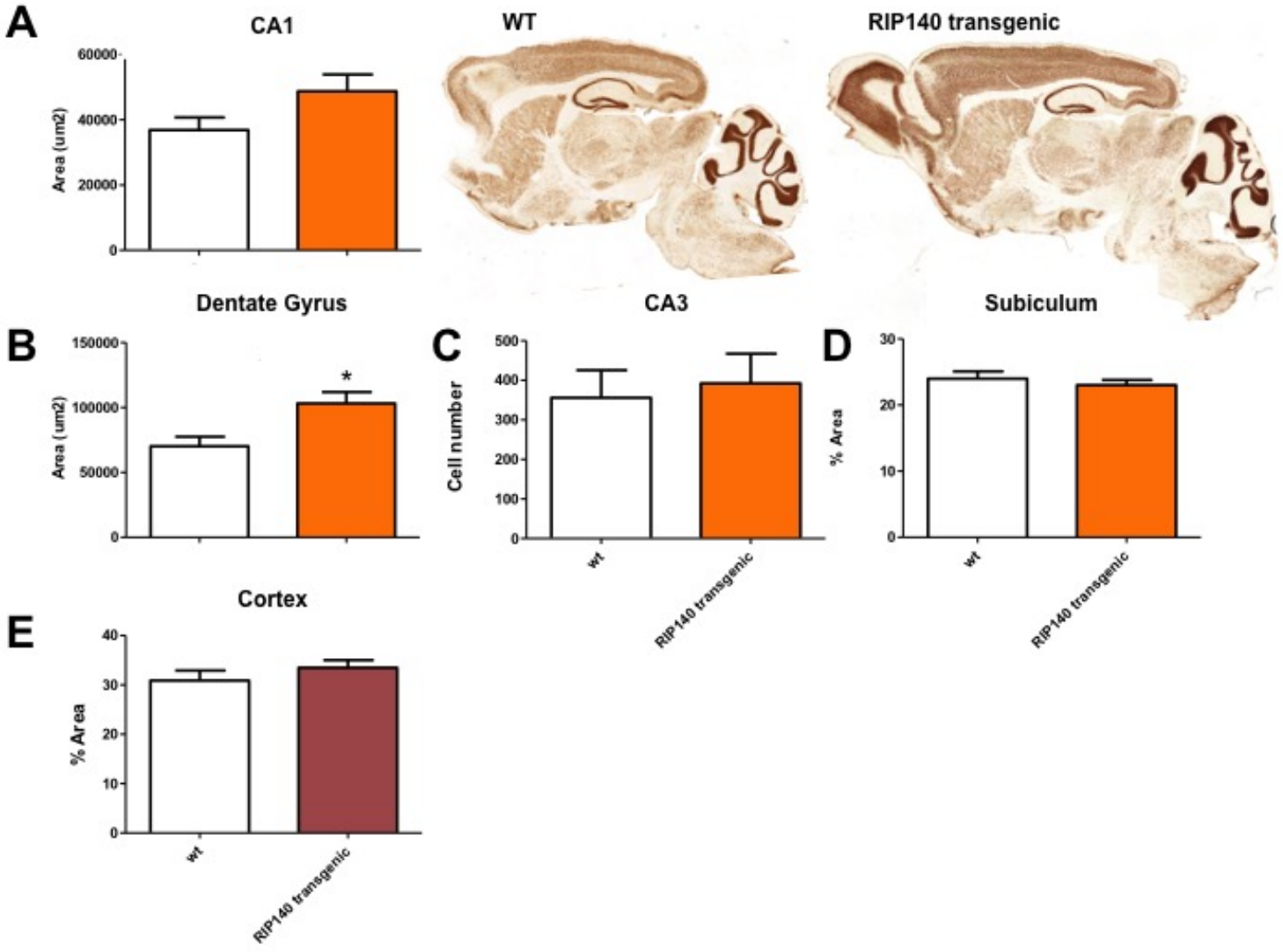


Figure 6.15: Neuronal density in RIP140 tg mice by NeuN staining. The hippocampal sub regions CA1 (A), CA3 (C) and Subiculum (D) did not show any changes in neuronal density or cell number in RIP140 mice in comparison to wild-types. An increase of neuronal cell density was observed in the dentate gyrus of RIP140 transgenic mice (B). No differences were observed in the Cortex region (E). Values shown in graphs represent the mean value ±SEM and are expressed as % area of wild-type control. Statistical analysis included student's t-test. *$p<0.05$. Quantification and analyses were performed by Mr. David Morrow).

6.4 Discussion of the effect of RIP140 overexpression in vivo in the expression of genes involved in AD

Evaluation of RIP140 knock out brains gave us insight on how certain genes are affected when this co-factor is missing. We were interested in studying the overexpression of RIP140 in vivo, since our in vitro studies pointed out that exogenous expression of human RIP140 in a neuroblastoma cell line had protective effects by reducing Aβ and BACE1 expression. BACE1 inhibition in human has been proven somehow controversial. The design of BACE1 inhibitors have some issues because most of these drugs do not cross the blood–brain barrier well. However, some BACE1 inhibitors are now in human clinical trials. Initial results suggest that some of these BACE1 inhibitor drugs are well tolerated, although others have been discontinued due to problems with liver toxicity and it is still unknown whether any will be effective for the prevention or treatment of AD (Vassar et al, 2014). The down-regulation of BACE1 is a continuing subject of research including approaches of various factors that could decrease level of this pro-amyloidogenic secretase (Zeng et al, 2015; Orejana et al, 2015).

We hypothesized, that RIP140 promotes neuro-protective and anti-inflammatory effects (Kapadia et al, 2008; reviewed by Landreth and Heneka, 2000) being therefore beneficial for AD. In this chapter we wanted to confirm the data obtained in chapters one and two to elucidate whether RIP140 overexpression in vivo is involved in the regulation of the same group of AD related genes.

However, because of low n numbers for the presented animal experiments, not all of our results present statistically significant results, that can reflect what we have previously observed in our in vitro cell studies and more experiments should be added to the currently presented ones. In addition, it has to be kept in mind that our results in vitro were performed in a neuroblastoma cell line and the brain present other types of cells, such as glial cells and vascular systems that may be affected differentially by RIP140 and therefore contribute to "dilute" the effect of RIP140 in neurons.

6.4.1 Effect of RIP140 on APP processing

In this section we show that BACE1 protein expression is strongly down-regulated in animals overexpressing RIP140, however only in the frontal cortex, while mRNA levels were found not significantly reduced in both hippocampus and frontal cortex. This might be due to insufficient number of animals; therefore with higher number of animals we could have reached statistical significance. This is in agreement with our in vitro results using N2a cells. However,

endogenous mouse Aβ levels in RIP140 tg were found unaltered in comparison to wild types. As we indicated in the previous chapter, BACE1 seems to have more affinity for APP with the Swedish mutation, which was used in our in vitro approach. In addition, it could be possible that the ELISA used is not sensitive enough to detect changes in endogenous Aβ. The reliability of the results is limited by the high background of many ELISAs for murine β-amyloid. A report examined the background signal of several murine β-amyloid ELISAs concluded that the majority of the background is from non-APP derived proteins (Teich et al, 2013). Ideally, RIP140 tg could be crossed with APP tg mice and determine if there is an effect on human Aβ deposition and in other fragments derived from BACE1 cleavage, such as the β-CTFs.

6.4.2 RIP140 overexpression results in elevation of the expression of Aβ degrading enzymes

Conversely to what we observed in the RIP140 knockout model, RIP140 overexpression induced increased mRNA levels of ApoE in the Hippocampus, however its protein levels were not different between RIP140 transgenic and wild-types. Therefore, other posttranscriptional modifications may prevent this and more research should follow up this point. In addition, lipidation levels of ApoE are important for its function, so this is something to be investigated in the future (Kim et al, 2009).

We did not find changes in the expression of other Aβ clearing enzymes, such as IDE and Neprilysin. This supports the possibility that RIP140 could affecting ApoE expression through ERRα signaling pathway or the PPARγ/LXR transcriptional regulation, as discussed in the previous chapter. ApoE is an important factor in AD as it is involved into the clearance of Aβ. If stimulation of RIP140 in the brain can actively increase amounts of this protein, it could serve as a good target for treatment during advanced but also earlier stages of AD, in order to clear Aβ to the blood stream. ApoE has also being involved in other potential mechanisms leading to AD, such as the differential modulation of neurotoxicity and Tau phosphorylation by ApoE isoforms as well as its role in synaptic plasticity and neuroinflammation (Kim et al., Neuron. 2009). ApoE is expressed basically in astrocytes and microglia, so it would be interesting to study in vitro the regulation of ApoE by RIP140 in primary astrocytes and microglia cultures.

6.4.3 RIP140 overexpression leads to an increase in neurotrophic growth factors and neuronal density

The two growth factors found in the initial screening in RIP140 ko mice which are linked to synaptic plasticity and memory were GAP43 and Igf2. Both of them exhibited increased mRNA levels in the transgenic RIP140 mouse brain in both Hippocampus and frontal cortex region. Although these changes were conspicuous, none of them appeared to be significant. It has been subject of discussion in the previous chapter that GAP43 mRNA may have been stabilized under low insulin level, a condition that does not occur in the transgenic mouse model of RIP140. In this non-stabilizing environment it may be harder to detect big changes in GAP43 mRNA as it can be degraded faster. As described by Duclot et al, mice lacking RIP140 exhibit diminished cognitive and memory functions and we were hoping to see factors involved into these processes to be up-regulated when RIP140 is overexpressed. We only examined two factors as these were changed in our preliminary array, but it is well possible that these cognitive and memory functions are regulated by others and/ or additional factors and not only mediated by GAP43 and IgF2, which could also explain our relatively mild response to RIP140 overexpression. An increase in the number animals could also help to explore further how strong is the trend that we observed or if it remains not significant. GAP43 and IgF2 role has only recently been linked to memory and cognition processes and they have been mainly described to be involved in other processes. GAP43 has been mainly described to be a neurotrophic factor, found in high amounts in neuronal growth cones during development and it is expressed selectively in associative regions of the adult human brain which includes the Hippocampus and cortex (Neve et al, 1988).

IgF2 is highly expressed in the developing brain where it has neurotrophic functions and is involved in determining cell identity, but unlike IgF1 its mRNA in the adult brain declines during maturation (Bondy et al, 1992). Although it has been clearly linked to improved memory consolidation and enhancement (Chen et al, 2001), it has to be noted that in most of these studies, IgF2 was administered. There-for, basal IgF2 level may be too low to detect changes in their expression.

Interestingly, NeuN staining in the brains of RIP140 tg mice revealed that one area of the Hippocampus (the DG) showed increased neuronal density in RIP140 tg mice, indicating that RIP140 may promote neurogenesis or to reduce neuronal death at least in certain areas. The dentate gyrus is one of the areas in the adult brain that exhibits high rates of neurogenesis (Cameron et al, 2001). The dentate gyrus is also thought to contribute to the formation of new episodic memories and the spontaneous exploration of novel environments (Amaral, et al, 2007; Saab, et al 2009). One test

performed on the RIP140 ko mice in the Duclot study included the water maze test, which affects episodic memories. Mice lacking RIP140 showed significant lower hippocampal dependent learning in the water maze in comparison to wild type. Although we did not see a decline in the neuronal density in the Hippocampus of RIP140 ko animals, the increase in the dentate gyrus in this chapter may still be an indicator how RIP140 is an inducer for neurogenesis in an area of the brain involved in spatial memory. It is possible that the excessive presence of RIP140 increases the turnover of neurogenesis, which may remain unaffected in its absence. To confirm whether RIP140 affects neurogenesis it would be interesting to perform staining with Ki67 and with doublecortin, which is a marker for immature neurons. It would also be worth carrying out behavioral tests in RIP140 transgenic mice, such as the water maze or the object location tests and see if they perform better than the wt's. Unfortunately, we did not have time and enough number of mice to perform these tests, which are available in our lab. This would be something to leave for future work.

6.4.4 Effect of RIP140 overexpression in the regulation of genes involved in Tau pathology

Examination of proteins involved into the Tau pathology in mice overexpressing RIP140 revealed that MAP2 mRNA are down regulated in the frontal cortex and up-regulated in the Hippocampus. Although this is contradicting, it should be noted that MAP2 expression in the Hippocampus RIP140 knockout mouse was a 4 fold higher than in wild types. This effect is more substantial than the 2 fold increased found in animals overexpressing RIP140. Experiments in N2a cells showed, that either overexpression or silencing of RIP140 resulted in up regulation of MAP2 (data not shown). There is less evidence of MAP2 being linked to the Tau pathological events of Alzheimer's Disease and in fact it is not present in paired helical filaments (PHF), which can be found in both, NFTs and Aβ plaques that accumulate in the degenerating neurites and neuronal cell bodies (Rosemblatt et al., 1989). MAP2 has been rather described to function as marker of neuronal differentiation and induces mitotic defects and is involved in neuronal growth, plasticity, and degeneration (Soltani et al, 2005; reviewed by Johnson and Jope, 1992). Recent studies in our lab revealed that overexpression of RIP140 does not affect total Tau expression either in the cell line SHSYSY transfected with RIP140 cDNA or in tissue from transgenic RIP140 mice.

Unexpectedly, CDK5 mRNA also appeared up-regulated in the Hippocampus of RIP140 transgenic mice, similar to what we described above for the RIP140ko mice, but also with a lower effect. Recent experiments in our lab have not found any differences in CDK5 protein expression either in the cell line N2asw transfected with RIP140

cDNA or in tissue from transgenic RIP140 mice. Although we described CDK5 so far to promote au pathology, because it phosphorylates Tau, it should be noted that cdK5 in itself is also responsible for neurite outgrowth and axon patterning (Nikolic et al., 1996; Connell-Crowley et al., 2000) and monomeric CDK5 has no enzymatic activity and requires association with a regulatory binding partner, p35 or p39, for its activation (Ko et al, 2001). CDK5 is temporally regulated by the short half-life of p35 (about 20–30 min), through the rapid degradation of p35 (Tsai et al, 1998). Neurotoxic insults such as Aβ 42 treatment will activate the cysteine protease calpain, which will cleave p35 into two segments one being p25 (Lee at el, 2000). As mentioned before, p25 acts as an activator of CDK5 as it can bind with the same affinity as p35. Different to p35 it lacks the site responsible for the fast degradation and instead will form a much more stable p25-CDK5 complex resulting in prolonged activity of CDK5 (Patrick et al, 1999). This will then lead to hyper phoshphorylation of Tau, cytoskeletal disruptions and neuronal cell death (Patrick et al, 1999). Our experiments only target the CDK5 sequence and it is not sure if we detect the CDK5-p35, the monomer or the CDK5-p25 complex. Western Blots with antibodies against p25 and/ or p35 could give insight which complex we found to be regulated or a two hybrid screening could show with which version cdK5 is associated.

Regarding GSK3, we did not find significant differences in the expression of the active isoforms of GSK3α and GSK3β, by RIP140 overexpression, but the phosphorylated version of GSK3 was significantly lower in the Hippocampus of RIP140 tg mice. At this stage, we do not know if RIP140 is involved in the regulation of the transcription of GSK3, as observed in RIP140 knockout mice. It is also possible that RIP140 may affect the activity of kinases that phosphorylate GSK3 and lower its activity. Our recent in vitro experiments carried out in N2a cells seem to indicate that RIP140 overexpression reduces the levels of GSK3, particularly the GSK3α isoform. This effect does not seem to be mediated through PPARγ, since PPARγ activators do not affect GSK3 expression and PPARγ knockdown does not reverse the down-regulation of RIP140. Therefore, our results open a new door for future investigations of the role of RIP140 on GSK3 regulation. This is very important since GSK3 is an enzyme involved in the regulation of many processes and pathways in the brain, some of them involved in Aβ generation, Tau phosphorylation, synaptic plasticity and neuroinflammation.

6.4.5 RIP140 has anti-inflammatory function

PPARγ activation has been linked with an anti-inflammatory effects. Transgenic APP mice treated with pioglitazone showed reduced microglial activation (Heneka et al., 2005). A study using PPARγ activators in human chondrocytes

demonstrated that this treatment can reduce expression of IL-1β (Hassan et al, 2001). PPARγ activation sufficiently inhibits the production of TNFα, IL-1β, IL-6 and IL-8 (Su et al, 1999; Ricote et al, 1998; Jiang et al, 1998). Based on these studies we hypothesized that RIP140 overexpression may activate PPARγ and potentially down-regulate inflammatory cytokines.

Analysis of cytokines in the Hippocampus of RIP140 tg mice revealed that the inflammatory cytokine IL-1β is reduced compared to wild type animals, but this was not significant in the frontal cortex. IL-6 was found unchanged in the Hippocampus and due to limitations in sample numbers, no evaluation of the frontal cortex was made.

These results indicate that high presence of RIP140 in the Hippocampus can modulate the inflammatory response by effectively lowering IL-1β. As these mice should not have induced inflammation, a regulation of interleukins may be harder to detect that under inflammatory conditions.

Reactive microglia or astrocytes density was not found different in RIP140 transgenic mice. This is positive as it indicates that the overexpression of RIP140 has no inflammatory inducing side effects as RIP140 has been described before to promote inflammation in macrophages by activating expression of pro-inflammatory cytokines (Zschiedrich et al., 2008). The absence of any inflammatory response indicates that RIP140 expression does not have these pro-inflammatory effects in the brain. It would be interesting to see how RIP140 animals would cope with inflammatory stress in comparison to wild-type animals. This could be done like demonstrated previously, by systemic LPS administration into the brain (Hey-Kyeong et al, 2010) or in APP/RIP140 double transgenic

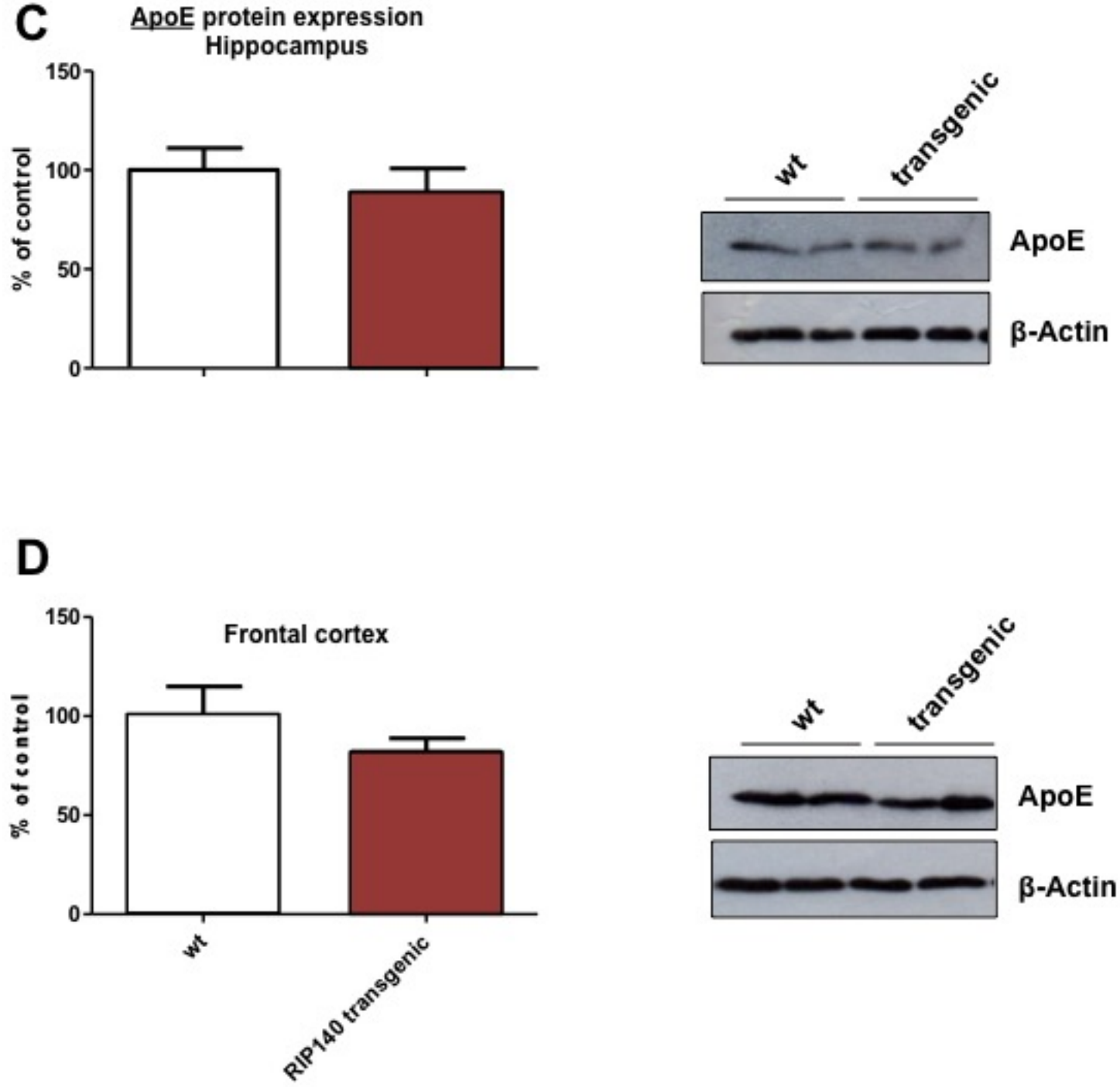


Figure 6.7: ApoE mRNA and protein expression in RIP140 tg mice. ApoE mRNA levels are significantly increased in the Hippocampus of RIP140 tg mice (A) and unchanged in the frontal cortex (B). ApoE protein levels are unaltered in both Hippocampus (C) and frontal cortex (D) of RIP140 tg. (n=5, RIP140 tg mice and n=5 for matching wild-type animals for both, hippocampus and frontal cortex. Values shown in graphs represent the mean value ±SEM and are expressed as % of wild-type control. Statistical analysis included student's t-test, *$p<0.05$).

Chapter 7

General Discussion

7.1 Findings of the study of RIP140

In this study we aimed to find out if and how the PPARγ Co factor RIP140 affects the progression of AD. The potential function of RIP140 in the brain is so far almost unknown, therefore we aimed to find out if RIP140 may have neuroprotective role in Alzheimer's disease by affecting the production of Aβ and can reduce neuroinflammation, because PPARγ, the main transcription factor regulated by RIP140 has been reported to affect Aβ generation and the transcription of pro-inflammatory molecules.

We were able to show that overexpression of RIP140 in a neuronal cell line can reduce multiple key factors involved in the generation Aβ includingBACE1, the key enzyme to produce this peptide. RIP140 can reduce BACE1 transcription, expression and its activity . Interestingly, these effects were reversed when RIP140 expression was knock down by siRNA transfection.

Furthermore, two mouse models one overexpressing and one lacking RIP140 confirmed the results observed in cell lines regarding the regulation of BACE1 byRIP140. We discovered that in addition to this, a range of genes that are all involved in the pathology of AD show changed expression patterns when RIP140 was not expressed or overexpressed, such as GSK3.

Role of PPARγ linking type-2 diabetes and AD

PPARγ could be the link between type-2 diabetes and AD, because insulin sensitivity has been associated with the down-regulation of PPARγ and PPARγ is also involved in the transcriptional regulation of genes involved in AD. The primary effects of PPARγ on gene transcription were initially described in adipose tissue, where it is most abundantly expressed, which ultimately lead to improved insulin action in muscle and liver (Moller et al., 2001). Activation of PPARγ using artificial high affinity ligands such as TZDs is widely used to increase peripheral insulin sensitivity leading to decreased plasma glucose level (Wagstaff and Goa, 2002). It is there for not surprising that PPARγ has become the predominant molecular target for insulin-sensitizing thiazolidinedione (TZD) drugs (Wilson et al., 2000; Moller et al., 2001). However, TZDs only show a modest efficiency accompanied by several side effects resulting in the expansion of research for improved PPARγ ligands and treatments as potential drugs and targets. Interestingly, loss of function mutations of PPARγ leads to severe insulin resistance and type 2 diabetes in mice (Barroso et al, 1999). A very recent study demonstrated that PPARγ activation in the brain ameliorates diabetes induced cognitive dysfunction and improves brain-derived neurotrophic factor (BDNF) expression hippocampal neuronal cells (Kariharan et al., 2015).

PPARγ has also been shown to suppress expression of pro-inflammatory genes in myeloid lineage cells, such as microglia and macrophages (Daynes et al., 2002). PPARs inhibit pro-inflammatory gene expression by a mechanism of transcriptional trans repression, which is not mediated by their binding to PPREs. They suppress the action of other transcription factors like NFκB, AP-1 and STAT1 (Daynes et al., 2002). Similarly, suppression of TNF-α gene expression by PPARγ in adipose tissue has been reported. TNF-αa is also a cytokine involved in systemic inflammation and potential systemic mediator of insulin resistance.

Another model suggests that trans repression of PPARγ is co-factor dependent. Under basal conditions NFκB-regulated inflammatory genes are maintained in a repressed state by the PPARγ cofactor N-Cor (nuclear co-repressor) containing co-repressor complexes. When exposed to pro-inflammatory stimuli this N-Cor containing complex is dismissed and gene expression is initiated, which can be prevented by sumoylated PPARγ. PPARγ agonist complexes stabilize N-Cor complexes at the promoters of NFκB-regulated genes, thus preventing inflammatory gene expression (Ghisletti et al., 2007; Ogawa et al., 2005). This observation points out an important potential role of PPAR regulation by co-factors and not only ligands alone. Taken this together, it can be assumed that the specific modification of inflammatory factors might also alter insulin resistance. The observation that PPARs are able to suppress the inflammatory response in peripheral macrophages and in several models of human autoimmune diseases, lead to the

idea that PPARs might be beneficial for CNS disorders possessing an inflammatory component. Inflammatory factors such as C-reactive protein, interleukin-6 and TNF-α are also elevated in type 2 diabetes (van de Ree et al., 2003).

The investigation of the PPARγ co-factor RIP140 appeared interesting and necessary as it is involved in many of the processes described along this thesis, such as the association between metabolic disease and neurodegeneration. Therefore RIP140 could represent another link and treatment target for AD and type-2 diabetes. Like PPARγ, RIP140 has been associated to insulin-resistance as well as pro-inflammatory factor expression; however, it is thought that RIP140 promotes inflammation and type 2 diabetes and its absence can improve insulin sensitivity (Zschiedrich et al, 2008). However these studies have been mainly focused and carried out in tissue linked to diabetes and obesity, such as white and brown adipocytes and actions of RIP140 in the brain have not been yet described with regard to insulin signaling. As RIP140 has been shown to act potentially as a co-activator or co-repressor dependent on the tissue, we were curious to find out how it would act on PPARγ and other transcription factors in the brain and whether it may contribute to or inhibit the beneficial effects promoted by this nuclear receptor. Nuclear receptor signaling seems therefore to play an important role linking energy metabolism and neuroinflam-matory processes. The results of this work provide molecular insights into the function of factors linking metabolic disease with AD and may offer opportunities for therapeutic intervention.

7.1.1 Effect of RIP140 on Aβ generation

In the present study we demonstrated that BACE1 protein levels are lower in a neuronal cell line, which is overexpressing the co-factor RIP140. This effect was enhanced when the cells were simultaneously treated with the TZD and PPARγ agonist pioglitazone. We additionally showed that BACE1 regulation by RIP140 did not only affected protein level but acts as early as on its promoter activity, which was also decreased in the overexpressed presence of RIP140 and consequently, BACE1 mRNA levels were down-regulated as well. The effect of RIP140 on BACE1 transcription seems to be mediated by PPARγ, since PPARγ knockdown reverses the effect (data not shown). Absence of RIP140, induced by transfection with RIP140 siRNA was able to show the opposite effects on BACE1 expression in vitro.

This suggests strong regulatory actions of RIP140 on BACE1, possibly mediated by binding to PPARγ which has shown to have a consensus binding sequence in the BACE1 promoter, leading to reduced BACE1 promoter activity and hence decreased BACE1 expression (Sastre et al., 2006). As PPARγ has been described to mediate the BACE1 promoter repression in an activated state, it is to be assumed that RIP140 has co-activating functions in this neuronal

cell line. Another possibility is that BACE1 interacts with other transcription factors such as NFκB or the estrogen receptor which both have consensus binding sites in the BACE1 promoter which could be affected by RIP140 expression levels (Rossner et al, 2006; Zheng et al., 2015.) . In fact it has been shown a long time ago that RIP140 interacts with the estrogen receptor and modulates its activity (Cavailles et al., 1995). It has also been shown that RIP140 has co-activating functions for NFκB in macrophages (Zschiedrich et al., 2008). Future experiments using a NFκB siRNA could reveal if BACE1 reductions mediated by RIP140 act through NFκB. In addition, Chromatin immunoprecipitation experiments could reveal if RIP140 indeed forms a complex with PPARγ in PPRE sites located at the BACE1 promoter.

Our In vivo studies revealed that BACE1 mRNA is elevated in the Hippocampus when RIP140 is knocked out and BACE1 protein level was strongly reduced in the frontal cortex when RIP140 is overexpressed, which is in agreement with the in vitro results. Therefore, our in vitro findings may be translated to an in vivo background and RIP140 could serve indeed as a target to modulate BACE1 in the brain. As a consequence of the decrease in BACE1 expression by RIP140 overexpression, less of the toxic Aβ peptide is generated, as we were able to demonstrate in vitro. We hypothesize that RIP140 inhibits BACE1 transcription and therefore down regulates the amyloidogenic cleavage of APP, resulting in less Aβ (Fig. 7.1). In the in vivo model of RIP140 overexpression, we were however unable to detect these changes in Aβ. It is noteworthy, that the neuronal cell line was stably expressing APP with the Swedish mutation, which will have increased APP expression and more efficient β-cleavage and therefore is a lot more sensitive to changes in β-secretase activity than the in vivo model. It would be interesting to cross breed RIP140 transgenic mice with an AD mouse or APP overexpressing model to study the effects on BACE1 and resulting cleavage products. But there could be other reasons why we wouldn't be able to detect a change in Aβ in vivo by RIP140 overexpression. The tissue examined in the in vivo studies is consistent of various cell types, while in vitro we examined a cell culture made up of 100% neuronal cells. The mixture of cells in vivo can mask effects seen in vitro by different factors expressed in the different cell types, which could contribute to the clearance of Aβ, for instance Aβ phagocytosis by microglia. Another possibility is that the reliability of the ELISA results is limited by the high background of many ELISAs for murine β-amyloid, revealed in a report on examination of human murine β-amyloid ELISA assays, which concluded that the majority of the background is from non-APP derived proteins (Teich et al., 2013).

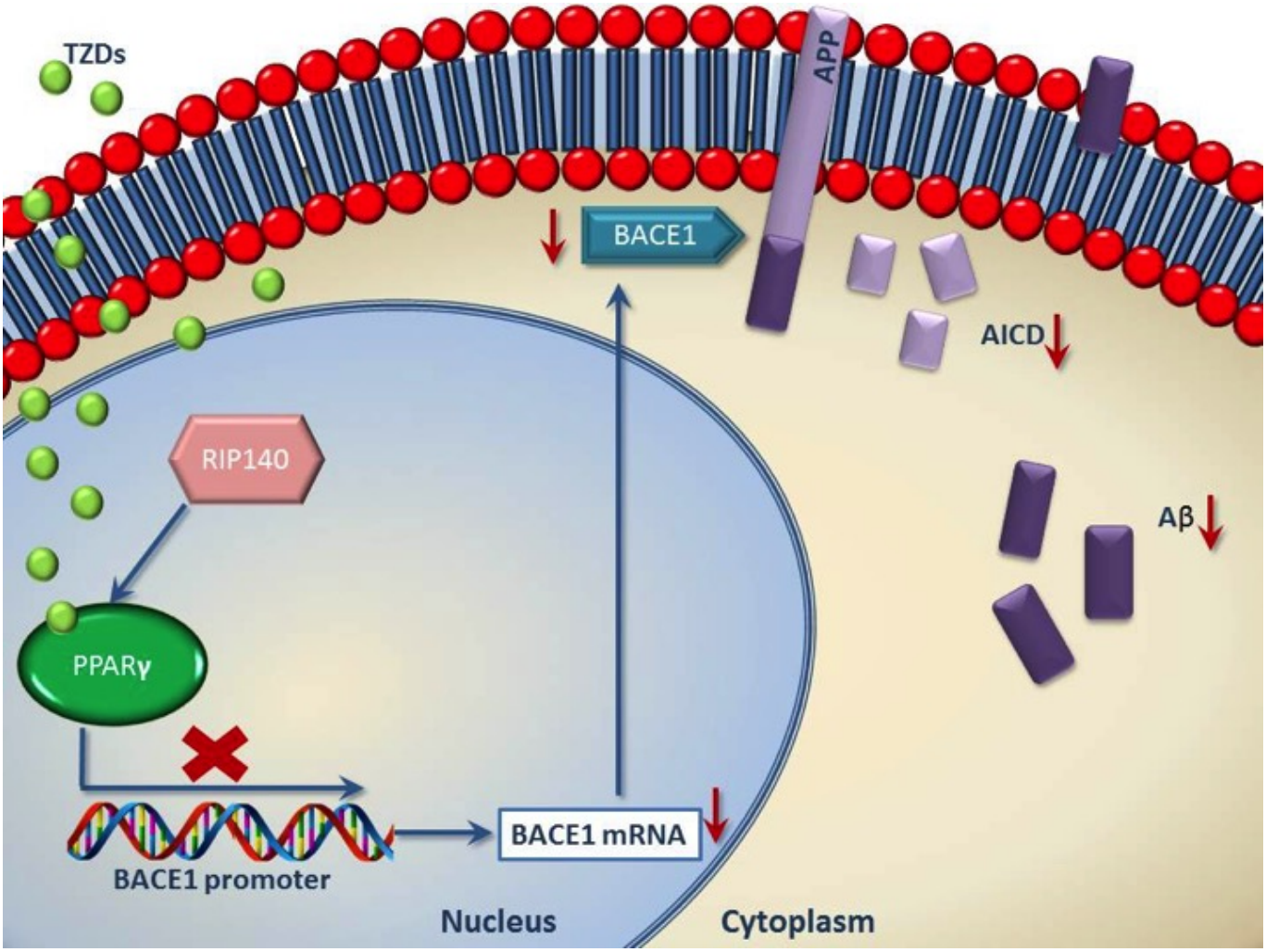


Figure 7.1: Proposed mechanism of RIP140 on APP processing. When activated by ligands, PPARγ will bind to a PPRE element in the BACE1 promoter and form a heterodimer complex with LXR (not shown) and repress BACE1 promoter activity. RIP140 co-activates by binding to PPARγ in a ligand dependent manner, repressing BACE1 promoter further and possibly increasing the stability of the complex. Consequently, less BACE1 mRNA will be transcribed leading to decreased expression of BACE1 protein. This results in a reduction of beta cleavage of APP, producing lower amounts of the toxic Aβ.

7.1.2 Effects of RIP140 on Aβ clearance

We have shown that Aβ level are reduced by RIP140 overexpression in vitro. We proposed that the underlying mechanism is a decrease in BACE1, cleaving less APP. Another way to decrease Aβ is by enzymatic degradation

and/or by receptor-mediated clearance (Tanzi et al). The most famous and reported mechanism involved in Aβ clearance in AD is probably ApoE, as mutations in this gene account for sporadic, inherited cases of AD.

We found that in the Hippocampus of mice lacking RIP140 ApoE mRNA is down-regulated, while up-regulated in animals overexpressing RIP140. This suggests that ApoE expression levels are modulated by the expression of RIP140. Examination of ApoE expression level in our cell experiments could give insight whether the decrease observed in Aβ level is possibly ApoE mediated or at least partially accounting for it. Although ApoE is mainly expressed by astrocytes, it may not be possible to pick up changes in a neuronal cell line and only the co-culture of astrocytes and neurons can reveal such changes in vivo.

Another additional mechanism by which RIP140 could affect ApoE function is through its receptor LRP. It has been shown that the low-density lipoprotein receptor (LDLR)-related protein, (LRP) functions as a receptor for ApoE (Besiege et al., 1989). Interestingly, LRP expression is also regulated by PPARγ (Gauthier et al., 2003). In the latter study, they found a predicted PPRE for PPARγ in the LRP gene and also demonstrated that rosiglitazone directly stimulates transcription of the LRP gene through activation of PPARγ, increasing functional LRP expression. Within the CNS, LRP is highly expressed in neuronal cell bodies and it is possible that RIP140 co-activates PPARγ during regulation of the LRP gene expression, resulting in higher neuronal LRP that can then bind ApoE. The strong association of ApoE4 with sporadic AD raised the possibility that ApoE is mediating its powerful effect at least in part through the receptors to which it binds. The role of LRP in AD has been described whereby a polymorphism in the LRP1 gene has been linked to AD development (Buffer el a., 1999).

In the future, other studies could be performed to further investigate the role of RIP140 on Aβ clearance. It would be interesting to investigate if RIP140 can mediate Aβ degradation via Aβ-phagocytosis in microglia, as this way of degradation has also been shown to be modulated by PPARγ (Yamanaka et al., 2012).

7.1.3 Effects on Tau pathology

RIP140 does not only play a part on Aβ pathology but also on Tau pathology as our study firstly described. The microtubule-associated contributor MAP2 has been found to be highly up-regulated in the Hippocampus of mice that do not express RIP140. However mice overexpressing RIP140 also show an increase in MAP2 in the Hippocampus in comparison to wild type mice, but with a response of only half the intensity than seen in RIP140 ko mice. This does suggest that RIP140 expression levels do affect MAP2 expression strongly. Some MAPs have been shown to be

regulated by the tumor suppressor protein p53, which negatively regulates the expression of MAP (Murphy et al., 1997). Usually low levels of p53 are maintained but it has been shown that it is elevated in AD and promotes Tau pathology (Hooper et al., 2007). PPARγ has shown to interact with p53 and TZD treatment leads to cell apoptosis in cancerous cells through a p53 dependent mechanism (Nag amine et al., 2003). It is possible that RIP140/ PPARγ interaction can modulate MAP expression through p53 signaling in different ways than observed in other tissues, leading to an increase in MAP expression, when RIP140 is depleted and not co-activating PPARγ .

Because we did not detect changes in total Tau expression in RIP140 knockout an transgenic mice (data do not shown), probably the most likely mechanism by which RIP140 affects Tau pathology is by altering Tau phosphorylation. We have shown that CDK5 was up-regulated in the Hippocampus of RIP140 knockout and transgenic animals suggesting again that expression level of this co-factor regulates those of cdK5. Apparently, CDK5 is a direct target of PPARγ ligands such as TZDs resulting in phosphorylation of PPARγ (Choi et al., 2010). It was demonstrated by Choi and colleagues that phosphorylation of PPARγ by the protein kinase CDK5 neither activates nor suppresses general receptor transcriptional activity, but changes the expression of specific genes. However, phosphorylation of PPARγ by other kinases has demonstrated how phosphorylation decreases its activity (Hu et al., 1996; Adams et al., 1997).

The second kinase we investigated and is also involved in Tau pathology is GSK3, which also appeared to be regulated by RIP140 expression. Lack of RIP140 lead to an increase on GSK3β protein level in both the Hippocampus and frontal cortex. GSK3α protein levels were also increased in the frontal cortex of RIP140 knockout mice, while in RIP140 overexpressing animals, phosphorylated GSK3 protein level were strongly down-regulated. Both isoforms of GSK3, GsK3β and GSK3α can lead to hyper phosphorylation of Tau. Phosphorylated GSK3 is the less active form of GSK3.

GSK3 is not only important for regulating Tau but also Aβ generation and recently our group demonstrated that GsK3 inhibition promotes lysosome biogenesis and autophagic degradation of Aβ , CTFs and APP (Parr et al., 2012). Another study on GsK3 in our group showed that activation of the Wnt pathway by overexpression of the agonist Wnt or β-catenin or by inhibition of GSK3 in N2a cells resulted in a reduction in Aβ levels and in the activity and expression of BACE1 (Parr et al., 2015). Alterations in the Wnt signaling pathway have been implicated in AD and activation of the canoncial Wnt-β-catenin pathway, leading to inhibition of cytosolic GSK3. Signaling via the canonical Wnt- β-catenin pathways has also been shown to inhibit PPARγ mRNA expression (reviewed in Ichiro et al., 2009), although other studies have shown that β-catenin can bind PPARγ (Liu et al., 2006) and elevate PPARγ protein levels,

possibly through sequestration by activated β-catenin in colon cancer cell lines (Jansson et al., 2005). Interestingly, TCF4 can bind to PPARγ and mutations in TCF4 have also been linked with type-2 diabetes (Jan et al, 2008).

In summary the regulation by RIP140 of the GSK3 gene can have beneficial effects on both the Tau and Aβ pathology. This could be through two mechanisms. Firstly by indirectly affecting the insulin signaling (as previously discussed) or secondly via PPARγ and Wnt- β-catenin pathway. It would be interesting in the future to determine whether GSK3 promoter has consensus sites for transcription factors regulated by RIP140.

7.1.4 Effects of RIP140 on inflammation

In the study of RIP140 knockout mice we found an increased density of reactive astrocytes in the hippocampus of those animals and a trending increase in IL1β and IL6, suggesting that presence of RIP140 is involved in the regulation of cytokine expression and the inflammatory response in a moderate state, most likely through PPARγ co-activation, as PPARγ can suppress expression of pro-inflammatory genes (described above).

Overexpression of RIP140 lead to a down-regulation in IL-1β expression in the Hippocampus, although no other cytokines were changed and no alteration in the activation of astrocytes or microglia was detected. This is interesting, as RIP140 has been described to drive the expression of inflammatory factors such as cytokines in macrophages and our results suggest that overexpression of RIP140 has opposite effects in cerebral tissue acting as an inhibitor of inflammation, like the down-regulation of IL-1β suggest. Maybe in combination with activation of PPARγ with TZDs this effect can be enhanced and also observed for further cytokines and pro-inflammatory genes including TNF-alpha, iNOS, etc. This would put RIP140 into a position to serve as a target for any condition associated with neuroinflammation. Therefore, it would be interesting to study the effect of RIP140 in models of neurodegenerative diseases, such as Multiple Sclerosis (MS). One suggestion would be to generate the experimental autoimmune encephalomyelitis (EAE) model of MS in RIP140 tg mice and see if the disease symptoms are reduced.

7.1.5 Effects of RIP140 on neuronal density, neuronal growths factors and neuroprotection

In this study, we found that excessive expression of RIP140 induced and increased the density of neuronal cells in the dentate gyrus, a sub region of the hippocampus. The dentate gyrus exhibits high rates of neurogenesis (Cameron et al, 2001) and it is possible that RIP140 can enhance or promote neurogenesis in this area. PPARγ activation was recently

demonstrated to be protective and promote neurogenesis and memory by suppressing the effects of LPS-produced transient illness (Brandi et al, 2013), suggesting an involvement of the nuclear receptor on neurogenesis.

GAP43, another factor involved in neurogenesis, appeared up-regulated when RIP140 was knocked out. As previously discussed, this might be due to alterations in circulating insulin levels in mice lacking RIP140, which will have an effect on stabilization of GAP43 mRNA. This effect would not be promoted by changed expression level in the brain but as a consequence of the whole RIP140 body knock out and its secondary effects. A neuronal conditional RIP140 knock out or transgene would give more insights on this aspect, as it could be free of these interferences and reveal neuron specific functions and regulations by RIP140.

7.2 Limitations of the study and future work

We studied effects of RIP140 overexpression and knockdown in vitro and in vivo, using genetically modified mice . This revealed how RIP140 affects processes involved in the Alzheimer's pathology and regulates directly or indirectly a wide range of genes, which are associated to AD.

Using an immortalized neuroblastoma cell line is a good start to do a proof-of-principle study but it has always to be kept in mind that the conditions are artificial and differentially regulated, as it is a tumor cell line. Therefore, it might not reflect what is actually happening in real life. The N2a cell line accounts as a fast growing line and origins from a neuroblastoma and is likely to exhibit alterations in its metabolism in comparison to real-life neurons. Therefore, primary neuronal cell culture would be more reliable approach to study the effect of RIP140 on APP processing. Cell could even be obtained from an AD mouse model to effectively study effects on AD.

In addition, the cerebral tissue is composed of multiple cell types, which are in constant interaction with each other, and study of a single cell line cannot take these interactions into account. We would suggest to use neuronal-glial co-cultures in future studies.

Additionally, the cells have been permanently transfected with an APP construct carrying the Swedish mutation, to generate rapid and increased Aβ production, which is again a good model for proof-of-principle research on APP processing. On the other hand, this introduces another artificial factor that could potentially alter the ongoing biochemistry in these cells, which drives it far away from real life applications. Moreover, the Swedish mutation itself does not represent APP processing like it happens in all cases for AD and only accounts for a small percentage of sporadic cases. This mutation leads to overproduction of Aβ and provides a better substrate to BACE1. There are also concerns

that N2a-sw cells (N2a cells permanently transfected with APP carrying the Swedish mutation construct), will lose the construct after a period of time in culture and that only a small number of cells will actually express the Swedish mutation. Unexpectedly, these cell might be able to adjust to the selection conditions with culture using geneticin in the conditioned media and grow just as normal as N2a untransfected cells. Different mouse models represent different versions of AD and could make future data more robust and ensure that effects are not only applicable to one specific type of AD. Our lab has also started to establish organotypic cultures, which allows to study a whole section of intact brain tissue in vivo. This model goes even a step further than primary cultures and takes into account all cell types and interactions with glial cells. However, the closer the method actually is to real-life the more challenging, time and money consuming it will be and therefore needs to be carefully planned. This is why testing a hypothesis in a simple cell line, like we did, is appropriate preliminary work to plan more challenging experiments.

The transgenic and knockout mouse model of RIP140 provided a good opportunity to study effects of RIP140 expression changes in the brain with relation to AD. In contrast with the study using the cell line, all cerebral cell types were affected similarly and could interact as under natural conditions. Although this reflects a more close approach to nature background, it is also possible that other cell types react different to RIP140 overexpression. Therefore, the effects of RIP140 in neuronal cells could be masked by opposing alterations in other cell types.

The genetically modified RIP140 mouse models may also not be ideal to study effects on AD by themselves, as they lack key features of AD pathology, such as amyloid deposition and neuroinflammation. Another problem is, that these were whole body knockout or transgenic mouse models and RIP140 could affect other tissues than the brain. RIP140 knockout mice are lean, with a 70% reduction of body fat and a 20% reduction in body weight. They are resistant to high-fat diet (HFD) induced obesity with an increase in insulin sensitivity and female's animals are infertile. This not only has side effects on the pathways we want to study in the brain, but also other issues, such as female infertility.

The RIP140 transgenic have cardiac issues, including hypertrophy of the cardiac muscle and increased calcification of the arteries leading to lower survival rates.

These issues severely limited the numbers of animals in our study and sometimes affected the statistical significance of our data.

In the future, two new approaches would be interesting to carry out in animals. To either cross breed RIP140 tg/ko mice with an AD mouse model to study effects on Aβ more accurately and see if conclusions form the cell work are reproducible. The other possibility would be to deliver a lentivirus vector carrying RIP140 gene to overexpress

RIP140 in the hippocampus or frontal cortex region of an AD mouse model and study how these animals improve their symptoms. We have experience in this technology, as this type of study has been previously done in our lab by delivering with another PPARγ co-factor, PGC-1α in the brain of APP23 mice. This seems to be a promising therapeutically approach (Katsouri et al, under revision, 2015).

Another idea is to generate conditional RIP140 tg/ ko mice using the cre-lox recombination system and overexpress RIP140 exclusively in neurons. Other interactions and side effects such as changed insulin signaling and cardiac issues would be diminished.

7.3 Final Conclusion

In the present study we have demonstrated that RIP140 expression has beneficial effects on AD pathology by disrupting APP processing, reducing inflammation and increasing the expression of neurotropic factors in the brain. Additionally, in this study we have shown that RIP140 affects a number of genes that have been implicated in other aspects of AD, such as kinases involved in Tau phosphorylation. Our final conclusions of this study are:

1. Exogenous overexpression of human RIP140 reduces the transcription of the BACE1, a key enzyme involved in the generation of Aß. This effect is mediated through the nuclear factor PPARγ and it is enhanced in combination with activating PPARγ-ligands, but can also act on its own.

2. Lack of RIP140 results in the opposite effects, increasing BACE1 levels. RIP140 down regulation observed in the brains of AD patients may therefore favor disease progression.

3. RIP140 regulates the expression of enzymes like ApoE and Neprilysin, which are both involved in Aß clearance and degradation. Overexpression of RIP140 leads to higher ApoE protein levels. Conversely, RIP140 knockout brains, exhibit lower expression levels for both Neprilysin and ApoE. Overall, RIP140 affects Aβ levels by reducing its generation and increasing its degradation.

4. Additionally, RIP140 also affects the expression of factors related to Tau pathology, namely Mtap2 and the kinases cdK5 and GsK3. It has to be noted that the latter can also be associated to the Aß pathology.

5. RIP140 is also involved in the regulation of the expression of growth factors in the brain, such as GAP43 and IgF2, which could lead to neuroprotection.

6. Furthermore, we describe here that RIP140 may have anti-inflammatory properties by reducing the levels of certain cytokines and the density of glial cells. In summary, our results provide further insight on how alterations in

nuclear factor signaling lead to AD pathology and emphasizes the role of RIP140 as novel treatment target for AD.

7.4 Literature

References

Adams M, Reginato MJ, Shao D, Lazar MA, Chatterjee VK.
Transcriptional activation by peroxisome proliferator-activated receptor gamma is inhibited by phosphorylation at a consensus mitogen-activated protein kinase site.
J Biol Chem. 1997 Feb 21;272(8):5128-32.

Andrew F. Teich,* Mitesh Patel, and Ottavio Arancio
A Reliable Way to Detect Endogenous Murine β-Amyloid.
PLoS One. 2013; 8(2): e55647. Published online 2013 Feb 1.
doi: 10.1371/journal.pone.0055647

Acquati F, Accarino M, Nucci C, Fumagalli P, Jovine L, Ottolenghi S, Taramelli R.
The gene encoding DRAP (BACE2), a glycosylated transmembrane protein of the aspartic protease family, maps to the down critical region.
FEBS Let, 2000.;468:59–64 ,

Ahmed RR, Holler CJ, Webb RL, Li F, Beckett TL, Murphy MP.
BACE1 and BACE2 enzymatic activities in Alzheimer's disease.
J Neurochem. 2010 Feb;112(4):1045-53. doi: 10.1111/j.1471-4159.2009.06528.x. Epub 2009 Dec 4.

Aigner L, Arber S, Kapfhammer JP, Laux T, Schneider C, Botteri F, Brenner HR, Caroni P.
Overexpression of the neural growth-associated protein GAP-43 induces nerve sprouting in the adult nervous system of transgenic mice.
Cell. 1995 Oct 20;83(2):269-78.

Akiyama H, Arai T, Kondo H, Tanno E, Haga C, Ikeda K
Cell mediators of inflammation in the Alzheimer disease brain.
Alzheimer Dis Assoc Disord. 2000;14 Suppl 1:S47-53

Alvarez, J.P. Munoz, R.B. Maccioni
A Cdk5-p35 stable complex is involved in the beta-amyloid-induced deregulation of Cdk5 activity in hippocampal neurons *Exp. Cell Res., 264 (2001), pp. 266–274*
Am J Geriatr Psychiatry. 2005 Nov;13(11):950-8.

Anders, S. Gilbert, W. Garten, R. Postina, F. Fahrenholz
Regulation of the alpha-secretase ADAM10 by its prodomain and proprotein convertases
FASEB J.2001, 15 , pp. 1837–1839

Arriagada PV, Growdon JH, Hedley-White T, Hyman BT.
Neurofibrillary tangles and not senile plaques parallel duration and severity of Alzheimer's disease.
Neurology 1992; 42: 1681–1688

Arvanitakis Z, Wilson RS, Bienias JL, Evans DA, Bennett DA.
Diabetes mellitus and risk of Alzheimer disease and decline in cognitive function.
Arch Neurol. 2004 May;61(5):661-6.

Asmaà Fritah , Mark Christian , Malcolm G. Parker
The metabolic coregulator RIP140: An update.
American Journal of Physiology - Endocrinology and Metabolism Published 1 September 2010 Vol. 299no. 3, E335-E340DOI: 10.1152/ajpendo.00243.2010

Auron, A.C. Webb
Interleukin-1: a gene expression system regulated at multiple levels
Eur Cytokine Netw, 5 (1994), pp. 573–592

B Zhang, C Gaiteri, L-G Bodea
Integrated systems approach identifies genetic nodes and networks in late-onset Alzheimer's disease
Cell, 153 (2013), pp. 707–720

Ayala-Grosso C, Ng G, Roy S, Robertson GS
Caspase-cleaved amyloid precursor protein in Alzheimer's disease.
Brain Pathol. 2002 Oct;12(4):430-41.

Barrosoa, Jaume del Vallea, David Porqueta, Ana M. Vieira Santosa, Laia Salvadóa, Rosalía Rodríguez-Rodrígueza, Patrícia Gutiérreza, Marta Anglada-Huguetc, Jordi Alberchc, dAntoni Caminsa, Xavier Palomera, Mercè Pallàsa, Liliane Michalikf, Walter Wahlif, Manuel Vázquez-Carreraa Tau hyperphosphorylation and increased BACE1 and RAGE levels in the cortex of PPARβ/δ-null mice *August 2013. Biochimica et Biophysica Acta; 1832(8).*

I. Barroso, M. Gurnell, V. E. F. Crowley, M. Agostini, J. W. Schwabe, M. A. Soos, G. LI Maslen, T. D. M. Williams, H. Lewis, A. J. Schafer, V. K. K. Chatterjee & S. O'Rahilly
Dominant negative mutations in human PPARgamma associated with severe insulin resistance, diabetes mellitus and hypertension
Nature 402, 880-883 (23 December 1999) | doi:10.1038/47254; Received 18 September 1999; Accepted 30 September 1999

Basi G, Frigon N, Barbour R, Doan T, Gordon G, McConlogue L, Sinha S, Zeller M.
Antagonistic effects of beta-site amyloid precursor protein-cleaving enzymes 1 and 2 on beta-amyloid peptide production in cells.
J Biol Chem. 2003;278:31512–31520.

Beffert U, Arguin C, Poirier J.
The polymorphism in exon 3 of the low density lipoprotein receptor-related protein gene is weakly associated with Alzheimer's disease.
Neurosci Lett. 1999 Jan 4;259(1):29-32.

Beisiegel U, Weber W, Ihrke G, Herz J, Stanley KK.
The LDL-receptor-related protein, LRP, is an apolipoprotein E-binding protein.
Nature. 1989 Sep 14;341(6238):162-4.

Ben Menachem-Zidon O, Avital A, Ben-Menahem Y, Goshen I, Kreisel T, Shmueli EM, Segal M, Ben Hur T, Yirmiya R (17 November 2010).
Astrocytes support hippocampal-dependent memory and long-term potentiation via interleukin-1 signaling.
Brain, Behaviour, and Immunity 25 (5): 1008–1016. doi:10.1016/j.bbi.2010.11.007

Bernardo A, Levi G, Minghetti L.
Role of the peroxisome proliferator-activated receptor-γ (PPAR-γ) and its natural ligand 15-deoxy-Δ(12,14)-prostaglandin J in the regulation of microglial functions.
European Journal of Neuroscience. 2000;12(7):2215–2223.

Billingsley ML, Kincaid RL (May 1997).
Regulated phosphorylation and dephosphorylation of tau protein: effects on microtubule interaction, intracellular trafficking and neurodegeneration.
Biochem. J. 323 (3): 577–91. PMC 1218358. PMID 9169588.

Black, C.T. Rauch, C.J. Kozlosky, J.J. Peschon, J.L. Slack, M.F. Wolfson, B.J. Castner, K.L. Stocking, P. Reddy, S. Srinivasan, N. Nelson, N. Boiani, K.A. Schooley, M. Gerhart, R. Davis, J.N. Fitzner, R.S. Johnson, R.J. Paxton, C.J. March, D.P. Cerretti
A metalloproteinase disintegrin that releases tumour-necrosis factor-alpha from cells
Nature, 385 (1997), pp. 729–733

Bodles AM1, Varma V, Yao-Borengasser A, Phanavanh B, Peterson CA, McGehee RE Jr, Rasouli N, Wabitsch M, Kern PA.
Pioglitazone induces apoptosis of macrophages in human adipose tissue.
J Lipid Res. 2006 Sep;47(9):2080-8. Epub 2006 Jun 23.

Bordet R., Ouk T., Petrault O.
PPAR: a new pharmacological target for neuroprotection in stroke and neurodegenerative diseases.
(2006) Biochem. Soc. Trans. 34, 1341–1346.

Bot, N., Schweizer, C., Ben Halima, S. & Fraering, P. C.
Processing of the synaptic cell adhesion molecule neurexin-3beta by Alzheimer disease alpha- and gamma-secretases.
J. Biol. Chem. 286, 2762–2773 (2011).

Breidert, J. Callebert, M.T. Heneka, G. Landreth, J.M. Launay, E.C. Hirsch
Protective action of the peroxisome proliferator-activated receptor-gamma agonist pioglitazone in a mouse model of Parkinson's disease
J. Neurochem., 82 (2002), pp. 615–624

Brou, F. Logeat, N. Gupta, C. Bessia, O. LeBail, J.R. Doedens, A. Cumano, P. Roux, R.A. Black, A. Israel
A novel proteolytic cleavage involved in Notch signaling: the role of the disintegrin-metalloprotease TACE
Mol. Cell Biol., 5 (2000), pp. 207–216

Bu, J. Li, P. Davies, I. Vincent
Deregulation of cdk5, hyperphosphorylation, and cytoskeletal pathology in the Niemann-Pick type C murine model
J. Neurosci., 22 (2002), pp. 6515–6525

Buxbaum, K.N. Liu, Y. Luo, J.L. Slack, K.L. Stocking, J.J. Peschon, R.S. Johnson, B.J. Castner, D.P. Cerretti, R.A. Black
Evidence that tumor necrosis factor alpha converting enzyme is involved in regulated alpha-secretase cleavage of the Alzheimer amyloid protein precursor
J. Biol. Chem., 273 (1998), pp. 27765–27767

Cai H, Wang Y, McCarthy D, Wen H, Borchelt DR, Price DL, Wong PC.
BACE1 is the major beta-secretase for generation of Abeta peptides by neurons.
Nat Neurosci. 2001;4:233–234.

Capell A, J. Grunberg, B. Pesold, A. Diehlmann, M. Citron, R. Nixon, K. Beyreuther, D.J. Selkoe, C. Haass
The proteolytic fragments of the Alzheimer's disease-associated presenilin-1 form heterodimers and occur as a 100–150-kDa molecular mass complex
J. Biol. Chem., 273 (1998), pp. 3205–3211

Caporaso, K. Takei, S.E. Gandy, M. Matteoli, O. Mundigl, P. Greengard, P. De Camilli
Morphologic and biochemical analysis of the intracellular trafficking of the Alzheimer beta/A4 amyloid precursor protein
J. Neurosci., 14 (1994), pp. 3122–3138

Cavailles, et al.
Interaction of proteins with transcriptionally active estrogen receptors
Proc. Natl. Acad. Sci. U.S.A., 91 (1994), pp. 10009–10013

V Cavaillès, S Dauvois, F L'Horset, G Lopez, S Hoare, P J Kushner, and M G Parker
Nuclear factor RIP140 modulates transcriptional activation by the estrogen receptor.
EMBO J. 1995 Aug 1; 14(15): 3741–3751. PMCID: PMC394449

Chen DY, Stern SA, Garcia-Osta A, Saunier-Rebori B, Pollonini G, Bambah-Mukku D, Blitzer RD, Alberini CM.
A critical role for IGF-II in memory consolidation and enhancement.
Nature. 2011 Jan 27;469(7331):491-7. doi: 10.1038/nature09667.

Choy RW, Cheng Z, Schekman R.
Amyloid precursor protein (APP) traffics from the cell surface via endosomes for amyloid beta (Abeta) production in the trans-Golgi network.
Proc Natl Acad Sci USA 2012;109:E2077–E2082.

Jang Hyun Choi, Alexander S. Banks, Jennifer L. Estall, Shingo Kajimura,Pontus Bostrom, Dina Laznik, Jorge L. Ruas, Michael J. Chalmers, Theodore M. Kamenecka, Matthias Bluher, Patrick R. Griffin, and Bruce M. Spiegelman
Obesity-linked phosphorylation of PPARγ by cdk5 is a direct target of the anti-diabetic PPARγ ligands
Nature. 2010 Jul 22; 466(7305): 451–456.
doi: 10.1038/nature09291PMCID: PMC2987584

Christian M, Kiskinis E, Debevec D, Leonardsson G, White R, Parker MG.
RIP140-targeted repression of gene expression in adipocytes.
Mol Cell Biol 25: 9383–9391, 2005.

Christian M, White R, Parker MG.
Metabolic regulation by the nuclear receptor corepressor RIP140.
Trends Endocrinol Metab 17: 243–250, 2006

Christina Priller, Thomas Bauer, Gerda Mitteregger, Bjarne Krebs, Hans A. Kretzschmar, and Jochen Herms
Synapse Formation and Function Is Modulated by the Amyloid Precursor Protein
JNEUROSCI.1450-06.2006 Progress in Neurobiology Volume 70, Issue 1, May 2003, Pages 1–32

Cimini A, Benedetti E, Cristiano L
Expression of peroxisome proliferator-activated receptors (PPARs) and retinoic acid receptors (RXRs) in rat cortical neurons.
Neuroscience. 2005;130(2):325–337.

Citron M, Oltersdorf T, Haass C, McConlogue L, Hung AY, Seubert P, Vigo-Pelfrey C, Lieberburg I, Selkoe DJ (December 1992).
Mutation of the beta-amyloid precursor protein in familial Alzheimer's disease increases beta-protein production.
Nature 360 (6405): 672–4.

Collino M, N.S. Patel, C. Thiemermann
PPARs as new therapeutic targets for the treatment of cerebral ischemia/reperfusion injury
Ther. Adv. Cardiovasc. Dis., 2 (2008), pp. 179–197

Cramer PE, Cirrito JR, Wesson DW, Lee CY, Karlo JC, Zinn AE, Casali BT, Restivo JL, Goebel WD, James MJ, Brunden KR, Wilson DA, Landreth GE.
ApoE-directed therapeutics rapidly clear β-amyloid and reverse deficits in AD mouse models.
Science. 2012 Mar 23;335(6075):1503-6. doi: 10.1126/science.1217697. Epub 2012 Feb 9.

Cruts M, H. Backhovens, S.Y. Wang, G. Van Gassen, J. Theuns, C.D. De Jonghe, A. Wehnert, J. De Voecht, G. De Winter, P. Cras,
Molecular genetic analysis of familial early-onset Alzheimer's disease linked to chromosome 14q24.3
Hum. Mol. Genet., 4 (1995), pp. 2363–2371

Cullingford TE, Bhakoo K, Peuchen S, Dolphin CT, Patel R, Clark JB.
Distribution of mRNAs encoding the peroxisome proliferator-activated receptor α, β, and γ and the retinoid X receptor α, β, and γ in rat central nervous system.
Journal of Neurochemistry. 1998;70(4):1366–1375.

Dahms SO, Hoefgen S, Roeser D, Schlott B, Gührs KH, Than ME (March 2010).
Structure and biochemical analysis of the heparin-induced E1 dimer of the amyloid precursor protein.
Proc Natl Acad Sci U S A 107 (12): 5381–6. doi:10.1073/pnas.0911326107

Dawson, G.R. Seabrook, H. Zheng, D.W. Smith, S. Graham, G. O'Dowd, B.J. Bowery, S. Boyce, M.E. Trumbauer, H.Y. Chen, L.H.T. Van der Ploeg, J.S. Sirinathsingji
Age-related cognitive deficits, impaired long-term potentiation and reduction in synaptic marker density in mice lacking the beta-amyloid precursor protein
Neuroscience, 90 (1999), pp. 1–13

Daynes RA, Jones DC.
Emerging roles of PPARs in inflammation and immunity.
Nat Rev Immunol. 2002 Oct;2(10):748-59.

de la Monte, S. C. Ng, and D. W. Hsu
Aberrant GAP-43 gene expression in Alzheimer's disease.
Am J Pathol. 1995 Oct; 147(4): 934–946. PMCID: PMC1871017

De Strooper B, Simons M, Multhaup G, Van Leuven F, Beyreuther K, Dotti CG (1995)
Production of intracellular amyloid-containing fragments in hippocampal neurons expressing human amyloid precursor protein and protection against amyloidogenesis by subtle amino acid substitutions in the rodent sequence.
EMBO J 14:4932–4938.

De Strooper, B. et al.
A presenilin-1-dependent gamma-secretase-like protease mediates release of Notch intracellular domain.
Nature 398, 518–522 (1999).

De Strooper, P. Saftig, K. Craessaerts, H. Vanderstichele, G. Guhde, W. Annaert, K. Von Figura, F. Van Leuven
Deficiency of presenilin-1 inhibits the normal cleavage of amyloid precursor protein
Nature, 391 (1998), pp. 387–390

Debevec D, Christian M, Morganstein D, Seth A, Herzog B, Parker M, White R.
Receptor interacting protein 140 regulates expression of uncoupling protein 1 in adipocytes through specific peroxisome proliferator activated receptor isoforms and estrogen-related receptor alpha.
Mol Endocrinol. 2007 Jul;21(7):1581-92. Epub 2007 Apr 24

Dehmer, M.T. Heneka, M. Sastre, J. Dichgans, J.B. Schulz
Protection by pioglitazone in the MPTP model of Parkinson's disease correlates with I kappa B alpha induction and block of NF kappa B and iNOS activation
J. Neurochem., 88 (2004), pp. 494–501

Desvergne B, Michalik L, Wahli W.
Be fit or be sick: peroxisome proliferator-activated receptors are down the road.
Molecular Endocrinology. 2004;18(6):1321–1332.
development and plasticity. *Trends Neurosci. 1997 Feb;20(2):84-91.*

DeWitt Perry G, Cohen M, Doller C, Silver
Astrocytes regulate microglial phagocytosis of senile plaque cores of Alzheimer's disease.
J. Exp Neurol. 1998 Feb;149(2):329-40.

Dominguez D, Tournoy J, Hartmann D, et al.
Phenotypic and biochemical analyses of BACE1- and BACE2-deficient mice.
J Biol Chem. 2005;280:30797–30806

Doster SK, Lozano AM, Aguayo AJ, Willard MB.
Expression of the growth-associated protein GAP-43 in adult rat retinal ganglion cells following axon injury.
Neuron. 1991 Apr;6(4):635-47.

Duce JA et al (2010).
Iron-Export Ferroxidase Activity of β- Amyloid Precursor Protein Is Inhibited by Zinc in Alzheimer's Disease.
Cell 142 (6): 857–67.

Duclot
Cognitive impairments in adult mice with constitutive inactivation of RIP140 gene expression Genes
Brain Behav., 11 (2012), pp. 69–78

Esler, W.T. Kimberly, B.L. Ostaszewski, W. Ye, T.S. Diehl, D.J. Selkoe, M.S. Wolfe
Activity-dependent isolation of the presenilin-gamma-secretase complex reveals nicastrin and a gamma substrate
Proc. Natl. Acad. Sci. U.S.A., 99 (2002), pp. 2720–2725

Esterbauer, H.,Oberkofler, H.,Krempler, F., andPatsch, W. (1999)
Human peroxisome proliferator activated receptor gamma coactivator 1 (PPARGC1) gene: cDNA sequence, genomic organization, chromosomal localization, and tissue expression.
Genomics 62, 98–102.

Farris W, Mansourian S, Chang Y, Lindsley L, Eckman EA, Frosch MP, Eckman CB, Tanzi RE, Selkoe DJ, Guenette S.
Insulin-degrading enzyme regulates the levels of insulin, amyloid beta-protein, and the beta-amyloid precursor protein intracellular domain in vivo.
Proc Natl Acad Sci U S A. 2003 Apr 1;100(7):4162-7. Epub 2003 Mar 12.

Farzan M, Schnitzler CE, Vasilieva N, Leung D, Choe H.
BACE2, a beta-secretase homolog, cleaves at the beta-site and within the amyloid-beta region of the amyloid-beta precursor protein.
Proc Natl Acad Sci USA. 2000;97:9712–9717.

Fawzia Al Rouqa, Eman El Etera,
PPAR-γ activator induces neuroprotection in hypercholesterolemic rats subjected to global cerebral ischemia/reperfusion injury: In vivo and in vitro inhibition of oxidative stress
DOI: 10.1016/j.exger.2013.12.008

Francesca Ruberti, Christian Barbato and Carlo Cogoni
Post-transcriptional regulation of amyloid precursor protein by microRNAs and RNA binding proteins
Commun Integr Biol. 2010 Nov-Dec; 3(6): 499–503. Published online Nov 1, 2010. doi: 10.4161/cib.3.6.13172 PMCID: PMC3038048

Fritah, et al.
levated expression of the metabolic regulator receptor-interacting protein 140 results in cardiac hypertrophy and impaired cardiac function
Cardiovasc. Res., 86 (2010), pp. 443–451

Gauthier A, Vassiliou G, Benoist F, McPherson R.
Adipocyte low density lipoprotein receptor-related protein gene expression and function is regulated by peroxisome proliferator-activated receptor gamma.
J Biol Chem. 2003 Apr 4;278(14):11945-53. Epub 2003 Jan 27.

Gezginci-Oktayoglu S1, Karatug A, Bolkent S.
The relation among NGF, EGF and insulin is important for triggering pancreatic β cell apoptosis.
Diabetes Metab Res Rev. 2012 Nov;28(8):654-62. doi: 10.1002/dmrr.2339.

Ghisletti S, Huang W, Ogawa S, Pascual G, Lin ME, Willson TM, Rosenfeld MG, Glass CK.
Parallel SUMOylation-dependent pathways mediate gene- and signal-specific transrepression by LXRs and PPARgamma.
Mol Cell. 2007 Jan 12;25(1):57-70.

Goedert M, Spillantini MG, Crowther RA.
Tau Proteins and Neurofibrillary Degeneration.
Brain Pathology (Zurich, Switzerland). 1991;1(4):279–86. doi:10.1111/j.1750-3639.1991.tb00671.x. PMID 1669718.

Goedert M, Wischik CM, Crowther RA, Walker JE, Klug A (June 1988).
Cloning and sequencing of the cDNA encoding a core protein of the paired helical filament of Alzheimer disease: identification as the microtubule-associated protein tau.
Proc. Natl. Acad. Sci. U.S.A. 85 (11): 4051–5. doi:10.1073/pnas.85.11.4051. PMC 280359. PMID 3131773.

Goldstein BJ.
Insulin resistance as the core defect in type 2 diabetes mellitus.
Am J Cardiol. 2002 Sep 5;90(5A):3G-10G.

Gong, B.,Chen, F.,Pan, Y.,Arrieta-Cruz, I.,Yoshida, Y., et al. (2010)
SCFFbx2-E3-ligase-mediated degradation of BACE1 attenuates Alzheimer's disease amyloidosis and improves synaptic function.
Aging Cell 9, 1018–1031.

Gotz, R.M. Nitsch Compartmentalized tau hyperphosphorylation and increased levels of kinases in transgenic mice *Neuroreport, 12 (2001), pp. 2007–2016*

Greenfield JP, Tsai J, Gouras GK, Hai B, Thinakaran G, Checler F, Sisodia SS, Greengard P, Xu H (1999)
Endoplasmic reticulum and trans-Golgi network generate distinct populations of Alzheimer beta-amyloid peptides.
Proc Natl Acad Sci USA 96:742–747.

Griffin, L.C. Stanley, C. Ling, L. White, V. MacLeod, L.J. Perrot, C.L. White, C. Araoz
Brain interleukin 1, and S-100 immunoreactivity are elevated in Down syndrome, and Alzheimer disease
Proc Natl Acad Sci USA, 86 (1989), pp. 7611–7615

Gupta P, Ho PC, Huq MD, Khan AA, Tsai NP, Wei LN. PKC
epsilon stimulated arginine methylation of RIP140 for its nuclear-cytoplasmic export in adipocyte differentiation.
PloS one 3: e2658, 2008.

Gupta, V.L. Dawson, T.M. Dawson
What causes cell death in Parkinson's disease?
Ann. Neurol., 64 (Suppl. 2) (2008), pp. S3–S15

H. Koike, S. Tomioka, H. Sorimachi, T.C. Saido, K. Maruyama, A. Okuyama, A. Fujisawa-Sehara, S. Ohno, K. Suzuki, S. Ishiura
Membrane-anchored metalloprotease MDC9 has an alpha-secretase activity responsible for processing the amyloid precursor protein
Biochem. J., 343 (1999), pp. 371–375

H. Tomimoto, I. Akiguchi, H. Wakita, S. Nakamura, J. Kimura
Ultrastructural localization of amyloid protein precursor in the normal and postischemic gerbil brain *Brain Res., 672 (1995), pp. 187–195*

Hallberg M, Morganstein DL, Kiskinis E, Shah K, Kralli A, Dilworth SM, White R, Parker MG, Christian M.
A functional interaction between RIP140 and PGC-1alpha regulates the expression of the lipid droplet protein CIDEA.
Mol Cell Biol 28: 6785–6795, 2008.

Haniu, P. Denis, Y. Young, E.A. Mendiaz, J. Fuller, J.O. Hui, B.D. Bennett, S. Kahn, S. Ross, T. Burgess, V. Katta, G. Rogers, R. Vassar, M. Citron
Characterization of Alzheimer's beta-secretase protein BACE. A pepsin family member with unusual properties

Harada A, Oguchi K, Okabe S, Kuno J, Terada S, Ohshima T, Sato-Yoshitake R, Takei Y, Noda T, Hirokawa N (June 1994).
Altered microtubule organization in small-calibre axons of mice lacking tau protein
Nature 369 (6480): 488–91. doi:10.1038/369488a0. PMID 8202139.

Hashiguchi, T. Saito, S.I. Hisanaga, T. Hashiguchi
Truncation of CDK5 activator p35 induces intensive phosphorylation of Ser202/Thr205 of human tau
J. Biol. Chem., 277 (2002), pp. 44525–44530

Heneka M. T. and Landreth G. E. (2007)
PPARs in the brain.
Biochim. Biophys. Acta 1771, 1031–1045.

Herzog B, Hallberg M, Seth A, Woods A, White R, Parker MG.
The nuclear receptor cofactor, receptor-interacting protein 140, is required for the regulation of hepatic lipid and glucose metabolism by liver X receptor.
Mol Endocrinol (Baltimore, Md) 21: 2687–2697, 2007

Herzog B, Hallberg M, Seth A, Woods A, White R, Parker MG.
The nuclear receptor cofactor, receptor-interacting protein 140, is required for the regulation of hepatic lipid and glucose metabolism by liver X receptor.
Mol Endocrinol (Baltimore, Md) 21: 2687–2697, 2007

Herzog
The nuclear receptor cofactor, receptor-interacting protein 140, is required for the regulation of hepatic lipid and glucose metabolism by liver X receptor *Mol. Endocrinol., 21 (2007), pp. 2687–2697*

Ho
NF-kappaB-mediated degradation of the coactivator RIP140 regulates inflammatory responses and contributes to endotoxin tolerance
Nat. Immunol., 13 (2012), pp. 379–386

Ho PC, Lin YW, Tsui YC, Gupta P, Wei LN.
A negative regulatory pathway of GLUT4 trafficking in adipocyte: new function of RIP140 in the cytoplasm via AS160.
Cell Metab 10: 516–523, 2009.

Ho L, Qin W, Pompl PN, Xiang Z, Wang J, Zhao Z, Peng Y, Cambareri G, Rocher A, Mobbs CV, Hof PR, Pasinetti GM.
Diet-induced insulin resistance promotes amyloidosis in a transgenic mouse model of Alzheimer's disease.
FASEB J. 2004 May;18(7):902-4. Epub 2004 Mar 19.

Hof PR, Bierer LM, Purohit DP
Neurofibrillary tangles correlate with dementia severity in Alzheimer's disease.
Arch Neurol 1995; 52: 81–88. 16. Curr Alzheimer Res. 2008 Dec;5(6):548-54.

Holsinger RM, McLean CA, Beyreuther K, Masters CL, Evin G.
Increased expression of the amyloid precursor beta-secretase in Alzheimer's disease.
Ann Neurol. 2002;51:783–786.

Claudie Hooper, Eirini Meimaridou, Mahvash Tavassoli, Gerry Melino, Simon Lovestone, and Richard Killick
p53 is upregulated in Alzheimer's disease and induces tau phosphorylation in HEK293a cells
Neurosci Lett. 2007 May 11; 418(1): 34–37.
doi: 10.1016/j.neulet.2007.03.026 PMCID: PMC1885960

Hoyer S, Lee SK, Löffler T, Schliebs R.
Inhibition of the neuronal insulin receptor. An in vivo model for sporadic Alzheimer disease? *Ann N Y Acad Sci. 2000;920:256-8.*

Hu E, Kim JB, Sarraf P, Spiegelman BM.
Inhibition of adipogenesis through MAP kinase-mediated phosphorylation of PPARgamma.
Science. 1996 Dec 20;274(5295):2100-3.

Hussain I, Powell D, Howlett DR
Identification of a Novel Aspartic Protease (Asp 2) as beta-Secretase.
Mol Cell Neurosci. 1999;14:419–427.

Hutton, F. Busfield, M. Wragg, R. Crook, J. Perez-Tur, R.F. Clark, G. Prihar, C. Talbot, H. Phillips, K. Wright, M. Baker, C. Lendon, K. Duff, A. Martinez, H. Houlden, A. Nichols, E. Karran, G. Roberts, P. Roques, M. Rossor, J.C. Venter, M.D. Adams, R.T. Cline, C.A. Phillips, A. Goate.
Complete analysis of the presenilin 1 gene in early onset Alzheimer's disease
NeuroReport, 7 (1996), pp. 801–805

Iqbal K, Alonso Adel C, Chen S, Chohan MO, El-Akkad E, Gong CX, Khatoon S, Li B, Liu F, Rahman A, Tanimukai H, Grundke-Iqbal I.
Tau Pathology in Alzheimer Disease and Other Tauopathies.
Biochimica Et Biophysica Acta. 2005;1739(2–3):198–210.

Irizarry MC, Locascio JJ, Hyman BT.
beta-site APP cleaving enzyme mRNA expression in APP transgenic mice: anatomical overlap with transgene expression and static levels with aging.
Am J Pathol. 2001;158:173–177

J.L. Madrigal, S. Kalinin, J.C. Richardson, D.L. Feinstein
Neuroprotective actions of noradrenaline: effects on glutathione synthesis and activation of peroxisome proliferator activated receptor delta
J. Neurochem., 103 (2007), pp. 2092–2101

Jonsson T, Atwal JK, Steinberg S, Snaedal J, Jonsson PV, Bjornsson S, Stefansson H, Sulem P, Gudbjartsson D, Maloney J, Hoyte K, Gustafson A, Liu Y, Lu Y, Bhangale T, Graham RR, Huttenlocher J, Bjornsdottir G, Andreassen OA, Jönsson EG, Palotie A, Behrens TW, Magnusson OT, Kong A, Thorsteinsdottir U, Watts RJ, Stefansson K (July 2012).
A mutation in APP protects against Alzheimer's disease and age-related cognitive decline
Nature 487 (7409): 96–9. doi:10.1038/nature11283. PMID 2280150

Jope RS, Yuskaitis CJ, Beurel E
Glycogen synthase kinase-3 (GSK3): inflammation, diseases, and therapeutics.
Neurochem Res. 2007 Apr-May; 32(4-5):577-95

Kaether C, Haass C, Steiner H (2006).
Assembly, trafficking and function of gamma-secretase.
Neurodegener Dis 3 (4–5): 275–83. doi:10.1159/000095267. PMID 17047368.

Kalinin, J.C. Richardson, D.L. Feinstein
A PPARdelta agonist reduces amyloid burden and brain inflammation in a transgenic mouse model of Alzheimer's disease *Curr. Alzheimer Res., 6 (2009), pp. 431–437 37.*

Kapadia R, Yi JH, Vemuganti R.
Mechanisms of anti-inflammatory and neuroprotective actions of PPAR-gamma agonists.
Front Biosci. 2008 Jan 1;13:1813-26.

Kariharan T, Nanayakkara G, Parameshwaran K, Bagasrawala I, Ahuja M, Abdel-Rahman E, Amin AT, Dhanasekaran M, Suppiramaniam V, Amin RH
Central activation of PPAR-gamma ameliorates diabetes induced cognitive dysfunction and improves BDNF expression.
Neurobiol Aging. 2015 Mar;36(3):1451-61. doi: 10.1016/j.neurobiolaging.2014.09.028. Epub 2014 Oct 2.

Katsouri, L.,Parr, C.,Bogdanovic, N.,Willem, M., and Sastre, M. (2011)
PPARgamma co-activator-1alpha (PGC-1alpha) reduces amyloid-beta generation through a PPARgamma-dependent mechanism.
J. Alzheimers Dis. 25, 151–162.

Kidd M.
Paired helical filaments in electron microscopy of Alzheimer's disease.
Nature 1963; 197: 192–193.

Kim, D.,Nguyen, M. D.,Dobbin, M. M.,Fischer, A.,Sananbenesi, F., et al. (2007)
SIRT1 deacetylase protects against neurodegeneration in models for Alzheimer's disease and amyotrophic lateral sclerosis.
EMBO J. 26, 3169–3179.

Kim, Jacob M. Basak, and David M. Holtzman
The Role of Apolipoprotein E in Alzheimer's Disease
Neuron. 2009 Aug 13; 63(3): 287–303.doi: 10.1016/j.neuron.2009.06.026

Kirazov, T. Loffler, R. Schliebs, V. Bigl
Glutamate-stimulated secretion of amyloid precursor protein from cortical rat brain slices
Neurochem. Int., 30 (1997), pp. 557–563

Kong GK, Adams JJ, Harris HH, Boas JF, Curtain CC, Galatis D, Masters CL, Barnham KJ, McKinstry WJ, Cappai R, Parker MW (March 2007).
Structural studies of the Alzheimer's amyloid precursor protein copper-binding domain reveal how it binds copper ions
J Mol Biol 367 (1): 148–61. doi:10.1016/j.jmb.2006.12.041. PMID 17239395.; 2007
PDB IDs 2FJZ, 2FK2, 2FKL. PDB 1RW6;

Koo EH, Squazzo SL.
Evidence that production and release of amyloid beta-protein involves the endocytic pathway.
J Biol Chem 1994;269:17386–17389.

Kurochkin IV, Goto S.
Alzheimer's beta-amyloid peptide specifically interacts with and is degraded by insulin degrading enzyme.
FEBS Lett. 1994 May 23;345(1):33-7.

L'Horset
RIP-140 interacts with multiple nuclear receptors by means of two distinct sites
Mol. Cell. Biol., 16 (1996), pp. 6029–6036

Laffitte BA, Repa JJ, Joseph SB, Wilpitz DC, Kast HR, Mangelsdorf DJ, Tontonoz P.
LXRs control lipid-inducible expression of the apolipoprotein E gene in macrophages and adipocytes.
Proc Natl Acad Sci U S A. 2001 Jan 16;98(2):507-12. Epub 2001 Jan 9.

Lammich, R. Postina, S. Gilbert, R. Pfeiffer, M. Jasionowski, C. Haass, F. Fahrenholz
Constitutive and regulated alpha-secretase cleavage of Alzheimer's amyloid precursor protein by a disintegrin metalloprotease
Proc. Natl. Acad. Sci. U.S.A., 96 (1999), pp. 3922–3927

Landreth GE1, Heneka MT.
Anti-inflammatory actions of peroxisome proliferator-activated receptor gamma agonists in Alzheimer's disease.
Neurobiol Aging. 2001 Nov-Dec;22(6):937-44.

Leibson CL1, Rocca WA, Hanson VA, Cha R, Kokmen E, O'Brien PC, Palumbo PJ.
Risk of dementia among persons with diabetes mellitus: a population-based cohort study.
Am J Epidemiol. 1997 Feb 15;145(4):301-8.

Leonardsson G, Steel JH, Christian M, Pocock V, Milligan S, Bell J, So PW, Medina-Gomez G, Vidal-Puig A, White R, Parker MG.
Nuclear receptor corepressor RIP140 regulates fat accumulation.
Proc Natl Acad Sci USA 101: 8437–8442, 2004.

Leonardsson, et al.
Nuclear receptor corepressor RIP140 regulates fat accumulation
Proc. Natl. Acad. Sci. U.S.A., 101 (2004), pp. 8437–8442

Liang K, Yang L, Yin C, Xiao Z, Zhang J, Liu Y, Huang J.
Estrogen stimulates degradation of beta-amyloid peptide by up-regulating neprilysin.
J Biol Chem. 2010 Jan 8;285(2):935-42. doi: 10.1074/jbc.M109.051664. Epub 2009 Nov 6.

Lin X, Koelsch G, Wu S, Downs D, Dashti A, Tang J.
Human aspartic protease memapsin 2 cleaves the beta-secretase site of beta-amyloid precursor protein.
Proc Natl Acad Sci U S A. 2000;97:1456–1460.

Liu, K. Iqbal, I. Grundke-Iqbal, C.X. Gong
Involvement of aberrant glycosylation in phosphorylation of tau by cdk5 and GSK-3beta
FEBS Lett., 530 (2002), pp. 209–214

Liu J, Wang H, Zuo Y, Farmer SR.
Functional interaction between peroxisome proliferator-activated receptor gamma and beta-catenin.
Mol Cell Biol. 2006 Aug;26(15):5827-37.

Lopez-Perez E1, Zhang Y, Frank SJ, Creemers J, Seidah N, Checler F.
Constitutive alpha-secretase cleavage of the beta-amyloid precursor protein in the furin-deficient LoVo cell line: involvement of the pro-hormone convertase 7 and the disintegrin metalloprotease ADAM10.
J Neurochem. 2001 Mar;76(5):1532-9.

Lu DC, Soriano S, Bredesen DE, Koo EH.
Caspase cleavage of the amyloid precursor protein modulates amyloid beta-protein toxicity.
J Neurochem. 2003
Nov;87(3):733-41.

Luchsinger JA, Tang MX, Stern Y, Shea S, Mayeux R.
Diabetes mellitus and risk of Alzheimer's disease and dementia with stroke in a multiethnic cohort.
Am J Epidemiol. 2001 Oct 1;154(7):635-41.

Lund, R. McKenna, D.B. Evans, S.K. Sharma, W.R. Mathews
Characterization of the in vitro phosphorylation of human tau by tau protein kinase II (cdk5/p20) using mass spectrometry
J. Neurochem., 76 (2001), pp. 1221–1232

Luo Y, Bolon B, Kahn S
Mice deficient in BACE1, the Alzheimer's beta-secretase, have normal phenotype and abolished beta-amyloid generation.
Nat Neurosci. 2001;4:231–232.

Madani R, Poirier R, Wolfer DP, Welzl H, Groscurth P, Lipp HP, Lu B, El Mouedden M, Mercken M, Nitsch RM, Mohajeri MH.
Lack of neprilysin suffices to generate murine amyloid-like deposits in the brain and behavioral deficit in vivo.
J Neurosci Res. 2006 Dec;84(8):1871-8.

Mahmoud Kiaei, , Khatuna Kipiani, Junyu Chen, Noel Y. Calingasan, M. Flint Beal
Peroxisome proliferator-activated receptor-gamma agonist extends survival in transgenic mouse model of amyotrophic lateral sclerosis
10.1016/j.expneurol.2004.10.007

Marambaud, P.,Zhao, H., andDavies, P. (2005)
Resveratrol promotes clearance of Alzheimer's disease amyloid-beta peptides.
J. Biol. Chem. 280, 37377–37382.

Marcinkiewicz M, Seidah NG.
Coordinated expression of beta-amyloid precursor protein and the putative beta-secretase BACE and alpha-secretase ADAM10 in mouse and human brain.
J Neurochem. 2000;75:2133

Matsui T, Ingelsson M, Fukumoto H, Ramasamy K, Kowa H, Frosch MP, Irizarry MC, Hyman BT (August 2007).
Origins of amyloid-beta.
BMC Genomics 14 (1): 290. doi:10.1186/1471-2164-14-290. PMID 23627794.

Matsuyama S, Teraoka R, Mori H, Tomiyama T. (2007).
Inverse correlation between amyloid precursor protein and synaptic plasticity in transgenic mice.
Neuroreport 18(10):1083-7. PMID 17558301

May PC, Mergott DJ, Cocke PJ, Monk SA, Boggs LN, Sanchez-Felix MV, Audia JE, Calligaro DO, Citron M, Dean RA, Lowe SL, Daugherty LL, Gonzales CR, Nakano M, Willis BA, Martenyi F:
Preclinical and Phase I clinical characterization of LY2886721, a BACE inhibitor in Phase II development Alzheimer's disease.
The 11th International Conference On Alzheimer's & Parkinson's Diseases, Florence, Italy, March 6-10, 2013.

McGeer PL, Schulzer M, McGeer EG
Arthritis and anti-inflammatory agents as possible protective factors for Alzheimer's disease: a review of 17 epidemiologic studies.
Neurology. 1996 Aug; 47(2):425-32.

McTigue D. M., Tripathi R., Wei P. and Lash A. T. (2007)
The PPAR gamma agonist Pioglitazone improves anatomical and locomotor recovery after rodent spinal cord injury.
Exp. Neurol. 205, 396–406.

Michel, M. Mercken, M. Murayama, K. Noguchi, K. Ishiguro, K. Imahori, A. Takashima
Characterization of tau phosphorylation in glycogen synthase kinase-3beta and cyclin dependent kinase-5 activator (p25) transfected cells
Biochim. *Biophys. Acta, 1380 (1998), pp. 177–182*

Mitko Dimitrov, Jean-René Alattia, Thomas Lemmin, Rajwinder Lehal, Andrzej Fligier, Jemila Houacine, Ishrut Hussain, Freddy Radtke, Matteo Dal Peraro, Dirk Beher & Patrick C. Fraering
Alzheimer's disease mutations in APP but not γ-secretase modulators affect epsilon-cleavage-dependent AICD production
Nature Communications 4, Article number: 2246 doi:10.1038/ncomms3246 Received 13 December 2012 Accepted 03 July 2013 Published 02 August 2013

Moller, D. E. & Greene, D. A.
Peroxisome proliferator-activated receptor (PPAR) γ agonists for diabetes.
Adv. Prot. Chem. (Drug Discovery) 56, 181-212 (2001)

Moreno S, Farioli-vecchioli S, Cerù MP.
Immunolocalization of peroxisome proliferator-activated receptors and retinoid X receptors in the adult rat CNS.
Neuroscience. 2004;123(1):131–145.

Morrison JH, Hof PR. Life and death of neurons in the aging brain. *Science 1997; 278: 412–419.*

Mostaqul Huq MD, Gupta P, Tsai NP, White R, Parker MG, Wei LN.
Suppression of receptor interacting protein 140 repressive activity by protein arginine methylation.
EMBO J 25: 5094–5104, 2006.

Mostaqul Huq MD, Gupta P, Wei LN.
The metabolic coregulator RIP140: an update Post-translational modifications of nuclear co-repressor RIP140: a therapeutic target for metabolic diseases.
Curr Med Chem 15: 386–392, 2008

Motonaga K, Itoh M, Becker LE, Goto Y, Takashima S.
Elevated expression of beta-site amyloid precursor protein cleaving enzyme 2 in brains of patients with Down syndrome.
Neurosci Lett. 2002;326:64–66.

Mucke, E. Masliah, W.B. Johnson, M.D. Ruppe, M. Alford, E.M. Rockenstein, S. Forss-Petter, M. Pietropaolo, M. Mallory, C.R. Abraham
Synaptotrophic effects of human amyloid beta protein precursors in the cortex of transgenic mice
Brain Res., 666 (1994), pp. 151–167

Mukai F, Ishiguro K, Sano Y, Fujita SC.
Alternative splicing isoform of tau protein kinase I/glycogen synthase kinase 3beta.
J. Neurochem. 2002;81:1073–1083.

Murphy M, Hinman A, Levine AJ.
Wild-type p53 negatively regulates the expression of a microtubule-associated protein.
Genes Dev. 1996 Dec 1;10(23):2971-80.

Murzin, A.M. Lesk, C. Chothia
β-Trefoil fold. Patterns of structure and sequence in the Kunitz inhibitors interleukins-1β and 1α and fibroblast growth factors
J Med Biol, 223 (1992), pp. 531–543

Nagayach A, Patro N, Patro I.
Astrocytic and microglial response in experimentally induced diabetic rat brain.
Metab
Brain Dis. 2014 Sep;29(3):747-61. doi: 10.1007/s11011-014-9562-z. Epub 2014 May 16

Nagamine M, Okumura T, Tanno S, Sawamukai M, Motomura W, Takahashi N Kohgo Y.
PPAR gamma ligand-induced apoptosis through a p53-dependent mechanism in human gastric cancer cells.
Cancer Sci. 2003 Apr;94(4):338-43.

Nagele RG, Wegiel J, Venkataraman V, Imaki H, Wang KC, Wegiel J. J
Contribution of glial cells to the development of amyloid plaques in Alzheimer's disease.
J. Neurobiol Aging. 2004 May-Jun;25(5):663-74.

Nautiyal J, Steel JH, Rosell MM, Nikolopoulou E, Lee K, Demayo FJ, White R, Richards JS, Parker MG.
The nuclear receptor cofactor receptor-interacting protein 140 is a positive regulator of amphiregulin expression and cumulus cell-oocyte complex expansion in the mouse ovary.
Endocrinology 151: 2923–2932, 2010.

Nautiyal J, Steel JH, Rosell MM, Nikolopoulou E, Lee K, Demayo FJ, White R, Richards JS, Parker MG.
The nuclear receptor cofactor receptor-interacting protein 140 is a positive regulator of amphiregulin expression and cumulus cell-oocyte complex expansion in the mouse ovary.
Endocrinology 151: 2923–2932, 2010.

Nautiyal, et al.
The transcriptional co-factor RIP140 regulates mammary gland development by promoting the generation of key mitogenic signals
Development, 140 (2013), pp. 1079–1089

Nemoto S, Fergusson MM, Finkel T (Apr 2005).
SIRT1 functionally interacts with the metabolic regulator and transcriptional coactivator PGC-1 alpha
J Biol Chem. 280 (16): 16456–60

Nesto, R. W. et al. Thiazolidinedione use, fluid retention, and congestive heart failure: *a consensus statement from the American Heart Association and American Diabetes Association.*
Diabetes Care 27, 256–263 (2004)

Nichol D, Christian M, Steel JH, White R, Parker MG.
RIP140 expression is stimulated by estrogen-related receptor alpha during adipogenesis.
J Biol Chem. 2006 Oct 27;281(43):32140-7. Epub 2006 Aug 21.

Nitsch, A. Deng, R.J. Wurtman, J.H. Growdon
Metabotropic glutamate receptor subtype mGluR1α stimulates the secretion of the amyloid β-protein precursor ectodomain
J. Neurochem., 69 (1997), pp. 704–712

Noble W, Olm V, Takata K, Casey E, Mary O, Meyerson J, Gaynor K, LaFrancois J, Wang L, Kondo T, Davies P, Burns M, Veeranna, Nixon R, Dickson D, Matsuoka Y, Ahlijanian M, Lau LF, Duff K.
Cdk5 is a key factor in tau aggregation and tangle formation in vivo.
Neuron. 2003 May 22;38(4):555-65.

O'Brien RJ, Wong PC.
Amyloid precursor protein processing and Alzheimer's disease.
Annu Rev Neurosci. 2011;34:185-204. doi: 10.1146/annurev-neuro-061010-113613. Review.

Ogawa S, Lozach J, Benner C, Pascual G, Tangirala RK, Westin S, Hoffmann A, Subramaniam S, David M, Rosenfeld MG, Glass CK.
Molecular determinants of crosstalk between nuclear receptors and toll-like receptors.
Cell. 2005 Sep 9;122(5):707-21.

Orejana L, Barros-Miñones L1, Jordan J2, Cedazo-Minguez A, Tordera RM1, Aguirre N, Puerta E.
Sildenafil Decreases BACE1 and Cathepsin B Levels and Reduces APP Amyloidogenic Processing in the SAMP8 Mouse.
J Gerontol A Biol Sci Med Sci. 2015 Jun;70(6):675-85. doi: 10.1093/gerona/glu106. Epub 2014 Jul 25.

Park S. W., Yi J. H., Miranpuri G., Satriotomo I., Bowen K., Resnick D. K. and Vemuganti R. (2007)
Thiazolidinedione class of peroxisome proliferator-activated receptor gamma agonists prevents neuronal damage, motor dysfunction, myelin loss, neuropathic pain, and inflammation after spinal cord injury in adult rats.
J. Pharmacol. Exp. Ther. 320, 1002–1012.

Parr C, Carzaniga R, Gentleman SM, Van Leuven F, Walter J, Sastre M.
Glycogen synthase kinase 3 inhibition promotes lysosomal biogenesis and autophagic degradation of the amyloid-β precursor protein.
Mol Cell Biol. 2012 Nov;32(21):4410-8. doi: 10.1128/MCB.00930-12. Epub 2012 Aug 27.

Patrick, L. Zukerberg, M. Nikolic, S. de la Monte, P. Dikkes, L.H. Tsai
Conversion of p35 to p25 deregulates Cdk5 activity and promotes neurodegeneration
Nature, 402 (1999), pp. 615–622

Peila R, Rodriguez BL, Launer LJ; Honolulu-Asia Aging Study.
Type 2 diabetes, APOE gene, and the risk for dementia and related pathologies: The Honolulu-Asia Aging Study.
Diabetes. 2002 Apr;51(4):1256-62.

Perez, H. Zheng, L.H.T. Van der Ploeg, E.H. Koo
The β-amyloid precursor protein of Alzheimer's disease enhances neuron viability and modulates neuronal polarity
J. Neurosci., 17 (1997), pp. 9407–9414

Phinney, M.E. Calhoun, D.P. Wolfer, H.P. Lipp, H. Zheng, M. Jucker
No hippocampal neuron or synaptic bouton loss in learning-impaired aged β-amyloid precursor protein-null mice
Neuroscience, 90 (1999), pp. 1207–1216

Puigserver P, Spiegelman BM.
Peroxisome proliferator-activated receptor-gamma coactivator 1 alpha (PGC-1 alpha): transcriptional coactivator and metabolic regulator.
Endocr Rev 24: 78–90, 2003.

Puigserver, P. (2005)
Tissue-specific regulation of metabolic pathways through the transcriptional coactivator PGC1-alpha.
Int. J. Obes. (Lond.) 29, S5–S9.

Puigserver, P.,Wu, Z.,Park, C. W.,Graves, R.,Wright, M (1998)
A cold-inducible coactivator of nuclear receptors linked to adaptive thermogenesis.
Cell 92, 829–839.

Qin, W.,Haroutunian, V.,Katsel, P.,Cardozo, C. P.,Ho, L., et al. (2009)
PGC-1alpha expression decreases in the Alzheimer disease brain as a function of dementia.
Arch. Neurol. 66, 352–361.

Quinn, B. Crook, M.E. Hows, M. Vidgeon-Hart, H. Chapman, N. Upton, A.D. Medhurst, D.J. Virley
The PPARgamma agonist pioglitazone is effective in the MPTP mouse model of Parkinson's disease through inhibition of monoamine oxidase B Br.
J. Pharmacol., 154 (2008), pp. 226–233

R. White, et al.
The nuclear receptor co-repressor nrip1 (RIP140) is essential for female fertility
Nat. Med., 6 (2000), pp. 1368–1374

Rai Ajit K. Srivastava, Neelam Srivastava, Maurizio Averna, Renee C. Lin, Kenneth S. Korach, Dennis B. Lubahn, and Gustav Schonfeld
Estrogen Up-regulates Apolipoprotein E (ApoE) Gene Expression by Increasing ApoE mRNA in the Translating Pool via the Estrogen Receptor α-Mediated Pathway
J. Biol. Chem. 1997 272: 33360-33366. doi:10.1074/jbc.272.52.33360

Rekart JL, Meiri K, Routtenberg A.
Hippocampal-dependent memory is impaired in heterozygous GAP-43 knockout mice.
Hippocampus. 2005;15(1):1-7.

Ridder DA, Schwaninger M.
In search of the neuroprotective mechanism of thiazolidinediones in Parkinson's disease.
2012 Dec;238(2):133-7. doi: 10.1016/j.expneurol.2012.08.012. Epub 2012 Aug 19.

Rodgers, J. T.,Lerin, C.,Gerhart-Hines, Z., and Puigserver, P. (2008)
Metabolic adaptations through the PGC-1 alpha and SIRT1 pathways.
FEBS Lett. 582, 46–53.

Rodgers, J. T.,Lerin, C.,Haas, W.,Gygi, S. P.,Spiegelman, B. M., et al. (2005)
Nutrient control of glucose homeostasis through a complex of PGC-1alpha and SIRT1.
Nature 434, 113–118.

Rodionova E, Conzelmann M, Maraskovsky E, Hess M, Kirsch M, Giese T, Ho AD, Zöller M, Dreger P, Luft T
GSK-3 mediates differentiation and activation of proinflammatory dendritic cells.
Blood. 2007 Feb 15; 109(4):1584-92.

Rossjohn J, Cappai R, Feil SC, Henry A, McKinstry WJ, Galatis D, Hesse L, Multhaup G, Beyreuther K, Masters CL, Parker MW (April 1999).
Crystal structure of the N-terminal, growth factor-like domain of Alzheimer amyloid precursor protein.
Nat Struct Biol 6 (4): 327–31. doi:10.1038/7562. PMID 10201399.

Ryder, J., Su, Y., Liu, F., Li, B., Zhou, Y. & Ni, B. 2003.
Divergent roles of GSK3 and CDK5 in APP processing.
Biochem Biophys Res Commun, 312, 922-9. 7.

Rytinki MM, Palvimo JJ.
SUMOylation attenuates the function of PGC-1alpha.
J Biol Chem 284: 26184–26193, 2009.

Sarkar IN, Tharp G (April 2013).
Proteins in normal cerebrospinal fluid not found in serum.
CLAUSEN J.

Satpute-Krishnan, P.; Degiorgis, J. A.; Conley, M. P.; Jang, M.; Bearer, E. L. (2006).
A peptide zipcode sufficient for anterograde transport within amyloid precursor protein.
Proceedings of the National Academy of Sciences 103 (44): 16532. 70 (1): 1–32. doi:10.1016/S0301-0082(03)00089-3. PMID 12927332.

Saura, T. Tomita, F. Davenport, C.L. Harris, T. Iwatsubo, G. Thinakaran
Evidence that intra-molecular associations between presenilin domains are obligatory for endoproteolytic processing
J. Biol. Chem., 274 (1999), pp. 13818–13823

Schaffer B, Wiedau-Pazos M, Geschwind DH.
Gene structure and alternative splicing of glycogen synthase kinase 3 beta (GSK-3beta) in neural and non-neural tissues.
Gene. 2003;302:73–81.

Schlondorff, J.D. Becherer, C.P. Blobel
Intracellular maturation and localization of the tumour necrosis factor alpha convertase (TACE)
Biochem. J., 347 (2000), pp. 131–138

Schnegg, M.E. Robbins
Neuroprotective mechanisms of PPARdelta: modulation of oxidative stress and inflammatory processes
PPAR. Res. (2011), p. 373560

Schubert, R. Prior, A. Weidemann, H. Dircksen, G. Multhaup, C.L. Masters, K. Beyreuther
Localization of Alzheimer beta A4 amyloid precursor protein at central and peripheral synaptic sites
Brain Res., 563 (1991), pp. 184–194

Seabrook, D.W. Smith, B.J. Bowery, A. Easter, T. Reynolds, S.M. Fitzjohn, R.A. Morton, H. Zheng, G.R. Dawson, D.J.S. Sirinathsinghji, C.H. Davies, G.L. Collingridge, R.G. Hill
Mechanisms contributing to the deficits in hippocampal synaptic plasticity in mice lacking amyloid precursor protein
Neuropharmacology, 38 (1999), pp. 349–359

Seidah, M. Chrétien
Proprotein and prohormone convertases: a family of subtilases generating diverse bioactive polypeptides
Brain Res., 848 (1999), pp. 45–62

Selkoe D, Kopan R (2003).
Notch and Presenilin: regulated intramembrane proteolysis links development and degeneration.
Annu. Rev. Neurosci. 26 (1): 565–97. doi:10.1146/annurev.neuro.26.041002.131334. PMID 12730322.

Seth
The transcriptional corepressor RIP140 regulates oxidative metabolism in skeletal muscle
Cell Metab., 6 (2007), pp. 236–245

Shigematsu K1, McGeer PL, McGeer EG.
Localization of amyloid precursor protein in selective postsynaptic densities of rat cortical neurons.
Brain Res. 1992 Oct 2;592(1-2):353-7.

Shirotani K, Edbauer D, Prokop S, Haass C, Steiner H.
Identification of distinct gamma-secretase complexes with different APH-1 variants
J Biol Chem 279 (40): 41340–5. doi:10.1074/jbc.M405768200. PMID 15286082.

Sinha S, Anderson JP, Barbour R
Purification and cloning of amyloid precursor protein beta-secretase from human brain.
Nature. 1999;402:537–540.

Sisodia Koo EH, Squazzo SL.
Beta-amyloid precursor protein cleavage by a membrane-bound protease.
Proc Natl Acad Sci U S A. Jul 1, 1992; 89(13): 6075–6079. PMCID: PMC49440

Sisodia
Beta-amyloid precursor protein cleavage by a membrane-bound protease *Proc. Natl. Acad. Sci. U.S.A., 89 (1992), pp. 6075–6079*

St-Pierre, J.,Drori, S.,Uldry, M.,Silvaggi, J. M.,Rhee, J., et al. (2006)
Suppression of reactive oxygen species and neurodegeneration by the PGC-1 transcriptional coactivators.
Cell 127, 397–408.

Steen E, Terry BM, Rivera EJ, Cannon JL, Neely TR, Tavares R, Xu XJ, Wands JR, de la Monte SM.
Impaired insulin and insulin-like growth factor expression and signaling mechanisms in Alzheimer's disease--is this type 3 diabetes?
J Alzheimers Dis. 2005 Feb;7(1):63-80.

Stern SA, Kohtz AS, Pollonini G, Alberini CM.
Enhancement of memories by systemic administration of insulin-like growth factor II.
Neuropsychopharmacology. 2014 Aug;39(9):2179-90. doi: 10.1038/npp.2014.69. Epub 2014 Mar 19.

Stone JR, Okonkwo DO, Singleton RH, Mutlu LK, Helm GA, Povlishock JT
Caspase-3-mediated cleavage of amyloid precursor protein and formation of amyloid Beta peptide in traumatic axonal injury.
J Neurotrauma. 2002 May;19(5):601-14.

Straus DS, Glass CK.
Anti-inflammatory actions of PPAR ligands: new insights on cellular and molecular mechanisms.
Trends in Immunology. 2007;28(12):551–558.

Ichiro Takada, Alexander P. Kouzmenko & Shigeaki Kat
Wnt and PPARgamma signaling in osteoblastogenesis and adipogenesis
Nature Reviews Rheumatology 5, 442-447 (August 2009) | doi:10.1038/nrrheum.2009.137

Tanaka, S. Shiojiri, Y. Takahashi, N. Kitaguchi, H. Ito, M. Kameyama, J. Kimura, K. Ueda
Tissue-specific expression of three types of beta-protein precursor mRNA: enhancement of protease inhibitor-harboring types in Alzheimer's disease brain
Biochem. Biophys. Res. Commun., 165 (1989), pp. 1406–1414

Tazawa H, Osman W, Shoji Y, Treuter E, Gustafsson JA, Zilliacus J.
Regulation of subnuclear localization is associated with a mechanism for nuclear receptor corepression by RIP140.
Mol Cell Biol 23: 4187–4198, 2003.

Teich AF1, Patel M, Arancio O.
A reliable way to detect endogenous murine β-amyloid.
PLoS One. 2013;8(2):e55647. doi: 10.1371/journal.pone.0055647. Epub 2013 Feb 1.

Thinakaran, D.R. Borchelt, M.K. Lee, H.H. Slunt, L. Spitzer, G. Kim, T. Ratovitsky, F. Davenport, C. Nordstedt, M. Seeger, J. Hardy, A.I. Levey, S.E. Gandy, N.A. Jenkins, N.G. Copeland, D.L. Price, S.S. Sisodia
Endoproteolysis of presenilin 1 and accumulation of processed derivatives in vivo
Neuron, 17 (1996), pp. 181–190

Tritos, N. A.,Mastaitis, J. W.,Kokkotou, E. G.,Puigserver, P.,Spiegelman, B. M., (2003)
Characterization of the peroxisome proliferator activated receptor coactivator 1 alpha (PGC 1alpha) expression in the murine brain.
Brain Res. 961, 255–260.

Tsai NP, Lin YL, Wei LN.
MicroRNA mir-346 targets the 5′-untranslated region of receptor-interacting protein 140 (RIP140) mRNA and up-regulates its protein expression.
Biochem J 424: 411–418, 2009.

Tsunemi, T. and La Spada, A. R. (2012)
PGC-1alpha at the intersection of bioenergetics regulation and neuron function: from Huntington's disease to Parkinson's disease and beyond.
Prog. Neurobiol. 97, 142–151.

Tullet JM, Pocock V, Steel JH, White R, Milligan S, Parker MG.
Multiple signaling defects in the absence of RIP140 impair both cumulus expansion and follicle rupture.
Endocrinology 146: 4127–4137, 2005.

Uemura, K. et al.
Characterization of sequential N-cadherin cleavage by ADAM10 and PS1. *Neurosci. Lett. 402, 278–283 (2006).*

van de Ree MA, Huisman MV, Princen HM, Meinders AE, Kluft C; DALI-Study Group.
Strong decrease of high sensitivity C-reactive protein with high-dose atorvastatin in patients with type 2 diabetes mellitus.
Atherosclerosis. 2003 Jan;166(1):129-35.

Vassar R, Bennett BD, Babu-Khan S, et al.
Beta-secretase cleavage of Alzheimer's amyloid precursor protein by the transmembrane aspartic protease BACE.
Science. 1999;286:735–741.

Vassilios Beglopoulos, Xiaoyan Sun, Carlos A. Saura, Cynthia A. Lemere, Richard D. Kim and Jie Shen
Molecular Basis of Cell and Developmental Biology: Reduced β-amyloid production and increased inflammatory responses in presenilin conditional knockout mice *J. Biol. Chem. published online September 1, 2004 Exp Neurol.*

Vitkovic, J. Bockaert, C. Jacque
Inflammatory cytokines: neuromodulators in normal brain?
J Neurochem, 74 (2000), pp. 457–471

Wagstaff AJ, Goa KL.
Rosiglitazone: a review of its use in the management of type 2 diabetes mellitus.
Drugs. 2002;62(12):1805-37.

Wang Y, Ha Y (August 2004).
The X-ray structure of an antiparallel dimer of the human amyloid precursor protein E2 domain.
Mol. Cell 15 (3): 343–53. doi

Wareski, P.,Vaarmann, A.,Choubey, V.,Safiulina, D.,Liiv, J., (2009)
PGC-1{alpha} and PGC-1{beta} regulate mitochondrial density in neurons.
J. Biol. Chem. 284, 21379–21385.

Watson GS, Cholerton BA, Reger MA, Baker LD, Plymate SR, Asthana S, Fishel MA, Kulstad JJ, Green PS, Cook DG, Kahn SE, Keeling ML, Craft S. Preserved cognition in patients with early Alzheimer disease and amnestic mild cognitive impairment during treatment with rosiglitazone: a preliminary study.

Wendy Noble, Vicki Olm, Kazuyuki Takata, Evelyn Casey, O Mary, Jordana Meyerson, Kate Gaynor, John LaFrancois, Lili Wang, Takayuki Kondo, Peter Davies, Mark Burns, Veeranna, Ralph Nixon, Dennis Dickson, Yasuji Matsuoka1, Michael Ahlijanian, Lit-Fui Lau, Karen Duff
Cdk5 Is a Key Factor in Tau Aggregation and Tangle Formation In Vivo
Neuron Volume 38, Issue 4, 22 May 2003, Pages 555–565

White R, Leonardsson G, Rosewell I, Ann Jacobs M, Milligan S, Parker M.
The nuclear receptor co-repressor nrip1 (RIP140) is essential for female fertility.
Nat Med 6: 1368–1374, 2000.

Willson, T. M., Brown, P. J., Sternbach, D. D. & Henke, B. R.
The PPARs: from orphan receptors to drug discovery.
*J. Med. Chem. **43**, 527-550 (2000).*

Wisniewski HM, Narang HK, Terry RD.
Neurofibrillary tangles of paired helical filaments.
J Neurol Sci 1976; 27: 173–181.

Wisniewski HM, Wegiel
Spatial relationships between astrocytes and classical plaque components.
Neurobiol Aging. 1991 Sep-Oct;12(5):593-600.

Wolfe, J. De Los Angeles, D.D. Miller, W. Xia, D.J. Selkoe
Are presenilins intramembrane-cleaving proteases? Implications for the molecular mechanism of Alzheimer's disease
Biochemistry, 38 (1999), pp. 11223–11230

Yamanaka M, Ishikawa T, Griep A, Axt D, Kummer MP, Heneka MT.
PPARγ/RXRα-induced and CD36-mediated microglial amyloid-β phagocytosis results in cognitive improvement in amyloid precursor protein/presenilin 1 mice.
J Neurosci. 2012 Nov 28;32(48):17321-31. doi: 10.1523/JNEUROSCI.1569-12.2012.

Yan R, Bienkowski MJ, Shuck ME
Membrane-anchored aspartyl protease with Alzheimer's disease beta-secretase activity.
Nature. 1999;402:533–537.

Yan R, Munzner JB, Shuck ME, Bienkowski MJ.
BACE2 functions as an alternative alpha-secretase in cells.
J Biol Chem. 2001;276:34019–34027

Yan Y, Wang C.
Protection mechanisms against Abeta42 aggregation.
Proc Soc Exp Biol Med. 1961 May;107:170-2.

Yu, M. Nishimura, S. Arawaka, D. Levitan, L. Zhang, A. Tandon, Y.Q. Song, E. Rogaeva, F. Chen, T. Kawarai, A. Supala, L. Levesque, H. Yu, D.S. Yang, E. Holmes P. Milman, Y. Liang, D.M. Zhang, D.H. Xu, C. Sato, E. Rogaev, M. Smith, C. Janus, Y. Zhang, R. Aebersold, L.S. Farrer, S. Sorbi, A. Bruni, P. Fraser, P. St George-Hyslop,
Nicastrin modulates presenilin-mediated notch/glp-1 signal transduction and betaAPP processing
Nature, 407 (2000), pp. 48–54

Zhao WQ, Chen H, Quon MJ, Alkon DL.
Insulin and the insulin receptor in experimental models of learning and memory. *Eur J Pharmacol. 2004 Apr 19;490(1-3):71-81.*

Zeng H, Huang P, Wang X, Wu J, Wu M, Huang J.
Zhang, P. Oliver, J.R. Lancaster, P.O. Schwarzenberger, M.S. Joshi, J. Cork, J.K. Kolls
Reactive oxygen species mediate tumor necrosis factor alpha-converting, enzyme-dependent ectodomain shedding induced by phorbol myristate acetate *FASEB J., 15 (2001), pp. 303–305*

Zheng H, Koo EH (2006).
Expression of APP pathway mRNAs and proteins in Alzheimer's disease
Brain Res. 1161: 116–23. doi:10.1016/j.brainres.2007.05.050. PMID 17586478.

Zheng H, Koo EH (2006).
The amyloid precursor protein: beyond amyloid.
Mol Neurodegener 1 (1): 5. doi:10.1186/1750-1326-1-5. PMC 1538601. PMID 16930452.

Zeng H, Huang P1, Wang X1, Wu J1, Wu M1, Huang J
Galangin-induced down-regulation of BACE1 by epigenetic mechanisms in SH-SY5Y cells.
Neuroscience. 2015 May 21;294:172-81. doi: 10.1016/j.neuroscience.2015.02.054. Epub 2015 Mar 14.

Zhu
A MicroRNA gene is hosted in an intron of a schizophrenia-susceptibility gene
Schizophr. Res., 109 (2009), pp. 86–89

Zschiedrich I, Hardeland U, Krones-Herzig A, Berriel Diaz M, Vegiopoulos A, Muggenburg J, Sombroek D, Hofmann TG, Zawatzky R, Yu X, Gretz N, Christian M, White R, Parker MG, Herzig S.
Coactivator function of RIP140 for NFkappaB/RelA-dependent cytokine gene expression.
Blood 112: 264–276, 2008.

Zschiedrich I, Hardeland U, Krones-Herzig A, Berriel Diaz M, Vegiopoulos A, Muggenburg J, Sombroek D, Hofmann TG, Zawatzky R, Yu X, Gretz N, Christian M, White R, Parker MG, Herzig S.
Coactivator function of RIP140 for NFkappaB/RelA-dependent cytokine gene expression.
Blood 112: 264–276, 2008.

Zschiedrich.
Coactivator function of RIP140 for NFkappaB/RelA-dependent cytokine gene expression
Blood, 112 (2008), pp. 264–276